



Published in final edited form as:

Chem Rev. 2018 May 09; 118(9): 4834–4885. doi:10.1021/acs.chemrev.7b00763.

Tetramethylpiperidine *N*-Oxyl (TEMPO), Phthalimide *N*-oxyl (PINO), and Related *N*-Oxyl Species: Electrochemical Properties and Their Use in Electrocatalytic Reactions

Jordan E. Nutting, Mohammad Rafiee*, and Shannon S. Stahl*

Department of Chemistry, University of Wisconsin-Madison, 1101 University Avenue, Madison, Wisconsin 53706, United States

Abstract

N-oxyl compounds represent a diverse group of reagents that find widespread use as catalysts for the selective oxidation of organic molecules in both laboratory and industrial applications. While turnover of *N*-oxyl catalysts in oxidation reactions may be accomplished with a variety of stoichiometric oxidants, *N*-oxyl reagents have also been extensively used as catalysts under electrochemical conditions in the absence of chemical oxidants. Several classes of *N*-oxyl compounds undergo facile redox reactions at electrode surfaces, enabling them to mediate a wide range of electrosynthetic reactions. Electrochemical studies also provide insights into the structural properties and mechanisms of chemical and electrochemical catalysis by *N*-oxyl compounds. This review provides a comprehensive survey of the electrochemical properties and electrocatalytic applications of aminoxyls, imidoxyls, and related reagents, of which the two prototypical and widely used examples are 2,2,6,6-tetramethylpiperidine *N*-oxyl (TEMPO) and phthalimide *N*-oxyl (PINO).

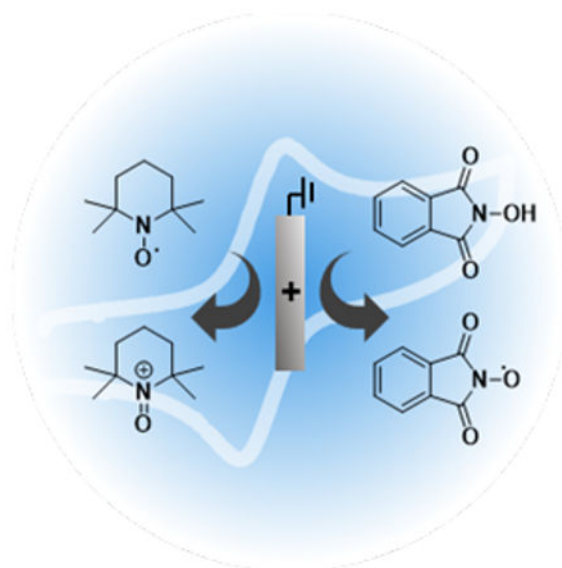
Graphical abstract

*Corresponding Author: mrafiee@chem.wisc.edu, stahl@chem.wisc.edu.

Dedication

We dedicate this work to the memory of Irving Shain (1926 - 2018), a pioneer in the field of electrochemistry and a valued member of the University of Wisconsin-Madison community.

The authors declare no competing financial interest.



1. Introduction

N-oxyl compounds represent a versatile class of organic radical reagents with unique properties and reactivity. The diverse chemistry of these compounds has enabled the use of *N*-oxyl species in applications ranging from use as spin labels in electron spin resonance (ESR) studies,¹ antioxidants in biological studies,^{2–4} charge carriers for energy storage,^{5–10} mediators in polymerization reactions,¹¹ and catalysts in chemical and electrochemical oxidation reactions.¹² In this review, we address the electrochemical properties and synthetic applications of several classes of *N*-oxyl compounds. The two most prominent classes of *N*-oxyl compounds are aminoxyl and imidoxyl species, of which the two most widely used members are 2,2,6,6-tetramethylpiperidine *N*-oxyl (TEMPO) and phthalimide *N*-oxyl (PINO), respectively (Scheme 1). TEMPO is stable under ambient conditions, whereas PINO is generated via oxidation of the stable precursor, *N*-hydroxyphthalimide (NHPI).

The first reports of stable organic aminoxyl radicals appeared in the early-to-mid 1900s,^{13–15} and during the subsequent century these species have emerged as versatile reagents and chemicals that continue to attract widespread research attention. Aminoxyl radicals are characterized by the general structure R₂N–O• (R = alkyl). The stability of aminoxyl radicals is enhanced when the sites adjacent to the *N*-oxyl functional group are fully substituted or are incorporated into the bridgehead position of a bi- or polycyclic framework. These structural features prevent otherwise facile disproportionation of the aminoxyl into the corresponding nitron and hydroxylamine (Scheme 2).¹⁶ Representative stable aminoxyl radicals include TEMPO and 9-azabicyclo[3.3.1]nonane *N*-oxyl (ABNO; cf. Scheme 1). The unusual stability observed with this class of organic radicals underlies the intensive investigations into their reactivity and applications.

Persistent aminoxyl radicals display unique redox properties that play a significant role in their reactivity (Scheme 3). Many aminoxyl radicals (**1**) undergo reversible 1 e[−] oxidation to the corresponding oxoammonium species (**2**), and the latter are relatively strong oxidants

(approx. 0.7–0.8 V vs. NHE).^{17–19} Aminoxy radicals can also undergo a quasi-reversible 1 e⁻/1 H⁺ reduction to hydroxylamines (**3**). These and related redox processes, structure-property relationships associated with these steps, and the implications of these steps for catalysis are elaborated in this review.

The oxoammonium species **2** may be isolated as a stable salt, and it serves as a 2 e⁻ oxidant in a number of organic oxidation reactions. In 1965, Golubev investigated various reactions of oxoammonium salts and observed the first stoichiometric oxidation of alcohols to ketones mediated by an oxoammonium species.²⁰ Since then, many applications of aminoxy radicals in organic oxidation reactions have focused on catalytic methods, in which the oxoammonium species is (re)generated by a stoichiometric secondary oxidant,^{11,12,21–23} such as NaOCl,²⁴ bromine,²⁵ NO_x/O₂,²⁶ or hypervalent iodide species.²⁷ This approach has been especially widely used for alcohol oxidation (Scheme 4).^{11,12,21–23,28} For example, the Anelli-Montanari protocol and related methods that use aminoxy and bromide co-catalysts with stoichiometric NaOCl have been widely implemented in industrial scale alcohol oxidation reactions.^{24,29,30} The oxoammonium also may be generated via electrochemical oxidation of the hydroxylamine or aminoxy species, and these reactions will be elaborated in this review.

A second class of organic *N*-oxyl species, denoted imidoxyl radicals, features carbonyl groups in the positions adjacent to the *N*-oxyl functional group. The imidoxyl radical PINO (Scheme 1) is the most prominent member of this class. Unlike aminoxy radicals, such as TEMPO and ABNO, imidoxyl radicals are not isolable at room temperature and are generally accessed via in situ oxidation of the corresponding *N*-hydroxyimides (Scheme 5). Imidoxyl radicals have been shown to mediate effective hydrogen-atom transfer (HAT) from weak C-H bonds, such as those in allylic and benzylic positions.^{21,31–33} In contrast, aminoxy radical species are generally unreactive with organic molecules, while their corresponding oxoammonium species mediate hydride transfer. The difference in reactivity between aminoxy and imidoxyl species reflects the much higher O-H bond strength of *N*-hydroxyimides (~88 kcal/mol for NHPI)³⁴ relative to hydroxylamines (~69–71 kcal/mol for TEMPOH).^{35,36} The strength of the O-H bonds in *N*-hydroxyimides is attributed, in part, to intramolecular hydrogen bonding and resonance stabilization of the hydroxylamine by the α-carbonyl pi system.³⁴

NHPI-catalyzed oxidation reactions are commonly utilized for the oxygenation of activated C-H bonds. The first synthetic application of PINO as a HAT catalyst was reported in 1977 by Grochowski.³⁷ Reports from Masui in the 1980s demonstrated the ability to access PINO from NHPI using electrochemical methods.^{38–44} Ishii demonstrated in 1995 that PINO could also be thermally accessed via autoxidation of NHPI,⁴⁵ and subsequent studies showed that metal cocatalysts, such as Co^{II} and Mn^{II}, improve aerobic NHPI-catalyzed oxidation reactions.^{21,31,32,46,47}

Electrochemical oxidation of aminoxy radicals to oxoammonium species and *N*-hydroxyimides to imidoxyl species provides the basis for mediated, or indirect, electrochemical processes for selective oxidation of organic molecules (Scheme 6a). In such processes, the mediator undergoes the electron transfer at the electrode surface and then diffuses away from the

electrode surface where it promotes a redox reaction with the organic substrate. Electrochemical mediators have been used extensively in the long history of electroorganic synthesis, and their use complements direct electrolysis methods (Scheme 6b), in which the organic substrate undergoes direct electron transfer at the electrode surface. The theory, application, and potential advantages of mediated electrolysis have been the subject of a number of reviews.^{48–51}

Several reviews and books have addressed the chemical properties of aminoxyl radicals and their use as reagents in chemical synthesis.^{11,12,21–23,28,30,31} Additionally, recent mini-reviews have highlighted alcohol oxidation methods employing electrode-supported aminoxyl radicals⁵² and the potential use of aminoxyl mediators in industrial-scale reactions.⁵³ This review provides the first comprehensive survey of the electrochemical properties of *N*-oxyl radicals and the use of these species as electrochemical mediators in synthetic organic transformations.

2. Electrochemistry of TEMPO and Other Aliphatic Cyclic Aminoxyl Derivatives

2.1. Electrochemical Properties of TEMPO

The first electrochemical study of TEMPO by cyclic voltammetric techniques was reported in 1973 by Tamura and co-workers (Scheme 7).⁵⁴ The cyclic voltammogram (CV) of TEMPO displays an anodic peak corresponding to the oxidation of TEMPO to the oxoammonium species, TEMPO⁺, and a cathodic peak corresponding to the reduction of the electrochemically generated TEMPO⁺ to TEMPO (Scheme 7a). A cathodic-to-anodic peak current ratio (i_{pc}/i_{pa}) of unity and a 60 mV peak-to-peak separation ($E_{pa}-E_{pc}$) satisfies the diagnostic criteria for a reversible electron transfer process. Controlled potential coulometry experiments and monitoring of the reaction by electron spin resonance (ESR) confirmed that the anodic oxidation of TEMPO to TEMPO⁺ is a 1 e⁻ process. Conversely, in the CV of *tert*-butyl nitroxide (DTBO), a stable open-chain radical, no cathodic peak is observed, suggesting a chemically irreversible reaction or decomposition of DTBO⁺ that prevents reduction of DTBO⁺ to DTBO in the cathodic scan (Scheme 7b). Coulometric studies indicate the passage of 0.33 e⁻/DTBO molecule, consistent with the involvement of non-electrochemical consumption of DTBO, such as side-reactions between DTBO⁺ and DTBO. The difference in the redox behavior of these aminoxyl radical species is attributed to structural features that provide the basis for higher stability of TEMPO⁺ relative to DTBO⁺.

It is important to note that use of the term “reversibility” is different in an electrochemical context relative to its usage in traditional chemical reactions. In electrochemistry, “reversibility” or “reversible electron transfer” is associated with the rate of heterogeneous electron transfer at the electrode surface (k^0), and electrochemical reversibility is achieved when electron transfer between the electrode and the analyte is fast on the time scale of mass transfer.⁵⁵ For “reversible” electron transfers, k^0 is typically greater than 0.05 cm s⁻¹, and mass transfer of the analyte to the electrode (i.e., diffusion, for voltammetric studies) is the rate-limiting step. When k^0 is less than ~10⁻⁵ cm·s⁻¹, electrochemically generated species can diffuse away from the electrode surface and will not undergo electron transfer reaction

in the reverse scan, yielding an “irreversible” electron transfer process. In some cases, a peak can be observed in the reverse scan for a slow electron transfer process and exhibits a large peak-to-peak separation.⁵⁶ Intermediate kinetic regimes, where k^0 ranges from $\sim 10^{-5}$ to $\sim 0.05 \text{ cm}\cdot\text{s}^{-1}$ and rates of electron transfer are comparable to mass transfer kinetics, are defined as “quasi-reversible”. Disappearance of the return peak in a CV due to a chemical reaction of the electrogenerated species is different from irreversible electron transfer and is classified as a coupled chemical electrochemical reaction. These distinctions and full discussion of these concepts are elaborated elsewhere.⁵⁷ Effort will be made to distinguish between electrochemical and chemical reversibility in the discussion throughout this review.

Motivated by interest in the interaction of aminoxyl radical species with biomolecules and biomembranes, Malinski and co-workers investigated the redox properties of TEMPO under aqueous conditions in 1988.⁵⁸ Under neutral conditions, a reversible, 1 e^- redox feature is observed at 0.49 V vs. SCE ($\sim 0.73 \text{ V vs. NHE}$) for the TEMPO/TEMPO⁺ couple (Scheme 8a). The product of the electrooxidation of TEMPO was monitored in situ by thin-layer spectroelectrochemistry (Scheme 8b). After generating TEMPO⁺ from TEMPO electrochemically, no spectral changes occurred over a period of 3 h. Upon applying a potential of $+0.35 \text{ V}$ to the solution of TEMPO⁺, the original spectrum of TEMPO was obtained. The apparent chemical stability of TEMPO⁺ and chemical reversibility of the TEMPO/TEMPO⁺ electron-transfer process observed here complements the electrochemical and chemical reversibility observed previously by Tamura.⁵⁴

In the same report, voltammetric and spectroelectrochemical techniques were used to demonstrate the electrochemical reduction of TEMPO to the corresponding hydroxylamine (TEMPOH) at -0.62 V vs. SCE (-0.38 V vs. NHE).⁵⁸ The reduction of TEMPO was found to be irreversible under these conditions, with no anodic peak observed for oxidation of TEMPOH to TEMPO in the reverse scan (Scheme 8a). Bulk electroreduction of TEMPO at -0.8 V vs. SCE yielded significant spectral changes due to the conversion of TEMPO to TEMPOH (Scheme 8c). However, application of an oxidative potential (0.35 V vs. SCE) to the solution of TEMPOH yielded no spectral change and no TEMPO was generated. This “irreversible” redox behavior was later shown by Kato and co-workers to arise from sluggish electron transfer for the proton-coupled TEMPOH/TEMPO redox couple.⁵⁹ Voltammetric studies revealed that oxidation of TEMPOH to TEMPO exhibits an anodic peak at potentials more positive than the peak associated with the TEMPO/TEMPO⁺ redox couple (Scheme 9, data are shown for 4-OH-TEMPO; similar results for TEMPO and other derivatives are also reported), thus reflecting “quasi-reversible” behavior with a very large anodic-to-cathodic peak separation. A recent study by Sigman and Minter tracked the pH-dependence of the anodic peak potential of the TEMPOH/TEMPO redox couple, E_{a2} , relative to the anodic peak potential of the TEMPO/TEMPO⁺ couple, E_{a1} (Scheme 10).⁶⁰ The trend highlights the shift of the TEMPOH/TEMPO anodic peak potential from a value positive relative to the TEMPO/TEMPO⁺ couple at low pH, to a value lower than that of the TEMPO/TEMPO⁺ couple at higher pH. The downward shift of this peak potential at higher pH values reflects both thermodynamic and kinetic effects: the proton-coupled redox process is both more favorable and more facile at higher pH.

Several efforts have been made to obtain a more rigorous assessment of the pH dependence of the TEMPOH/TEMPO redox couple. Kato showed that as the pH of the solution increased, the anodic-to-cathodic peak separation of the TEMPOH/TEMPO redox couple decreased.⁵⁹ Additionally, the $E_{1/2}$ of the TEMPOH/TEMPO couple showed a stronger pH dependence under acidic conditions, which was rationalized by the formation of hydroxylammonium ion (TEMPOH_2^+), rather than the neutral hydroxylamine, at sufficiently acidic pH. This behavior was later elaborated by Samuni and co-workers, who examined the redox behavior of the hydroxylamine/aminoxyl couple from pH 2–12 (Scheme 11a, data are shown for 4-OH-TEMPO).⁶¹ Under basic conditions (pH 7.5–12), the pH dependence of the potential for 4-OH-TEMPO exhibits a slope of -54 mV/pH , reflecting a $1 e^-/1 \text{ H}^+$ redox process (Scheme 11b). Consistent with earlier observations of Kato,⁵⁹ the pH dependence of the 4-OH-TEMPO/4-OH-TEMPOH redox potential under acidic conditions changes and displays a slope of -144 mV/pH , roughly corresponding to a $1 e^-/2 \text{ H}^+$ redox process (Scheme 11b). This change in pH dependence arises from protonation of the nitrogen atom of 4-OH-TEMPO under acidic conditions to afford the hydroxylammonium species, and the solution pH at which the change in pH dependence occurs corresponds to the $\text{p}K_a$ of the nitrogen atom. This CV analysis provides a $\text{p}K_a$ value of 7.1 for the 4-OH-TEMPO hydroxylammonium.^{61,62} The $\text{p}K_a$ value of TEMPOH_2^+ , which lacks the electron-withdrawing 4-OH, group, is slightly higher, and measured values range from 7.34–7.96.^{59,61,63} The aminoxyl species is significantly less basic, with the corresponding oxylammonium reported to have a $\text{p}K_a$ of -5.8 .⁶⁴

Stahl and co-workers recently reported a full Pourbaix analysis of TEMPO and other aminoxyl derivatives across a wide pH range (Scheme 12).⁶³ Voltammetric studies were complemented by independent UV-visible and NMR spectroscopic studies to determine $\text{p}K_a$ values. The TEMPO/TEMPO⁺ redox potential is pH insensitive, as expected, and the potential of the $1 e^-/1 \text{ H}^+$ TEMPOH/TEMPO redox couple exhibits the expected slope of -59 mV/pH . At lower pH values, the slope shifts to -118 mV/pH , reflecting a $1 e^-/2 \text{ H}^+$ process associated with the $\text{TEMPOH}_2^+/\text{TEMPO}$ redox couple. A $\text{p}K_a$ value of 7.34 was determined for the hydroxylammonium species, similar to previously reported values.^{59,61}

Differences in the basicity of the different TEMPO redox partners can lead to disproportionation-comproportionation equilibria. For example, the basicity of TEMPOH leads to the disproportionation of TEMPO under acidic conditions (Scheme 13).⁶¹ As noted above, cyclic voltammetry studies often reveal the oxidation wave for conversion of TEMPOH_2^+ to TEMPO⁺ at potentials higher than the TEMPO/TEMPO⁺ potential (cf. Schemes 10 and 1a), indicating that the comproportionation of hydroxylammonium and oxoammonium under acidic conditions is slow on the CV timescale. This kinetic behavior accounts for the presence of data for the TEMPO/TEMPO⁺ potential in the Pourbaix diagram (Scheme 12, black circles) at $\text{pH} < 3$, where TEMPO is unstable with respect to disproportionation into TEMPOH_2^+ and TEMPO⁺.

Malinski and co-workers noted an additional pH-dependent equilibrium for TEMPO⁺ at pH values greater than 12 during the course of electrochemical and spectroelectrochemical studies.⁵⁸ They attributed this process to the formation of TEMP(OH)O , a hydroxide adduct

of TEMPO⁺ (Scheme 14). The resulting electrochemically inert zwitterionic TEMP(OH)O adduct had been identified in an earlier pulse-radiolysis study.⁶⁵

In 2004, Grzeszczuk and co-workers examined the thermodynamic and kinetic parameters of TEMPO disproportionation and comproportionation (cf. Scheme 13) using cyclic and steady-state voltammetry in neutral to strongly acidic aqueous solutions.⁶⁶ A steady-state voltammogram was obtained using a rotating disc electrode (RDE). The limiting currents obtained from the steady-state plateau provided insight into the bulk concentration of redox-active species.⁵⁷ At pH 7, the steady-state voltammogram shows an anodic plateau due to TEMPO oxidation, and the current of this plateau is proportional to the concentration of TEMPO (Scheme 15). Upon addition of HClO₄, the anodic current decreases, reflecting depletion of TEMPO in the solution, and a cathodic plateau appears. At pH 0, the anodic plateau is absent (i.e., $I \sim 0$), and the cathodic current reaches a maximum value that is approximately half of the initial anodic current, indicating that the concentration of TEMPO⁺ is half of the original TEMPO concentration. These results provide direct insights into the disproportionation of TEMPO into TEMPO⁺ and TEMPOH₂⁺ that occurs under acidic conditions. The TEMPOH₂⁺ species is not electrochemically active in this potential range.

Grzeszczuk and co-workers employed digital simulation methods to determine kinetic parameters and the equilibrium constant for the disproportionation reaction at pH 0. There was good agreement between the simulated and experimental CVs, and the disproportionation rate was calculated to be $10^4 \text{ M}^{-1} \text{ s}^{-1}$. A hydrogen-bonded dimer resulting from interaction of TEMPO and TEMPOH₂⁺ was also proposed on the basis of CV simulations.

The disproportionation of TEMPO was later examined under acidic conditions in organic solvent by Kishioka and co-workers.⁶⁷ Steady-state voltammetry data revealed that 50% of the TEMPO converts to TEMPO⁺ upon addition of acid (Scheme 16). Addition of 2,6-lutidine to a solution of TEMPO⁺ and TEMPOH₂⁺ generated from disproportionation of TEMPO resulted in regeneration of TEMPO. Titration of TEMPO with *p*-toluenesulfonic acid (*p*-TSA) indicates 1 H⁺ is consumed for each molecule of TEMPO, again highlighting the formation of TEMPOH₂⁺ under acidic conditions.

To complement studies examining the disproportionation of TEMPO under acidic conditions, Samuni and co-workers investigated the comproportionation reaction of TEMPOH and TEMPO⁺ under basic conditions.⁶¹ The reaction of TEMPOH with TEMPO⁺ in aqueous solution was studied at various pH values using rapid-mixing stopped-flow methods and EPR spectrometry. Taking into account the acid dissociation constant for TEMPOH₂⁺ ($pK_{a1} = 7.5$) and assuming TEMPOH has a pK_a value similar to that of NH₂OH ($pK_{a2} = 13.7$), Samuni and co-workers evaluated the three relevant comproportionation reactions and derived the rate constants for each (Scheme 17). Rate constants for the comproportionation between TEMPO⁺ and the various protonation states of TEMPOH varied by several orders of magnitude. The faster comproportionation reactions at higher pH is consistent with the greater driving force for these reactions, evident in the pH-dependent shift in the TEMPO redox potentials (cf. Scheme 11).

The electrochemical kinetics of the TEMPOH/TEMPO redox couple are dependent on the identity of the electrode. Samuni and co-workers showed that a smaller cathodic-to-anodic peak separation is observed with a graphite electrode relative to that observed with a glassy carbon electrode.^{61,68,69} In a separate study by Kishioka, nearly reversible redox behavior, with 70 mV peak-to-peak separation, was reported at the surface of a mercury drop electrode under acidic and basic conditions (Scheme 18).⁷⁰ Similar behavior is observed at an oxidized carbon electrode.⁶³ Although the origin of these changes in redox behavior are not well understood, the results show the ability of the electrode material to affect the rate of this proton-coupled electron transfer step.⁷¹

The electron transfer of TEMPOH and the comproportionation reaction of TEMPO⁺ and TEMPOH are important factors for electrocatalytic applications of TEMPO, which are discussed in section 3 below. Oxidation reactions mediated by TEMPO often yield TEMPOH, and the regeneration of TEMPO⁺ can proceed by two possible pathways (Scheme 19): (a) direct 2 e⁻/1 H⁺ oxidation of TEMPOH to TEMPO⁺ at the electrode surface, and (b) comproportionation of TEMPOH and TEMPO⁺ in solution, followed by 1 e⁻ oxidation of TEMPO to TEMPO⁺ at the electrode.

2.3. Structural Effects on the Electrochemical Properties of Cyclic Aminoxy Radicals

The well-characterized electrochemical reactivity of TEMPO has enabled the use of electrochemical methods to study structural effects on the redox behavior of other cyclic aminoxy radicals. Modification of the structural and electronic properties of the aminoxy radical can significantly alter the redox potentials of aminoxy radicals and provide the basis for the design of new compounds with defined electrochemical properties.

The substantial effects of structural modifications on the redox chemistry of cyclic aminoxy radicals are highlighted in the Pourbaix diagram for 4-NH₂-TEMPOH (Scheme 20).⁶³ 4-NH₂-TEMPO possesses a basic functional group. Protonation of the amino group strongly modulates the effect of the substituent on the redox properties of the aminoxy radical. At low pH, a strong inductive effect from the protonated amine increases the redox potential of the aminoxy/oxoammonium couple to 0.926 V vs. NHE (cf. 0.745 V vs. NHE for TEMPO in Scheme 12). Under more basic conditions (pH > 9), 4-NH₂-TEMPO is neutral, and it displays chemically irreversible oxidation by voltammetric analysis, probably arising from oxidation of the free amino group. The p*K*_a of the hydroxylamine bearing a 4-NH₃⁺ group is 5.6, considerably lower than the value of 7.34 determined for TEMPO by similar methods (Scheme 11b). Changes in the pH-dependence of the redox potentials for this species result in no disproportionation of the 4-NH₂-TEMPO aminoxy radical under acidic conditions.

Efforts to probe the effects of structural modifications on electrochemical properties of aminoxy radicals were reported as early as 1975.⁷² However, the majority of data focuses only on the aminoxy/oxoammonium redox couple. As expected, substitution of electron-donating groups lowers the redox potentials, while electron-withdrawing moieties lead to an increase.^{60,73–80} The experimental aminoxy/oxoammonium redox potentials of a wide range of stable cyclic aminoxy radical species are shown in Table 1. Where available, the redox potentials of aminoxy species in different solvents have been included. Redox potentials in aqueous and non-aqueous (i.e., CH₃CN) solvents are difficult to compare

precisely; however, the redox potentials for the aminoxyl/oxoammonium couple of TEMPO, ABNO, and AZADO is somewhat more positive under non-aqueous conditions.¹⁷

As noted above, the oxoammonium redox state is susceptible to formation of an electrochemically inactive hydroxide adduct at high pH (cf. Scheme 14). Less hindered bi- and polycyclic oxoammonium species, such as ABNO⁺ and 2-azaadamantane-2-oxoammonium (AZADO⁺), exhibit greater affinity for hydroxide, relative to TEMPO⁺. This behavior was characterized recently for ABNO,^{63,73} and is manifested as a pH-dependence in the oxidation of ABNO to the ABNO⁺ species (Scheme 21). Oxoammonium species are also susceptible to base-induced decomposition at high pH, arising from an elimination reaction that leads to cleavage of a C-N bond and opening of the ring (Scheme 22).⁸¹⁻⁸³ This reactivity is especially problematic for the most electron-deficient aminoxyl derivatives (e.g., X = O in Scheme 22), and is evident in voltammetric studies by the presence of irreversible CVs under basic conditions.⁷³

Further differences between the redox chemistry of ABNO and more sterically hindered aminoxyls are apparent in the respective Pourbaix diagrams of these species (cf. Scheme 12 and Scheme 21). While the redox potential for the aminoxyl/oxoammonium couple of ABNO and TEMPO were found to differ by < 5 mV, the redox potential for the hydroxylamine/aminoxyl of ABNO (0.80 V) is 150 mV more positive than that of TEMPO (0.65 V, cf. Scheme 12). This difference may be ascribed to the greater acidity of ABNOH₂⁺ relative to TEMPOH₂⁺ arising from decreased inductive stabilization of the cation in ABNOH₂⁺. The relatively more positive redox potential of the ABNOH/ABNO couple results in a narrower region of stability for ABNO compared to TEMPO. Additionally, ABNO demonstrates a kinetically facile 2 e⁻/2 H⁺ equilibrium for the ABNOH₂⁺/ABNO⁺ couple at pH < 3.

A few studies have examined the effect of structure on the redox potential of the hydroxylamine/aminoxyl couple. In 1991, Morris, Swartz and co-workers measured the redox potentials of the hydroxylamine/aminoxyl couple of substituted piperidine-, pyrrolidine-, and pyrroline-derived aminoxyls using voltammetric techniques (Scheme 23).⁸⁴ Among aminoxyl derivatives with the same backbone structure, the redox potentials of the hydroxylamine/aminoxyl couples correlate with substituent inductive effects: more electron-withdrawing substituents result in less negative redox potentials whereas electron-donating substituents give more negative redox potentials. Pyrroline derivatives display the lowest response to substituent inductive effects, and the 5-membered-ring aminoxyl species were generally reduced at lower potentials compared to the 6-membered-ring aminoxyls.

Anzai and co-workers later demonstrated in 2007 that substitution at the β-position of 2,2,5,5-tetramethylpyrrolidine *N*-oxyl (PROXYL) derivatives with electron-withdrawing and donating groups alters the potential of the hydroxylamine/aminoxyl redox couple.⁷⁴ A linear relationship was demonstrated between the Pauling group electronegativity of the substituent and this redox potential (Scheme 24). A 1 e⁻ reduction process was invoked in this report; however, the use of protic solvents (H₂O, MeOH) in this study suggests that the reaction likely corresponds to a 1 e⁻/1 H⁺ reduction process.

The Pourbaix analysis of different aminoxyls, reported by Stahl and coworkers, showed that ancillary substituents more strongly affect the aminoxyl/oxoammonium couple than the hydroxylamine/aminoxyl couple (Table 2).⁶³ For the aminoxyl series consisting of TEMPO, 4-AcNH-TEMPO (ACT) and 4-NH₃⁺-TEMPO, the aminoxyl/oxoammonium couples vary by 180 mV, while the standard hydroxylamine/aminoxyl potentials exhibit a range of only 60 mV. This effect is further illustrated by the relative uniformity of the R₂NO-H BDEs. The different response evident in the two redox processes may be rationalized by a “redox leveling effect” of proton-coupled electron transfer (PCET) processes⁸⁵ (i.e., the hydroxylamine/aminoxyl redox process), whereby substituent electronic effects have an opposite influence on electron- and proton-transfer steps.

Various computational studies have analyzed substituent effects on aminoxyl redox potentials within several different aminoxyl structural classes.^{87,88} In 2008, Bottle and coworkers computed the oxidation potentials of over 20 aminoxyl radical species with piperidine, pyrrolidine, azaphenalene and isoindoline core structures.⁷⁸ The results were correlated with experimental oxidation potentials to benchmark the computational studies. Using the same computational methods, earlier studies had calculated the redox potential for over 50 different hydroxylamine/aminoxyl and aminoxyl/oxoammonium couples, but these computed values were not validated with experimental results.⁸⁸ Determination of the gas phase and solvation free energies of the aminoxyl radical and the corresponding closed shell oxoammonium species provided the basis for computed oxidation potentials. Good agreement between computed and experimental oxidation potentials ($E^0 < 0.05$ V) was observed for pyrrolidine, piperidine, and isoindoline derivatives (Table 3). Azaphenalene derivatives, however, displayed much higher experimental oxidation potentials compared to the computed values (E^0 up to 0.5 V), which was tentatively attributed to pi-stacking effects that are not accounted for in the computations.

3. Electrochemical Reactions Mediated by TEMPO and Related Cyclic Aminoxyl Radicals

3.1. Alcohol Oxidation

3.1.1. Mechanism of Aminoxyl-Mediated Alcohol Oxidation—In 1965, Golubev reported the first stoichiometric reactions between TEMPO-derived oxoammonium salts and alcohols.²⁰ Since then, cyclic aminoxyls species have found extensive use as reagents for the oxidation of alcohols to the corresponding aldehydes, ketones, and carboxylic acids.^{11,12,21–23,28} Electrochemical conditions may be used as an alternative to chemical oxidants to promote the formation of oxoammonium species from the corresponding aminoxyls, and the electrochemical properties and redox reactions of aminoxyls described in section 2 underlie aminoxyl-mediated electrochemical oxidation of alcohols.

In 1983, Semmelhack and co-workers reported the first use of an aminoxyl radical as an electrocatalyst for alcohol electrooxidation and examined certain mechanistic aspects of this reactivity.⁸⁹ The reaction between electrogenerated TEMPO⁺ with primary alcohols in the presence of base (here, 2,6-lutidine) was found to be fast, even at –60 °C, and up to 40 catalytic turnovers were achieved. The TEMPO⁺-mediated oxidation of primary alcohols

was found to be relatively insensitive to substrate electronic effects, but secondary alcohols were oxidized at significantly slower rates. In the absence of base, alcohol oxidation was sluggish.

In a subsequent study, Semmelhack and co-workers investigated the mechanism of TEMPO⁺-catalyzed alcohol oxidation.⁹⁰ Four potential routes were considered (Scheme 25): (a) direct hydride abstraction from the alcohol by the oxoammonium to afford hydroxylamine and an oxocarbenium ion that undergoes subsequent deprotonation; (b) H⁺/e⁻ transfer from alcohol to oxoammonium, generating TEMPO, H⁺, and an alkoxy radical; (c) nucleophilic attack of an alkoxide at the nitrogen atom of TEMPO⁺ to generate a reactive N-O adduct; and (d) nucleophilic attack of the alkoxide at the oxygen atom of TEMPO⁺ to generate a reactive O-O adduct. Hammett studies and deuterium kinetic isotope effects were interpreted in favor of path (c), with alcohol oxidation arising from a cyclic transition state involving the N-O TEMPO⁺/alkoxide adduct.

Later work by Tokuda and co-workers in 1998 further probed the potential formation of an intermediate oxoammonium-alcohol adduct.⁹¹ Using UV-visible spectroelectrochemical methods, they obtained evidence for the formation of an adduct over the course of the TEMPO-mediated electrooxidation of 4-methoxybenzyl alcohol in CH₃CN containing 0.2 M NaClO₄ under N₂. In the absence of alcohol, only TEMPO and TEMPO⁺ were observed during the electrochemical oxidation of TEMPO. In a solution of 4-methoxybenzyl alcohol and TEMPO, application of the same range of potentials led to a significant increase in the absorbance at 265 nm, supporting the formation of a new species during the electrolysis. The authors proposed this new species to be the N-O oxoammonium-alkoxide adduct proposed by Semmelhack (Scheme 25, path c). This was the first experimental evidence for the formation of an adduct between TEMPO⁺ and alcohol.

Although other mechanisms are sometimes proposed in the literature,^{28,92} a preponderance of experimental and computational evidence suggests that, under basic conditions, the alcohol substrate forms an adduct at the nitrogen atom of the oxoammonium species, followed by intramolecular hydride transfer to provide TEMPOH and the organic carbonyl (Scheme 26a). Much of this evidence comes from studies of non-electrochemical aminoxyl-mediated alcohol oxidation reactions, including stoichiometric reactions of oxoammonium species with alcohols or catalytic alcohol oxidation reactions with chemical oxidants.⁹³⁻⁹⁵ Primary alcohols have lower p*K*_a values and smaller steric demands than secondary alcohols, and both properties account for their preferential oxidation under basic conditions (selected data will be elaborated below).^{12,93} The mechanism and selectivity of the reaction between alcohols and TEMPO⁺ has been shown to change at lower pH. Golubev and co-workers were the first to show that, under acidic conditions (i.e., pH < 4), secondary alcohols react faster than primary alcohols.⁹⁶ Computational studies by Bailey, Wiberg, and co-workers attribute this change in selectivity under acidic conditions to a bimolecular hydride-transfer mechanism (Scheme 26b).⁹³ This mechanism is consistent with the better hydride-donor ability of secondary alcohols, relative to primary alcohols.

In 1996, Ohmori and co-workers reported a CV study of TEMPO under basic conditions in the presence of alcohol substrates (Scheme 27).⁹⁷ The reactivity of the electrochemically

generated TEMPO⁺ species with alcohols under basic conditions is evident in the voltammetric behavior of the TEMPO/TEMPO⁺ redox couple. The increase in the anodic peak current and disappearance (or decrease) in the cathodic peak current is characteristic of a catalytic electrochemical-chemical pathway (EC') (Scheme 28). In an oxidative EC' reaction, the reduced mediator, Med_{red}, undergoes an electrochemical oxidation (E) to generate Med_{ox}, which then undergoes a chemical redox reaction (C') with the reduced substrate, Sub_{red}, to generate Sub_{ox} and Med_{red}. Consumption of Med_{ox} in the chemical step results in the lack of a cathodic peak. Regeneration of Med_{red} in the chemical reaction enables another electrochemical oxidation on the CV timescale, resulting in an increase in the anodic peak current.⁹⁸

Mechanistic studies of aminoxyl-catalyzed electrochemical alcohol oxidation were conducted by Brown and co-workers in connection with their development of a flow electrolysis method for alcohol oxidation.^{69,99} CV experiments were conducted under aqueous alkaline conditions (pH 9.3–13.2), analogous to the conditions employed for the preparative method. As shown in Scheme 29, the oxidation of TEMPO in the presence of benzyl alcohol is electrochemically irreversible, and the oxidation current significantly increases at higher pH. The pH-dependent response of the current could be attributed to the role of base in promoting a) reoxidation of TEMPOH or b) TEMPO⁺-mediated oxidation of the alcohol. Brown noted that regeneration of TEMPO⁺ from TEMPOH after conversion of alcohol to aldehyde cannot be rate-limiting under alkaline conditions as the oxidation wave for conversion of TEMPOH to TEMPO appears at lower potentials than the oxidation wave for oxidation of TEMPO to TEMPO⁺ (cf. Scheme 11). Further, they noted that the comproportionation of TEMPOH and TEMPO⁺ to generate TEMPO is thermodynamically favorable and fast under basic conditions.⁶¹ Consistent with previous mechanistic proposals for TEMPO-catalyzed alcohol oxidation using chemical oxidants, the base dependence on the reaction was attributed to base-promoted formation of the TEMPO⁺/alkoxide adduct.^{90,93} This productive role of base was found to compete with base-promoted decomposition of TEMPO⁺ (cf. Scheme 22) and formation of the catalytically inert zwitterionic hydroxide adduct of TEMPO⁺, TEMP(OH)O (cf. Scheme 14). The full proposed mechanism for electrocatalytic oxidation of benzyl alcohol by TEMPO is shown in Scheme 30.

In 2014, Rafiee and co-workers used voltammetric techniques to determine the catalytic activity and rate constants for TEMPO-mediated electrooxidation of a series of primary and secondary alcohols.⁶⁸ The ratio of the TEMPO oxidation current in the presence (i_{cat}) and absence (i_0) of alcohol is proportional to the turnover frequency of the mediated alcohol oxidation process.⁹⁸ Comparison of i_{cat}/i_0 at fixed concentrations of TEMPO and substrate allows for comparison of the relative reactivity of TEMPO⁺ with different substrates. The highest reactivity was observed with primary alcohols, with considerably slower reactivity observed with secondary alcohols (Scheme 31). Voltammetric studies show that the catalytic rate increases at higher alcohol concentration, and studies of the reaction with benzyl alcohol reveal a linear correlation between the anodic plateau current and [benzyl alcohol]^{1/2}, consistent with classical electrocatalytic kinetics involving diffusion of the substrate to the electrode (Scheme 32).^{98,100} Digital simulations of the cyclic voltammograms under various electrocatalytic conditions led to the conclusion that reoxidation of TEMPOH during catalytic turnover involves both (a) direct electrochemical

oxidation of TEMPOH and (b) comproportionation of TEMPO⁺/TEMPOH to form TEMPO followed by electrochemical oxidation of TEMPO to TEMPO⁺.

Badalyan and Stahl recently examined the mechanism of TEMPO-catalyzed alcohol electrooxidation in an organic solvent (CH₃CN) with *N*-methylimidazole as an added base.¹⁰¹ Kinetic analysis of the oxidation of benzyl alcohol (PhCH₂OH) was performed by CV. A beneficial role of base was observed, similar to the effect of higher pH under aqueous conditions. In addition, a kinetic isotope effect of 3.2 was observed on the basis of independent rate measurements for the electrooxidation of PhCH₂OH and PhCD₂OH, and Hammett analysis of various para-substituted benzyl alcohol derivatives revealed a negative slope, $\rho = -0.24$ (Scheme 33, i.e., faster rates observed with more electron-rich substrates). Collectively, the data support an electrocatalytic mechanism involving base-promoted formation of the TEMPO⁺/alkoxide adduct, followed by turnover-limiting intramolecular hydride transfer within this complex, similar to that shown in Scheme 26a.

A report by Marken and co-workers in 2016 utilized a hydrodynamic rocking disc electrode technique to further examine the TEMPO-mediated oxidation of primary alcohols.¹⁰² This and other mechanistic studies for aminoxyl-catalyzed alcohol electrooxidation corroborate the mechanistic findings and trends discussed above.^{103–105} The majority of these mechanistic studies have focused on basic conditions, owing to the enhanced rates of aminoxyl-mediated alcohol oxidation at higher pH. Slower alcohol oxidation under acidic conditions often prevents the use of CV studies to investigate reaction kinetics. Krzyczmonik and co-workers, however, examined rate constants for alcohol oxidation by electrogenerated 4-OH-TEMPO⁺ at pH 4–5 using coulometric methods.¹⁰⁶ Initial and steady-state currents measured for mediated bulk electrolyses were used to derive the rate constants for oxidation of various alcohols by 4-OH-TEMPO⁺. The coulometric data demonstrate a pH-dependence on the reaction rate and selectivity under mildly acidic conditions (Scheme 34). At pH 4, secondary alcohols are oxidized more rapidly than primary alcohols by 4-OH-TEMPO⁺, but the difference in relative reactivity between primary and secondary alcohols narrows as the pH is increased to 5.

3.1.2. Performance of Aminoxyl Derivatives for Electrochemical Alcohol Oxidation

—Two recent studies have probed the effect of different aminoxyl derivatives on electrochemical alcohol oxidation. Using chronoamperometry and CV techniques, Stahl and coworkers examined a series of TEMPO analogs and bi-/polycyclic aminoxyls with a range of redox potentials for the oxidation of alcohols under basic conditions.⁷³ As with voltammetric responses, the ratio of chronoamperometric anodic currents in the presence and absence of substrate is proportional to the rate of the catalytic reaction, enabling determination of the reaction TOF (Scheme 35).¹⁰⁷ The low-cost aminoxyl derivative 4-AcNH-TEMPO (ACT) was identified as a particularly effective mediator (Table 4) based on these studies. The less hindered oxoammonium species (e.g., those derived from AZADO and ABNO) were shown to be more susceptible to inhibition at high pH by formation of the hydroxide adduct (analogous to the reaction in Scheme 14; see also, Scheme 21). This adduct is electrochemically inactive and competes with formation of the productive alkoxide-aminoxyl adduct.

This study drew attention to a contrast between the use of electrochemical versus chemical methods for reoxidation of the oxoammonium-based oxidant. With chemical oxidants, such as bleach (NaOCl), AZADO, ABNO, and other sterically less-hindered aminoxyls have been shown to exhibit significantly higher activity for alcohol oxidation than TEMPO and various TEMPO analogs.^{75108–110} Under electrochemical conditions, however, the redox potential of the aminoxyl was shown to be even more influential than steric effects on the catalytic rate (Table 4). For example, the sterically hindered, but higher-potential aminoxyl ACT ($E_{1/2} = 650$ mV vs. Ag/AgCl) exhibited faster rates than the sterically less-hindered, lower-potential aminoxyls ABNO and AZADO ($E_{1/2} = 480$ mV and 450 mV vs. Ag/AgCl, respectively) for the oxidation of primary alcohols (Table 4). Even for the oxidation of secondary alcohols, the activity of ACT was comparable to the activity of ABNO and AZADO. Additional analysis was conducted with seven different aminoxyls to obtain catalytic rate constants for the oxidation of 1-butanol using both chemical and electrochemical oxidation methods. As shown in Scheme 36, the reaction rates exhibit opposite trends with respect to the aminoxyl/oxoammonium redox potential. The less hindered aminoxyls, which exhibit comparatively low redox potentials, are much faster than TEMPO derivatives when NaOCl is used as the oxidant. In contrast, the rates are faster with higher-potential TEMPO derivatives under electrochemical conditions. It was observed that low-potential aminoxyl mediators were more rapidly oxidized by NaOCl and exhibited higher steady-state concentration of the oxoammonium relative to high-potential aminoxyls. The increased rate of alcohol oxidation by low-potential aminoxyl mediators under chemical oxidation conditions correlates with the more rapid generation of the corresponding oxoammonium species under these conditions. Under electrochemical conditions, however, the rate of mediator reoxidation and the steady state oxoammonium concentration is normalized by adjustment of the applied potential and leads to a catalytic rate that reflects the oxidizing ability of the oxoammonium. These data suggest that, when normalized for effective oxoammonium concentration, the reaction driving force is more significant than steric effects in aminoxyl-mediated electrochemical oxidation of alcohols.

Sigman, Minter, and co-workers examined the catalytic activity of an even wider range of aminoxyl radicals in their study of glycerol oxidation using voltammetric and computational methods.⁶⁰ The ratio $(i_{pa}/i_{pc})_{cat}$ of the peak oxidative current (i_{pa}) and the peak reductive current (i_{pc}) in the presence of glycerol and the difference (E_a) between the anodic peak potentials of the hydroxylamine/aminoxyl (E_{pa2}) and the aminoxyl/oxoammonium (E_{pa1}) redox couples (see Scheme 10a for definition of E_{pa1} and E_{pa2}) were measured by CV under aqueous conditions at pH 7. The catalytic activity towards glycerol was found to increase as E_a decreased, with $(i_{pa}/i_{pc})_{cat}$ showing a correlation with $1/(E_{pa2} - E_{pa1})$ (cf. Scheme 37a). Though the basis for this correlation is not yet clear, the trend is suggested to arise from the relative stability of the off-cycle hydroxylammonium species. A model developed from this correlation was used to predict the catalytic activity of a series of aminoxyl radicals using computationally derived E_{a1} and E_{a2} values. Eight aminoxyl derivatives were used as a training set to develop the parameterized model, and variety of other aminoxyl radicals were used to validate the model (Scheme 37b). A linear correlation with $R^2 = 0.80$ was observed between the predicted and experimental values for the $(i_{pa}/i_{pc})_{cat}$ validation set. A large deviation observed in the predicted reactivity for one particular TEMPO derivative, 4-(*N,N*-

dimethyl-*N*-benzylammonium)-TEMPO, was hypothesized to be due to the large size and permanent charge of the bulky ammonium substituent (cf. Scheme 37b). This model may be used to predict the catalytic activity of aminoxyl derivatives from in silico-determined values of E_{a1} and E_{a2} , precluding the need to independently synthesize and probe various aminoxyl structures.

After identifying these relationships, aminoxyl species with similar properties were grouped into four categories according to their potential practical applications (Scheme 38): aminoxyl radicals with lower potentials and high catalytic activity (quadrant I) could serve as anodic oxidation catalysts for fuel cell applications; aminoxyl radicals with high redox potentials and high catalytic activity (quadrant II) could present advantages in electrosynthetic applications; aminoxyl radicals with low redox potentials and low catalytic activity (quadrant III) are well-suited for use as antioxidants or radical traps; and aminoxyl radicals with high redox potentials and low catalytic activity (quadrant IV) have properties aligned with spin-labeling applications. These classifications and the correlation studies provide a route to readily predict and identify aminoxyl radicals that are suitable for a particular application.

3.1.3. Cooperative Copper/Aminoxyl Catalyzed Electrochemical Alcohol

Oxidation—In 2016, Badalyan and Stahl characterized a cooperative Cu/aminoxyl electrocatalyst for alcohol oxidation.^{101,111} The catalyst system, composed of Cu^I(OTf), (2,2'-bipyridine) (bpy), NEt₃, and an aminoxyl co-catalyst (TEMPO or ABNO), mediates the electrooxidation of diverse alcohols in CH₃CN, demonstrating electrocatalytic behavior at the Cu^I/Cu^{II} potential (Scheme 39a). This process operates at an applied potential nearly 0.5 V lower than electrocatalytic alcohol oxidation with TEMPO alone as a catalyst (Scheme 39b). This significant lowering of the applied potential arises from the involvement of two low-potential 1 e⁻ oxidants (Cu^{II} and TEMPO) rather than one high-potential 2 e⁻ oxidant (TEMPO⁺) in the alcohol oxidation process. The TOFs of both processes were determined using the ratio of the currents at the plateau peak potential in the presence and absence of 20 mM benzyl alcohol (i_{cat}/i_0).¹⁰⁷ In spite of the lower driving force, the Cu/TEMPO-catalyzed reaction exhibits a turnover frequency 4–5-fold higher than the corresponding TEMPO-only catalytic process.

Mechanistic studies showed that the Cu/aminoxyl system exhibits a kinetic isotope effect of 1.0 and Hammett analysis of *para*-substituted benzyl alcohols gives a slope (ρ) of +0.37. These results contrast data obtained with the TEMPO-only catalyst system (cf. Scheme 33 and associated text). In the proposed reaction mechanism (Scheme 39c), oxidation of Cu^I(bpy) to Cu^{II}(bpy) occurs at the electrode surface, and the electrogenerated Cu^{II}(bpy) then plays a dual role: a) oxidation of TEMPOH to TEMPO, and b) oxidation of the alcohol in cooperation with TEMPO via a bpy-ligated Cu^{II}(TEMPO)(alkoxide) adduct, similar to that characterized previously for Cu/TEMPO-catalyzed alcohol oxidation under aerobic conditions.^{112–115} The base plays a proton-acceptor role in formation of the Cu^{II}-alkoxide species and in the oxidation of TEMPOH.

3.1.4. Synthetic Alcohol Oxidation—The use of aminoxyl radical catalysts for the preparative electrochemical oxidation of alcohols was first reported in 1983 when

Semmelhack and co-workers demonstrated efficient electrooxidation of primary aliphatic alcohols in the presence of catalytic quantities of TEMPO (Scheme 40).⁸⁹ Semmelhack's report pre-dated the widely-used Anelli conditions for TEMPO-catalyzed alcohol oxidation, which employ biphasic conditions with co-catalytic bromide and NaOCl as the stoichiometric oxidant.²⁴ Previous methods for electrochemical alcohol oxidation utilized high-potential mediators, such as bromide and iodide (ca. 1.4 V vs. NHE),^{116,117} whereas Semmelhack's method could operate at the significantly lower TEMPO/TEMPO⁺ redox potential (ca. 0.77 V vs. NHE). Primary alcohols were found to undergo significantly faster oxidation than secondary alcohols, and no overoxidation to the corresponding carboxylic acid was observed, even in the presence of water.

In 1991, Torii and co-workers demonstrated the use of a two-phase bromide/4-benzoate-TEMPO (4-BzO-TEMPO) double mediatory system for the oxidation of both primary and secondary alcohols.¹¹⁸ This work was inspired by previous chemical studies in which a terminal oxidant in the aqueous phase oxidizes an aminoxyl species at the aqueous-organic phase boundary.^{24,119,120} At an anode submerged in a basic aqueous solution of NaBr, Br⁻ is oxidized to an oxidized bromine species (i.e., Br⁺, BrO⁻, Br[•], Br₂, Br₃⁻). The oxidized bromine species then oxidizes the aminoxyl species to the corresponding oxoammonium at a H₂O-CH₂Cl₂ boundary layer. Alcohol oxidation by the generated oxoammonium occurs in the organic phase (Scheme 41).

Lower aminoxyl loadings were possible with this method (ca 1 mol%), relative to the Semmelhack conditions, and secondary alcohols were reported to undergo oxidation to the ketone, albeit at slower rates than primary alcohols. While TEMPO was found to be a successful catalyst for this method, 4-BzO-TEMPO exhibited higher yields and selectivity. Again, no overoxidation of the aldehyde to the carboxylic acid was reported (Scheme 42). One limitation of this method is that alcohol substrates containing sterically-unhindered electron-rich arene groups are susceptible to bromination. For 1,6- and 1,5-diols, the corresponding lactone product was observed. In the same year, Ogibin and co-workers expanded the scope of Torii's double mediatory system and achieved effective electrooxidation of cyclopropylcarbinols (Scheme 43).¹²¹ The excellent yields for these substrates is consistent with a non-radical mechanism for alcohol oxidation.

In 1994, Torii and co-workers reported the electrooxidation of dihydroxyalkanoates to the corresponding vicinal tricarbonyl products using the bromide/4-BzO-TEMPO double mediatory system (Scheme 44).¹²² The electrooxidation system generally produced di- and tricarbonyl compounds in higher yields than a corresponding chemical oxidation method, which used catalytic 4-BzO-TEMPO in the presence of NaBrO₂ as the stoichiometric oxidant.

Ogibin later applied this method to the electrooxidation of 6 β -methyl-3 β ,5 α -dihydroxy-16 α ,17 α -cyclohexanopregnan-20-one **4** to 6 β -methyl-5 α -dihydroxy-16 α ,17 α -cyclohexanopregnan-3,20-dione **5**, an intermediate in the preparation of progesterin (6 α -methyl-16 α ,17 α -cyclohexanoprogesterone, **6**).¹²³ Oxidation of the 3,5-diol motif of **4** to **5** can be carried out with chromic acid in acetone (Scheme 45). However, **4** is poorly soluble in acetone (0.015 M) and requires large amounts of solvent. This consideration, together

with the formation of toxic chromium byproducts, made large scale chemical synthesis of progestin impractical. Using the NaBr and 4-hydroxy-TEMPO-benzoate catalyst system under biphasic conditions, **4** was oxidized to **5** in 90% yield on a 12-g scale with a concentration in CH₂Cl₂ of 0.1 M.

Tanaka and co-workers have reported a series of aminoxyl-catalyzed electrooxidations of alcohols under aqueous conditions in an undivided cell. In 2005, a series of secondary aliphatic alcohols were shown to undergo effective oxidization to the corresponding ketones using a water-soluble cationic TEMPO derivative (Scheme 46).¹²⁴ Only two examples of primary alcohol oxidation were reported, and both aldehyde and carboxylic acid products were obtained. A bromide co-mediator is required to achieve efficient reactivity. A protocol employing an anionic water-soluble TEMPO derivative was developed later (Scheme 46).¹²⁵ This anionic TEMPO derivative was effective in the absence of bromide, thereby enabling oxidation of electron-rich benzylic alcohols without competing arene bromination. Both the anionic and cationic derivatives could be recovered and recycled following electrolysis. Later reports from Tanaka showed that oxidation of amphiphilic alcohols in water may be achieved with unmodified TEMPO in the absence of bromide salts.^{126,127} The formation of an emulsion in the aqueous electrolysis medium was shown to contribute to efficient catalysis with this system.

Bicyclic aminoxyl mediators have also been used successfully in the electrooxidation of alcohols. In 2008, Onomura and co-workers reported the use of azabicyclo-*N*-oxyls as electrochemical mediators for the oxidation of sterically-hindered secondary alcohols (Scheme 47).¹²⁸ Biphasic conditions with a bromide co-mediator were used, analogous to the conditions reported earlier by Torii.¹¹⁸ The reduced steric bulk of the bicyclic *N*-oxyl species facilitated oxidation of sterically bulky, secondary alcohols such as menthol.

Chiral aminoxyl mediators have been used to enable kinetic resolution of chiral secondary alcohols under electrochemical conditions.^{129–131} In 1999, Kashiwagi, Anzai, and co-workers evaluated the reaction of chiral alcohols with **7** as a chiral TEMPO mediator.¹²⁹ Voltammetric studies showed that the anodic peak current of **7** was significantly greater in the presence of (*R*)-1-phenylethanol than in the presence of the (*S*)-isomer (Scheme 48). The closely related chiral aminoxyl radical **8** was later applied for the preparative electrooxidation of racemic *sec*-benzylic alcohols with moderate selectivity (Scheme 49).¹³¹

Preparative kinetic resolution alcohol electrooxidation was later reported by Onomura and co-workers using a chiral bicyclic aminoxyl catalyst. The sterically less-hindered nortropane-derived aminoxyl **9** was shown to enable kinetic resolution of racemic secondary alcohols with moderate selectivity (Scheme 50).¹³²

All of the methods discussed above were carried out in batch electrolysis reactions, but recent reports have examined the use of flow methods for electrochemical aminoxyl-catalyzed alcohol oxidation. In 2012, Brown and co-workers described the first protocol for TEMPO-mediated alcohol electrooxidation in a single channel microfluidic electrolysis cell.⁹⁹ Efficient electrooxidation was achieved in a 1:1 *tert*-butanol:carbonate buffer (pH 11.5), and high selectivity for the aldehyde and ketone products was observed with only trace

carboxylic acid formation. Depending on the substrate, product could be generated at a rate of 30–100 mg h⁻¹, with only a single pass through the electrolysis cell. Roughly 60% of TEMPO was recovered after electrolysis.

3.1.4.1. Biomass Oxidation: The successful electrooxidation of simple alcohol functional groups by aminoxyl mediators led to the implementation of this methodology for the catalytic oxidation of carbohydrates, biomass-derived polyols, lignin-related compounds, and derivatives thereof. These processes generate unique polymeric materials and value-added chemicals and have also been considered for energy-conversion applications.

Chemical methods for aminoxyl-mediated oxidation of carbohydrates were reported in the early 1990s and were carried out using co-catalytic TEMPO or 4-OMe-TEMPO and bromide salts with hypochlorite as the terminal oxidant.²⁸ Early electrochemical precedents reported the use of TEMPO as a mediator for the electroanalytical detection of carbohydrates.^{97,133,134} The first synthetic application of carbohydrate electrooxidation mediated by TEMPO was reported by Schäfer and co-workers in 1999 (Scheme 51).¹³⁵ Under alkaline aqueous conditions, TEMPO was shown to mediate selective oxidation of primary hydroxyl groups in preference to secondary hydroxyl groups of non-reducing carbohydrates. Monosaccharide derivatives of glucose, mannose, and galactose were readily oxidized at the primary hydroxyl group in moderate to excellent yields (Scheme 51). Di-, oligo- and polysaccharides were also effectively oxidized at the primary hydroxyl groups. Electrooxidation of potato starch gave a polycarboxylic acid in 63% yield with 93% conversion of the primary hydroxyl groups to the carboxylic acid. The electromediated oxidation of potato starch led to lower yields compared to Anelli conditions (ca 98%) but provided a means to avoid high concentrations of NaBr. Later reports expanded the reaction scope to include aminopyranosides, unsaturated carbohydrates, glycosyl azides, and additional non-reducing di-saccharides, all of which were isolated as the methyl ester (Scheme 51).^{136,137}

In 2005, Belgsir and co-workers reported the TEMPO-mediated electrooxidation of reducing disaccharides, maltose and cellobiose, at pH 10 in a divided cell.⁹² Oxidation occurred at both the primary hydroxyl groups and at the anomeric position. Similar behavior was observed in the oxidation of the acetal groups in 1,4-dioxane-2,3-diol.

Barbier compared the use of Schäfer's electrochemical TEMPO-mediated oxidation of carbohydrates to TEMPO/NaOCl/NaOClO₂ oxidation conditions.¹³⁸ Shorter reaction times were observed for the electrochemical process. While the electrochemical oxidation was performed at pH 10, the chemical oxidation method was performed in a mixed organic-aqueous system buffered to pH 6.2, which likely accounts for the shorter reaction times under the electrochemical conditions. The TEMPO/NaOCl conditions generally provided higher yields of oxidation at the primary hydroxyl of non-reducing carbohydrates with protected *sec*-hydroxyl groups. For unprotected non-reducing sugars, however, electrochemical reaction conditions provided higher yields.

TEMPO-mediated electrooxidation of carbohydrates has been extended for the efficient oxidation of cellulosic materials. Oxidation of the primary hydroxyls in the carbohydrate

monomer units can provide carboxylated cellulosic polymers (Scheme 52), which can potentially be used as biomass-derived solvents, carrier reagents, binders, swelling agents, and other applications.¹³⁹

Reports of TEMPO-mediated chemical oxidation of cellulosic materials emerged in the late 1990s that utilized the bleach/TEMPO system with a bromide co-catalyst.^{140–142} In 2010, Bettencourt reported the first electrooxidation of mercerized microcrystalline cellulose by TEMPO.¹³⁹ During electrolysis in alkaline aqueous media (pH 10), the initially insoluble cellulose powder gradually solubilized, yielding a transparent solution after the reaction. Analysis of the material recovered after electrolysis by elemental analysis and titration studies indicated nearly complete oxidation of the primary hydroxyl groups to the corresponding carboxylic acid. No discussion of the morphology or degree of polymerization of the oxidation product was provided.

Soon after, Isogai and co-workers achieved near quantitative electrochemical oxidation of viscose rayon fibers using catalytic ACT under mildly acidic reaction conditions.¹⁴³ It was hypothesized that the mildly acidic conditions could prevent base-promoted depolymerization often observed under catalytic TEMPO/NaOCl conditions for the chemical oxidation of cellulose.¹⁴⁴ Indeed, under the electrooxidation conditions, the degree of polymerization (DP) only decreased from approximately 300 to 100 whereas a chemical oxidation method mediated by 4-NH₂-TEMPO at pH 10 reported previously resulted in reduction of the DP to ~40.¹⁴⁵ A later report from Isogai examined aminoxyl-mediated electrooxidation of a softwood bleached kraft pulp native cellulose under both mildly acidic and basic conditions.¹⁴⁶ As expected, electrooxidation of the native cellulose under basic conditions resulted in significant depolymerization while depolymerization was suppressed under the mildly acidic electrooxidation conditions (Scheme 53). The overall aldehyde and carboxylic acid content was similar in the oxidation products of both electrolysis methods. The oxidized cellulose nanofibrils obtained after electrolysis demonstrated a higher aldehyde content and lower carboxylate content compared to corresponding nanofibrils obtained from a chemical TEMPO/NaOCl oxidation system.

Carlsson, Mhryan, and co-workers recently demonstrated the TEMPO-mediated electrooxidation of native *Cladophora* nanocellulose and achieved a comparable degree of oxidation in the product as observed under a TEMPO/NaOCl cellulose oxidation system.¹⁴⁷ The degree of oxidation observed (9.8%) corresponded to quantitative oxidation of the cellulose fibril surface. Though approximately 20% depolymerization was observed after electrolysis under alkaline conditions, the surface morphology of the water-insoluble products remained largely unchanged, indicating the oxidation did not proceed significantly beyond the fibril surface.

The valorization of biomass-derived feedstock chemicals by conversion to building block organic molecules and the utilization of biomass for energy production has been the focus of increasing recent interest.^{148–151} In 2006 Pagliaro and co-workers reported the TEMPO-mediated electrooxidation of glycerol to 1,3-dihydroxyacetone (DHA), a valuable material used in the cosmetic and fungicide industries (Scheme 54).¹⁵² DHA is conventionally produced via microbial fermentation by *Gluconobacter oxydans*, the activity of which is

susceptible to product inhibition. The fermentation process also presents challenging downstream purification. The reported TEMPO-mediated electrooxidation of glycerol to DHA under mildly basic conditions provided access to DHA, and overoxidation to carboxylic acid byproducts was only observed following longer reaction times. The observed selectivity for oxidation of the secondary hydroxyl group was unexpected owing to the typical steric sensitivity of TEMPO-catalyzed oxidations. Although not investigated or rationalized by the authors, this observation may arise from isomerization of initially formed glyceraldehyde.

In 2014, Sigman, Minteer, and co-workers described an electrochemical aminoxyl/enzyme co-catalyst system for the complete oxidation of glycerol to CO₂, a process that could be utilized in biofuel cell applications.¹⁵³ It was hypothesized that an aminoxyl species could catalyze the oxidation of glycerol to mesoxalic acid (Scheme 55), which is a suitable substrate for further oxidation by oxalate oxidase. Oxalate oxidase operates under acidic conditions, but most reports on synthetic aminoxyl-catalyzed electrochemical alcohol oxidation operate under basic conditions. 4-NH₂-TEMPO was identified as a mediator capable of promoting efficient glycerol electrooxidation under mildly acidic conditions where oxalate oxidase is still active (Scheme 56). The enhanced performance of 4-NH₂-TEMPO under acidic conditions could be attributed, at least in part, to protonation of the amine functional group below pH 5.6, which increases the redox potential and reactivity of the corresponding oxoammonium (cf. Scheme 20).⁶³ Overall, the electrooxidation of glycerol by this cooperative 4-NH₂-TEMPO and oxalate oxidase system can generate 16 electrons per molecule of glycerol, upon complete oxidation of glycerol to CO₂ (Scheme 55). Complete oxidation of glycerol to CO₂ was achieved in 22 hours at room temperature, with 90.6 C of charge collected.

A 2015 report from Choi and co-workers demonstrated the operation of a photoelectrochemical process for TEMPO-mediated electrooxidation of 5-hydroxymethylfurfural (HMF) to 2,5-furandicarboxylic acid (FDCA) (Scheme 57).¹⁵⁴ HMF is derived from cellulosic materials and has been widely targeted as a biomass-based feedstock for the downstream generation of valuable, industrially-relevant materials, such as FDCA. FDCA is a monomer for important polymers including polyethylene terephthalate and poly(ethylene-2,5-furandicarboxylate). The TEMPO-mediated oxidation of HMF was applied in a photoelectrochemical cell where FDCA generation at a photoanode (BiVO₄) was coupled to H₂ fuel generation at the cathode (Scheme 58). Near quantitative yields of FDCA were obtained with 100% Faradaic efficiency using 1.5 equivalents of TEMPO mediator. The work included a demonstration of the process with simulated solar light as the energy input.

Ananikov and co-workers later reported the electrooxidation of HMF to 2,5-diformylfuran (DFF) in a two-phase solution, with ACT and iodide as a double-mediator system (Scheme 59).¹⁵⁵ DFF is a monomer and a building block for polymer and pharmaceutical applications, but selective oxidation of HMF to DFF is challenging due to the oxidatively-sensitive formyl groups present in both HMF and DFF. For the TEMPO-mediated method, however, DFF was obtained in 61–63% yields. Bromide was found to be ineffective as a co-mediator in this reaction.

Aminoxyl-mediated electrooxidation of alcohols in biomass has also been leveraged for the efficient synthesis of betulinic acid **12** from betulin **10** (Scheme 60). Betulin is present in the bark of various species of birch trees and comprises 5–25% of the bark material. Betulinic acid is of interest as an anti-tumor and anti-HIV agent. Previous chemical method to access betulinic acid from betulin required multiple steps, installation and removal of protecting groups, costly reagents, and purification steps which were prohibitive on a commercial scale.^{156–159} In a 2006 patent, Krasutsky and co-workers described the electrooxidation of betulin to betulin aldehyde **11** using catalytic quantities of TEMPO.¹⁶⁰ The betulin aldehyde was then oxidized further to betulinic acid using stoichiometric NaClO₂. No competing oxidation of the secondary hydroxyl group of betulin was observed. The electrooxidation reaction was reported on a 120-g scale.

Lignin is an abundant biopolymer with a highly functionalized aromatic backbone, and the depolymerization of lignin provides a potential means to produce aromatic chemicals.^{161,162} Selective oxidation of the benzylic alcohol in the β-O-4 linkage of lignin to a ketone has been shown to facilitate this process (Scheme 61). Stahl and coworkers showed that a catalyst system consisting of 5 mol% ACT in combination with catalytic HNO₃ and HCl enabled effective oxidation of lignin with O₂ as the stoichiometric oxidant,¹⁶³ and subsequent hydrolysis of the oxidized polymer in the presence of formic acid and sodium formate led to low molecular-weight aromatics in yields of >50%.¹⁶⁴ This work and other studies highlight the utility of TEMPO and related aminoxyl catalysts for selective oxidation of lignin, and by modifying the oxidant and/or reaction conditions, different selectivities can be achieved.^{165–171} For example, Bolm and coworkers reported that use of TEMPO in combination with diacetyliodobenzene as the stoichiometric oxidant leads to selective oxidation of the primary alcohol in lignin.¹⁷¹

In 2017, Takano and co-workers investigated TEMPO and ACT as mediators for electrochemical oxidation of non-phenolic lignin β-O-4 model compound **13**.¹⁷² Various mixed aqueous-organic solvent mixtures were tested with several bases and buffering conditions (Scheme 62). The results showed that under different buffering conditions with aminoxyl mediator (20 mol%), the selectivity of the oxidation reaction changes. Electrolysis of **13** in 95:5 CH₃CN/water in the presence of excess 2,6-lutidine, led to selective oxidation of the benzylic alcohol to the corresponding ketone, albeit only in low yields (3% and 11%, respectively). In a 10:90 dioxane:phosphate buffer (pH 7) solution, electrolysis instead led to high yields for selective oxidation of the primary hydroxyl group to the carboxylic acid. Electrolysis in 10:90 dioxane:carbonate buffer (pH 10) also yielded oxidation of the primary hydroxyl group, but significant yields of C-C cleavage products were also observed. In all cases, ACT demonstrated enhanced catalytic efficiency compared to TEMPO. The electrochemical reaction did not proceed well under acidic conditions (acetate buffer, pH 4).

3.1.4.2. Supported Aminoxyls for Electrocatalytic Alcohol Oxidation: Immobilization of aminoxyl mediators on electrode surfaces can lead to significantly enhanced rates of alcohol oxidation and facilitate isolation relative to methods that use dissolved aminoxyl mediators. Pagliaro and co-workers reviewed this topic in 2015.⁵² Content from this earlier review is summarized here, together with highlights of more recent examples and methods

not summarized previously. The content below is organized according the type of immobilization method employed for the aminoxyl catalysts.

Polymeric films: The earliest reports of supported aminoxyl radicals for electrocatalytic alcohol oxidation employed electrode-supported polymeric films modified with aminoxyl species. In 1987, Moutet and co-workers reported electrooxidation of alcohols with an electrode modified by electropolymerization of a pyrrole-tethered 2,2,5,5-tetramethyl-3-pyrrolin-1-oxyl (Scheme 63).^{173,174} The modified electrode exhibited reversible redox couples corresponding to polypyrrole/polypyrrole⁺ (0.58 V vs. NHE) and aminoxyl/oxoammonium (0.98 V vs. NHE) (Scheme 64). Though the film facilitated electrooxidation of several benzyl alcohol substrates, it displayed rather poor stability, losing 70 to 80% of its initial electroactivity during the course of the electrolysis. Using a similar approach, Walton and co-workers electrochemically polymerized thiophene-tethered TEMPO onto platinum electrodes.¹⁷⁵ The resulting film facilitated electrooxidation of *p*-methoxybenzyl alcohol to the corresponding aldehyde in 50% yield without significant film degradation.

In later reports from 1988 and 1990, Osa, Bobbitt, and co-workers modified cross-linked poly(acrylic acid) (PAA) with 4-NH₂-TEMPO via amide bond formation.^{176,177} The TEMPO-PAA polymer was then cast-coated onto carbon electrodes. The modified electrode was competent for the oxidation of nerol, a monoterpene bearing a primary allylic alcohol. Methylation of free carboxylic acid functional groups (Scheme 65) enhanced the stability of the electrode, and the methylated electrode demonstrated a TON of more than 1560 for nerol oxidation compared to approximately 500 TON achieved by the non-methylated electrode.

PAA electrode films modified with chiral aminoxyls have been used for asymmetric oxidative lactonization of alcohols.¹⁷⁸ Asymmetric lactonization and kinetic resolution of alcohols has also been reported for aminoxyl-modified PAA electrode films using the chiral base sparteine rather than a chiral aminoxyl species.^{179,180} Later reports have called these results into question, however, by demonstrating competitive electrooxidation of sparteine at the electrolysis potentials.¹⁸¹

Both the polypyrrole and PAA aminoxyl-linked polymeric films described above were used for electrochemical alcohol oxidation in organic solvents. Belgsir and co-workers later sequestered TEMPO within a Nafion® film-coated graphite felt electrode that demonstrated some stability in water.¹⁸² The polymer film facilitated electrooxidation of several methyl glycosides to the corresponding uronic acids in excellent to moderate yields; however, 40–50% of the TEMPO leached from the Nafion® film by the end of the electrolysis.

Additional aminoxyl-polymer electrode films have been reported in the literature, but have not been applied to preparative bulk electrolyses.^{183–187} For example, Sigman, Minter, and co-workers covalently linked TEMPO to linear poly(ethylamine) which was subsequently crosslinked on a glassy carbon electrode.¹⁸⁸ The modified electrode demonstrated improved reactivity for alcohol electrooxidation compared to homogenous 4-OMe-TEMPO (Scheme 66).

Silica films: Aminoxy radicals incorporated into silica films have been used to functionalize conductive oxide electrodes. Pagliaro and co-workers reported the first application of this approach for alcohol electrooxidation using aminoxy-doped sol-gel electrodes.^{189,190} Electrodeposition of a (trimethoxy)silane derivative bearing an aminopropyl-tethered TEMPO onto an indium-tin oxide (ITO) electrode provided an amorphous film that was active for alcohol oxidation under buffered alkaline conditions. A series of benzylic and allylic alcohols were oxidized selectively in high yields to the corresponding aldehydes and ketones (Scheme 67). No carboxylic acid products were detected. Though a 40% reduction in catalytic activity was observed after the first bulk electrooxidation, no further degradation was observed in subsequent electrolyses, and the electrode was reused for multiple preparative bulk electrolyses. Long electrolysis times were required for complete conversion, however (ca 180 hours for oxidation of 0.5 mmol benzyl alcohol). The authors note that benzyl alcohol did not undergo oxidation at a bare ITO electrode or a TEMPO-free sol-gel coated ITO electrode under the same electrolysis conditions.

Karimi, Rafiee, and co-workers later developed an electrode-supported aminoxy-modified mesoporous silica film which displayed enhanced reactivity and stability compared to amorphous sol-gel systems.¹⁹¹ In this study, an ordered mesoporous silica (MCM-41) film was constructed on the electrode surface using a technique known as electro-assisted self-assembly (EASA)¹⁹² where a sol-gel precursor is templated with surfactant molecules on a carbon electrode at reducing potentials. Aminopropyl groups contained within the film were functionalized with 4-oxo-TEMPO via reductive amination. The resulting film contained ordered channels aligned perpendicular to the electrode surface (Scheme 68). A variety of benzylic, allylic, and alkyl-substituted alcohols were oxidized to the corresponding aldehydes in good to excellent yields over short reaction times under buffered alkaline conditions (Scheme 69). The modified electrode could be used for five subsequent electrolyses with only a small decrease in yield. Turnover frequencies up to 3070 h⁻¹ were observed with this electrode. The improved reactivity and stability was attributed to the ordered, porous nature of the silica film, whereby the orientation of the channels should allow facile electron transfer from anchored TEMPO to the electrode surface while additionally making the catalyst molecules accessible to the dissolved substrates. However, the comparatively high potentials used in these electrolyses (1.0 V vs. Ag/AgCl) may reflect the resistance of the nonconductive silica film deposited at the electrode surface, which could contribute to significant Ohmic drop during bulk electrolysis.

Covalent functionalization of carbon electrodes: Geneste and co-workers reported the covalent linking of TEMPO to carbon electrodes using amine bridges.¹⁹³ Electrochemical oxidation of 4-NH₂-TEMPO was reported to generate a nitrogen-centered aminyl radical that could be grafted to the graphite felt electrode surface. This covalently-modified electrode was shown to oxidize 4-nitrobenzylalcohol under aqueous conditions with a TON of 290.¹⁹⁴

Mediated electrolysis with dispersed TEMPO-functionalized particles and polymers:

Tanaka and co-workers reported a method for electrochemical alcohol oxidation that

employed bromide as an electrochemically regenerable mediator in combination with supported-TEMPO catalysts dispersed in solution.^{195–199} Under buffered alkaline conditions with a bromide mediator, various primary and secondary alcohols were oxidized in the presence of aminoxyl catalysts supported by silica gel or polymeric particles. Instead of being immobilized at the electrode, these particles were freely dispersed within the electrolysis cell (Scheme 70). After electrolysis, the particles were filtered and recovered from the reaction solution, facilitating product purification and catalyst recycling. TEMPO-immobilized poly(*p*-phenylene benzobisthiazole) particles could be reused five times with no loss in yield for the electrooxidation of 4-chlorobenzyl alcohol. As in homogenous bromide-aminoxyl co-mediator systems, bromination of electron-rich arenes was observed as a side reaction.

Francke and co-workers recently reported the attachment of TEMPO to a soluble poly(methacrylate) backbone (Scheme 71).²⁰⁰ Tethering the mediator to a soluble support is reported to enhance the kinetics of electron transfer between the mediator and the electrode relative to disperse TEMPO-functionalized particles while still facilitating recovery of the mediator. The M_w of the polymeric mediator was adjusted to approximately 2700 g mol⁻¹, which corresponds to 11 monomer units for each polymer. By CV, the diffusion coefficient, D , of the polymeric TEMPO mediator is measured to be 8.8×10^{-6} cm² s⁻¹, lower than the value measured for TEMPO (3.2×10^{-5} cm² s⁻¹). The polymeric TEMPO mediator demonstrates enhanced activity towards the electrochemical oxidation of alcohols relative to molecular TEMPO: under kinetically controlled and pseudo-first order conditions, the rate of benzyl alcohol oxidation is approximately 60 times greater for poly(methacrylate)-TEMPO. A soluble poly(methacrylate)-supported electrolyte was also developed and provided sufficient ionic conductivity for use in bulk electrolysis reactions. Bulk electrochemical oxidation of various primary alcohols was carried out to generate the corresponding aldehydes in the presence of both the polymeric mediator and polyelectrolyte. The electrolysis reactions proceed with good Faradaic efficiency and can be carried out on a gram scale. The polymeric materials could be recovered after the electrolysis reactions via dialysis and could be reused up to five times.

Non-covalent immobilization: Das and Stahl recently reported a pyrene-tethered TEMPO derivative that was noncovalently immobilized at electrodes coated with multi-walled carbon nanotubes (MWCNTs) (Scheme 7a).²⁰¹ This approach takes advantage of pi-pi stacking interactions between the pyrene and the MWCNTs and draws upon precedents for non-covalent immobilization of molecular catalysts for energy storage and conversion applications.²⁰² Preparation of the modified electrode by adding a solution of pyrene-TEMPO to the electrolysis cell with a carbon-cloth anode coated with MWCNTs is a particularly facile protocol relative to other methods to prepare functionalized electrodes. The supported pyrene-TEMPO catalyst demonstrated high activity at low mediator loadings for alcohol electrooxidation (Scheme 72b). Bulk electrolysis using ACT as an electronically similar dissolved mediator exhibited a TOF of 25 h⁻¹ while the immobilized pyrene-TEMPO catalyst exhibited a TOF of 2000 h⁻¹ under otherwise identical conditions for benzyl alcohol oxidation, and TOFs of up to 4000 h⁻¹ were observed in the study. This rate enhancement led to much better electrosynthetic performance, allowing for full conversion

of diverse benzylic alcohol substrates at a loading of only 0.05 mol% of the pyrene-TEMPO derivative (Scheme 73).^{179,180} The method was further validated by oxidation of a sterically hindered heterocyclic benzylic alcohol derivative that is an intermediate toward the cholesterol-lowering drug rosuvastatin. These results, together with those of Geneste¹⁹⁴ and Karimi¹⁹¹, demonstrate the enhanced rates accessible from catalyst immobilization, which avoids kinetic losses associated with catalyst mass transfer to and from the electrode surface when using dissolved mediators.

Other strategies for aminoxyl immobilization on the electrode surfaces have been reported, though their use for preparative-scale alcohol oxidation has not been investigated.^{203,204} Electrode-supported aminoxyls have additionally been applied to other synthetic oxidation reactions. The latter results are addressed in sections below, in connection with the use of dissolved mediators for each of the respective synthetic applications.

3.2. Amine Oxidation

Electrocatalytic oxidation of amines using aminoxyl mediators has been explored, although not as extensively as for alcohol oxidation. Use of TEMPO as an electrochemical mediator for amine oxidation was first reported by Semmelhack and Schmid in 1983.²⁰⁵ Under conditions similar to those reported for electrocatalytic alcohol oxidation, primary amines were readily oxidized to the corresponding aldehyde under aqueous conditions (CH₃CN/H₂O), or to the nitrile when the reaction was conducted in anhydrous CH₃CN (Scheme 74). The oxidation of several *sec*-primary amines to the corresponding ketone was reported as well. The two methods provide moderate to excellent yields for oxidation of aliphatic and benzylic amines. Higher efficiencies were observed for the oxidation of aliphatic amines with slow addition of substrate. The oxidation of *N*-methyl benzylamine resulted in cleavage of the *N*-methyl group and formation of benzaldehyde in 89% yield.

In 1999, Kashiwagi and co-workers reported an electrocatalytic method for kinetic resolution of racemic primary benzylic amines using chiral aminoxyl catalyst **8** (Scheme 75).²⁰⁶ Moderate discrimination was observed between the two enantiomers of the amine substrates, favoring oxidation of the (*S*) configuration to the corresponding ketone where *s* = 4.7–5.8. The same chiral aminoxyl catalyst was previously used for kinetic resolution of benzylic alcohols.¹³¹ Similar *s* values were observed in each system (cf. Scheme 49).

Kashiwagi and co-workers demonstrated the electrocatalytic oxidation of *N*-alkyl-*N*-methylanilines to *N*-alkylformanilides using 10 mol% 4-BzO-TEMPO as a mediator in a divided cell (Scheme 76).²⁰⁷ Oxidation of the tertiary amine was hypothesized to produce the corresponding iminium ion. Water addition to the iminium would afford the α -amino alcohol, which could then undergo oxidation to the formanilide product.

In 2013, Little, Zeng, and co-workers reported the TEMPO-mediated electrooxidation of a series of tetrahydroisoquinolines to give the corresponding isoquinolinones under biphasic conditions with a bromide co-mediator (Scheme 77).²⁰⁸ As proposed by Kashiwagi, the amine was hypothesized to first undergo oxidation to the iminium ion, which could then react with water and undergo further oxidation of the hemiaminal to give the lactam product. Similar reactivity was observed with the cyclic ether isochroman. Acyclic substrates were

not amenable to oxidation under these conditions. Cyclic amines lacking benzylic sites were not tested for oxidation.

In 2016, Li, Shen, and co-workers reported a method for synthesis of nitriles from aldehydes via aminoxyl-mediated electrooxidation of an imine generated in situ (Scheme 78).²⁰⁹ Hexamethyldisilazane (HMDS) was used as the nitrogen source and underwent condensation with the aldehyde to provide the imine, which was observed under the reaction conditions. Oxidation of the condensation product yielded the nitrile. Aromatic and heteroaromatic aldehydes were readily oxidized to the corresponding nitriles in moderate to excellent yields. Aliphatic aldehydes underwent competitive aldol reactions in the presence of HMDS, requiring dropwise addition of HMDS, and electron-rich substrates such as 4-methoxy-benzaldehyde required higher aminoxyl loadings than electron-deficient substrates. The method for conversion of benzaldehydes to nitriles was improved by using the less expensive and easier-to-handle nitrogen source, ammonium acetate (NH₄OAc), instead of HMDS.²¹⁰ Electrooxidation of aliphatic aldehydes in the presence of NH₄OAc was not reported.

Li and Shen later reported a one-pot method for electrooxidation of alcohols to nitriles, catalyzed by TEMPO (Scheme 79).²¹¹ Electrooxidation of the primary alcohol substrates provides the aldehyde, which condenses with NH₄OAc to provide an imine capable of undergoing further TEMPO⁺-mediated oxidation to the nitrile. Under the reported conditions, only benzylic and allylic substrates were demonstrated and, as in the earlier reports, electron-rich substrates required higher TEMPO loadings. Though aliphatic alcohols were consumed under the reaction conditions, no nitrile products were observed, even with longer reaction times. Though a large overpotential is applied in these reactions to reduce reaction time, the yield of byproducts was observed to not vary greatly between electrolyses conducted at 1.5 V versus 0.8 V (vs. Ag/AgNO₃).

Lei and co-workers recently reported TEMPO-mediated electrochemical dehydrogenation of saturated *N*-heterocycles.²¹² Using catalytic quantities of TEMPO, tetrahydroisoquinolines, tetrahydroquinazolines, indoline, and dihydrobenzothiazole derivatives undergo dehydrogenation to the corresponding unsaturated heterocycles in moderate-to-good yields (Scheme 80). An imine intermediate was observed in the electrochemical oxidation of a tetrahydroisoquinoline derivative. Further oxidation yields the fully dehydrogenated product.

Several reports address the use of electrode-supported aminoxyl catalysts for the oxidation of amines. In 1990, Crayston, Walton, and co-workers prepared a polyacrylic ester-supported aminoxyl polymer that could be dip-coated onto platinum or carbon cloth electrodes.²¹³ Bulk electrolysis of benzylamine in mixed 25:1 CH₃CN:H₂O using a carbon cloth anode coated with the polymer provided benzaldehyde (78%) and benzonitrile (22%). No stability tests of the polymer were conducted. Later, in 1998, Kashiwagi and co-workers reported the oxidation of several primary benzylic and aliphatic amines using a graphite felt anode coated with a PAA-immobilized TEMPO mediator.²¹⁴ The nitrile products were obtained in good yields in CH₃CN. During electrolysis, the electrode underwent steady inactivation. The polymer-linked TEMPO was proposed to decompose to the corresponding

piperidine leading to electrode inactivation. Treatment of the electrode with *m*-CPBA could restore activity, presumably via reoxidation of the amine to the aminoxy.

The mechanism of alkyl amine oxidation by oxoammonium has not been investigated as extensively as that of alcohol oxidation. Several mechanisms have been proposed for the reaction, largely drawing on mechanisms considered for alcohol oxidation (Scheme 81).^{207,215,216} Computational studies by Wiberg, Bailey, and co-workers implicate outer-sphere hydride transfer from the amine to the oxoammonium species as the rate-limiting step in the sequence leading to generation of the hydroxylamine and the protonated aldimine (Scheme 82, left), corresponding to path a in Scheme 81.²¹⁵ This mechanism for oxidation of primary amines by oxoammonium resembles the mechanism of alcohol oxidation under acidic conditions. The formation of an adduct between the amine and oxoammonium species (i.e., Scheme 81, paths b and c) was not considered in this report. Oxidation of the aldimine to nitrile was also evaluated, and the proposed mechanism features pyridine base-promoted transfer of a hydride from the iminyl C-H position to a second equivalent of oxoammonium (Scheme 82, right).

In 2017, Zhang and co-workers reported CV studies of TEMPO-mediated electrooxidation of glycine, with glyoxal proposed as the product by analogy to previous reports of amine oxidation (the product identity was not confirmed).^{205,216} They observed that pyridine-derived bases of higher basicity increased the rate of glycine oxidation in mixed CH₃CN/H₂O solvent (Scheme 83). The hydride transfer mechanism proposed by Wiberg and Bobbitt does not account for this base effect, and Zhang and co-workers instead proposed base-promoted formation of a covalent N-N bonded TEMPO⁺/glycine adduct (Scheme 81, path b). Formation of an N-O adduct (Scheme 81, path c), which has been suggested (without evidence) by Kashiwagi and co-workers, is also consistent with this data.²⁰⁷ Additional studies will be required to resolve these mechanistic uncertainties.

3.3. C-H Functionalization

The electrochemical activation of C-H bonds by aminoxy mediators has been reported for a number of activated substrates. In 1993, Osa and co-workers used PAA-immobilized TEMPO (cf. Scheme 65) supported on a graphite felt electrode to facilitate the electrocatalytic homocoupling of 2-naphthol and 2-methoxynaphthalene.²¹⁸ Electrolyses were performed in CH₃CN with 2,6-lutidine in a divided cell. Quantitative yields were obtained for the 1,1'-bi(2-naphthol) homocoupling products. 1-Naphthol and 1-methoxynaphthalene were also oxidized under these conditions, and a mixture of the 1,1'-, 2,2'-, and 1,2'-homocoupling products were observed. It was reported that the film was not deactivated after electrolysis and could be used for multiple reactions. The reaction was proposed to go through one-electron transfer between the oxoammonium and electron-rich substrate.

In 2005, Belgsir and co-workers reported electrochemical allylic oxygenation of activated alkenes using catalytic quantities of TEMPO (Scheme 84a).²¹⁹ A putative carbocation intermediate was proposed to be trapped by water or hydroxide to give the allylic alcohol which then undergo facile oxidation by a second equivalent of TEMPO⁺ to afford the ketone product. Isomerization of *cis*-alkenes to the *trans*-isomers was observed. Upon subjecting α -

terpinene and γ -terpinene to the electrolysis conditions, the aromatization product *p*-cymene was obtained rather than carbonyl products (Scheme 84b). This aromatization of cyclohexadiene species by TEMPO⁺ was expanded to other substrates in a later report by Breton and co-workers (Scheme 85).²²⁰

3.4. Palladium Co-Catalyzed Reactions

Homogeneous Pd catalysts have been widely used for selective oxidation of organic molecules. Many different terminal oxidants have been used in these reactions for oxidation of Pd⁰ and/or Pd^{II} intermediates, including Ag^I and Cu^{II} salts, benzoquinone, PhI(OAc)₂, *N*-bromosuccinimide, peroxides, and molecular oxygen.^{221–226} Considerable effort has been directed toward the development of electrochemical variants of these methods, typically through the use of a mediator that can oxidize the Pd-based intermediates and then undergo facile regeneration at the electrode. Quinones and triaryl amines are the most commonly used mediators for Pd electrocatalysis, as documented in several reviews,^{227–229} but aminoxyl mediators have also been investigated.

In 2007, Tanaka and co-workers demonstrated a Pd-catalyzed Wacker-type electrooxidation reaction that used TEMPO as a mediator (Scheme 86).²³⁰ Various Pd⁰ sources were tested, but Pd(OAc)₂ gave the highest yields of product. The enhanced reactivity of Pd(OAc)₂ was attributed to Kolbe-type decarboxylation of the acetate anion proposed to promote generation of especially reactive dicationic Pd^{II} species (Scheme 87). In the absence of TEMPO, only trace product was observed in these reactions. A later report focused on optimization of the Pd(OAc)₂/TEMPO system for electrochemical Wacker-type oxidative cyclizations, and TEMPO was found to be a more effective co-catalyst than hydroquinone and triphenylamine.²³¹ This system was later found to mediate electrochemical oxidative homocoupling of arylboronic acids²³² and arylboronic esters²³³ and cross-coupling of arylboronic acids with silver acetylides.²³⁴

3.5. Alkene Aminooxygenation

In 2014, Xu and co-workers reported the intramolecular aminooxygenation of unactivated alkenes via the electrochemical generation of a nitrogen-centered radical from *N*-aryl carbamates and *N*-aryl amides.²³⁵ The reaction was proposed to proceed via intramolecular addition of the nitrogen-centered radical to an alkene, followed by trapping of the resulting carbon-centered radical by TEMPO to yield the cyclized aminooxygenation product (Scheme 88). In addition to serving as a radical trap, TEMPO was proposed to mediate the electrochemical oxidation of the carbamate or amide substrates under the reaction conditions. Indeed, carrying out the reaction in the absence of current with the addition of excess TEMPO⁺[BF₄⁻] provided the same aminooxygenation products. Under the electrolysis conditions, high yields of the cyclized aminooxygenation products were obtained with excellent *trans*-diastereoselectivity (Scheme 89). Acyclic substrates were also amenable to the aminooxygenation reaction.

3.6. Alkyne Hydroxybromination

In 1992, Torii and co-workers expanded upon their work with biphasic aminoxyl/bromide co-mediated electrolysis by exploring the synthesis of α,α -dihaloketones from alkynes

(Scheme 90).²³⁶ These products represent an appealing synthetic alternative to relatively unstable 1,2-diketones.^{237,238} The reaction was proposed to proceed via oxidation of Br^- to Br^+ or Br^\bullet , either of which could react with the alkyne. Pendant acetate and amide groups and water are thought to subsequently participate in oxygenation of the activated alkyne (e.g., as a bromonium species): in the absence of the aminoxyl, the yield of the α,α -dihaloketone is diminished and 1,2-dibrominated alkenes were obtained as the major product. The neighboring acetate or amide groups were necessary to form the hydroxybromination product: oxidation of 1-decyne provided only the 1,2-dibromo-alkene product (84% yield), with no α,α -dihaloketone product.

3.7. Oxidation of Sulfur-Containing Compounds

In 2017, Xu and co-workers reported a TEMPO-mediated electrochemical method for an oxidative C-S coupling reaction.²³⁹ In the presence of catalytic quantities of TEMPO, a variety of *N*-arythioamides and amino-pyridine thioamides underwent electrooxidation in good yields to give the corresponding benzothiazole and thiazolopyridine products, respectively (Scheme 91). Substrates containing primary and secondary hydroxyl groups were tolerated, presumably due to the reduced rate of aminoxyl-catalyzed alcohol oxidation under neutral conditions. On the basis of voltammetric analysis and radical clock experiments, the researchers hypothesized that electrogenerated TEMPO^+ reacts with the thiocarbonyl group of the substrate to give a S-O adduct. The bond strength of the S-O bond was calculated to be $12.5 \text{ kcal mol}^{-1}$ (Scheme 92), and homolytic cleavage of the weak S-O bond would afford TEMPO and a thioamidyl radical that could undergo radical addition to the (hetero)arene. Further oxidation and deprotonation then provides the benzothiazole or thiazolopyridine product. Direct oxidation of the substrate was noted to be unlikely due to the more positive redox potential of the thioamide relative to the TEMPO redox potential.

Fors, Lin, and co-workers recently reported the TEMPO-mediated electrochemical cationic polymerization of vinyl ethers using a dithiocarbamate chain transfer agent (CTA).²⁴⁰ Previous efforts demonstrated that upon photochemical oxidation, the dithiocarbamate CTA undergoes mesolytic cleavage to produce a propagating oxocarbenium ion and the dithiocarbamate radical. A similar strategy was exploited under electrochemical oxidation conditions. Direct oxidation of the dithiocarbamate CTA at 0.325 V vs. Fc/Fc^+ in the presence of isobutyl vinyl ether (IBVE) results in the formation of a polymer with M_n of 10.9 kg/mol, but with a relatively broad dispersity (PDI = 1.97). By adding one equivalent of TEMPO relative to the dithiocarbamate and performing the electrolysis at the same potential, a polymer with M_n of 8.4 kg/mol and a narrower dispersity (PDI = 1.23) was obtained. Constant current electrolyses allowed full conversion of the monomer units. It was found that by applying a reducing potential, the dithiocarbamate radical is reduced to the corresponding anion which quenches the cationic polymerization process. Polymer growth is reinitiated by reapplying an oxidative current, indicating the ability to exert electrochemical control over the mediated polymerization. This method is compatible with a variety of vinyl ethers. Additionally, 4-methoxystyrene undergoes polymerization under these conditions, which could not be achieved under photochemical conditions. The polymerization reaction is proposed to proceed via initial attack of TEMPO^+ by the dithiocarbamate CTA to generate

a cationic intermediate (Scheme 93). Subsequent fragmentation provides TEMPO, the dithiocarbamate radical, and the propagating cation.

4. Electrochemistry and Electrochemical Applications of Imidoxyl Derivatives

4.1. Electrochemical Properties of NHPI

Imidoxyl radicals, such as PINO, represent a second class of *N*-oxyl species and display distinct redox properties and reactivity relative to aminoxyl radicals. In 1983, Masui and co-workers demonstrated the ability to access PINO from NHPI under electrochemical conditions.³⁸ Bulk electrolysis experiments demonstrated that unlike hydroxamic acids which undergo 2 e⁻ electrochemical oxidation, NHPI undergoes 1 e⁻ oxidation to form PINO.²⁴¹ In CH₃CN, the 1 e⁻/1 H⁺ NHPI/PINO couple exhibits a redox potential of 1.44 V vs. SCE and is quasi-reversible. Addition of one or two equivalents of pyridine shifts the potential of NHPI to 0.85 V and 0.78 V, respectively, vs. SCE in CH₃CN.⁴⁴ Later studies by Kishioka probed the redox behavior of NHPI in the presence of different amounts of 2,6-lutidine in CH₃CN and corroborated the base effects on the NHPI/PINO redox couple observed by Masui (Scheme 94).²⁴² Deprotonation of NHPI under these conditions is unlikely, due to the difference between the relative p*K*_a values of NHPI and pyridine bases in CH₃CN (23.5 for NHPI and 12–16 for pyridine bases). Instead, the anodic oxidation of NHPI to PINO is best attributed to a concerted PCET process.⁸⁶

In 1987, Masui and co-workers examined the stability of PINO in the presence of excess pyridine.⁴⁴ The rate of PINO decomposition was monitored spectroelectrochemically by observing the change in absorbance at 400 nm (corresponding to the λ_{max} for PINO) upon bulk electrolysis of a solution of NHPI and subsequent stirring of the solution at open circuit (Scheme 95a). In the bulk electrolysis period, the growth in absorbance at 400 nm was nearly linear (Scheme 95a) and correlated directly with the amount of charge passed. When the electrolysis was stopped, the absorbance of the solution showed a second-order kinetic decay (Scheme 95b), and the rate constant of PINO decomposition was determined to be 24.1 M⁻¹ s⁻¹ at 25 °C. Independent studies by Espenson and co-workers monitored the decomposition of PINO (generated by oxidation of NHPI by Pb(OAc)₄ in acetic acid at 25 °C and found it to be second-order with respect to PINO. A slower rate constant was observed under these conditions (0.61 M⁻¹ s⁻¹).²⁴³ Baciocchi, Lanzalunga, and co-workers later corroborated these findings, measuring a rate constant of 0.4 M⁻¹ s⁻¹ under conditions similar to those of Espenson.²⁴⁴ They also determined second-order decomposition rate constants of 0.9, 4.0, and 0.4 M⁻¹ s⁻¹ in 1,1,1,3,3,3-hexafluoroisopropanol (HFIP), CCl₄, and CH₃CN in the presence of 1% acetic acid, respectively. Pedulli and co-workers reported evidence for first-order decay of PINO in 9:1 benzene:CH₃CN solutions.³⁴

The origin of the differences between the second-order and first-order PINO decay processes and specific mechanisms of PINO decomposition have not been fully elucidated. However, Masui identified the trimeric species **14** (Scheme 96) as the major PINO decomposition product after bulk electrooxidation of NHPI in CH₃CN.⁴⁴ This product was obtained in 71% yield, together with phthalic acid (2.5%), phthalic anhydride (8%), phthalimide (trace), and

recovered NHPI (3.5%). The rate of decomposition was not affected by the base (pyridine) concentration under these conditions. The latter observation contrasts with later results obtained in aqueous solution. Rafiee and co-workers used voltammetric studies to examine the effect of solution pH on the rates of PINO decomposition,⁶⁸ and they observed that the NHPI/PINO redox couple becomes less reversible under increasingly basic conditions (Scheme 97). They attributed this observation to a base-promoted pathway for PINO decomposition. Stahl and coworkers noted a related deleterious effect of base on the reversibility of the NHPI/PINO redox couple in their study of an electrocatalytic C-H iodination reaction (see below), which was conducted in CH₃CN solution with pyridine derivatives as the source of base.²⁴⁵ It is worth noting that, in spite of the faster rate of PINO decomposition under basic conditions, many electrosynthetic applications with NHPI as a mediator are performed in the presence of base due to the significant reduction in the potential of the proton-coupled NHPI/PINO redox process.

The electrochemical properties of structurally modified NHPI derivatives are less extensively explored relative to TEMPO derivatives and other cyclic aminoxyl species. However, it has been observed that the redox potential of NHPI is sensitive to electronically varied substituents on the phthalimide ring. Lepretre, Saint-Aman, and co-workers noted a linear correlation between substituent Hammett parameters σ and the redox potential of NHPI derivatives with a positive slope (i.e., electron-withdrawing groups shift the redox potential more positively) (Scheme 98).²⁴⁶

The electrochemical properties of *N*-hydroxysuccinimide (NHSI; Table 5, entry 2) and *N*-hydroxymaleimide (NHMI; Table 5, entry 3) exhibit redox potentials higher than NHPI under analogous conditions. In the presence of excess collidine in CH₃CN, the redox potentials of NHPI, NHMI, and NHSI are 0.69, 0.77, and 0.92 V, respectively, vs. SCE (i.e., approximately 0.93, 1.01, and 1.16 V respectively, vs. NHE).²⁴⁷ NHMI displays a less reversible redox feature compared to NHPI and NHSI, suggesting that the corresponding imidoxyl radical is less stable, possibly due to side reactions of the alkene in the backbone of NHMI in the presence of reactive radicals.²⁴⁸ A summary of the redox potentials of various *N*-hydroxyimide derivatives is shown in Table 5.^{246,247,249} It is challenging to compare redox potentials of *N*-hydroxyimide/imidoxyl redox couples obtained under different conditions because the involvement of proton transfer in this process leads to a significant dependence of the measured potential on the conditions employed. For example, the higher NHPI redox potential under aqueous conditions relative to potentials measured under non-aqueous conditions (cf. Table 5, entry 1) could be attributed to the slightly acidic conditions of the aqueous system or to stabilization of NHPI via hydrogen bonding to water.

4.2 Electrochemical Reactions Mediated by NHPI and Related Derivatives

4.2.1. Alcohol Oxidation: Synthetic and Mechanistic Considerations—The first use of NHPI as an electrochemical mediator in a preparative synthetic method was reported in 1983 by Masui and co-workers for the NHPI-mediated electrooxidation of alcohols (Scheme 99).³⁸ Secondary alcohols were oxidized by PINO at constant potential (0.85 V vs. SCE) to the corresponding ketone in excellent yields. Only low yields were obtained under the same conditions for the oxidation of primary alcohols to the corresponding aldehydes,

except for ethanol. The improved reactivity of ethanol relative to other primary alcohols was not addressed.

Mechanistic investigations of NHPI-mediated alcohol oxidation have been pursued in several reports. Masui and co-workers reported a kinetic study of the reaction of PINO-mediated oxidation of benzhydrol and observed a first-order dependence of the rate on [benzhydrol] and no dependence on the concentration of base.⁴⁴ A large deuterium isotope effect of 10.6 was obtained from independent measurement of the rates for oxidation of H- and D-substituted benzhydrol,⁴⁴ and the NHPI-mediated reaction was proposed to proceed via a rate-limiting hydrogen atom transfer (HAT) from the alcohol substrate by PINO. Subsequent conversion of the radical intermediate to the carbonyl product is expected to be facile (i.e., via sequential or concerted loss of a proton and electron) (Scheme 100).²⁵¹ Shiraishi and co-workers have proposed that cleavage of the O-H bond from the radical intermediate is also mediated by PINO,²⁵¹ but direct insights into this step are not yet available.

Masui and co-workers measured the second order rate constants for the reaction of PINO with different alcohol substrates (Table 6), and the trend in rate constants tracked with the relative C-H bond strengths. For example, benzylic alcohols exhibited the highest rates, and the primary aliphatic alcohols reacted more slowly than secondary alcohols.

In 2014, Rafiee and co-workers used voltammetric techniques to compare the catalytic activity of NHPI in the oxidation of a diverse set of alcohols under mildly acidic, aqueous conditions.⁶⁸ The acidic conditions minimized complications arising from decomposition of PINO under neutral or basic conditions. Comparison of the current for the oxidation of NHPI in the absence (i_0) and presence (i_{cat}) of substrate provided a relative measure of PINO reactivity toward substrate oxidation. As shown in Scheme 101, NHPI demonstrated higher reactivity for the oxidation of allylic and benzylic alcohols compared to aliphatic ones. No significant catalytic activity was observed for oxidation of aliphatic alcohols, except for cyclohexanol, under these conditions.

The electrochemical reactivity of other imidoxyl derivatives for alcohol oxidation have received limited attention. In 1998, Lepretre and Saint-Aman examined the redox properties of a series of substituted N-hydroxyphthalimides and the effect of the substituents on alcohol oxidation (cf. Table 5, entries 1, 4, and 9–16).²⁴⁶ It was shown that NHPI derivatives with electron-withdrawing groups displayed higher i_{cat}/i_0 for the oxidation of borneol in the presence of excess collidine. Among the various derivatives examined, the electron-deficient F₄-NHPI (Table 5, entry 13) had the highest reported redox potential in the presence of collidine (1.03 V vs. NHE) and was found to be a competent mediator for electrochemical alcohol oxidation. The i_{cat}/i_0 value for borneol oxidation by NHPI was measured to be 1.65, while that for F₄-NHPI was 2.35. Similar enhancement in reactivity was observed for cyclohexanol and 2-octanol.

4.2.2. Biomass Oxidation—The electrocatalytic activity of NHPI towards alcohol oxidation has been applied to the oxidation of biomass-derived alcohols. Imidoxyl-mediated electrooxidation of lignin, in particular, has received attention. In 2012, Shiraishi and co-

workers developed a method for the electrooxidation of lignin β -O-4 models with catalytic quantities of NHPI (Scheme 102).²⁵¹ High yields were obtained for the oxidation products. The catalytic performance of NHPI was compared to 2,2'-azinobis(3-ethylbenzothiazoline-6-sulfonate) (ABTS), a single-electron-transfer reagent. Poor yields of oxidation and cleavage products were observed with ABTS, showing that mediated single-electron oxidation of the lignin models is inefficient compared to HAT-mediated oxidation.

Stephenson and co-workers recently expanded upon Shiraishi's work by applying NHPI-catalysis to the electrooxidation of lignin β -O-4 model compounds and native lignin.²⁵² They reported excellent yields for the NHPI-mediated electrochemical oxidation of 1-(3,4-dimethoxyphenyl)ethanol to the corresponding ketone. Following electrooxidation, the crude oxidation products could then be fragmented under flow conditions using a previously reported photocatalytic method for reductive C-O bond cleavage.¹⁶⁸ This sequential oxidation-reductive cleavage method was subsequently applied to a variety of lignin β -O-4 model compounds, providing cleavage products in moderate-to-excellent yields. Native pine lignin was then subjected to the reaction conditions, and afforded oligomeric (45 wt%) and lower molecular weight units (55 wt%). The major monomeric units depicted in Scheme 103 were obtained in yields of 1.30 wt% and 1.14 wt%.

4.2.3. C-H Oxygenation—NHPI and its derivatives have been studied extensively as mediators for oxygenation of benzylic, allylic, and other activated C-H bonds. In 1983, Masui and co-workers reported the electrochemical oxygenation of simple benzylic and allylic substrates with catalytic quantities of NHPI (Scheme 104).^{39,40} The electrolyses were carried out with 20–50 mol% NHPI and excess pyridine. Though several substrates underwent successful electrolysis in an undivided cell, the majority of the bulk electrolyses were carried out in a divided cell. The oxygenation reaction is believed to be initiated by H-atom abstraction of the benzylic or allylic C-H bond by PINO (Scheme 105). Subsequent capture of the organic radical by dissolved O₂ affords an organic peroxy radical that leads to formation of the ketone product.³²

Masui later expanded upon these synthetic studies by investigating the rates of NHPI-mediated oxidation of various substrates containing benzylic and allylic C-H bonds, as well as C-H bonds with α -heteroatoms (Table 7).⁴⁴ Efforts to establish quantitative structure-activity relationships among these results were not successful, but several qualitative observations could be made. Successful reactivity with PINO required the presence of a weak C-H bond, such as those in benzylic or allylic positions or adjacent to a heteroatom; the presence of two of these structural activation features led to further rate enhancement (e.g., *kisochroman* > *ktetralin*). Cyclic substrates tend to show higher reactivity than structurally related acyclic substrates (tetrahydropyran and tetrahydrothiopyran represent exceptions), and five-membered rings are more reactive than six-membered rings.

Following the work of Masui, little attention was given to NHPI-mediated electrochemical oxygenation reactions for over 20 years. In the intervening period, however, Ishii developed numerous examples of NHPI (co)catalyzed aerobic oxidation reactions for the oxidation of hydrocarbon C-H bonds and alcohol. The addition of catalytic metal salts, such as Co(OAc)₂ or Mn(OAc)₂, led to highly effective oxidation methods, including industrial applications.

32,253–255 During the development of $\text{Co}(\text{OAc})_2/\text{NHPI}$ -catalyzed methods for C-H oxygenation of pharmaceutically relevant molecules containing heterocycles, Stahl and co-workers encountered challenges with certain substrates.²⁵⁶ The problem was speculated to arise from inhibition of the cobalt catalyst by chelation of the heterocycle, and this hypothesis prompted exploration of electrochemical PINO generation as a means to bypass the need for a metal co-catalyst. The electrolysis was performed in an undivided cell with catalytic quantities of pyridine, and improved yields of the oxygenated products were obtained for these problematic substrates under the electrochemical conditions relative to the metal-catalyzed conditions (Scheme 106).

Derivatives of NHPI have also been investigated for electrochemical oxygenation of allylic C-H bonds. Baran and co-workers examined a number *N*-hydroxy reagents and oxygen atom donors for the allylic oxygenation of diverse terpene-derived structures and other pharmaceutically-relevant molecules. The optimal conditions, which featured tetrachloro-NHPI ($\text{Cl}_4\text{-NHPI}$; Table 5, entry 11) as the mediator, *tert*-butyl hydrogen peroxide as the oxygen-atom donor, and 2 equivalents of pyridine, enabled oxidation of valencene to nootkatone **15** in 77% yield.²⁵⁷ The outcome contrasts a 6% yield of **15** when the original Masui conditions with NHPI and O_2 were employed. The use of *t*BuOOH as a soluble oxygen atom source was identified as a primary contributor to the improved conditions. The method was applied to a wide range of terpenoid, steroid, cyclohexene, and acyclic alkene and alkyne structures (Scheme 107), and it was demonstrated on 100-gram scale for several substrates.

4.2.4. Other NHPI-Mediated Electrooxidation Reactions—Masui and co-workers applied their NHPI-catalysis conditions to a variety of other oxidation reactions, including the α -oxygenation of amides and the conversion of aldehyde acetals to β - and γ -hydroxy esters.^{41–43} The oxidation of aldehyde acetal species proceeded to the desired product even when O_2 was excluded (Scheme 108). It was hypothesized that adventitious water in the solvent served as the oxygen source that trapped an intermediate oxocarbenium ion generated via HAT followed by single-electron transfer, though no further studies were conducted to validate this suggestion. The ester products could then be readily hydrolyzed to provide the corresponding carboxylic acid.

In 2017, Stahl and co-workers demonstrated the use of NHPI as an electrochemical mediator for iodination of methylarenes (Scheme 109a)²⁴⁵ representing the first electrochemical application of NHPI mediated C-H functionalization that did not form a C-O bond. As in other methods, electrochemical generation of PINO is followed by H-atom abstraction, and the resulting radical is trapped rapidly by I_2 . Benzylic iodination of a range of methylarenes was achieved, including those containing electron-rich and electron-deficient functional groups such as methoxy, phenoxy, acetyl and acetoxy groups (Scheme 109b). When pyridine/pyridinium was used as the electrolyte rather than 2,6-lutidine, the benzyl iodide product underwent in situ displacement of iodide by pyridine to afford benzyl pyridinium products (Scheme 109c). In the latter reactions, the iodide formed in the nucleophilic substitution step could undergo reoxidation at the anode, thereby allowing the use of catalytic quantities of I_2 . The iodination method was showcased in the preparation of pharmaceutical targets that used an inexpensive methylarene as an alkylating agent.

This HAT-mediated method for benzylic oxidation was compared to related electrochemical methods that are initiated by electron-transfer.²⁵⁸ Use of PINO as an HAT mediator enabled oxidation of methylarenes at electrode potentials 0.5–1.2 V lower than those required for direct electrooxidation (Scheme 110). The HAT pathway was also shown to be much less sensitive to substrate electronic effects, which provides the basis for functionalization of electronically diverse substrates.

5. Electrochemistry of Other *N*-oxyl Radicals

The sections above describe the relatively thorough characterization of cyclic aliphatic aminoxyl radicals and *N*-hydroxy imide compounds and their applications as mediators in electrochemical syntheses. Other classes of *N*-oxyl compounds have been evaluated, but they are generally not as well characterized nor have been investigated as extensively as electrocatalytic mediators.

Nitrosodisulfonate, commonly known as Frémy's salt, was discovered in 1845 by Edmond Frémy and was the first *N*-oxyl species reported in the literature (Table 8, entry 1).^{259,260} This inorganic *N*-oxyl radical has been widely used for stoichiometric selective oxidation of phenols and aromatic amines.²⁶¹ Frémy's salt is isolable and relatively stable under ambient conditions. In 1972, Aoyagui and co-workers found that nitrosodisulfonate could be generated electrochemically from the corresponding hydroxylamine.²⁶² Raspi and co-workers later investigated the redox behavior of nitrosodisulfonate and the hydroxylamine derivative under aqueous basic conditions.²⁶³ Between pH 8.5 and 12, nitrosodisulfonate was stable and displayed nearly reversible behavior on the time scale of the voltammetric studies, but was unstable under more acidic conditions. At pH of 9.8, the redox potential of the nitrosodisulfonate and the hydroxylamine was found to be 0.24 V vs. SCE (0.48 V vs. NHE). The standard redox potential of the nitrosodisulfonate and corresponding oxoammonium was calculated from the Nernst equation to be 1.36 V vs. NHE in water by Toropova and Degtyareva (Table 8, entry 1).²⁶⁴ Studies of Frémy's salt have not yet been extended beyond these fundamental studies to electrosynthetic applications.

Acyclic organic *N*-oxyl radicals are generally less stable than TEMPO and related cyclic aminoxyls, and studies of their electrochemical generation are limited.⁵⁴ For example, the oxoammonium derived from di-*tert*-butyl nitroxide (DTBO) is rather unstable, as discussed above (cf. Scheme 7).⁵⁴ Kashiwagi reported the electrochemical properties of an α -phosphonylated *N*-oxyl radical (Table 8, entry 3).²⁶⁵ The aminoxyl exhibited a reversible redox feature at 0.81 V vs Ag/AgCl (1.01 V vs. NHE) and mediated the electrooxidation of 4-methylbenzyl alcohol, yielding the corresponding aldehyde in 97% yield.

Inclusion of aromatic functional groups in conjugation with the aminoxyl radical can enhance the stability of the corresponding oxoammonium species relative to oxoammonium species with aliphatic substituents. In 2006, Nakahara and co-workers studied the electrochemical behavior of several aminoxyl radicals bearing aryl substituents (e.g., Table 8, entries 10 and 11), all of which demonstrated reversible electrochemical behavior for the aminoxyl/oxoammonium redox couple.²⁶⁶ In 2006, Scholhorn studied substituent effects on the redox potential and electrochemical behavior of *N*-*t*-butyl-*N*-aryl aminoxyl radicals by

CV in CH₃CN.²⁶⁷ The presence of an adjacent carboxylate group was shown to significantly reduce the redox potential of the aminoxyl/oxoammonium couple relative to the corresponding methyl ester (Table 8, entries 13 and 14). This effect was mitigated as the distance between the anionic and *N*-oxyl functional groups was increased (Table 8, entries 15 and 16). Schelter and co-workers later examined substituent effects on the redox potentials of substituted *N*-*t*-butyl-*N*-2-pyridylhydroxylamines (Table 8, entries 4–9).²⁶⁸ These aminoxyl species exhibited electrochemically reversible behavior for the hydroxylamine/aminoxyl and aminoxyl/oxoammonium redox couples (Scheme 111a). The anodic-to-cathodic ratio of the peak currents for the aminoxyl/oxoammonium couple approached unity for substrates bearing more electron-donating substituents *o*- or *p*- to the aminoxyl group, indicating enhanced stability of these oxoammonium species. The results also demonstrated that the aminoxyl/oxoammonium redox potential strongly depends on the electron-donating and withdrawing ability of the substituents and may be modulated by 0.95 V (Scheme 111b).

Hydroxyamic acids (i.e., *N*-hydroxy amides) and related *N*-hydroxy derivatives have received limited attention in the electrochemistry literature and have not been used effectively as mediators in electro synthetic applications. In 1977, Masui and co-workers examined the electrochemical oxidation of hydroxamic acids (Scheme 112).²⁴¹ Voltammetric analysis of a range of derivatives displayed irreversible CVs with only anodic peaks observed. Bulk electrooxidation of the hydroxamic acids was reported to generate the corresponding carboxylic acids together with nitrous oxide or organic nitroso compounds.

Many hydroxamic acid species and related *N*-hydroxy derivatives have been investigated as potential mediators for laccase-catalyzed oxidation of lignin and lignin models. Laccases are copper-containing oxidase enzymes that are involved in the biosynthesis and degradation of lignin, and they have also been investigated as catalysts in chemical approaches to lignin decomposition.^{269–271} The use of redox mediators has been shown to enhance the effectiveness of laccase-catalyzed aerobic oxidation of alcohols and other substrates (Scheme 113).²⁷² The rate of mediator oxidation by laccases depends, in part, on the redox potential of the mediator such that high potential mediators are more slowly oxidized.^{250,273} The electrochemical properties of various *N*-hydroxy compounds have therefore been explored.^{247,250,273,274} Tables 9 and 10 summarize the reported redox potentials for these *N*-hydroxy derivatives.

In 2001, Xu and co-workers reported redox potentials for an extensive series of *N*-hydroxyacetanilide (Table 9) and 1-hydroxybenzotriazole (Table 10, entries 5–7) derivatives.²⁵⁰ Over 30 derivatives were studied, and electronic and steric effects of the substituents were investigated. Derivatives with electron-withdrawing substituents exhibited higher redox potentials. Comparison of the anodic-to-cathodic peak currents demonstrated the *N*-oxyl species bearing *N*-aryl or *N*-carbonyl groups are more stable than those bearing *N*-alkyl groups, presumably due to enhanced stabilization of the radical through conjugation. *N*-azo substitution (cf. Table 9, entry 13 and Table 10, entries 5–7) resulted in a less stable *N*-oxyl species. In 2009, Falcón and co-workers assessed the catalytic efficiency of TEMPO, NHPI and selected *N*-hydroxy compounds (e.g., entries 1 and 5 in Table 10) for laccase-catalyzed oxidation of kraft lignin and veratryl alcohol (3,4-dimethoxybenzyl alcohol), a non-phenolic

lignin model.²⁷⁴ As a test for catalytic activity, voltammetry studies in the absence of laccase were conducted with individual mediators. CV studies in the presence and absence of veratryl alcohol or lignin provided anodic peak current ratios (i_{cat}/i_0). With veratryl alcohol, NHPI and 1-hydroxybenzotriazole (Table 10, entry 5) displayed the largest i_{cat}/i_0 ratio, indicating that these mediators exhibited the highest electrocatalytic activity. The observed electrochemical reactivity of these mediators did not correlate with the effectiveness of their reactivity under aerobic, laccase-catalyzed oxidation conditions. In 2005, Galli and co-workers had shown that NHPI and 1-hydroxybenzotriazole mediators were less effective in laccase-catalyzed aerobic oxidation of 4-methoxybenzyl alcohol relative to TEMPO and violuric acid (Table 10, entry 1).²⁷³ This difference in relative performance under the electrocatalytic and laccase-catalyzed conditions may be rationalized as follows: the higher-potential mediators (NHPI and 1-hydroxybenzotriazole) exhibit higher intrinsic reactivity for alcohol oxidation, and undergo efficient regeneration under electrochemical conditions because the electrode potential may be tuned to the potential of the mediator; laccase, however, does not operate at sufficiently high potentials to promote efficient reoxidation of the high-potential mediators. While lower-potential mediators (TEMPO and violuric acid) are less reactive catalysts for alcohol oxidation, their effectiveness in the laccase-catalyzed reactions in the studies by Falcón and Galli reflects the ability of laccase to promote their reoxidation.

6. Conclusions and Outlook

The electrochemical properties of aminoxyls, imidoxyls and related *N*-oxyl radicals have been the focus of considerable study, as elaborated throughout this review. These studies have led to considerable understanding of the effect of substituents, structure, and reaction conditions on the redox behavior of these species and their reactivity with organic molecules. Oxidation of aminoxyls, such as TEMPO, generates oxoammonium species that commonly promote hydride transfer from organic molecules, such as alcohols and amines, to afford the hydroxylamine. Other reaction pathways have also been identified, including those involving the hydroxylamine/aminoxyl and aminoxyl/oxoammonium redox couples. Oxidation of *N*-hydroxyimides, such as NHPI, generates imidoxyl species that promote the abstraction of hydrogen atoms from C-H bonds of many organic molecules. This method for the generation of carbon-centered radicals in the absence of stoichiometric chemical oxidants provides a versatile strategy for the functionalization of organic molecules. Collectively, aminoxyl- and imidoxyl-mediated processes have led to a number of synthetically useful electrochemical oxidation reactions, with applications ranging from pharmaceutical synthesis to biomass conversion. The use of electrochemical methods to (re)generate the oxidized mediator provides a compelling alternative to the use of stoichiometric chemical oxidants. Advantages include the ability to tune the electrode to any applied potential, thereby enabling efficient reoxidation of mediators, including high-potential derivatives that are difficult to regenerate with chemical oxidants. These mediated electrochemical reactions can lead to improved functional group compatibility in chemical reactions by avoiding side reactions caused by strong stoichiometric oxidants. In addition, they offer a potentially “greener” approach to achieve selective oxidation reactions on larger scale. Indeed, the successful implementation of *N*-oxyl catalyst systems with chemical

oxidants in commercial applications^{255,275–277} and direct electrochemical oxidation reactions in industrial settings²⁷⁸ portend the successful application of electrochemical *N*-oxyl-catalyzed reactions beyond the lab scale syntheses presented herein.

New electrochemical processes will undoubtedly continue to emerge from the development of novel reactions and synthetic applications employing *N*-oxyl mediators. These efforts would benefit from increased attention directed toward the design of mediators that show increased stability. For example, the limited lifetime of PINO and related imidoxyl mediators limits the scope of accessible oxidation reactions to molecules bearing particularly reactive C-H bonds. Identification of structural changes that enhance the stability, tune the redox properties, and/or modulate the O-H bond strength of these compounds could have a major impact on this field. Such efforts could include the identification of new classes of *N*-oxyl or related radical mediators that enable other electrosynthetic reactions. Fundamental characterization of such structures, similar to the work described above with TEMPO and PINO, will provide a foundation for such applications. As the methodological studies continue to grow, additional efforts will undoubtedly be directed toward the development of improved process conditions for large-scale applications that allow the “green chemistry” opportunities of these methods to be realized.

Acknowledgements

Our work in this field has been supported financially by the Center for Molecular Electrocatalysis, as an Energy Frontier Research Center funded by the U.S. Department of Energy, Office of Science, Office of Basic Energy Sciences; the NIH (R01 GM100143); and the Great Lakes Bioenergy Research Center (DOE BER Office of Science DE-FC02-07ER64494).

Biography

Jordan Nutting obtained her B.A. degree in Chemistry from Ripon College in 2015. She conducted research during the summers of 2013 and 2014 in the groups of Prof. Shannon S. Stahl at the University of Wisconsin-Madison and Prof. Steven R. Kass at the University of Minnesota, respectively. In 2015, she returned to the University of Wisconsin-Madison to pursue her doctoral studies in organic chemistry. Her graduate work focuses on the development of mediated electrochemical reactions.

Mohammad Rafiee was born in 1979 and raised in Iran. In 2001, he earned his B.A. degree in chemistry from Bu-Ali Sina University, Hamadan, where he became intrigued with the use of electrons as “simple chemical reagents” to catalyze organic reactions. He then pursued his graduate studies at Bu-Ali Sina University under the supervision of Prof. D. Nematollahi, where his doctoral work focused on electrochemical synthesis and molecular electrochemistry. In 2008, he started an independent academic career at the Institute for Advanced Studies in Basic Sciences (IASBS) focusing on the development of electrodes modified with mediators for electrosynthetic applications. In 2014, he joined the Stahl group as a research scientist at the University of Wisconsin-Madison and is pursuing collaborative studies on mediated electrochemical reactions and electrosynthesis.

Shannon S. Stahl was an undergraduate at the University of Illinois at Urbana-Champaign, and a graduate student at Caltech (PhD, 1997), where he worked with Professor John

Bercaw. He was an NSF postdoctoral fellow with Professor Stephen Lippard at Massachusetts Institute of Technology from 1997–1999. He is currently a Professor of Chemistry at the University of Wisconsin-Madison, where he began his independent career in 1999. His research group specializes in catalysis, with an emphasis on the catalytic chemistry of molecular oxygen and aerobic oxidation reactions and electrocatalytic reactions related to chemical synthesis and energy conversion.

Abbreviations

ABNO	9-Azabicyclo[3.3.1]nonane <i>N</i> -oxyl
ABTS	2,2'-Azinobis(3-ethylbenzothiazoline-6-sulfonate)
Ac	Acetyl
AZADO	2-Azaadamantane <i>N</i> -oxyl
BHT	2,6-Di- <i>t</i> -butyl-4-methyl phenol
bpy	2,2'-Bipyridine
Bz	Benzoyl
CTA	Chain transfer agent
CV	Cyclic voltammogram
DFF	2,5-Diformylfuran
DHA	1,3-Dihydroxyacetone
DTBO	Di- <i>tert</i> -butyl nitroxide
E^0	Standard redox potential
$E_{1/2}$	Half wave potential
EASA	Electro-assisted self-assembly
EC'	Catalytic electrochemical-chemical
E_g	Pauling group electronegativity
E_{pa}	Anodic peak potential
E_{pc}	Cathodic peak potential
EPR	Electron paramagnetic resonance
ESR	Electron spin resonance
FDCA	2,5-Furandicarboxylic acid
GC	Glassy carbon

HAT	Hydrogen atom transfer
HMDS	Hexamethyldisilylazane
HMF	5-Hydroxymethylfurfural
<i>I</i>	Current
<i>i</i>₀	Current of electrochemical mediator in absence of substrate
<i>i</i>_{cat}	Current of electrochemical mediator in presence of substrate
<i>i</i>_{pa}	Anodic peak current
<i>i</i>_{pc}	Cathodic peak current
IBVE	Isobutyl vinyl ether
<i>j</i>	Current Density
<i>k</i>⁰	Rate of electron transfer at electrode surface
MeOH	Methanol
MWCNT	Multi-walled carbon nanotubes
NHE	Normal Hydrogen Electrode
NHMI	<i>N</i> -Hydroxymaleimide
NHPI	<i>N</i> -Hydroxyphthalimide
NHSI	<i>N</i> -Hydroxysuccinimide
OTf	Trifluoromethanesulfonate
PAA	Poly(acrylic acid)
PCET	Proton-coupled electron transfer
Ph	Phenyl
PhCD₂OH	Benzyl alcohol- α,α -d ₂
PhCH₂OH	Benzyl alcohol
PINO	phthalimide <i>N</i> -oxyl
PROXYL	2,2,5,5-Tetramethylpyrrolidine <i>N</i> -oxyl
<i>p</i>-TSA	<i>para</i> -Toluenesulfonic acid
RDE	Rotating disk electrode
RVC	Reticulated vitreous carbon
SCE	Saturated calomel electrode

<i>t</i>BuOOH	<i>tert</i> -Butylhydrogenperoxide
TEMPO	2,2,6,6-Tetramethylpiperidine <i>N</i> -oxyl
TOF	Turnover frequency
TON	Turnover Number

References

1. Keana JFW Newer Aspects of the Synthesis and Chemistry of Nitroxide Spin Labels. *Chem. Rev.* 1978, 78, 37–64.
2. Mitchell JB; Samuni A; Krishna MC; DeGraff WG; Ahn MS; Samuni U; Russo A Biologically Active Metal-Independent Superoxide Dimutase Mimics. *Biochemistry* 1990, 29, 2802–2807. [PubMed: 2161256]
3. Nilsson UA; Olsson L-I; Carlin G; Bylund-Fellenius A-C Inhibition of Lipid Peroxidation by Spin Labels. *J. Biol. Chem* 1989, 264, 11131–11135. [PubMed: 2738061]
4. Lafon-Cazal M; Pietri S; Culcasi M; Bockaert J NMDA-Dependent Superoxide Production and Neurotoxicity. *Nature* 1993, 364, 535–537. [PubMed: 7687749]
5. Kato F; Kikuchi A; Okuyama T; Oyaizu K; Nishide H Nitroxide Radicals as Highly Reactive Redox Mediators in Dye-Sensitized Solar Cells. *Angew. Chem., Int. Ed* 2012, 51, 10177–10180.
6. Bergner BJ; Schurmann A; Peppler K; Garsuch A; Janek J TEMPO: A Mobile Catalyst for Rechargeable Li-O₂ Batteries. *J. Am. Chem. Soc* 2014, 136, 15054–15064. [PubMed: 25255228]
7. Janoschka T; Martin N; Hager MD; Schubert US An Aqueous Redox-Flow Battery with High Capacity and Power: The TEMPTMA/MV System. *Angew. Chem., Int. Ed* 2016, 55, 14427–14430.
8. Zhang Z; Chen P; Murakami TN; Zakeeruddin SM; Gratzel M The 2,2,6,6-Tetramethyl-1-piperidinyloxy Radical: An Efficient, Iodine-Free Redox Mediator for Dye-Sensitized Solar Cells. *Adv. Funct. Mater* 2008, 18, 341–346.
9. Bergner BJ; Schurmann A; Peppler K; Garsuch A; Janek J TEMPO: A Mobile Catalyst for Rechargeable Li-O₂ Batteries. *J. Am. Chem. Soc* 2014, 136, 15054–15064. [PubMed: 25255228]
10. Bergner BJ; Hofmann C; Schurmann A; Schroder D; Peppler K; Schreiner PR; Janek J Understanding the Fundamentals of Redox Mediators in Li-O₂ Batteries: A Case Study on Nitroxides. *Phys. Chem. Chem. Phys* 2015, 17, 31769–31779. [PubMed: 26563563]
11. Tebben L; Studer A Nitroxides: Applications in Synthesis and in Polymer Chemistry. *Angew. Chem., Int. Ed* 2011, 50, 5034–5068.
12. Bobbitt JM; Brückner C; Merboub N Oxoammonium- and Nitroxide-Catalyzed Oxidations of Alcohols In *Organic Reactions*; Wiley: Hoboken, 2009; pp 103–424.
13. Wieland H; Offenbacher M Diphenylstickstoffoxyd, ein Neues Organisches Radikal mit Vierwertigem Stickstoff. *Ber. Dtsch. Chem. Ges* 1914, 47, 2111–2115.
14. Lebedev OL; Kazarnovskii SN Catalytic Oxidation of Aliphatic Amines with Hydrogen Peroxide. *Zh. Obshch. Khim* 1960, 30, 1631–1635.
15. Hoffman AK; Henderson AT A New Stable Free Radical: Di-*t*-Butylnitroxide. *J. Am. Chem. Soc* 1961, 83, 4671–4672.
16. Bowman DF; Gillan T; Ingold KU Kinetic Applications of Electron Paramagnetic Resonance Spectroscopy. III. Self-Reactions of Dialkyl Nitroxide Radicals. *J. Am. Chem. Soc* 1971, 93, 6555–6561.
17. For a more uniform presentation of redox potentials, reported values are normalized with respect to the normal hydrogen electrode (NHE). Conversions are based on values reported in the following references 18 and 19.
18. Pavlishchuk VV; Addison AW Conversion constants for redox potentials measured versus different reference electrodes in acetonitrile solutions at 25 °C. *Inorg. Chim. Acta* 2000, 298, 97–102.
19. Smith TJ; Stevenson KJ Reference Electrodes In *Handbook of Electrochemistry*; Zoski CG, Eds. Elsevier: Amestrdam, 2007; pp 75–76.

20. Golubev VA; Rozantsev EG; Neiman MB Some Reactions of Free Iminoxyl Radicals with the Participation of the Unpaired Electron. *Bull. Acad. Sci. USSR, Chem. Ser.*, 1965, 14, 1898–1904.
21. Sheldon RA; Arends IWCE Organocatalytic Oxidations Mediated by Nitroxyl Radicals. *Adv. Synth. Catal* 2004, 346, 1051–1071.
22. Vogler T; Studer A Applications of TEMPO in Synthesis. *Synthesis* 2008, 1979–1993.
23. Wertz S; Studer A Nitroxide-Catalyzed Transition-Metal-Free Aerobic Oxidation Processes. *Green Chem* 2013, 15, 3116–3134.
24. Anelli PL; Biffi C; Montanari F; Quici S Fast and Selective Oxidation of Primary Alcohols to Aldehydes or to Carboxylic Acids and of Secondary Alcohols to Ketones Mediated by Oxoammonium Salts under Two-Phase Conditions. *J. Org. Chem* 1987, 52, 2559–2562.
25. Mei Z-W; Omote T; Mansour M; Kawafuchi H; Takaguchi T; Jutand A; Tsuboi S; Inokuchi T A High Performance Oxidation Method for Secondary Alcohols by Inductive Activation of TEMPO in Combination with Pyridine-Bromine Complexes. *Tetrahedron* 2008, 64, 10761–10766.
26. He X; Shen Z; Mo W; Sun N; Hu B; Hu X TEMPO-tert-Butyl Nitrite: An Efficient Catalytic System for Aerobic Oxidation of Alcohols. *Adv. Synth. Catal* 2009, 351, 89–92.
27. De Mico A; Margarita R; Parlanti L; Vescovi A; Piancatelli G A Versatile and Highly Selective Hypervalent Iodine (III)/2,2,6,6-Tetramethyl-1-piperidinyloxy-Mediated Oxidation of Alcohols to Carbonyl Compounds. *J. Org. Chem* 1997, 62, 6974–6977.
28. de Nooy AEJ; Besemer AC; van Bekkum H On the Use of Stable Organic Nitroxyl Radicals for the Oxidation of Primary and Secondary Alcohols. *Synthesis* 1996, 1153–1174.
29. Caron S; Dugger RW; Ruggeri SG; Ragan JA; Ripin DHB Large Scale Oxidations in the Pharmaceutical Industry. *Chem. Rev* 2006, 106, 2943–2989. [PubMed: 16836305]
30. Ciriminna R; Pagliaro M Industrial Oxidations with Organocatalyst TEMPO and Its Derivatives. *Org. Process Res. Dev* 2010, 14, 245–251.
31. Ishii Y; Sakaguchi S A New Strategy for Alkane Oxidation with O₂ Using *N*-Hydroxyphthalimide (NHPI) as a Radical Catalyst. *Catal. Surv. from Asia* 1999, 3, 27–35.
32. Recupero F; Punta F Free Radical Functionalization of Organic Compounds Catalyzed by *N*-Hydroxyphthalimide. *Chem. Rev* 2007, 107, 3800–3842. [PubMed: 17848093]
33. Galli C; Gentili P; Lanzalunga O Hydrogen Abstraction and Electron Transfer with Aminoxyl Radicals: Synthetic and Mechanistic Issues. *Angew. Chem., Int. Ed* 2008, 47, 4790–4796.
34. Amorati R; Lucarini M; Mugnaini V; Pedulli GF; Minisci F; Recupero F; Fontana F; Astolfi P; Greci L Hydroxylamines as Oxidation Catalysts: Thermochemical and Kinetic Studies. *J. Org. Chem* 2003, 68, 1747–1754. [PubMed: 12608787]
35. Mahony LR; Mendenhall GD; Ingold KU Calorimetric and Equilibrium Studies on Some Stable Nitroxide and Iminoxyl Radicals. Approximate O-H Bond Dissociation Energies in Hydroxylamines and Oximes. *J. Am. Chem. Soc* 1973, 95, 8610–8614.
36. Bordwell FG; Liu W-Z Solvent Effects on Homolytic Bond Dissociation Energies of Hydroxylic Acids. *J. Am. Chem. Soc* 1996, 118, 10819–10823.
37. Grochowski E; Boleslawska T; Jurczak J Reactions of Diethyl Azodicarboxylate with Ethers in the Presence of *N*-Hydroxyimides as Catalysts. *Synthesis* 1977, 718–720.
38. Masui M; Ueshima T; Ozaki S *N*-Hydroxyphthalimide as an Effective Mediator for the Oxidation of Alcohols by Electrolysis. *J. Chem. Soc., Chem. Commun* 1983, 479–480.
39. Masui M; Hara S; Ueshima T; Kawaguchi T; Ozaki S Anodic Oxidation of Compounds Having Benzylic or Allylic Carbon and α -Carbon to Hetero Atom Using *N*-Hydroxyphthalimide as a Mediator. *Chem. Pharm. Bull* 1983, 31, 4209–4211.
40. Masui M; Hosomi K; Tsuchida K; Ozaki S Electrochemical Oxidation of Olefins Using *N*-Hydroxyphthalimide as a Mediator. *Chem. Pharm. Bull* 1985, 33, 4798–4802.
41. Masui M; Kawaguchi T; Ozaki S A Simple and Effective Electrocatalytic Deprotection of the 4-Phenyl-1,3-dioxolane Protecting Group. *J. Chem. Soc., Chem. Commun* 1985, 1484–1485.
42. Masui M; Kawaguchi T; Yoshida S; Ozaki S A Simple Electrochemical Oxidation of Aldehyde Acetals to Esters in Neutral Solution. *Chem. Pharm. Bull* 1986, 34, 1837–1839.
43. Masui M; Hara S; Ozaki S Anodic Oxidation of Amides and Lactams Using *N*-Hydroxyphthalimide as a Mediator. *Chem. Pharm. Bull* 1986, 34, 975–979.

44. Ueda C; Noyama M; Ohmori H; Masui M Reactivity of Phthalimide-*N*-oxyl: A Kinetic Study. *Chem. Pharm. Bull* 1987, 35, 1372–1377.
45. Ishii Y; Nakayama K; Tkeno M; Sakaguchi S; Iwahama T; Nishiyama Y A Novel Catalysis of *N*-Hydroxyphthalimide in the Oxidation of Organic Substrates by Molecular Oxygen. *J. Org. Chem* 1995, 60, 3934–3935.
46. Yoshino Y; Hayashi Y; Iwahama T; Sakaguchi S; Ishii Y Catalytic Oxidation of Alkylbenzenes with Molecular Oxygen under Normal Pressure and Temperature by *N*-Hydroxyphthalimide Combined with Co(OAc)₂. *J. Org. Chem* 1997, 62, 6810–6813.
47. Fukuda O; Sakaguchi S; Ishii Y Preparation of Hydroperoxides by *N*-Hydroxyphthalimide-Catalyzed Aerobic Oxidation of Alkylbenzenes and Hydroaromatic Compounds and Its Application. *Adv. Synth. Catal* 2001, 343, 809–813.
48. Steckhan E Indirect Electroorganic Syntheses- A Modern Chapter of Organic Electrochemistry. *Angew. Chem., Int. Ed* 1986, 25, 683–701
49. Steckhan E Organic Syntheses with Electrochemically Regenerable Redox Systems. *Top. Curr. Chem* 1987, 142, 1–69.
50. Ogibin YN; Elinson MN; Nikishin GI Mediator Oxidation Systems in Organic Electrosynthesis. *Russ. Chem. Rev* 2009, 7S, 89–140.
51. Francke R; Little RD Redox Catalysis in Organic Electrosynthesis: Basic Principles and Recent Developments. *Chem. Soc. Rev* 2014, 43, 2492–2521. [PubMed: 24500279]
52. Ciriminna R; Palmisano G; Pagliaro M Electrodes Functionalized with the 2,2,6,6-Tetramethylpiperidinyloxy Radical for the Waste-Free Oxidation of Alcohols. *Chem. Cat. Chem* 2015, 7, 552–558.
53. Ciriminna R; Ghahremani M; Karimi B; Pagliaro M Electrochemical Alcohol Oxidation Mediated by TEMPO-like Nitroxyl Radicals. *ChemistryOpen* 2017, 6, 5–10. [PubMed: 28168142]
54. Tsunaga M; Iwakura C; Tamura H Electrode Reactions of Nitroxide Radicals at Platinum in Acetonitrile. *Electrochim. Acta* 1973, 18, 241–245.
55. Khalafi L; Rafiee M Cyclic Voltammetry In Encyclopedia of Physical Organic Chemistry; Wang Z, Ed.; Wiley: Hoboken, 2017; Vol. 5, pp. 3437–3478.
56. Pletcher D; Greff R; Peat R; Peter LM; Robinson J Instrumental Methods in Electrochemistry, 1st Ed.; Woodhead Publishing: Cambridge, 2001.
57. Bard AJ; Faulkner LR Electrochemical Methods: Fundamentals and Applications; Wiley: Hoboken, 2002.
58. Fish JR; Swarts SG; Sevilla MD; Malinski T Electrochemistry and Spectroelectrochemistry of Nitroxyl Free Radicals. *J. Phys. Chem* 1988, 92, 3745–3751.
59. Kato Y; Shimizu Y; Yijing L; Unoura K; Utsumi H; Ogata T Reversible Half-Wave Potentials of Reduction Processes on Nitroxide Radicals. *Electrochim. Acta* 1995, 40, 2799–2802.
60. Hickey DP; Schiedler DA; Matanovic I; Doan PV; Atanassov P; Minter SD; Sigman MS Predicting Electrocatalytic Properties: Modelling Structure-Activity Relationships of Nitroxyl Radicals. *J. Am. Chem. Soc* 2015, 137, 16179–16186. [PubMed: 26635089]
61. Israeli A; Patt M; Oron M; Samuni A; Kohen R; Goldstein S Kinetics and Mechanism of the Comproportionation Reaction Between Oxoammonium Cation and Hydroxylamine Derived from Cyclic Nitroxides. *Free Radical Bio. Med* 2005, 38, 317–324. [PubMed: 15629861]
62. Kato and co-workers report a 4-OH-TEMPO pK_a of 5.18 which lies outside the typical range of pK_a values reported for TEMPO-derived hydroxylamine species. See ref. 59.
63. Gerken JB; Pang YQ; Lauber MB; Stahl SS Structural Effects on the pH-Dependent Redox Properties of Organic Nitroxyls: Pourbaix Diagrams for TEMPO, ABNO and Three TEMPO Analogs. *J. Org. Chem*, 2018, in press.
64. Sen VD; Golubev VA Kinetics and Mechanism for Acid-Catalyzed Disproportionation of 2,2,6,6-Tetramethylpiperidine-1-oxyl. *J. Phys. Org. Chem* 2009, 22, 138–143.
65. Asmus K-D; Nigman S; Wilson RL Kinetics of Nitroxyl Radical Reactions. A PulseRadiolysis Conductivity Study. *Int. J. Radiat. Biol. Relat. Stud. Phys. Chem. Med* 1976, 29, 211–219. [PubMed: 1083844]

66. Janiszewska AM; Grzeszczuk M Mechanistic - Kinetic Scheme of Oxidation/Reduction of TEMPO Involving Hydrogen Bonded Dimer. RDE Probe for Availability of Protons in Reaction Environment. *Electroanalysis* 2004, 16, 1673–1681.
67. Kishioka S-y.; Ohsaka T; Tokuda K Electrochemical Studies of Acid-Promoted Disproportionation of Nitroxyl Radical. *Electrochim. Acta* 2003, 48, 1589–1594.
68. Rafiee M; Karimi B; Alizadeh S Mechanistic Study of the Electrocatalytic Oxidation of Alcohols by TEMPO and NHPI. *ChemElectroChem* 2014, 1, 455–462.
69. Green RA; Hill-Cousins JT; Brown RCD; Pletcher D; Leach SG A Voltammetric Study of the 2,2,6,6-Tetramethylpiperidin-1-oxyl (TEMPO) Mediated Oxidation of Benzyl Alcohol in *tert*-Butanol/Water. *Electrochim. Acta* 2013, 113, 550–556.
70. Kishioka S.-y.; Umeda M; Yamada A Effect of Oxygen on the Electrochemical Reduction of Nitroxyl Radical: Interpretation of the Mechanism for a Redox Probe in Biological Systems. *Anal. Sci* 2002, 18, 1379–1381.
71. For review see: McCreery RL Advanced Carbon Electrode Materials for Molecular Electrochemistry. *Chem. Rev* 2008, 108, 2646–2687.
72. Summermann W; Deffner U The Electrochemical Oxidation of Aliphatic Nitroxyl Radicals. *Tetrahedron* 1975, 31, 593–596.
73. Rafiee M; Miles KC; Stahl SS Electrocatalytic Alcohol Oxidation with TEMPO and Bicyclic Nitroxyl Derivatives: Driving Force Trumps Steric Effects. *J. Am. Chem. Soc* 2015, 137, 14751–14757. [PubMed: 26505317]
74. Manda S; Nakanishi I; Ohkubo K; Yakumaru H; Matsumoto K.-i.; Ozawa T; Ikota N; Fukuzumi S; Anzai K Nitroxyl Radicals: Electrochemical Redox Behavior and Structure-Activity Relationships. *Org. Biomol. Chem* 2007, 5, 3951–3955. [PubMed: 18043799]
75. Shibuya M; Pichierri F; Tomizawa M; Nagasawa S; Suzuki I; Iwabuchi Y Oxidation of Nitroxyl Radicals: Electrochemical and Computational Studies. *Tetrahedron Lett* 2012, 53, 2070–2073.
76. Hamada S; Furuta T; Wada Y; Kawabata T Chemoselective Oxidation by Electronically Tuned Nitroxyl Radical Catalysts. *Angew. Chem., Int. Ed* 2013, 52, 8093–8097.
77. Chabita K; Mandal PC Electrochemical Oxidation and Reduction of Nitroxides: A Cyclic Voltammetric and Simulation Study. *Indian J. Chem* 2002, 41A, 2231–2237.
78. Blinco JP; Hodgson JL; Morrow BJ; Walker JR; Will GD; Coote ML; Bottle SE Experimental and Theoretical Studies of the Redox Potentials of Cyclic Nitroxides. *J. Org. Chem* 2008, 73, 6763–6771. [PubMed: 18683980]
79. Goldstein S; Samuni A; Hideg K; Merenyi G Structure-Activity Relationship of Cyclic Nitroxides as SOD Mimics and Scavengers of Nitrogen Dioxide and Carbonate Radicals. *J. Phys. Chem. A* 2006, 110, 3679–3685. [PubMed: 16526651]
80. Mendkovich AS; Luzhkov VB; Syroeshin MA; Sen VD; Khartsii DI; Rusakov AI Influence of the Nature of Solvent and Substituents on the Oxidation Potential of 2,2,6,6-Tetramethylpiperidine 1-Oxyl Derivatives. *Russ. Chem. Bull. Int. Ed* 2017, 66, 684–689.
81. Martinez JJ; Krzyczmonik P; Scholl H; Grabowski G Electrode Reactions of Nitroxide Radicals. IX. Anodic Oxidations of 4-Hydroxyimino-2,2,6,6-tetramethylpiperidine-1-oxyl and 4-[(Aminocarbonyl)-hydrazone]-2,2,6,6-tetramethylpiperidine-1-oxyl in Water Solutions. *Electroanal* 1991, 3, 233–237.
82. Golubev VA; Sen VD Mechanism of Autoreduction of 2,2,6,6-Tetramethyl-1,4-dioxopiperidinium Cation in Alkaline Medium. *Russ. J. Org. Chem* 2011, 47, 869–876.
83. Nilsen A; Braslau R Nitroxide Decomposition: Implications toward Nitroxide Design for Applications in Living Free-Radical Polymerization. *J. Polym. Sci. Part A: Polym. Chem* 2006, 44, 697–717.
84. Morris S; Sosnovsky G; Hui B; Huber CO; Rao NU; Swartz HM Chemical and Electrochemical Reduction Rates of Cyclic Nitroxides (Nitroxyls). *J. Pharm. Sci* 1991, 80, 149–152. [PubMed: 2051318]
85. Huynh MVH; Meyer TJ Proton-Coupled Electron Transfer. *Chem. Rev* 2007, 107, 5004–5064. [PubMed: 17999556]
86. Warren JJ; Tronic TA; Mayer JM The Thermochemistry of Proton-Coupled Electron Transfer Reagents and its Implications. *Chem. Rev* 2010, 110, 6961–7001. [PubMed: 20925411]

87. Rychnovsky SD; Vaidyanathan R; Beauchamp T; Lin R; Farmer PJ AM1-SM2 Calculations Model the Redox Properties of Nitroxyl Radicals Such as TEMPO. *J. Org. Chem* 1999, 64, 6745–6749. [PubMed: 11674681]
88. Hodgson JL; Namazian M; Bottle SE; Coote ML One-Electron Oxidation and Reduction Potentials of Nitroxide Antioxidants: A Theoretical Study. *J. Phys. Chem. A* 2007, 111, 13595–13605. [PubMed: 18052257]
89. Semmelhack MF; Chou CS; Cortes DA Nitroxyl-Mediated Electrooxidation of Alcohols to Aldehydes and Ketones. *J. Am. Chem. Soc* 1983, 105, 4492–4494.
90. Semmelhack MF; Schmid CR; Cortés DA Mechanism of the Oxidation of Alcohols by 2,2,6,6-Tetramethylpiperidine Nitrosonium Cation. *Tetrahedron Lett* 1986, 27, 1119–1122.
91. Kishioka S-y.; Ohsaka T; Tokuda K Spectroelectrochemical Detection of an Intermediate in the Alcohol Oxidation Process with a Nitroxyl Radical. *Chem. Lett* 1998, 343–344.
92. Liaigre D; Breton T; Belgsir EM Kinetic and Selectivity Control of TEMPO ElectroMediated Oxidation of Alcohols. *Electrochem. Commun* 2005, 7, 312–316.
93. Bailey WF; Bobbitt JM; Wiberg KB Mechanism of the Oxidation of Alcohols by Oxoammonium Cations. *J. Org. Chem* 2007, 72, 4504–4509. [PubMed: 17488040]
94. Bobbitt JM; Bartelson AL; Bailey WF; Hamlin TA; Kelly CB Oxoammonium Salt Oxidations of Alcohols in the Presence of Pyridine Bases. *J. Org. Chem* 2014, 79, 1055–1067. [PubMed: 24386938]
95. Michel C; Belanzoni P; Gamez J; Reedijk J; Baerends EJ Activation of the C-H Bond by Electrophilic Attack: Theoretical Study of the Reaction Mechanism of the Aerobic Oxidation of Alcohols to Aldehydes by the Cu(bipy)²⁺/2,2,6,6-Tetramethylpiperidyl-1-oxy Cocatalyst System. *Inorg. Chem* 2009, 48, 11909–11920.
96. Golubev VA; Borislavskii VN; Aleksandrov AL Mechanism of Oxidation of Primary and Secondary Alcohols by Oxopiperdinium Salts. *Bull. Akad. Sci. USSR. Div. Chem. Sci* 1977, 1874–1881.
97. Yamauchi Y; Maeda H; Ohmori H Amperometric Detection of Alcohols and Carbohydrates Coupled with Their Electrocatalytic Oxidation by 2,2,6,6-Tetramethylpiperidyl-1-oxy (TEMPO). *Chem. Pharm. Bull* 1996, 44, 1021–1025.
98. Savéant J-M Elements of Molecular and Biomolecular Electrochemistry: An Electrochemical Approach to Electron Transfer Chemistry; Wiley: Hoboken, 2006.
99. Hill-Cousins JT; Kuleshova J; Green RA; Birkin PR; Pletcher D; Underwood TJ; Leach SG; Brown RC D. TEMPO-Mediated Electrooxidation of Primary and Secondary Alcohols in a Microfluidic Electrolytic Cell. *ChemSusChem* 2012, 5, 326–331.
100. Nicholson RS; Shain I Theory of Stationary Electrode Polarography. Single Scan and Cyclic Methods Applied to Reversible, Irreversible, and Kinetic Systems. *Anal. Chem* 1964, 36, 706–723.
101. Badalyan A; Stahl SS Cooperative Electrocatalytic Alcohol Oxidation with Electron-Proton-Transfer Mediators. *Nature* 2016, 535, 406–410. [PubMed: 27350245]
102. Ahn SD; Fisher AC; Buchard A; Bull SD; Bond AM; Marken F Hydrodynamic Rocking Disc Electrode Study of the TEMPO-mediated Catalytic Oxidation of Primary Alcohols. *Electroanal* 2016, 28, 2093–2103.
103. Comminges C; Barhdadi R; Doherty AP; O'Toole S; Troupel M Mechanism of 2,2,6,6'-Tetramethylpiperidin-*N*-oxyl-Mediated Oxidation of Alcohols in Ionic Liquids. *J. Phys. Chem. A* 2008, 112, 7848–7855. [PubMed: 18672867]
104. Herath AC; Becker JY 2,2,6,6-Tetramethyl Piperidine-1-oxyl (TEMPO)-Mediated Catalytic Oxidation of Benzyl Alcohol in Acetonitrile and Ionic Liquid 1-Butyl-3-methyl-imidazolium Hexafluorophosphate [BMIm][PF₆]: Kinetic Analysis. *Electrochim. Acta* 2008, 53, 4324–4330.
105. Zhang W; Xiong Z; Zhang Z; Gao H 2,2,6,6-Tetramethyl Piperidine-1-oxyl Mediated Electrocatalytic Oxidation of Ethylene Glycol in Water and Dichloromethane. *Int. J. Hydrogen Energ* 2017, 42, 2134–2138.
106. Chmielewska B; Krzyczmonik P; Scholl H Electrode Reactions of Nitroxyl Radicals XI: Coulometric Experiments on the Oxidation of Aliphatic Alcohols by Oxoammonium Cations. *J. Electroanal. Chem* 1995, 395, 167–172.

107. These coulometric and chronoamperometric experiments are conducted at the aminoxyl/oxoammonium redox potential or at slightly more positive potentials. For the voltammetric experiments, peak or plateau currents (i_{cat}/i_0) were considered for deriving the TOFs according to the method of Savéant and co-workers (see refs. 98). Therefore, the measured turnover frequencies correspond to maximum TOF values. TOFs and TONs are reported elsewhere in the review are also maximal values.
108. Shibuya M; Tomizawa M; Suzuki I; Iwabuchi Y 2-Azaadamantane *N*-oxyl (AZADO) and 1-Me-AZADO: Highly Efficient Organocatalysts for Oxidation of Alcohols. *J. Am. Chem. Soc* 2006, 128, 8412–8413. [PubMed: 16802802]
109. Hayashi M; Shibuya M; Iwabuchi Y Oxidation of Alcohols to Carbonyl Compounds with Diisopropyl Azodicarboxylate Catalyzed by Nitroxyl Radicals. *J. Org. Chem* 2012, 77, 3005–3009. [PubMed: 22352461]
110. Lauber MB; Stahl SS Efficient Aerobic Oxidation of Alcohols at Ambient Temperature with an ABNO/NO_x Catalyst System. *ACS Catal* 2013, 3, 2612–2616.
111. Hoover JM; Stahl SS Highly Practical Copper(I)/TEMPO Catalyst System for Chemoselective Aerobic Oxidation of Primary Alcohols. *J. Am. Chem. Soc* 2011, 133, 16901–16910. [PubMed: 21861488]
112. Hoover JM; Ryland BL; Stahl SS Mechanism of Copper(I)/TEMPO-Catalyzed Aerobic Alcohol Oxidation. *J. Am. Chem. Soc* 2013, 135, 2357–2367. [PubMed: 23317450]
113. Hoover JM; Ryland BL; Stahl SS Copper/TEMPO-Catalyzed Aerobic Alcohol Oxidation: Mechanistic Assessment of Different Catalyst Systems. *ACS Catal* 2013, 3, 2599–2605. [PubMed: 24558634]
114. Ryland BL; McCann SD; Brunold TC; Stahl SS Mechanism of Alcohol Oxidation Mediated by Copper(II) and Nitroxyl Radicals. *J. Am. Chem. Soc* 2014, 136, 12166–12173. [PubMed: 25090238]
115. Walroth RC; Miles KC; Lukens JT; MacMillan SM; Stahl SS; Lancaster KM Electronic Structural Analysis of Copper(II)-TEMPO/ABNO Complexes Provides Evidence for Copper(I)-Oxoammonium Character. *J. Am. Chem. Soc* 2017, 139, 13507–13517. [PubMed: 28921958]
116. Shono T; Matsumura Y; Hayashi Mizoguchi, M. Electrochemical Oxidation of Alcohols Using Iodonium Ion as an Electron Carrier. *Tetrahedron Lett* 1979, 20, 165–168.
117. Shono T; Matsumura Y; Hayashi J; Mizoguchi M Electrooxidation of Alcohols Using a New Double Mediator System. *Tetrahedron Lett* 1980, 21, 1867–1870.
118. Inokuchi T; Matsumoto S; Torii S Indirect Electrooxidation of Alcohols by a Double Mediator System with Two Redox Couples of [R₂N⁺=O]/R₂NO• and [Br• or Br⁺]/Br⁻ in an Organic-Aqueous Two-Phase Solution. *J. Org. Chem* 1991, 56, 2416–2421.
119. Inokuchi T; Matsumoto S; Nishiyama T; Torii S A Selective and Efficient Method for Alcohol Oxidations Mediated by *N*-Oxoammonium Salts in Combination with Sodium Bromite. *J. Org. Chem* 1990, 55, 462–466.
120. Inokuchi T; Matsumoto S; Fukushima M; Torii S A New Oxidizing System for Aromatic Alcohols by the Combination of *N*-Oxoammonium Salt and Electrosynthesized Tetralkylammonium Tribromide. *Bull. Chem. Soc. Jpn* 1991, 64, 796–800.
121. Ogibin YN; Khusid A. Kh.; Nikishin GI Electrochemical and Chemical Oxidation of Alcohols in a Two-Phase System Using *N*-Oxopiperidinium Salt: Synthesis of 4-Chlorobutanal, Formylcyclopropanes, and *m*-Phenoxybenzaldehyde. *Russ. Chem. Bull* 1992, 41, 941–946.
122. Inokuchi T; Liu P; Torii S Oxidations of Dihydroxyalkanoates to Vicinal Tricarbonyl Compounds with a 4-BzoTEMPO-Sodium Bromite System or by Indirect Electrolysis Using 4-BzoTEMPO and Bromide Ion. *Chem. Lett* 1994, 1411–1414.
123. Ogibin YN; Levina IS; Kamernitsky AV; Nikishin GI A Highly Efficient, Indirect Electrooxidation of 6β-Methyl-3β,5α-dihydroxy-16α,17α-cyclohexanopregnan-20-one to the Corresponding 5α-Hydroxy-3,20-dione Using a Mediator Couple of Sodium Bromide and Substituted 2,2,6,6-Tetramethylpiperidine-*N*-oxyl (TEMPO). *Mendelev Commun* 1995, 5, 184–185.

124. Kubota J; Shimizu Y; Mitsudo K; Tanaka H Water-Soluble *N*-oxyl Compounds Mediated Electrooxidation of Alcohols in Water: A Prominent Access to a Totally Closed System. *Tetrahedron Lett* 2005, 46, 8975–8979.
125. Yoshida T; Kuroboshi M; Oshitani J; Gotoh K; Tanaka H Electroorganic Synthesis in Oil-in-Water Nanoemulsion: TEMPO-Mediated Electrooxidation of Amphiphilic Alcohols in Water. *Synlett* 2007, 2691–2694.
126. Mitsudo K; Kumagai H; Takabatake F; Kubota J; Tanaka H Anionic WS-TEMPO-Mediatory Electrooxidation of Alcohols in Water: Halide-Free Oxidation Directed Towards a Totally Closed System. *Tetrahedron Lett* 2007, 48, 8994–8997.
127. Kuroboshi M; Yoshida T; Oshitani J; Goto K; Tanaka H Electroorganic Synthesis in Oil-in-Water (O/W) Nanoemulsion: TEMPO-Mediated Electrooxidation of Amphiphilic Alcohols in Water. *Tetrahedron* 2009, 65, 7177–7185.
128. Demizu Y; Shiigi H; Oda T; Matsumura Y; Onomura O Efficient Oxidation of Alcohols Electrochemically Mediated by Azabicyclo-*N*-oxyls. *Tetrahedron Lett* 2008, 49, 48–52.
129. Kashiwagi Y; Uchiyama K; Kurashima F; Kikuchi C; Anzai J.-i. Chiral Discrimination in Electrocatalytic Oxidation of (*R*)- and (*S*)-1-Phenylethanol Using a Chiral Nitroxyl Radical as Catalyst. *Chem. Pharm. Bull* 1999, 47, 1051–1052.
130. Kurashima F; Kashiwagi Y; Kikuchi C; Anzai J.-i.; Osa T Electrocatalytic Oxidation of Benzyl Alcohol and 1-Phenethyl Alcohol by a Decahydroquinolinyl-*N*-oxyl Radical. *Heterocycles* 1999, 50, 79–82.
131. Kashiwagi Y; Kurashima F; Kikuchi C; Anzai J.-i.; Osa T. Bobbitt. Enantioselective Electrocatalytic Oxidation of Racemic *sec*- Alcohols Using a Chiral 1-Azaspiro[5.5]undecane-*N*-oxyl Radical. *Tetrahedron Lett* 1999, 40, 6469–6472.
132. Shiigi H; Mori H; Tanaka T; Demizu Y; Onomura O Chiral Azabicyclo-*N*-oxyls Mediated Enantioselective Electrooxidation of *sec*-Alcohols. *Tetrahedron Lett* 2008, 49, 5247–5251.
133. Ito K; Bobbitt JM; Rusling JF Catalytic Oxidation of Sugars by 4-Acetylamino TEMPO In Proceedings of the 5th International Symposium on Redox Mechanisms and Interfacial Behavior of Molecules of Biological Importance, Shultz FA, Taniguchi I, Eds.; Electrochemical Society: Pennington, NJ, 1993; p. 260.
134. Yamauchi Y; Maeda H; Ohmori H Electrochemical Detection of Alcohols and Carbohydrates at a Glassy Carbon Electrode Coated with a Poly(phenylene oxide) Film Containing Immobilized 2,2,6,6-Tetramethylpiperinyl-1-oxy (TEMPO). *Chem. Pharm. Bull* 1997, 45, 2024–2028
135. Schnatbaum K; Schäfer HJ Electroorganic Synthesis 66: Selective Anodic Oxidation of Carbohydrates Mediated by TEMPO. *Synthesis* 1999, 864–872.
136. Schämamm M; Schäfer HJ TEMPO-Mediated Anodic Oxidation of Methyl Glycosides and 1-Methyl and 1-Azido Disaccharides. *Eur. J. Org. Chem* 2003, 351–358.
137. Schämamm M; Schäfer HJ Reaction of Enamines and Mediated Anodic Oxidation of Carbohydrates with the 2,2,6,6-Tetramethylpiperidine-1-oxoammonium Ion (TEMPO⁺). *Electrochim. Acta*, 2005, 50, 4956–4972.
138. Barbier M; Breton T; Servat K; Grand E; Kokoh B; Kovensky J Selective TEMPO-Catalyzed Chemicals vs. Electrochemical Oxidation of Carbohydrate Derivatives. *J. Carbohydr. Chem* 2006, 25, 253–266.
139. Parpot P; Servat K; Bettencourt AP; Huser H; Kokoh KB TEMPO Mediated Oxidation of Carbohydrates Using Electrochemical Methods. *Cellulose* 2010, 17, 815–824.
140. Chang PS; Robyt JF Oxidation of Primary Alcohol Groups of Naturally Occurring Polysaccharides with 2,2,6,6-Tetramethyl-1-piperidine Oxoammonium Ion. *J. Carbohydr. Chem* 1996, 15, 819–830.
141. Isogai A; Kato Y Preparation of Polyruonic Acid from Cellulose by TEMPO-Mediated Oxidation. *Cellulose* 1998, 5, 153–164.
142. Pierre G; Punta C; Delattre C; Melone L; Dubessay P; Fiorati A; Pastori N; Galante YM; Michaud P TEMPO-Mediated Oxidation of Polysaccharides: An Ongoing Story. *Carbohydr. Polym* 2017, 165, 71–85. [PubMed: 28363578]

143. Isogai T; Saito T; Isogai A TEMPO Electromediated Oxidation of Some Polysaccharides Including Regenerated Cellulose Fiber. *Biomacromolecules* 2010, 11, 1593–1599. [PubMed: 20469944]
144. Jin Y; Edler KJ; Marken F; Scott JL Voltammetric Optimisation of TEMPO-Mediated Oxidations at Cellulose Fabric. *Green Chem* 2014, 16, 3322–3327.
145. Shibata I; Yanagisawa M; Saito T; Isogai A SEC-MALS Analysis of Celluronic Acid Prepared from Regenerated Cellulose by TEMPO-Mediated Oxidation. *Cellulose* 2006, 13, 73–80.
146. Isogai T; Saito T; Isogai A Wood Cellulose Nanofibrils Prepared by TEMPO Electro-Mediated Oxidation. *Cellulose* 2011, 18, 421–431.
147. Carlsson DO; Lindh J; Nyholm L; Stramme M; Mihranyan A Cooxidant-Free TEMPO-Mediated Oxidation of Highly Crystalline Nanocellulose in Water. *RSCAdv* 2014, 4, 52289–52298.
148. Corma A; Iborra S; Velty A Chemical Routes for the Transformation of Biomass into Chemicals. *Chem. Rev* 2007, 107, 2411–2502. [PubMed: 17535020]
149. Pagliaro M; Ciriminna R; Kimura H; Rossi M; Della Pina C From Glycerol to Value-Added Products. *Angew. Chem., Int. Ed* 2007, 46, 4434–4440.
150. McKendry P Energy Production from Biomass (Part 1): Overview of Biomass. *Bioresour. Technol* 2002, 83, 37–46. [PubMed: 12058829]
151. Alonso DM; Bond JQ; Dumesic JA Catalytic Conversion of Biomass to Biofuels. *Green Chem* 2010, 12, 1493–1513.
152. Ciriminna R; Palmisano G; Della Pina C; Rossi M; Pagliaro M One-Pot Electrocatalytic Oxidation of Glycerol to DHA. *Tetrahedron Lett* 2006, 47, 6993–6995.
153. Hickey DP; McCammant MS; Giroud F; Sigman MS; Minteer SD Hybrid Enzymatic and Organic Electrocatalytic Cascade for the Complete Oxidation of Glycerol. *J. Am. Chem. Soc* 2014, 136, 15917–15920. [PubMed: 25350383]
154. Cha HG; Choi K-S Combined Biomass Valorization and Hydrogen Production in a Photoelectrochemical Cell. *Nature Chem* 2015, 7, 328–333. [PubMed: 25803471]
155. Kashparova VP; Klushin VA; Leontyeva DV; Smirnova NV; Chernyshev VM; Ananikov VP Selective Synthesis of 2,5-Diformylfuran by Sustainable 4-Acetamido-TEMPO/Halogen-Mediated Electrooxidation of 5-Hydroxymethylfurfural. *Chem. Asian J* 2016, 11, 2578–2585. [PubMed: 27432749]
156. Pezzuto JM; Kim DS H. L. Methods of Manufacturing Betulinic Acid. U.S. Patent 5,804,575, Sep. 8, 1998.
157. Krasutsky PA; Carlson RM; Nesterenko VV Method for Manufacturing Betulinic Acid U.S. Patent 6,232,481, 5 15, 2001.
158. Krasutsky PA; Carlson RM; Nesterenko VV Method for Manufacturing Betulinic Acid U.S. Patent 6,271,405 B2, Aug. 7, 2001.
159. Krasutsky PA; Carlson RM; Nesterenko VV Methods for Manufacturing Betulinic Acid U.S. Patent 6,407,270 B1 Jun. 18, 2002.
160. Krasutsky PA; Rudnitskava A; Khotkevych AB Electrochemical Method for the Production of Betulin Aldehyde U.S. Patent 20,080,308,426, Dec. 18, 2008.
161. Zakzeski J; Bruijninx PCA; Jongerius AL; Weckhuysen BM The Catalytic Valorization of Lignin for the Production of Renewable Chemicals. *Chem. Rev*, 2010, 110, 3552–3599. [PubMed: 20218547]
162. Rinaldi R; Jastrzebski R; Clough MT; Ralph J; Kennema M; Bruijninx PCA; Weckhuysen BM Paving the Way for Lignin Valorisation: Recent Advances in Bioengineering, Biorefining and Catalysis. *Angew. Chem., Int. Ed* 2016, 55, 8164–8215.
163. Rahimi A; Azarpira A; Kim H; Ralph J; Stahl SS Chemoselective Metal-Free Aerobic Alcohol Oxidation in Lignin. *J. Am. Chem. Soc* 2013, 135, 6415–6418. [PubMed: 23570328]
164. Rahimi A; Ulbrich A; Coon JJ; Stahl SS Formic-acid-Induced Depolymerization of Oxidized Lignin to Aromatics. *Nature* 2014, 515, 249–252. [PubMed: 25363781]
165. Fabbrini M; Galli C; Gentili P Comparing the Catalytic Efficiency of Some Mediators of Laccase. *J. Mol. Catal. B: Enzym* 2002, 16, 231–240.

166. Barreca AM; Fabbrini M, Galli C; Gentili P; Ljunggren S Laccase Mediated Oxidation of a Lignin Model for Improved Delignification Procedures. *J. Mol. Catal. B: Enzym* 2003, 26, 105–110.
167. Ma P; Fu S; Zhai H; Law K; Daneault C Influence of TEMPO Mediated Oxidation on the Lignin of Thermomechanical Pulp. *Bioresour. Technol* 2012, 118, 607–610. [PubMed: 22704831]
168. Nguyen JD; Matsuura BS; Stephenson CRJ A Photochemical Strategy for Lignin Degradation at Room Temperature. *J. Am. Chem. Soc* 2014, 136, 1218–1221. [PubMed: 24367945]
169. Patil ND; Yao SG; Meier MS; Mobley JK; Crocker M Selective Cleavage of the C α -C β Linkage in Lignin Model Compounds via Baeyer-Villiger Oxidation. *Org. Biomol. Chem* 2015, 13, 3243–3254. [PubMed: 25641654]
170. Wang M; Lu J; Zhang X; Li L; Li H; Luo N; Wang F Two-Step, Catalytic C-C Bond Oxidative Cleavage Process Converts Lignin Models and Extracts to Aromatic Acids. *ACS Catal* 2016, 6, 6086–6090.
171. Dabral S; Hernandez JG; Kamer PCJ; Bolm C Organocatalytic Chemoselective Primary Alcohol Oxidation and Subsequent Cleavage of Lignin Model Compounds and Lignin. *ChemSusChem* 2017, 10, 2707–2713. [PubMed: 28523820]
172. Sannami Y; Kamitakahara H; Takano T TEMPO-Mediated Electro-Oxidation Reactions of Non-Phenolic β -O-4-type Lignin Model Compounds. *Holzforschung* 2017, 71, 109–117.
173. Bidan G; Limosin D Electrochemical Synthesis and Behaviour of a Poly(Pyrrrole) Film Containing a Nitroxide Group. *Ann. Phys* 1986, 11, 5–16.
174. Deronzier A; Limosin D; Moutet J-C Electrochemical Oxidations of Carbinols Mediated by Nitroxyl Radicals in Solutions or Bonded to Polypyrrolic Coatings on Platinum and Carbon Electrodes. *Electrochim. Acta* 1987, 32, 1643–1647.
175. Iraqi A; Crayston JA; Walton JC; Harrison A Aminoxyl Functionalized Polythiophene: Synthesis and Electrochemical Applications. *J. Mater. Chem* 1995, 5, 1291–1295.
176. Osa T; Akiba U; Segawa I; Bobbitt JM Electrocatalytic Oxidation of Nerol with Nitroxyl Radical Covalently Immobilized to Poly(acrylic acid) Coated on Carbon Electrodes. *Chem. Lett* 1988, 17, 1423–1426.
177. Osa T; Kashiwagi Y; Mukai K; Ohsawa A; Bobbitt JM A Preparative Nitroxyl-Radical Coated, Graphite Felt Electrode for the Oxidation of Alcohols. *Chem. Lett* 1990, 19, 75–78.
178. Kashiwagi Y; Kurashima F; Chiba S; Anzai J.-i.; Osa T; Bobbitt JM Asymmetric Electrochemical Lactonization of Diols on a Chiral 1-Azasprio[5.5]undecane *N*-oxyl Radical Mediator-Modified Graphite Felt Electrode. *Chem. Commun* 2003, 114–115.
179. Kashiwagi Y; Yanagisawa T; Kurashima F; Anzai J.-i.; Osa T; Bobbitt JM Enantioselective Electrocatalytic Oxidation of Racemic Alcohols on a TEMPO-Modified Graphite Felt Electrode by Use of a Chiral Base (TEMPO = 2,2,6,6-tetramethylpiperdin-1-yloxy). *Chem. Commun* 1996, 2745–2746.
180. Yanagisawa T; Kashiwagi Y; Kurashima F; Anzai J.-i.; Osa T; Bobbitt JM Enantioselective, Electrocatalytic Lactonization of Methyl-substituted Diols on a TEMPO-modified Graphite Felt Electrode in the Presence of (–)-Sparteine. *Chem. Lett* 1996, 25, 1043–1044.
181. Belgsir EM; Schäfer HJ TEMPO-Modified Graphite Felt Electrodes: Attempted Enantioselective Oxidation of *rac*-1-Phenylethanol in the Presence of (–)-Sparteine. *Chem. Commun* 1999, 435–436.
182. Belgsir EM; Schäfer HJ Selective Oxidation of Carbohydrates on Nafion®-TEMPO-Modified Graphite Felt Electrodes. *Electrochem. Commun* 2001, 3, 32–35.
183. Hahn Y; Song SK Electrochemical Behavior of a TEMPO-Modified Electrode and Its Electrocatalytic Oxidation of Benzyl Alcohol. *Anal. Sci* 1997, 13, 329–332.
184. Kishioka S-y.; Ohki S; Ohsaka T; Tokuda K Reaction Mechanism and Kinetics of Alcohol Oxidation at Nitroxyl Radical Modified Electrodes. *J. Electroanal. Chem* 1998, 452, 179–186.
185. Kolodziej A; Ahn SD; Carta M; Malpass-Evans R; McKeown NB; Chapman RSL; Bull SD; Marken F Electrocatalytic Carbohydrate Oxidation with 4-Benzoyloxy-TEMPO Heterogenised in a Polymer of Intrinsic Microporosity. *Electrochim. Acta* 2015, 160, 195–201.

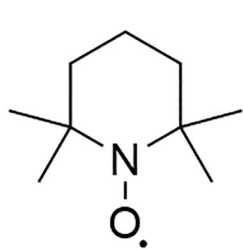
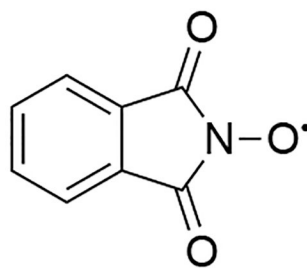
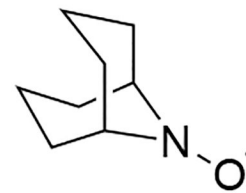
186. Lu J.-j.; Ma J.-q.; Yi J.-m.; Shen Z.-l.; Zhong Y.-j.; Ma C.-a.; Li M.-c. Electrochemical Polymerization of Pyrrole Containing TEMPO Side Chain on Pt Electrode and Its Electrochemical Activity. *Electrochim. Acta* 2014, 130, 412–417.
187. Ahn SD; Kolodziej A; Malpass-Evans R; Carta M; McKeown NB; Bull SD; Buchard A; Marken F Polymer of Intrinsic Microporosity Induces Host-Guest Substrate Selectivity in Heterogenous 4-Benzoyloxy-TEMPO-Catalysed Alcohol Oxidations. *Electrocatal* 2016, 7, 70–78.
188. Hickey DP; Milton RD; Chen D; Sigman MS; Minter SD TEMPO-Modified Linear Poly(ethylenimine) for Immobilization-Enhanced Electrocatalytic Oxidation of Alcohols. *ACS Catal* 2015, 5, 5519–5524.
189. Palmisano G; Ciriminna R; Pagliaro M Waste-Free Electrochemical Oxidation of Alcohols in Water. *Adv. Synth. Catal* 2006, 34S, 2033–2037.
190. Palmisano G; Mandler D; Ciriminna R; Pagliaro M Structural Insight on Organosilica Electrodes for Waste-Free Alcohol Oxidations. *Catal. Lett* 2007, 114, 55–58.
191. Karimi B; Rafiee M; Alizadeh S; Vali H Eco-Friendly Electrocatalytic Oxidation of Alcohols on a Novel Electro Generated TEMPO-Functionalized MCM-41 Modified Electrode. *Green Chem* 2015, 17, 991–1000.
192. Walcarius E Sibottier M. Etienne and Ghanbaja J, Electrochemically Assisted Self Assembly of Mesoporous Silica Thin Films. *Nat. Mater* 2007, 6, 602–608 [PubMed: 17589513]
193. Geneste F; Moinet C Electrochemically Linking TEMPO to Carbon *via* Amine Bridges. *New J. Chem* 2005, 29, 269–271.
194. Geneste F; Moinet C; Ababou-Girard S; Solal F Covalent Attachment of TEMPO onto a Graphite Felt Electrode and Application in Electrocatalysis. *New J. Chem* 2005, 29, 1520–1526.
195. Tanaka H; Kawakami Y; Goto K; Kuroboshi M An Aqueous Silica Gel Disperse Electrolysis System. *N-oxyl-Mediated Electrooxidation of Alcohols*. *Tetrahedron Lett* 2001, 45, 445–448.
196. Tanaka H; Kubota J; Itogawa S.-j.; Ido T; Kuroboshi M; Shimamura K; Uchida T Electrooxidation of Alcohols in a Disperse System with *N-oxyl*-Immobilized Polyethylene Particles as a Disperse Phase and Aqueous NaHCO₃/NaBr as Disperse Media: A Totally Closed Electrolysis System. *Synlett* 2003, 951–954.
197. Tanaka H; Kubota J; Miyahara S; Kuroboshi M Electrooxidation of Alcohols in an *N-oxyl*-Immobilized Poly(ethylene-*co*-acrylic acid)/Water Disperse System. *Bull. Chem. Soc. Jpn* 2005, 7S, 1677–1684.
198. Kubota J; Ido T; Kuroboshi M; Tanaka H; Uchida T; Shimamura K Electrooxidation of Alcohols in an *N-oxyl*-Immobilized Rigid Network Polymer Particles/Water Disperse System. *Tetrahedron* 2006, 62, 4769–4773.
199. Kuroboshi M; Goto K; Tanaka H Electrooxidation of Alcohols in *N-oxyl*-Immobilized Silica Gel/Water Disperse System: Approach to Totally Closed System. *Synthesis* 2009, 903–908.
200. Schille B; Ole Giltzau NO; Francke R On the Use of Polyelectrolytes and Polymediators in Organic Electrosynthesis. *Angew. Chem., Int. Ed* 2018, 57, 422–426.
201. Das A; Stahl SS Noncovalent Immobilization of Molecular Electrocatalysts for Chemical Synthesis: Efficient Electrochemical Alcohol Oxidation with a Pyrene-TEMPO Conjugate. *Angew. Chem., Int. Ed* 2017, 56, 8892–8897
202. See references from: Das A; Stahl SS Noncovalent Immobilization of Molecular Electrocatalysts for Chemical Synthesis: Efficient Electrochemical Alcohol Oxidation with a Pyrene-TEMPO Conjugate. *Angew. Chem., Int. Ed* 2017, 56, 8892–8897.
203. Blanchard P-Y; Alveveque O; Breton T; Levillain E TEMPO Mixed SAMs: Electrocatalytic Efficiency versus Surface Coverage. *Langmuir* 2012, 2S, 13741–13745.
204. Swiech O; Bilewicz R; Megiel E TEMPO Coated Au Nanoparticles: Synthesis and Tethering to Gold Surfaces. *RSC Adv* 2013, 3, 5979–5986.
205. Semmelhack MF; Schmid CR Nitroxyl-Mediated Electrooxidation of Amines to Nitriles and Carbonyl Compounds. *J. Am. Chem. Soc* 1983, 105, 6732–6734.
206. Kashiwagi Y; Kurashima F; Kikuchi C; Anzai J.-i.; Osa T; Bobbitt JM Enantioselective Electrocatalytic Oxidation of Racemic Amines Using a Chiral 1-Azaspiro[5.5]undecane *N-oxyl* Radical. *Chem. Commun* 1999, 1983–1984.

207. Kashiwagi Y; Anzai J.-i. Selective Electrocatalytic Oxidation of *N*-Alkyl-*N*-ethylanilines to *N*-Alkylformanilides Using Nitroxyl Radical. *Chem. Pharm. Bull* 2001, 49, 324–326. [PubMed: 11253925]
208. Li C; Zeng C-C; Hu L-M; Yang F-L; Yoo SJ; Little RD Electrochemically Induced C-H Functionalization Using Bromide Ion/2,2,6,6-Tetramethylpiperinyl-*N*-oxyl Dual Redox Catalysts in a Two-Phase Electrolytic System. *Electrochim. Acta* 2013, 114, 560–566.
209. Chen Q; Fang C; Shen Z; Li M Electrochemical Synthesis of Nitriles from Aldehydes Using TEMPO as a Mediator. *Electrochem. Commun* 2016, 64, 51–55.
210. Yang X; Fan Z; Shen Z; Li M Electrocatalytic Synthesis of Nitriles from Aldehydes with Ammonium Acetate as the Nitrogen Source. *Electrochim. Acta* 2017, 226, 53–59.
211. Fan Z; Yang X; Chen C; Shen Z; Li M One-Pot Electrochemical Oxidation of Alcohols to Nitriles Mediated by TEMPO. *J. Electrochem. Soc* 2017, 164, G54–G58.
212. Wu Y; Yi H; Lei A Electrochemical Acceptorless Dehydrogenation of *N*-Heterocycles Utilizing TEMPO as an Organo-Electrocatalyst. *ACS Catal* 2018, 8, 1192–1196.
213. MacCorquodale F; Crayston JA; Walton JC; Worsfold DJ Synthesis and Electrochemical Characterization of Poly(TEMPO-Acrylate). *Tetrahedron Lett* 1990, 31, 771–774.
214. Kashiwagi Y; Kurashima F; Kikuchi C; Anzai J.-i.; Osa T; Bobbitt JM Electrocatalytic Oxidation of Amines to Nitriles on a TEMPO-modified Graphite Felt Electrode (TEMPO = 2,2,6,6-Tetramethylpiperinyl-1-oxy). *J. Chin. Chem. Soc* 1998, 45, 135–138.
215. Lambert KM; Bobbitt JM; Eldirany SA; Wiberg KB; Bailey WF Facile Oxidation of Primary Amines to Nitriles Using an Oxoammonium Salt. *Org. Lett* 2014, 16, 6484–6487. [PubMed: 25495541]
216. Zhang W; Xiong Z; Gao Y; Gao H; Zhang Y Roles of the Base in the Electrocatalytic Reactions: A Case Study of Glycine Electrooxidation. *J. Electroanal. Chem* 2017, 785, 216–219.
217. Andon RJJ; Cox JD; Herington EFG The Ultra-Violet Absorption Spectra and Dissociation Constants of Certain Pyridine Bases in Aqueous Solution. *Trans. Faraday Soc* 1954, 50, 918–927.
218. Kashiwagi Y; Ono H; Osa T Electrocatalytic Coupling Reaction of Naphthols and Naphthol Ethers on a TEMPO Modified Graphite Electrode. *Chem. Lett* 1993, 81–84.
219. Breton T; Liaigre D; Belgsir EM Allylic Oxidation: Easy Synthesis of Alkenones from Activated Alkenes with TEMPO. *Tetrahedron Lett* 2005, 46, 2487–2490.
220. Breton T; Liaigre D; Belgsir EM Aromatization of Cyclohexadienes by TEMPO Electro-Mediated Oxidation: Kinetic and Structural Aspects. *Electrochem. Commun* 2005, 7, 1445–1448.
221. Henry PM Palladium Catalyzed Oxidation of Hydrocarbons; D. Reidel Publishing Co.: Dordrecht, The Netherlands, 1980, Vol. 2.
222. Heumann A; Jens K-J; Reglier M Palladium Complex Catalyzed Oxidation Reactions. *Prog. Inorg. Chem* 1994, 42, 483–576.
223. Piera J; Backvall JE Catalytic Oxidation of Organic Substrates by Molecular Oxygen and Hydrogen Peroxide by Multistep Electron Transfer- A Biomimetic Approach. *Angew. Chem, Int. Ed* 2008, 47, 3506–3523
224. Lyons TW; Sanford MS Palladium-Catalyzed Ligand-Directed C-H Functionalization Reactions. *Chem. Rev* 2010, 110, 1147–1169. [PubMed: 20078038]
225. Chen X; Engle KM; Wang D-H; Yu J-Q Palladium(II)-Catalyzed C-H Activation/C-C Cross-Coupling Reactions: Versatility and Practicality. *Angew. Chem., Int. Ed* 2009, 48, 5094–5115.
226. Wang D; Weinstein AB; White PB; Stahl SS Ligand-Promoted Palladium-Catalyzed Aerobic Oxidation Reactions. *Chem. Rev.* in press
227. Jutand A Contribution of Electrochemistry to Organometallic Catalysis. *Chem. Rev* 2008, 108, 2300–2347.
228. Jiao K-J; Zhao C-Q; Fang P; Mei T-S Palladium Catalyzed C-H Functionalization with Electrochemical Oxidation. *Tetrahedron Lett* 2017, 58, 797–802.
229. Kakiuchi F; Kochi T Selective C-H Functionalization by Electrochemical Reactions with Palladium Catalysts. *Isr. J. Chem* 2017, 57, 953–963.

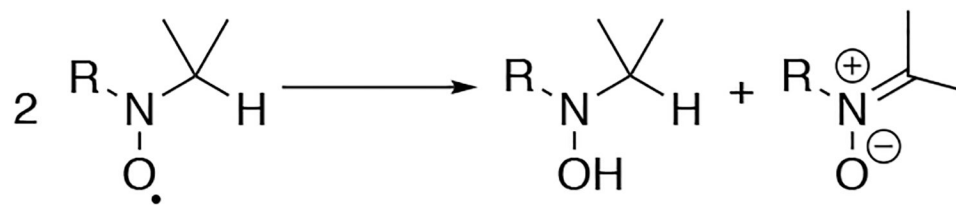
230. Mitsudo K; Kaide T; Nakamoto E; Yoshida K; Tanaka H Electrochemical Generation of Cationic Pd Catalysts and Application to Pd/TEMPO Double-Mediatory Electrooxidative Wacker-Type Reactions. *J. Am. Chem. Soc* 2007, 129, 2246–2247. [PubMed: 17279759]
231. Mitsudo K; Ishii T; Tanaka H Pd/TEMPO Double-Mediatory Electrooxidative Wacker-Type Cyclizations. *Electrochem* 2008, 859–861.
232. Mitsudo K; Shiraga T; Tanaka H Electrooxidative Homo-Coupling of Arylboronic Acids Catalyzed by Electrogenerated Cationic Palladium Catalysts. *Tetrahedron Lett* 2008, 49, 6593–6595.
233. Mitsudo K; Shiraga T; Kagen D; Shi D; Becker JY; Tanaka H Pd/TEMPO-Catalyzed Electrooxidative Synthesis of Biaryls from Arylboronic Acids or Arylboronic Esters. *Tetrahedron* 2009, 65, 8384–8388.
234. Mitsudo K; Shiraga T; Mizukawa J Suga S; Tanaka H Electrochemical Generation of Silver Acetylides from Terminal Alkynes with a Ag Anode and Integration into Sequential Pd-Catalysed Coupling with Arylboronic Acids. *Chem. Commun* 2010, 46, 9256–9258.
235. Xu F; Zhu L; Zhu S; Yan X; Xu H-C Electrochemical Intramolecular Aminooxygenation of Unactivated Alkenes. *Chem. Eur. J* 2014, 20, 12740–12744. [PubMed: 25145684]
236. Inokuchi T; Matsumoto S; Tsuji M; Torii S Electrohalogenation of Propargyl Acetates and Amides to Form the 1,1-Dibromo-2-oxo Functionality and a Facile Synthesis of Furaneol. *J. Org. Chem* 1992, 57, 5023–5027.
237. Verhe R; Courtheyn D; De Kimpe N; De Buyck L; Schamp N Preparation of 1,1-Dialkoxy-2-alkanones. *Synthesis* 1982, 667–670.
238. Tiecco M; Testaferri L; Tingoli M; Baroli D Selenium-Catalyzed Conversion of Methyl Ketones into α -Keto Acetals. *J. Org. Chem* 1990, 55, 4523–4528.
239. Qian X-Y; Li S-Q; Song J; Xu H-C TEMPO-Catalyzed Electrochemical C-H Thiolation: Synthesis of Benzothiazoles and Thiazolopyridines from Thioamides. *ACS Catal* 2017, 7, 2730–2734.
240. Peterson B; Lin S; Fors BP Electrochemically Controlled Cationic Polymerization of Vinyl Ethers. *J. Am. Chem. Soc* 2018, 140, 2076–2079. [PubMed: 29385348]
241. Ozaki S; Masui M Oxidation of Hydroxylamine Derivatives. I. Anodic Oxidation of Hydroxamic Acids. *Chem. Pharm. Bull* 1977, 25, 1179–1185.
242. Kishioka S; Yamada A Kinetic Study of the Catalytic Oxidation of Benzyl Alcohols by Phthalimide-*N*-oxyl Radical Electrogenerated in Acetonitrile using Rotating Disk Electrode Voltammetry. *J. Electroanal. Chem* 2005, 57S, 71–77.
243. Espenson JH; Saha B; Koshino N Kinetic Study of the Phthalimide *N*-oxyl Radical in Acetic Acid. Hydrogen Abstraction from Substituted Toluenes, Benzaldehydes, and Benzyl Alcohols. *J. Org. Chem* 2003, 6S, 9364–9370.
244. Baciocchi E; Gerini MF; Lanzalunga O Reactivity of Phthalimide *N*-oxyl Radical (PINO) toward the Phenolic O-H Bond. A Kinetic Study. *J. Org. Chem* 2004, 69, 8963–8966. [PubMed: 15575785]
245. Rafiee M; Wang F; Hruszkewycz DP; Stahl SS *N*-Hydroxyphthalimide-Mediated Electrochemical Iodination of Methylarenes and Comparison to Electron-Transfer-Initiated C-H Functionalization. *J. Am. Chem. Soc* 2008, 140, 22–25.
246. Gorgy K; Lepretre J-C; Saint-Aman E; Einhorn C; Einhorn J; Marcadal C; Pierre J-L Electrocatalytic Oxidation of Alcohols using Substituted *N*-Hydroxyphthalimides as Catalysts. *Electrochim. Acta* 1998, 44, 385–393.
247. Baciocchi E; Bietti M; DAlfonso C; Lanzalunga O; Lapi A; Salamone M One-Electron Oxidation of Ferrocenes by Short-Lived *N*-oxyl Radicals. The Role of Structural Effects on the Intrinsic Electron Transfer Reactivities. *Org. Biomol. Chem* 2011, 9, 4085–4090. [PubMed: 21541382]
248. Kishioka S; Yamada A Electro-oxidation of *N*-Hydroxy Imides for Redox Mediator in Acetonitrile Containing Lutidine as a Base. *Electrochim. Acta* 2006, 51, 4582–4588.
249. Annunziatini C; Baiocco P; Gerini MF; Lanzalunga O; Sjorgen B Aryl Substituted *N*-Hydroxyphthalimides as Mediators in the Laccase-Catalysed Oxidation of Lignin Model Compounds and Delignification of Wood Pulp. *J. Mol. Catal. B: Enzym* 2005, 32, 89–96.

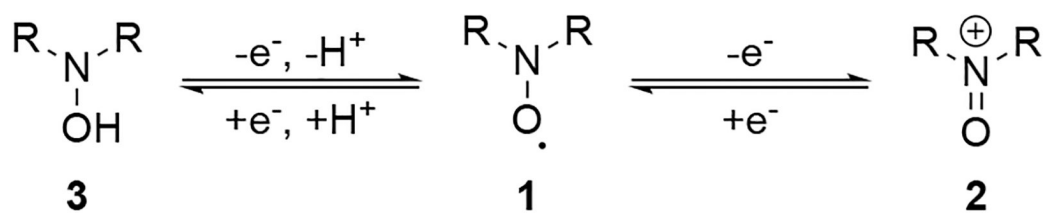
250. Xu F; Deussen H-JW; Lopez I B; Lam L; Li K Enzymatic and Electrochemical Oxidation of *N*-Hydroxy Compounds. Redox Potential, Electron-Transfer Kinetics, and Radical Stability. *Eur. J. Biochem* 2001, 26S, 4169–4176.
251. Shiraishi T; Takano T; Kamitakahara H; Nakatsubo F Studies on the Electro-Oxidation of Lignin and Lignin Model Compounds. Part 2: *N*-Hydroxyphthalimide (NHPI)-Mediated Indirect Electrooxidation of Non-Phenolic Lignin Model Compounds. *Holzforschung* 2012, 66, 311–315.
252. Bosque I; Magallanes G; Rigoulet M; Karkas MD; Stephenson CR J. Redox Catalysis Facilitates Lignin Depolymerization. *ACS Cent. Sci* 2017, 3, 621–628. [PubMed: 28691074]
253. Ishii Y; Sakaguchi S; Iwahama T Innovation of Hydrocarbon Oxidation with Molecular Oxygen and Related Reactions. *Adv. Synth. Catal* 2001, 343, 393–427.
254. Tashiro Y; Iwahama T; Sakaguchi S; Ishii Y A New Strategy for the Preparation of Terephthalic Acid by the Aerobic Oxidation of *p*-Xylene using *N*-Hydroxyphthalimide as a Catalyst. *Adv. Synth. Catal* 2001, 343, 220–225.
255. Melone L; Punta C *N*-Hydroxyphthalimide (NHPI)-Organocatalyzed Aerobic Oxidations: Advantages, Limits, and Industrial Perspectives In: *Liquid Phase Aerobic Oxidation Catalysis: Industrial Applications and Academic Perspectives*; Stahl SS; Alsters PL, Eds. Wiley- VCH: Weinheim, 2016; pp 253–265.
256. Hruszkewycz DP; Miles KC; Theil OR; Stahl SS Co/NHPI-Mediated Aerobic Oxygenation of Benzylic C-H bonds in Pharmaceutically Relevant Molecules. *Chem. Sci* 2016, 8, 1282–1287. [PubMed: 28451270]
257. Horn EJ; Rosen BR; Chen Y; Tang J; Chen K; Eastgate MD; Baran PS Scalable and Sustainable Electrochemical Allylic C-H Oxidation. *Nature* 2016, 533, 77–81. [PubMed: 27096371]
258. Zhu Y; Zhu Y; Zeng H; Chen Z; Little RD; Ma C A Promising Electro-Oxidation of Methyl-Substituted Aromatic Compounds to Aldehydes in Aqueous Imidazole Ionic Liquid Solutions. *J. Electroanal. Chem* 2015, 751, 105–110.
259. Fremy ME On a New Series of Acids Formed from Oxygen, Sulfur, Hydrogen, and Nitrogen. *Ann. Chim. Phys* 1845, 15, 408–488.
260. Divers E; Haga T Identification and Constitution of Fremy's Sulphazotised Salts of Potassium. *J. Chem. Soc., Trans* 1900, 77, 440–446.
261. Zimmer H; Lankin DC; Horgan SW Oxidations with Potassium Nitrosodisulfonate (Fremy's Radical). *Teuber Reaction. Chem. Rev* 1971, 71, 229–246.
262. Aoyagui S; Kato F Formal Oxidation-Reduction Potential of the Nitrosyldisulfonate/Hydroxylaminedisulfonate Redox System. *Electroanal. Chem. Interfacial Electrochem* 1972, 38, 243–244.
263. Raspi G; Cinquantini A; Cospito M Voltammetric Behavior of the Nitrosodisulfonate/Hydroxylaminedisulfonate Redox System. *J. Electroanal. Chem. Interfacial Electrochem* 1975, 59, 69–74
264. Toropova VF; Degtyareva VN Application of Nitrosodisulfonate Potassium Potentiometric Titration. *Izv. Vyssh. Uchebn. Zaved* 1974, 17, 175–178.
265. Kashiwagi Y; Nishimura T; Anzai J.-i. Voltammetric Behavior of β -Phosphonylated Nitroxide and Its Application to Electrocatalytic Oxidation of Alcohol. *Electrochim. Acta* 2002, 47, 1317–1320.
266. Nakahara K; Iwasa S; Iriyama J; Morioka Y; Suguro M; Satoh M; Cairns EJ Electrochemical and Spectroscopic Measurements for Stable Nitroxyl Radicals. *Electrochim. Acta* 2006, 52, 921–927.
267. Marx L; Scholhorn B Intramolecular Charge Effects in the Electrochemical Oxidation of Aminoxyl Radicals. *New J. Chem* 2006, 30, 430–434.
268. Bogart JA; Lee HB; Boreen MA; Jun M; Schelter EJ Fine-Tuning the Oxidative Ability of Persistent Radicals: Electrochemical and Computational Studies of Substituted 2-Pyridylhydroxylamines. *J. Org. Chem* 2013, 78, 6344–6349. [PubMed: 23721056]
269. Thurston CF The Structure and Function of Fungal Laccases. *Microbiol* 1994, 140, 19–26.
270. Call HP; Mucke I History, Overview and Applications of Mediated Lignolytic Systems, Especially Laccase-Mediator-Systems (Lignozym[®]-process). *J. Biotechnol* 1997, 53, 163–202.
271. Riva S Laccases: Blue Enzymes for Green Chemistry. *Trends Biotechnol* 2006, 24, 219–226. [PubMed: 16574262]

272. Solomon EI; Sundaram UM; Machonkin TE Multicopper Oxidases and Oxygenases. *Chem. Rev* 1996, 96, 2563–2606. [PubMed: 11848837]
273. Astolfi P; Brandi P; Galli C; Gentili P; Gerini MF; Greci L; Lanzalunga O New Mediators for the Enzyme Laccase: Mechanistic Features and Selectivity in the Oxidation of Non-Phenolic Substrates. *New J. Chem* 2005, 29, 1308–1317.
274. Gonzalez Arzola K; Arevalo MC; Falcon MA Catalytic Efficiency of Natural and Synthetic Compounds used as Laccase-Mediators in Oxidising Veratryl Alcohol and a Kraft Lignin, Estimated by Electrochemical Analysis. *Electrochim. Acta* 2009, 54, 2621–2629.
275. Steves JE; Stahl SS Copper-Catalyzed Aerobic Alcohol Oxidation In: *Liquid Phase Aerobic Oxidation Catalysis: Industrial Applications and Academic Perspectives*; Stahl SS; Alsters PL, Eds. Wiley- VCH: Weinheim, 2016; pp 85–96.
276. Zultanski SL; Stahl SS NO_x Cocatalysts for Aerobic Oxidation Reactions: Application to Alcohol Oxidation In: *Liquid Phase Aerobic Oxidation Catalysis: Industrial Applications and Academic Perspectives*; Stahl SS; Alsters PL, Eds. Wiley- VCH: Weinheim, 2016; pp 239–251.
277. Ciriminna R; Pagliaro M Industrial Oxidations with Organocatalyst TEMPO and Its Derivatives. *Org. Process Res. Dev* 2010, 14, 245–251.
278. Pletcher D; Walsh FC *Industrial Electrochemistry*; Chapman and Hall: London, 1990, Vol. 2.

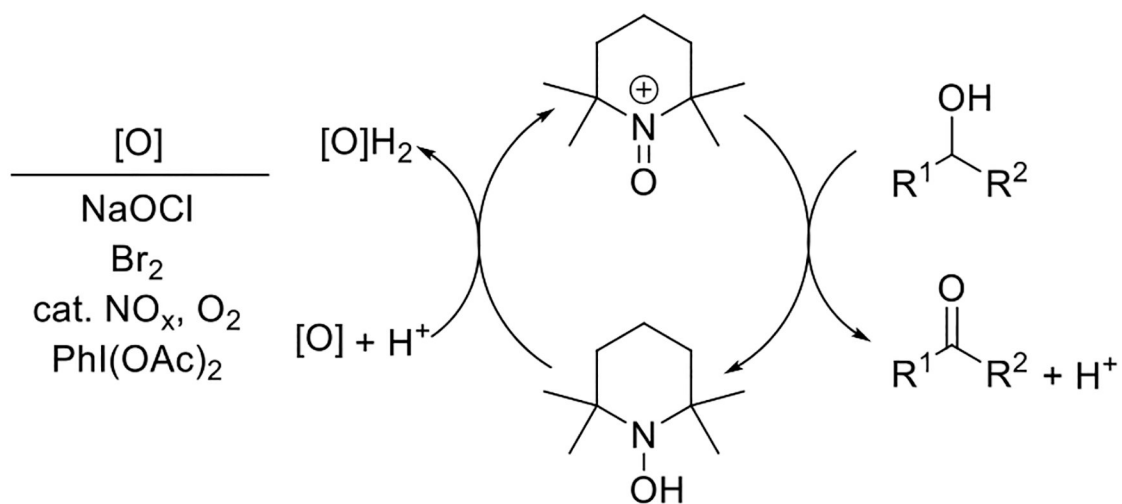
**TEMPO****PINO****ABNO**

Scheme 1.
Structures of TEMPO, PINO, and ABNO.

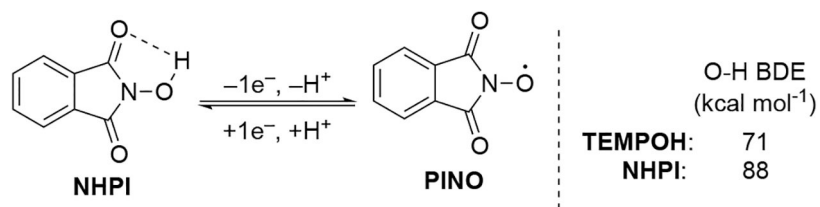
**Scheme 2.**Disproportionation of aminoxyl radicals with α -protons.



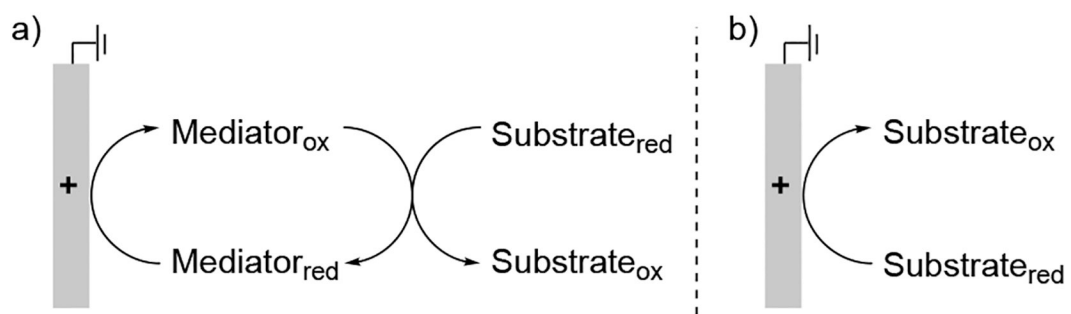
Scheme 3.
Simplified redox chemistry of aminoxyl radicals.



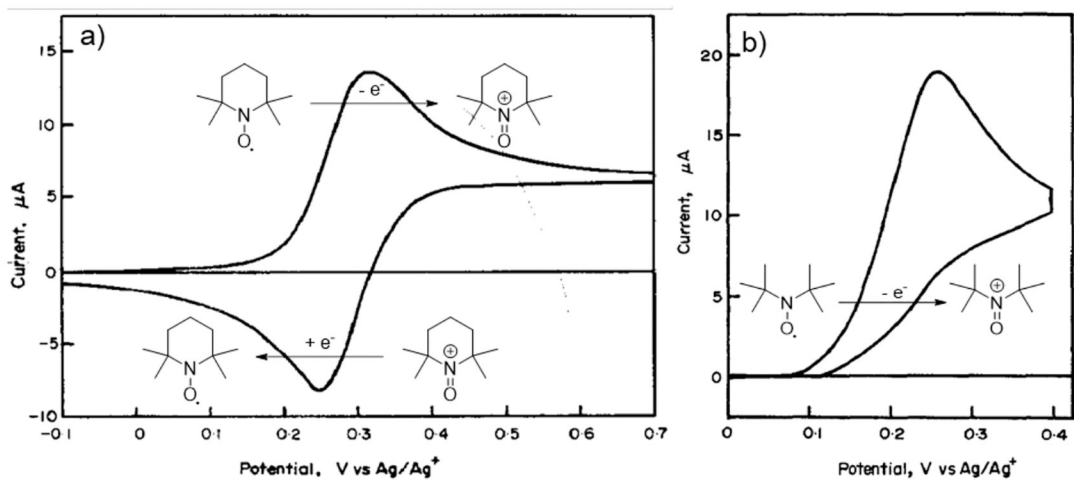
Scheme 4.
Alcohol oxidation methods employing aminoxyl (pre)catalysts.



Scheme 5.
Redox reaction of *N*-hydroxyphthalimide (NHPI) and PINO and the O–H bond strengths of TEMPOH and NHPI.^{32–36}

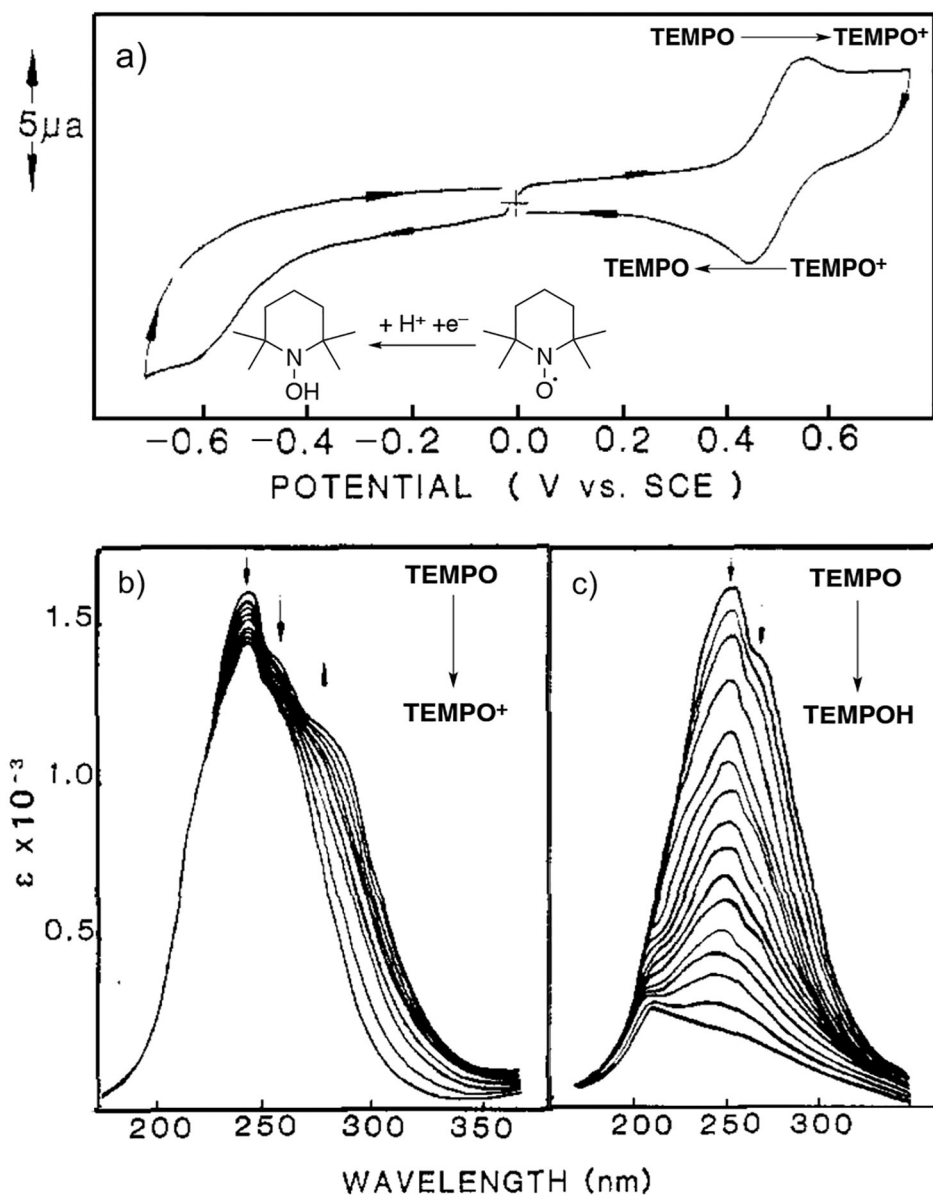
**Scheme 6.**

a) Mediated electrooxidation of organic substrates, and b) direct electrooxidation of an organic substrate at an anode surface.

**Scheme 7.**

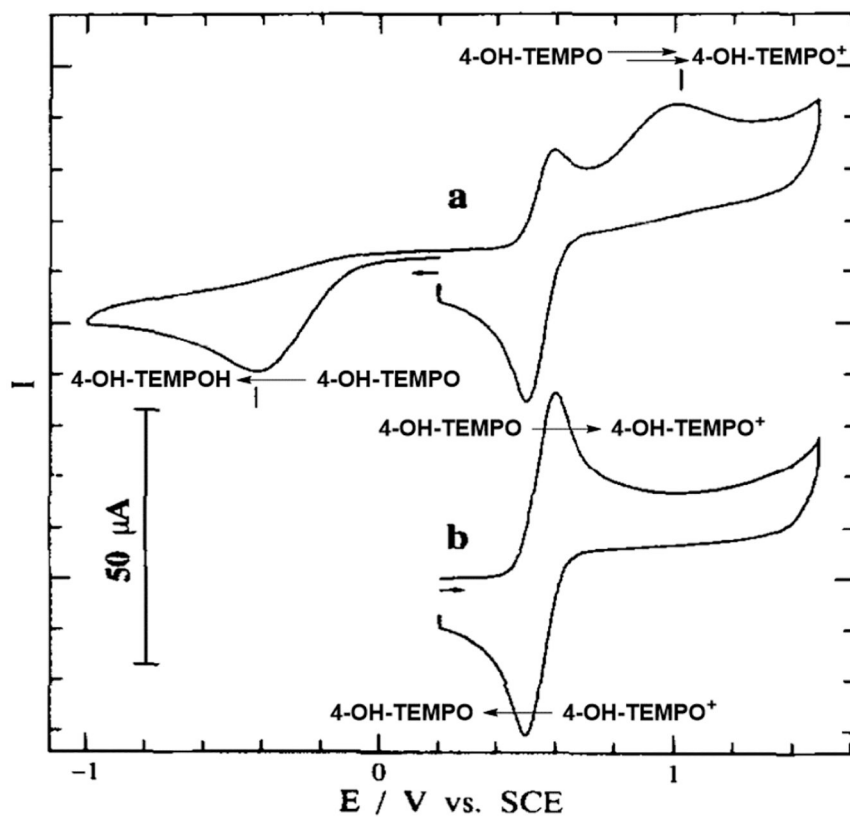
CV of (a) TEMPO and (b) DTBO. Analyses conducted with 5 mM aminoxyl radical in 0.5 M LiClO_4 in acetonitrile (CH_3CN) at a platinum electrode. Scan rate = 92 mV s^{-1} .

Aminoxyl redox reactions have been added for clarity. Adapted with permission from ref. 54. Copyright 1973 Elsevier.

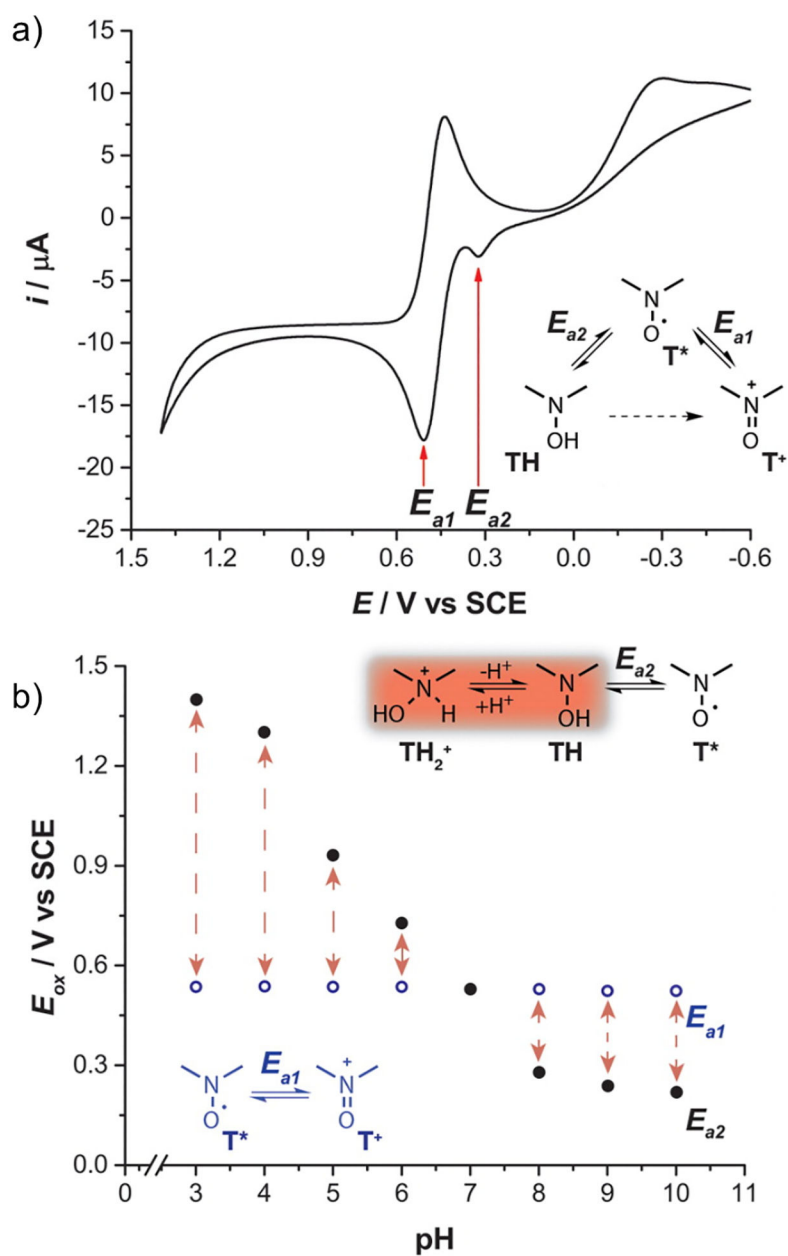


Scheme 8.

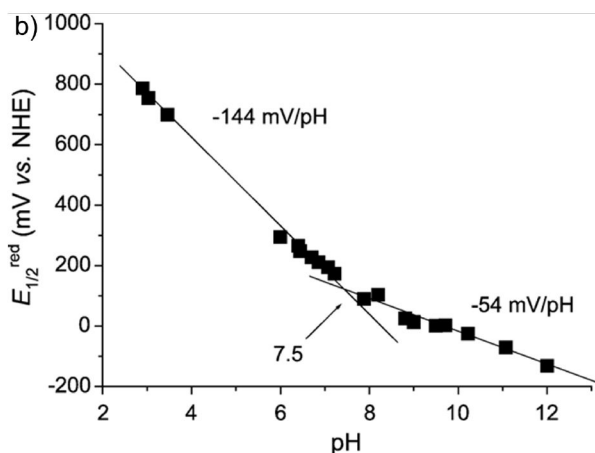
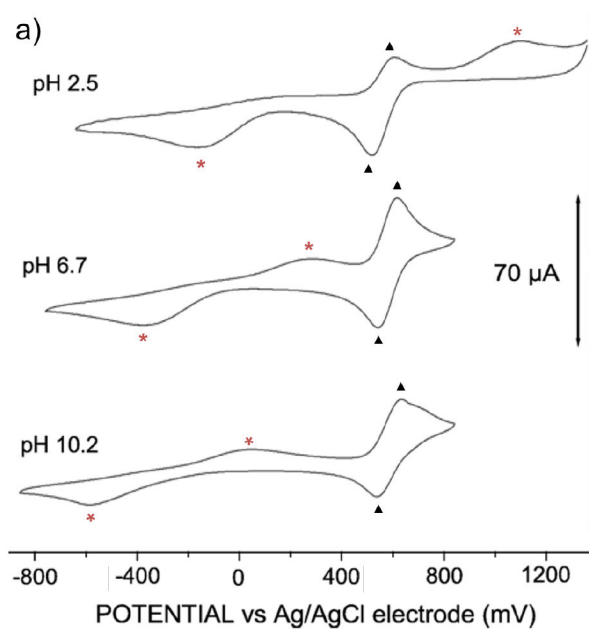
a) CV of TEMPO revealing the generation of TEMPOH and electronic absorption spectra of TEMPO recorded during (b) electrooxidation and (c) electroreduction. Potentials of +0.65 V and -0.80 V vs. SCE were applied for oxidation and reduction, respectively. Redox reactions have been added for clarity. Analyses conducted in an aqueous solution of NEt_4ClO_4 (0.08 M). Adapted with permission from ref. 58. Copyright 1988 American Chemical Society.

**Scheme 9.**

CVs of 4-OH-TEMPO (2.40 mM) with a (a) cathodic potential sweep prior to the anodic sweep, and (b) anodic sweep starting at 0.2 V. Redox reactions have been added for clarity. Analyses conducted in pH 4.3 Robinson buffer. Adapted with permission from ref. 59. Copyright 1995 Elsevier.

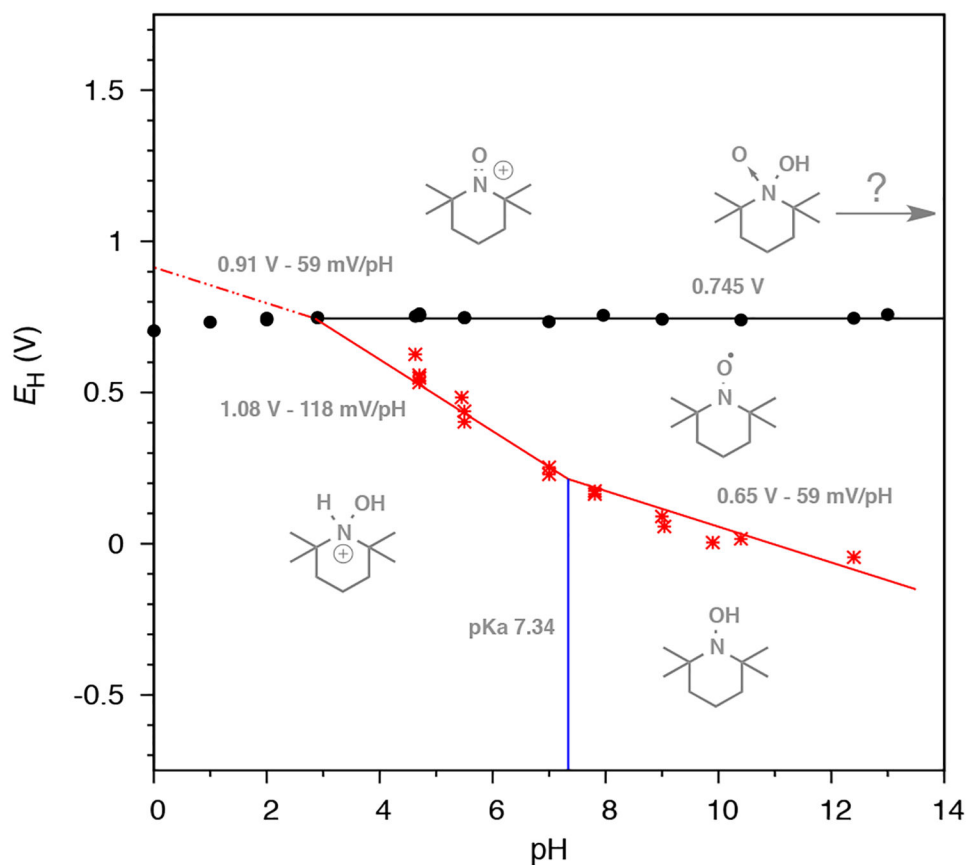
**Scheme 10.**

a) Representative CV of an aminoxyl radical highlighting the anodic peak potentials E_{a1} and E_{a2} . b) Comparison of the oxidation potentials for the (O) TEMPO/TEMPO⁺ and (●) TEMPO/TEMPOH redox couples at varying pH. Reprinted with permission from ref. 60. Copyright 2015 American Chemical Society.

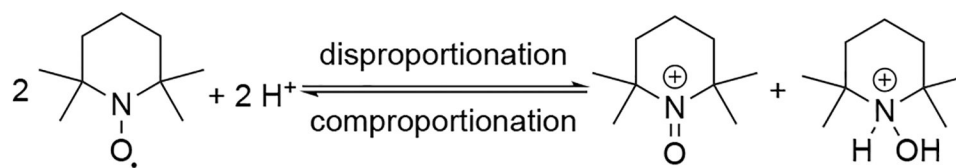


Scheme 11.

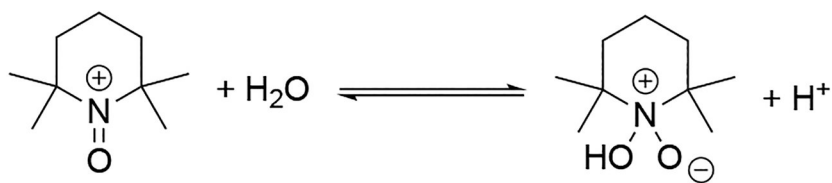
a) CVs of 4-OH-TEMPO (4.6 mM) in aqueous phosphate buffer. Labels for the (*) 4-OH-TEMPOH/4-OH-TEMPO and (\blacktriangle) 4-OH-TEMPO/4-OH-TEMPO⁺ redox couples have been added for clarity. Scan rate = 100 mV s⁻¹. b) Changing $E_{1/2}$ as a function of pH for TEMPO (4.6 mM) in aqueous phosphate buffer. Adapted with permission from ref. 61. Copyright 2009 John Wiley & Sons, Ltd.

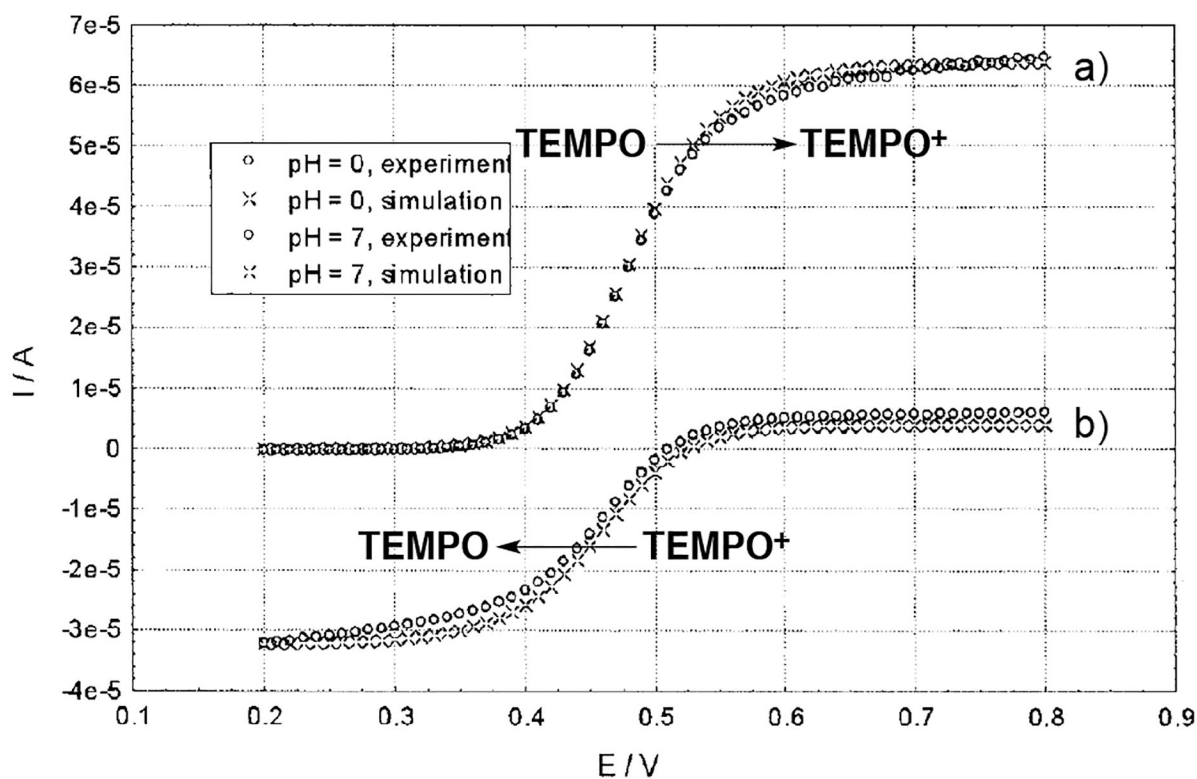
**Scheme 12.**

Pourbaix diagram of TEMPO under buffered aqueous solutions. The hydroxylammonium pK_a values shown were determined by NMR. Line fits have been constrained to have slopes corresponding to 0, 1, or 2 H^+/e^- , and to intersect at points. Black circles and lines correspond to oxoammonium reduction to the nitroxyl, red stars and solid lines correspond to aminoxyl reduction, and the dashed red line corresponds to the theoretical $2 e^-/2 H^+$ oxidation of hydroxylammonium to oxoammonium. E_H denotes redox potential referenced to NHE. Reprinted with permission from ref. 63. Copyright 2018 American Chemical Society.

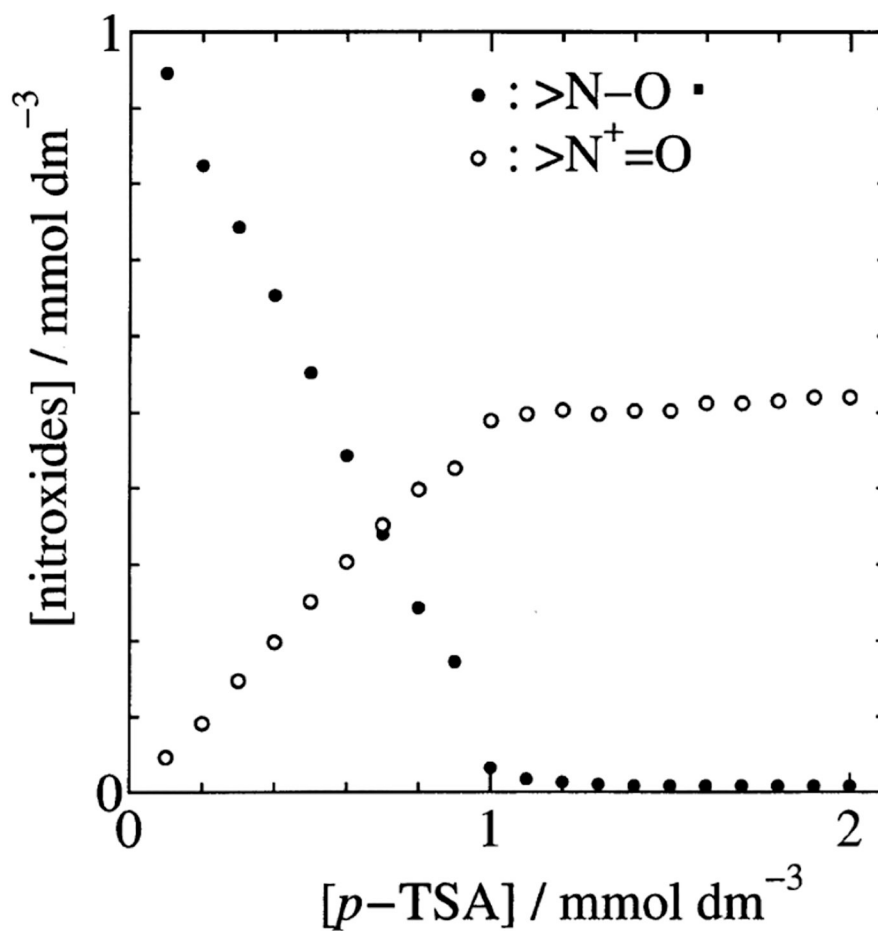
**Scheme 13.**

Disproportionation-comproportionation equilibrium of TEMPO and TEMPOH₂⁺/TEMPO⁺ under acidic conditions.

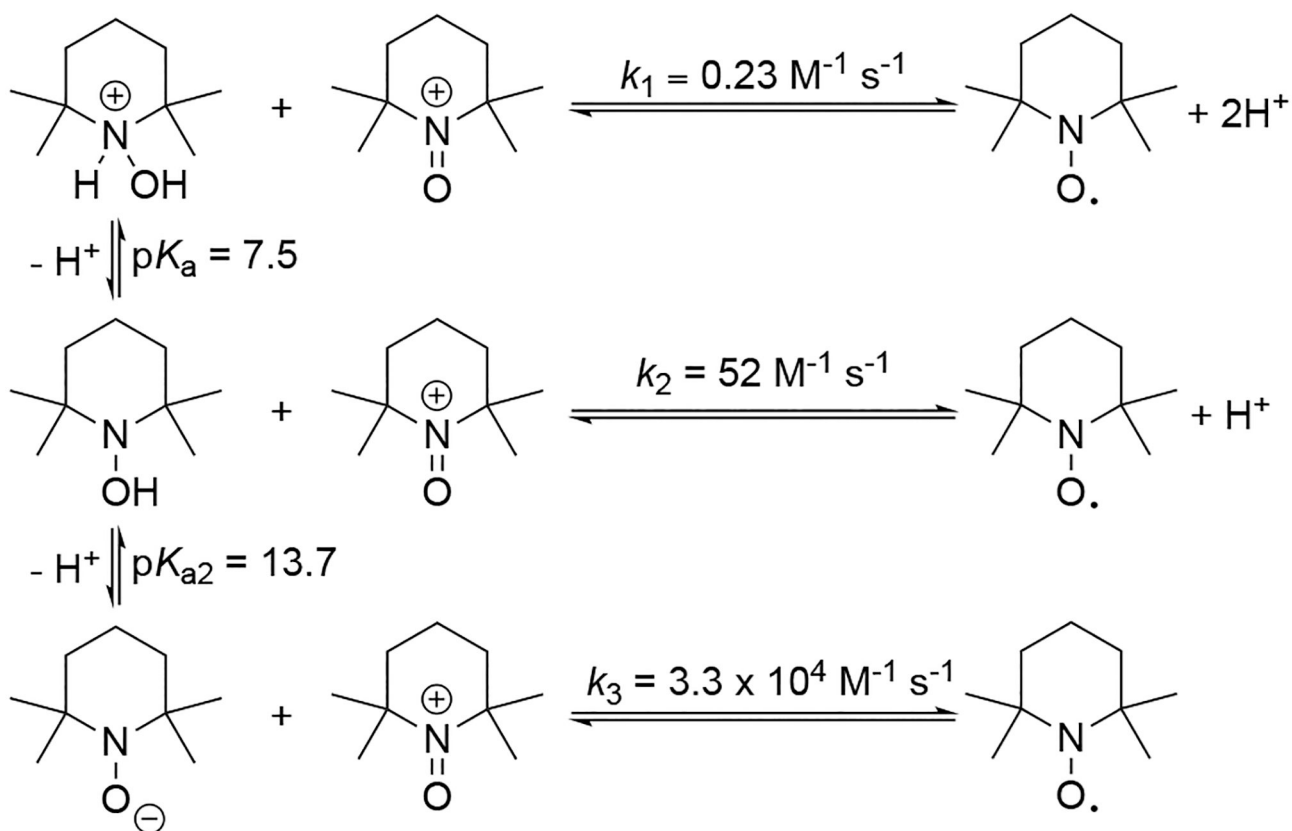
**Scheme 14.**Adduct formation of TEMPO⁺ with hydroxide ion.

**Scheme 15.**

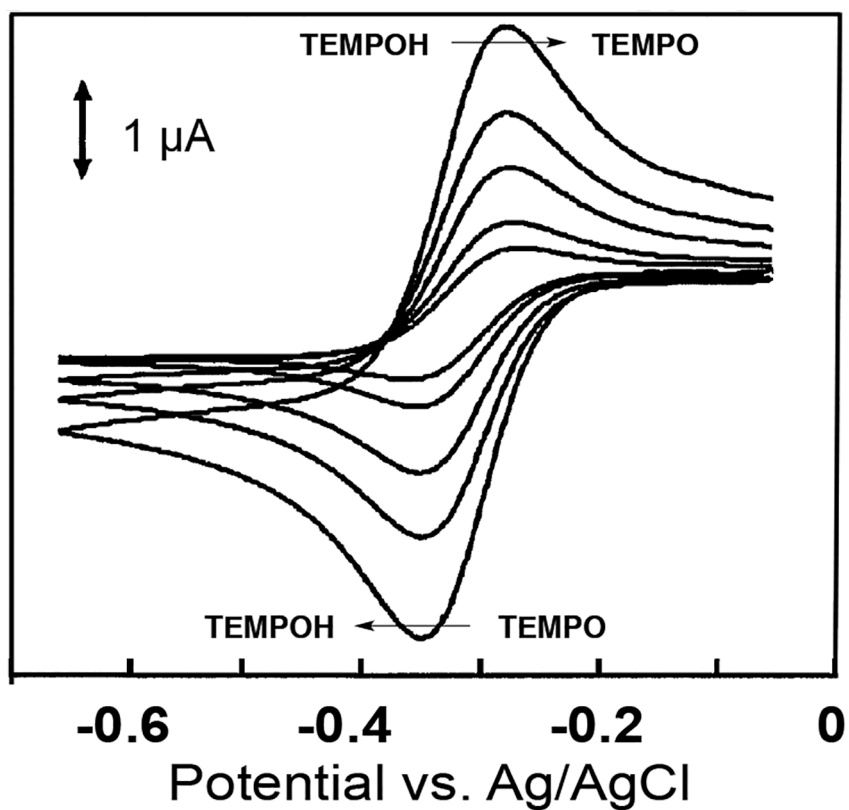
Digitally simulated and experimental steady-state voltammograms using RDE in aqueous solution under (a) neutral and (b) acidic conditions. Experimental data for 1 mM TEMPO in (a) 1 M NaClO₄ (pH 7) and (b) 1 M HClO₄ (pH 0). Redox reactions have been added for clarity. Adapted with permission from ref. 64. Copyright 2004 WILEY-VCH Verlag GmbH&Co. KGaA.

**Scheme 16.**

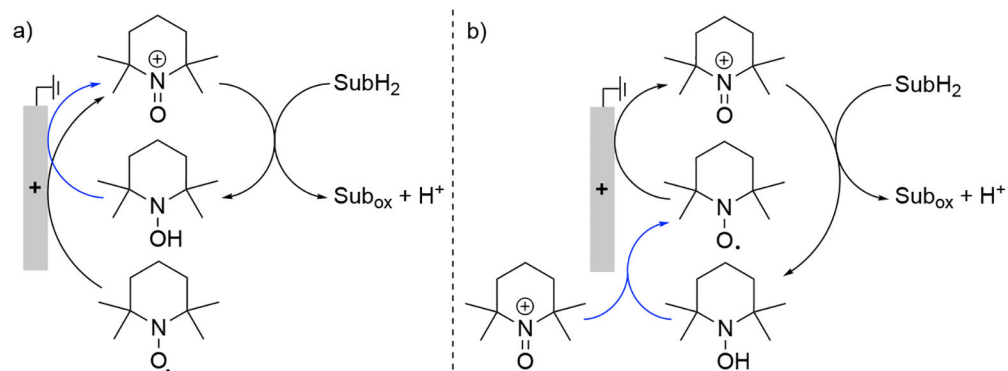
Concentration profile of (●) TEMPO and (○) TEMPO⁺ obtained from limiting currents as a function of the concentration of *p*-TSA in CH₃CN containing 0.2 M NaClO₄. Reprinted with permission from ref. 67. Copyright 2003 Elsevier.

**Scheme 17.**

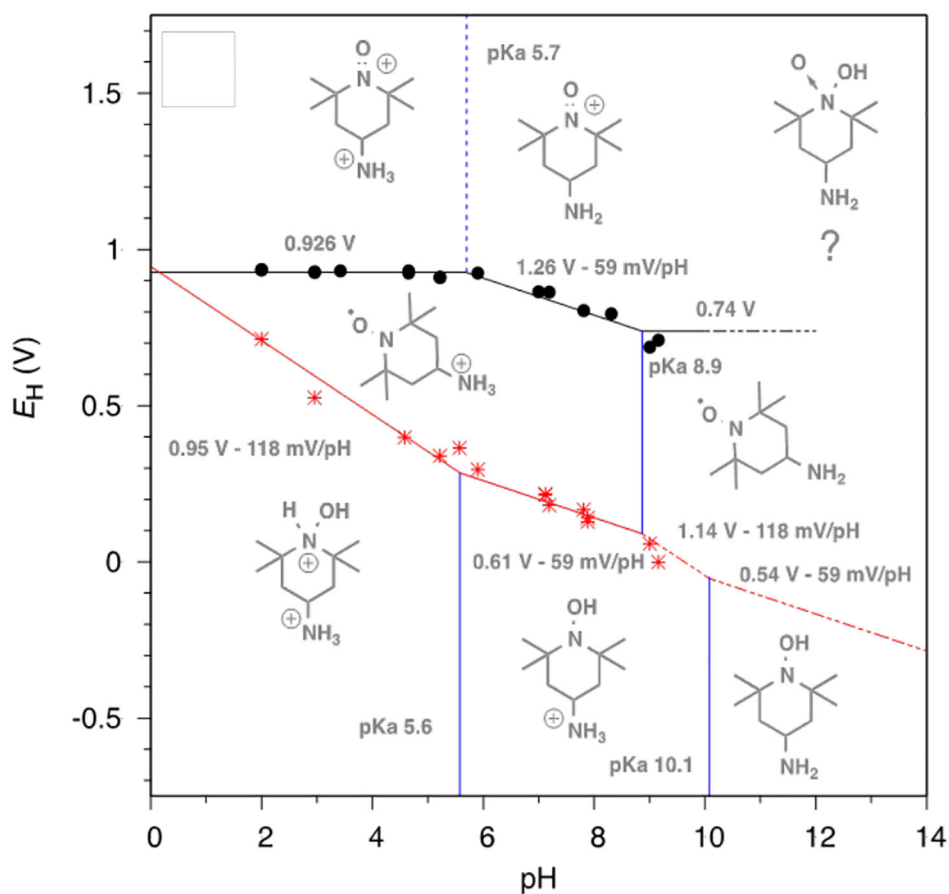
The acid-base equilibria of TEMPOH and the rate constants of the comproportionation reaction for the different forms of TEMPOH with TEMPO⁺.⁶¹

**Scheme 18.**

Reversible CVs, at different scan rates, of the TEMPOH/TEMPO redox couple at the surface of a mercury drop electrode. Redox reactions have been added for clarity. Adapted with permission from ref. 70. Copyright 2002 Japan Society for Analytical Chemistry.

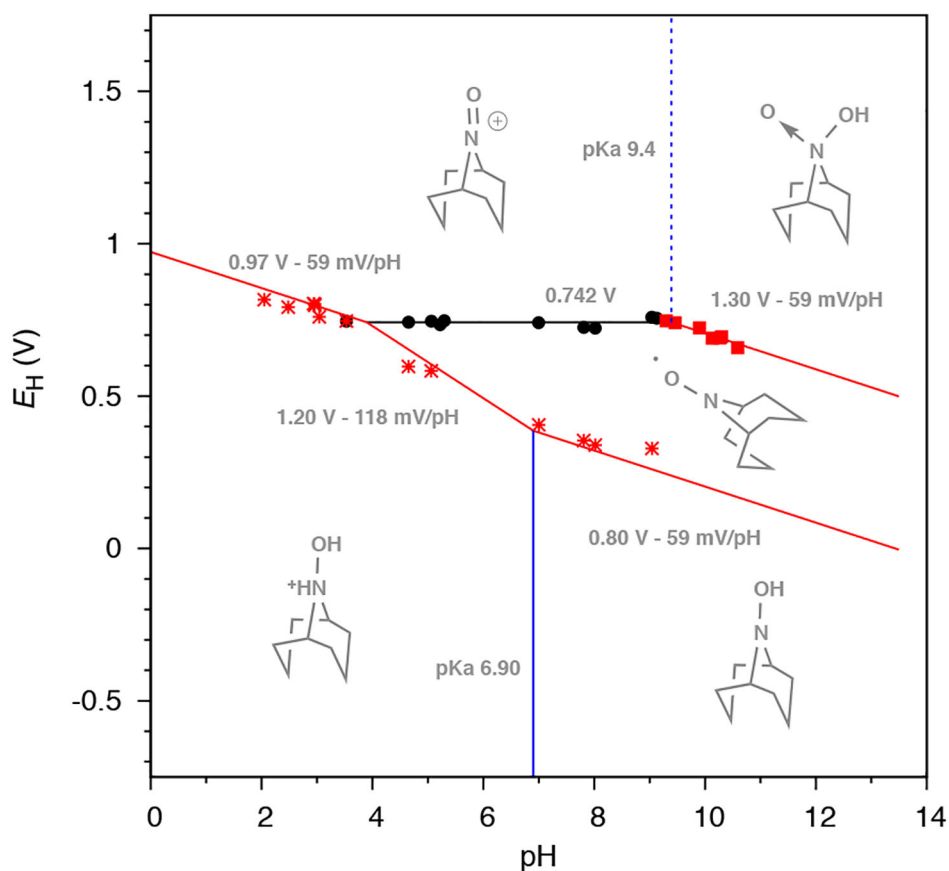
**Scheme 19.**

Possible mechanisms for regeneration of TEMPO⁺ in electrocatalytic reactions, a) direct electron transfer and b) comproportionation.

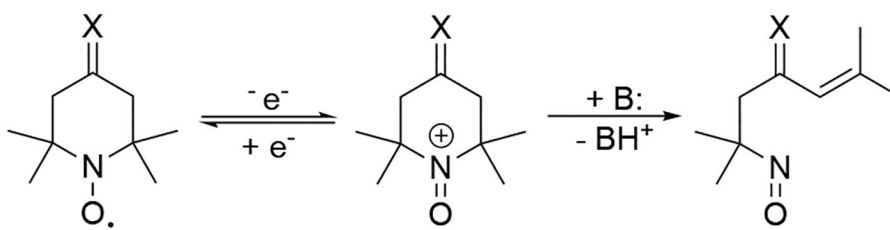


Scheme 20.

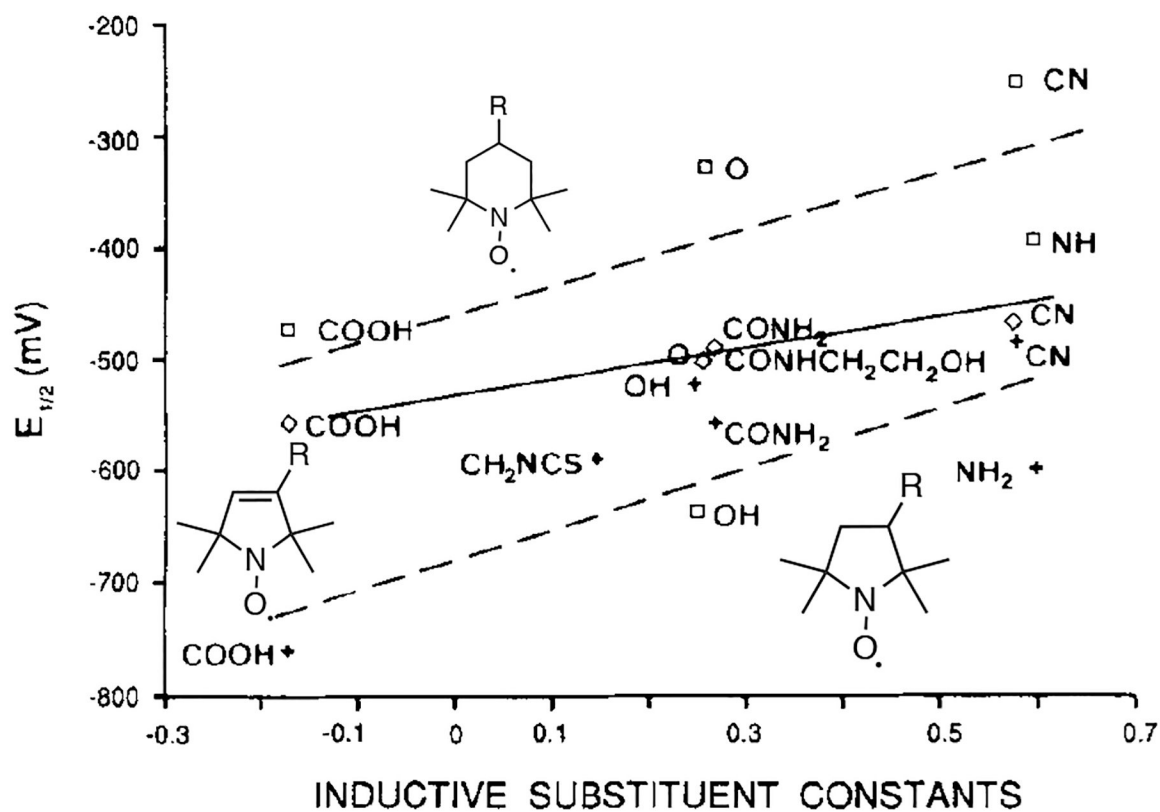
The Pourbaix diagram of 4-NH₂-TEMPO under buffered aqueous conditions. Line fits have been constrained to have slopes corresponding to 0, 1, or 2 H⁺/e⁻, and to intersect at points. Black circles and lines correspond to oxoammonium reduction, red stars and lines correspond to aminoxyl reduction. Dashed red lines are redox potentials inferred from spectroscopic pK_a data. Blue solid lines correspond to pK_a values measured by NMR, blue dashed line corresponds to pK_a value inferred by voltammetric data. E_H denotes redox potential referenced to NHE. Reprinted with permission from ref. 63. Copyright 2018 American Chemical Society.

**Scheme 21.**

The Pourbaix diagram of ABNO under buffered aqueous conditions. Line fits have been constrained to have slopes corresponding to 0, 1, or 2 H^+/e^- , and to intersect at points. Black circles and lines correspond to aminoxyl oxidation, red squares correspond to aminoxyl oxidation to hydroxylamine *N*-oxide, and red stars correspond to hydroxylamine or hydroxylammonium oxidation. Blue solid line corresponds to $\text{p}K_a$ measured by NMR, blue dashed line corresponds to $\text{p}K_a$ value inferred by voltammetric data. E_H denotes redox potential referenced to NHE. Reprinted with permission from ref. 63. Copyright 2018 American Chemical Society.

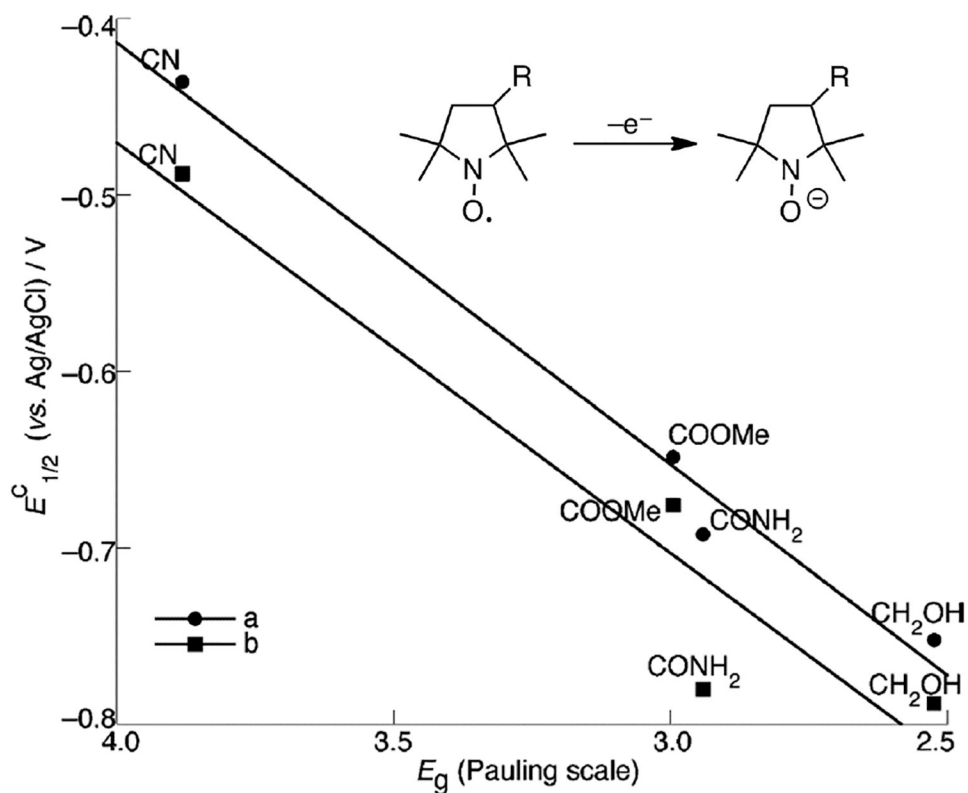
**Scheme 22.**

Suggested degradation pathway of electron-deficient oxoammonium ion under basic conditions.

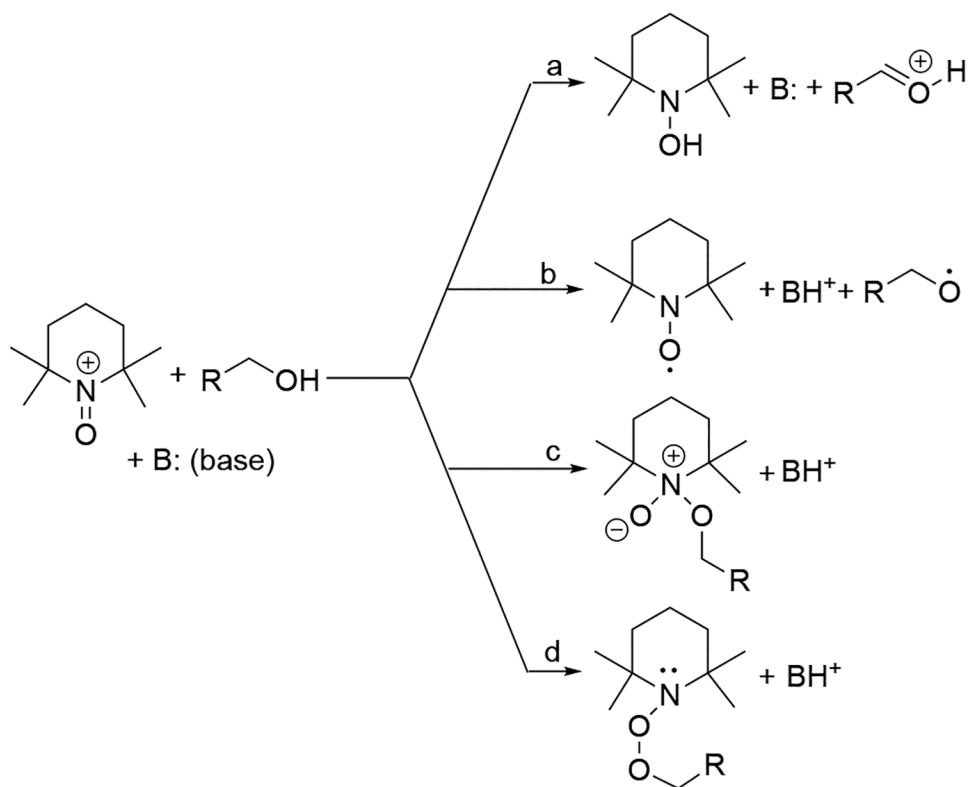


Scheme 23.

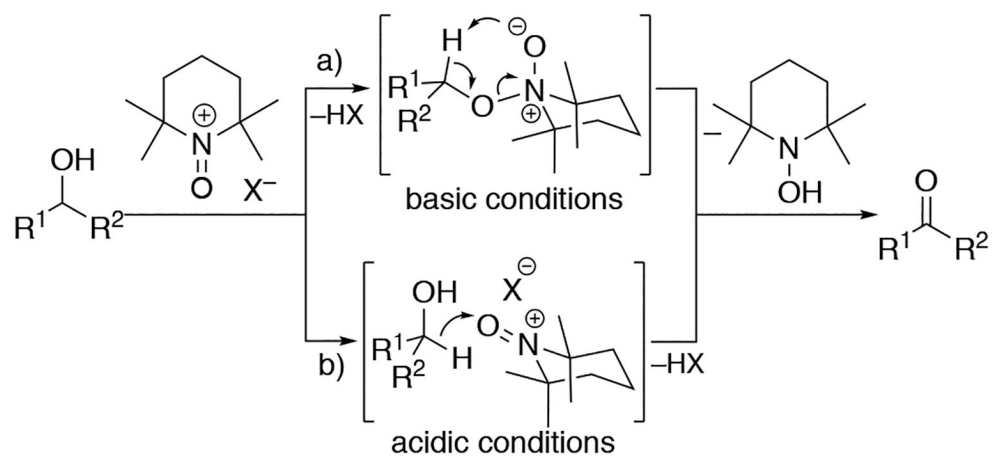
Correlation of inductive constants and half-wave potentials of different hydroxylamine/aminoxyl radicals couples for (□) piperidine structures, (+) pyrrolidine structures, (○) pyrroline structures. Analyses were conducted in pH 7.2–7.4 phosphate buffer at a Hg drop electrode. Adapted with permission from ref. 84. Copyright 1991 Elsevier.

**Scheme 24.**

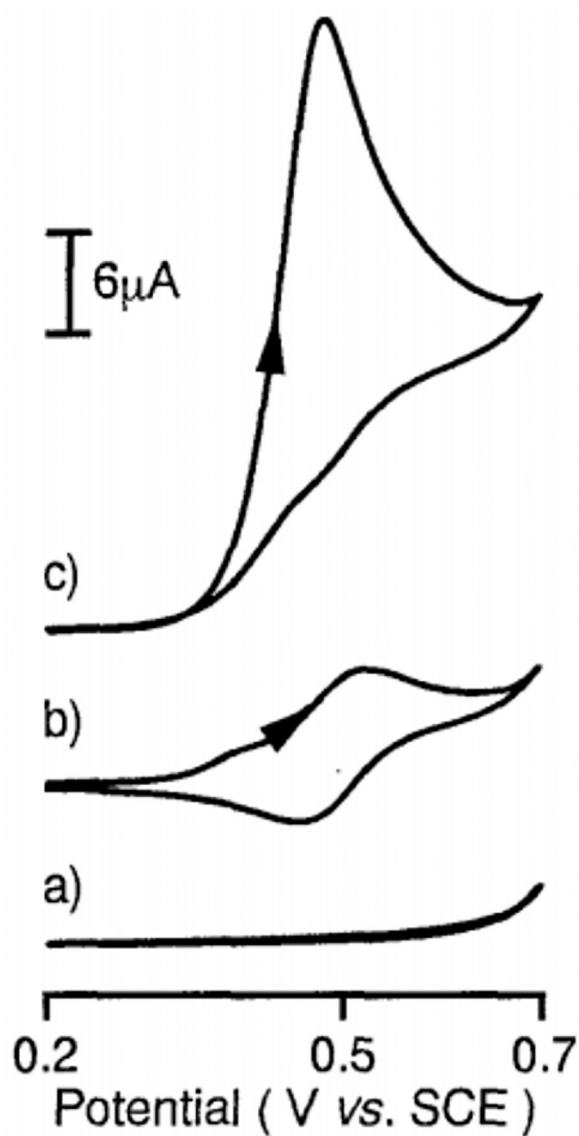
Correlation between the Pauling group electronegativity (E_g) of substituents vs. redox potentials ($E_{1/2}$) for the five-membered ring hydroxylamine/aminoxyl radicals in (a) MeOH (0.1 M Bu₄NClO₄) and (b) phosphate buffer (0.1 M, pH 7.4). The general structure of the aminoxyl radicals and the corresponding electron transfer reaction have been added. Adapted with permission from ref. 74. Copyright 2007 Royal Society of Chemistry.

**Scheme 25.**

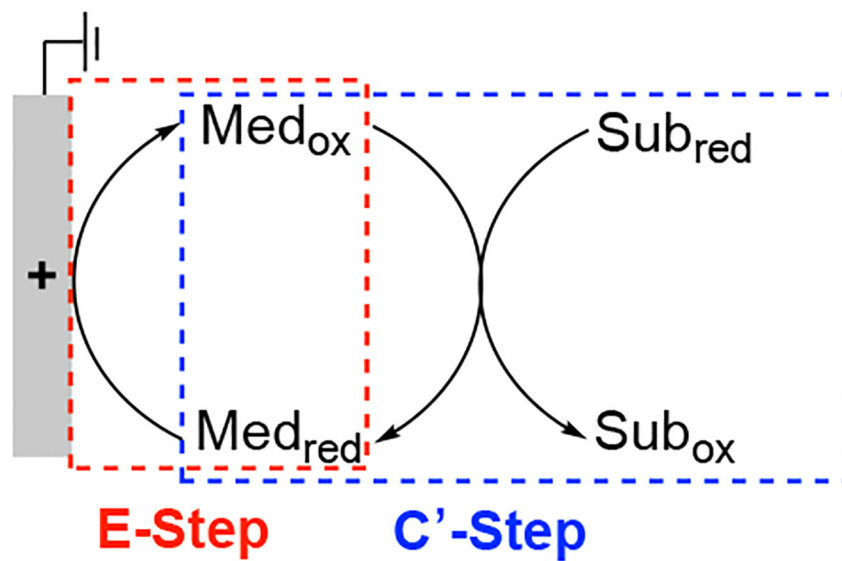
Proposed mechanistic paths for the TEMPO⁺-mediated oxidation of alcohols in the presence of base.⁹⁰

**Scheme 26.**

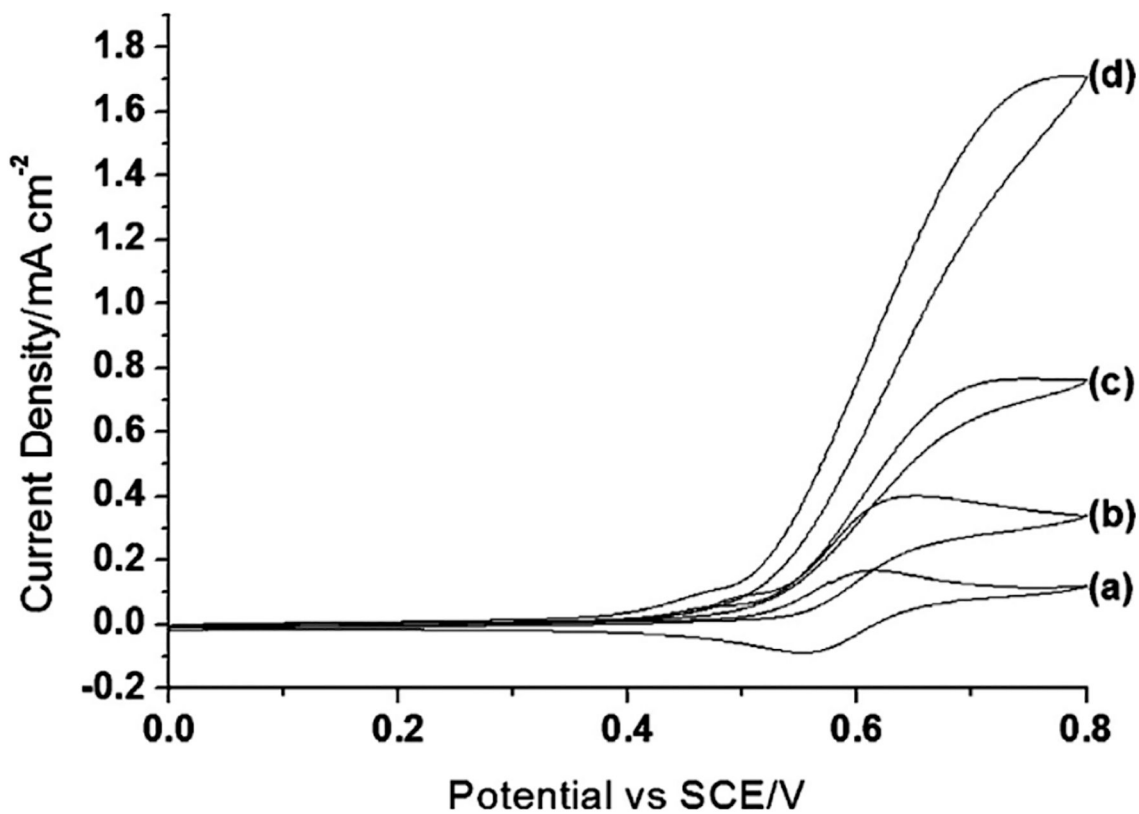
Rationale for the pH-dependent change in the mechanism and reaction selectivity in the reaction of TEMPO⁺ and alcohols under a) basic and b) acidic conditions.

**Scheme 27.**

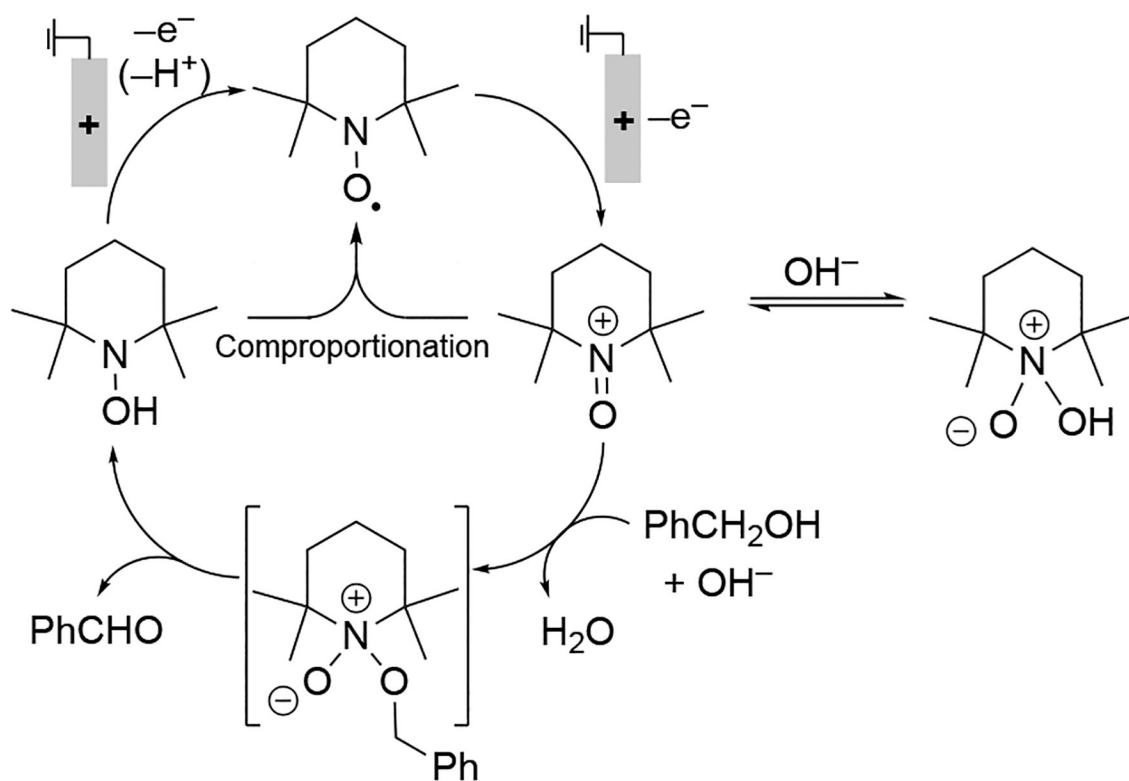
CVs of (a) blank electrolyte solution, (b) TEMPO, (c) TEMPO in the presence of 1-pentanol. Analyses conducted with 1 mM TEMPO, 1 mM 1-pentanol in aqueous solution of 150 mM NaOH at a glassy carbon electrode at 10 mV s^{-1} . Adapted with permission from ref. 97. Copyright 1996 The Pharmaceutical Society of Japan.



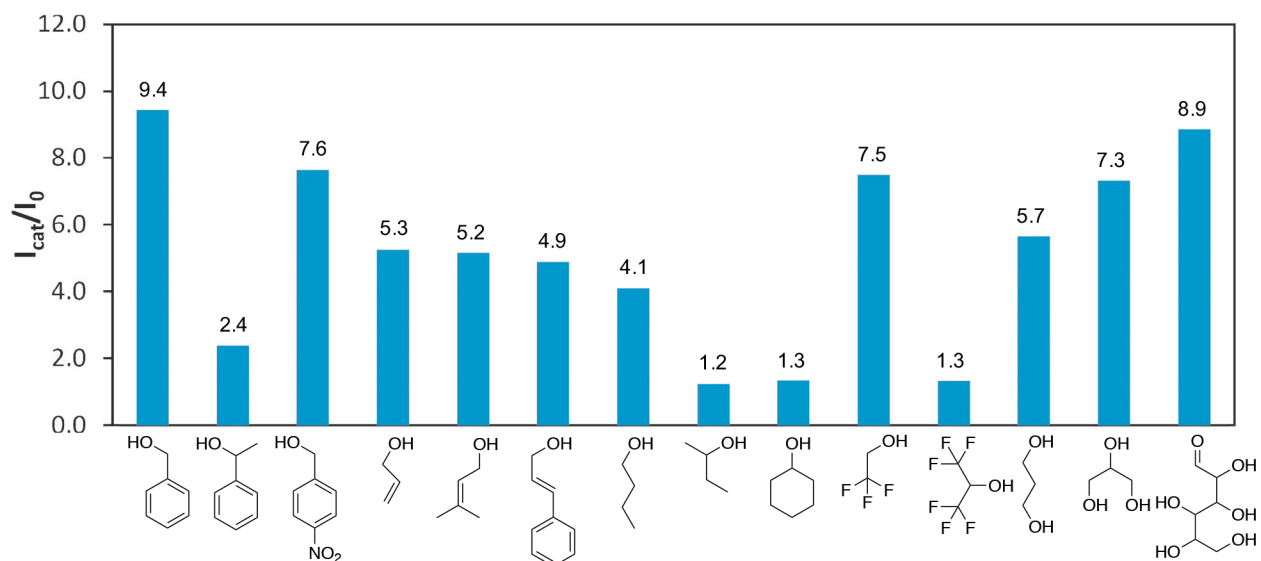
Scheme 28.
Generalized EC' mechanism

**Scheme 29.**

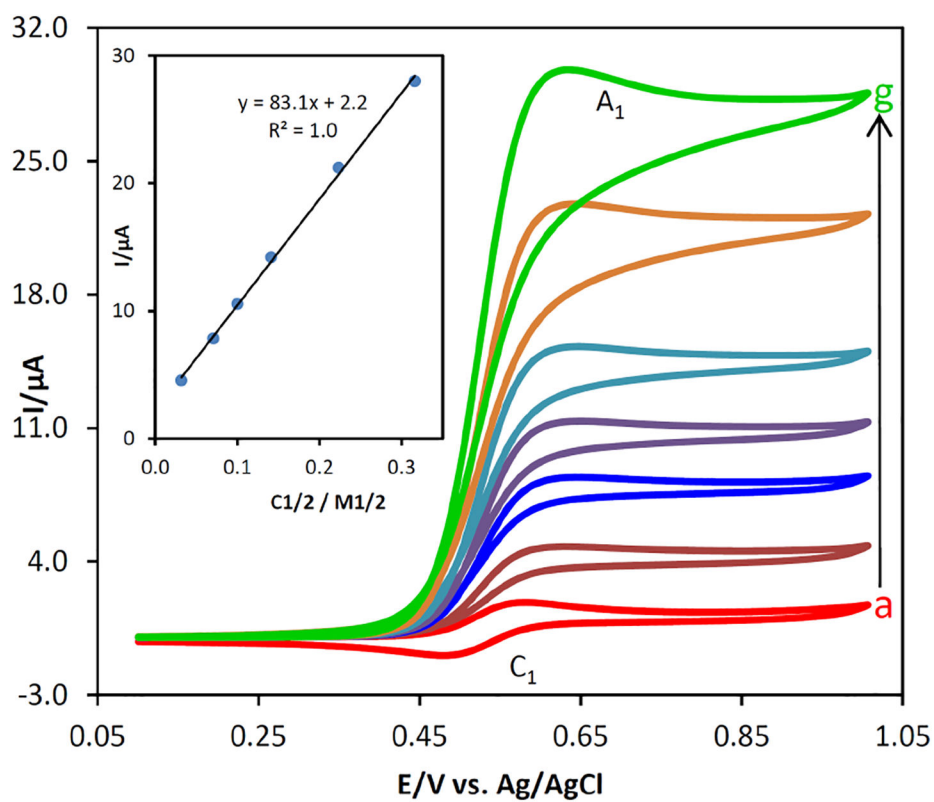
a) CV of 2 mM TEMPO at pH 9.3. CVs of 2 mM TEMPO in the presence of 16 mM benzyl alcohol at b) pH 9.3, c) pH 10.6, d) pH 11.5. Scan rate = 50 mV s⁻¹. Adapted with permission from ref. 69. Copyright 2013 Elsevier.



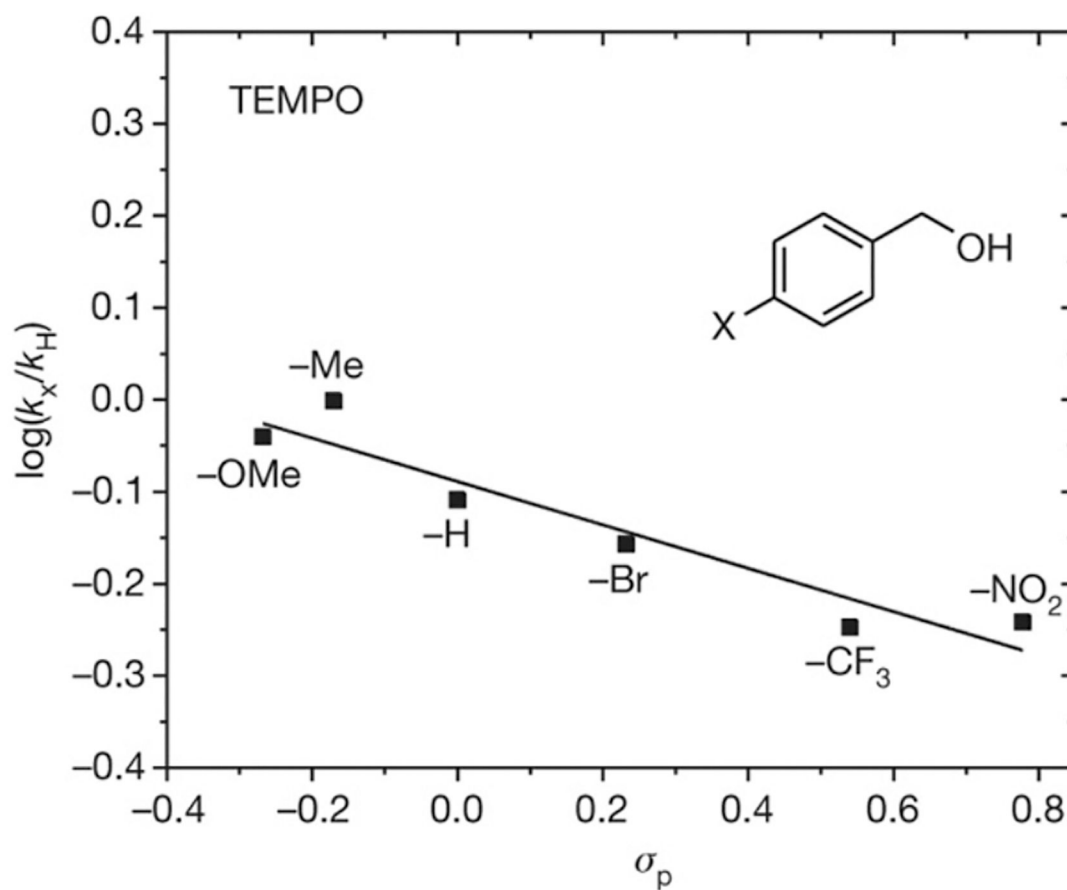
Scheme 30.
Mechanism of TEMPO catalyzed electrochemical oxidation of benzyl alcohol.

**Scheme 31.**

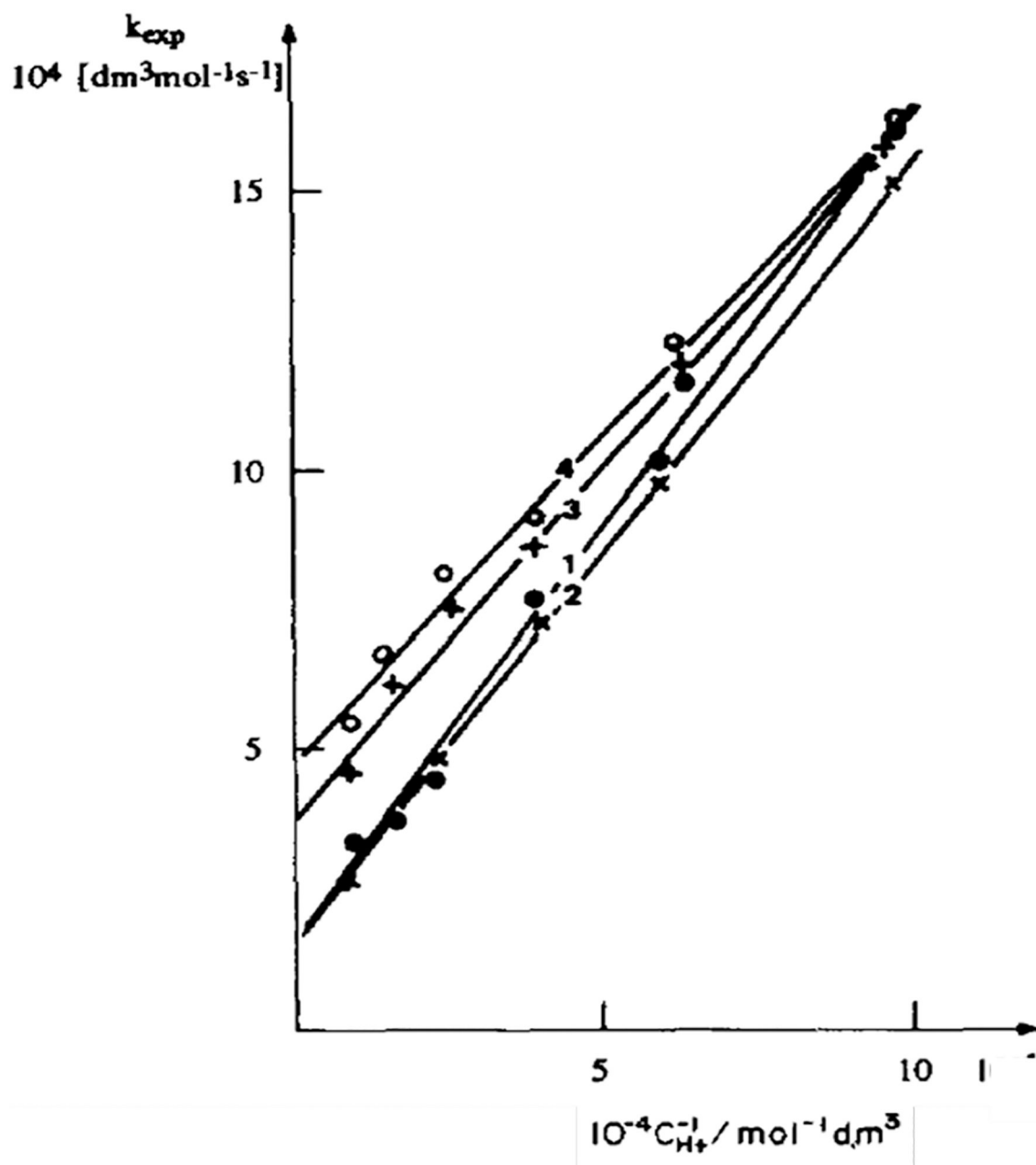
Ratio of the anodic-peak current of the TEMPO/TEMPO⁺ redox couple in the presence of alcohol substrates (i_{cat}) compared to the current in the absence of alcohols (i_0). Analyses conducted with 1 mM TEMPO, 10 mM alcohol in a pH 9.6 aqueous buffer solution at glassy carbon electrode. Reprinted with permission from ref. 68. Copyright 2014 John Wiley and Sons.

**Scheme 32.**

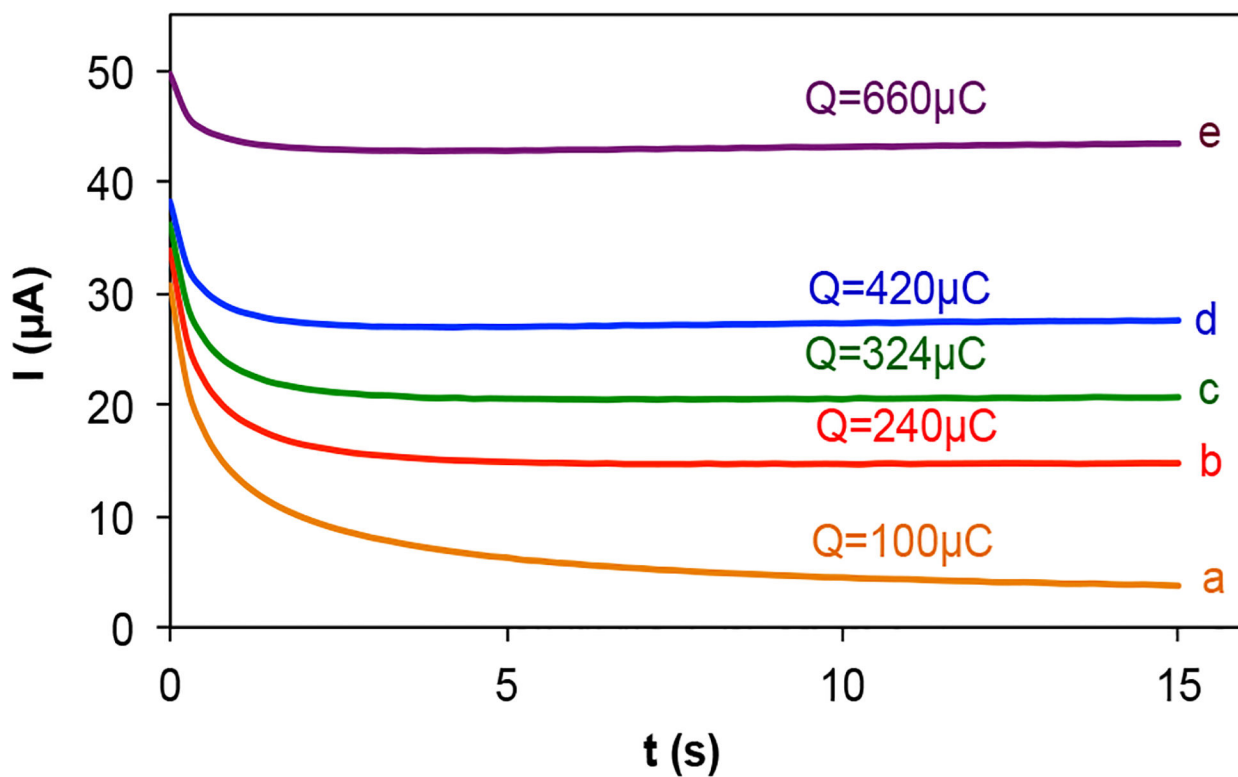
CVs of 1.0 mM TEMPO in the presence of various concentrations of benzyl alcohol at pH 9.6. The concentrations of benzyl alcohol are [increasing from (a) to (g)]: 0.0, 1.0, 5.0, 10.0, 20, 50.0 and 100 mM, and scan rate = 20 mV s^{-1} . The inset shows the linear dependence of the anodic peak current on the square root of the alcohol concentration. Reprinted with permission from ref. 68. Copyright 2014 John Wiley and Sons.

**Scheme 33.**

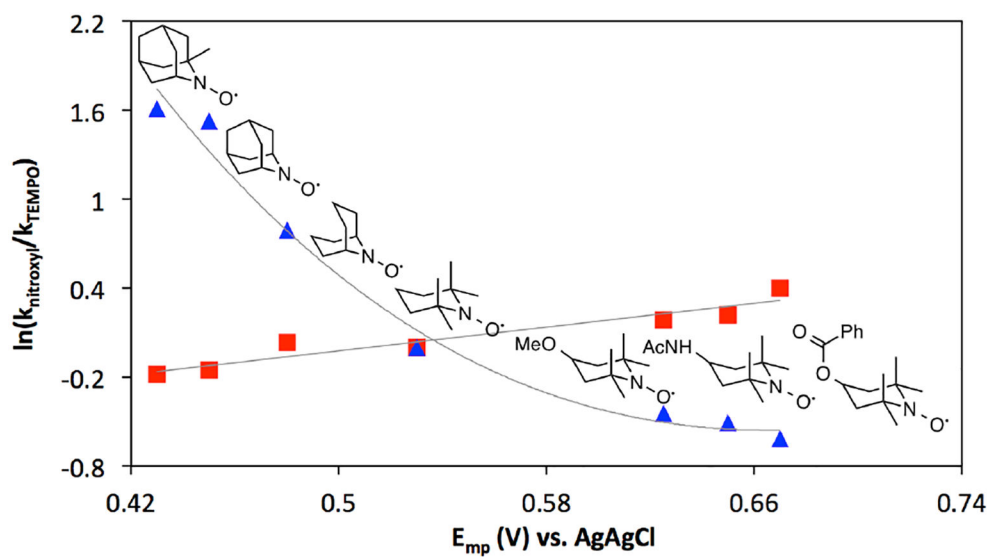
Electronic effects on the TEMPO-catalyzed electrochemical oxidation of benzyl alcohol derivatives. Analyses were conducted with 100 mM alcohol in 0.1 M Bu_4NClO_4 in CH_3CN with 1 mM TEMPO and 450 mM *N*-methylimidazole. Reprinted with permission from ref. 101. Copyright 2016 Nature Publishing Group.

**Scheme 34.**

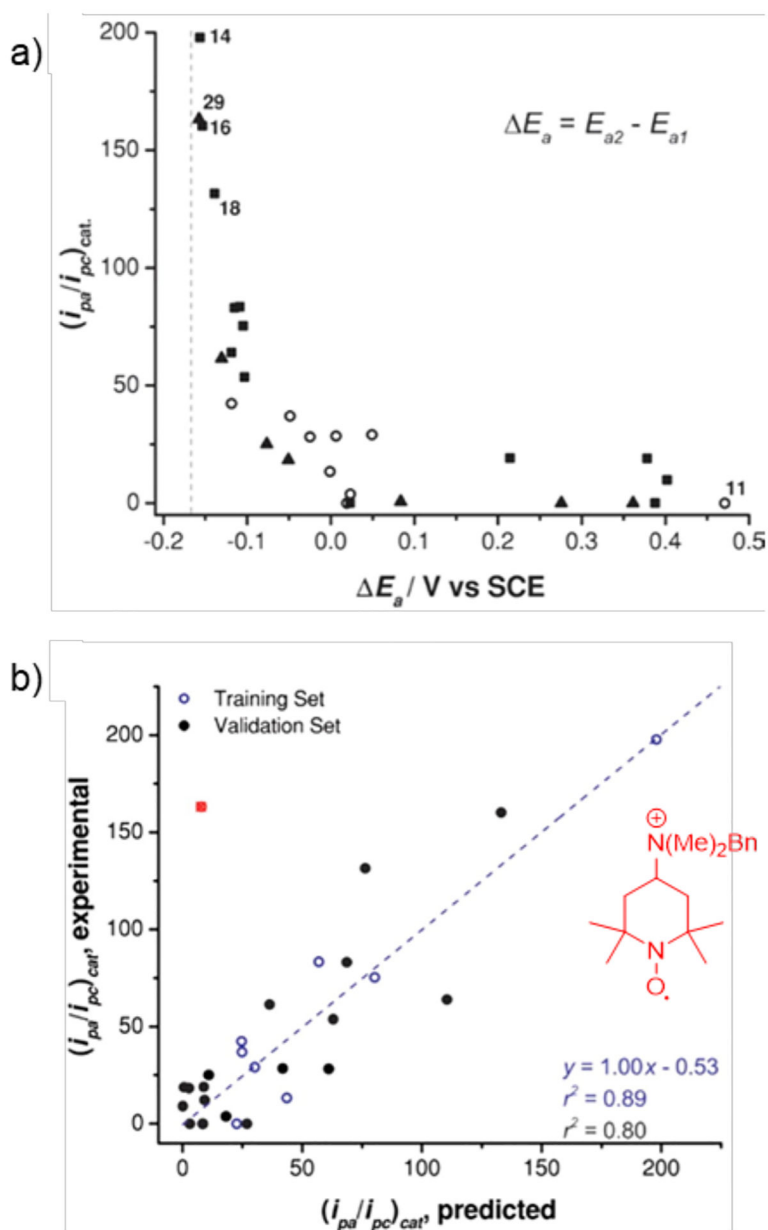
Rate constant of alcohol oxidation by 4-OH-TEMPO as a function of $1/[H^+]$ for (●) propan-1-ol, (x) butan-1-ol, (+) propan-2-ol, and (○) butan-2-ol. Adapted with permission from ref. 106. Copyright 1995 Elsevier.

**Scheme 35.**

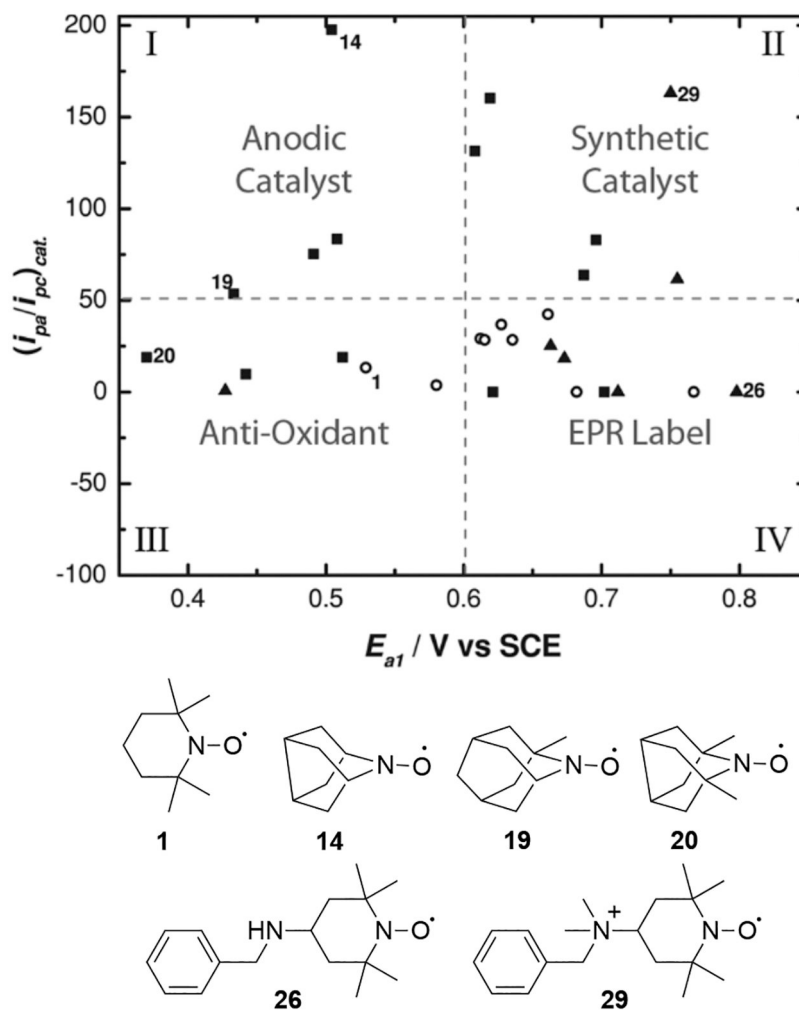
Chronoamperograms of ABNO (1 mM) in the (a) absence and presence of 1-butanol at (b) 5 mM, (c) 10 mM, (d) 20 mM and (e) 50 mM concentrations in $\text{HCO}_3^-/\text{CO}_3^{2-}$ electrolyte (pH 10), applied potential 0.7 V vs. Ag/AgCl. Reprinted with permission from ref. 73. Copyright 2015 American Chemical Society.

**Scheme 36.**

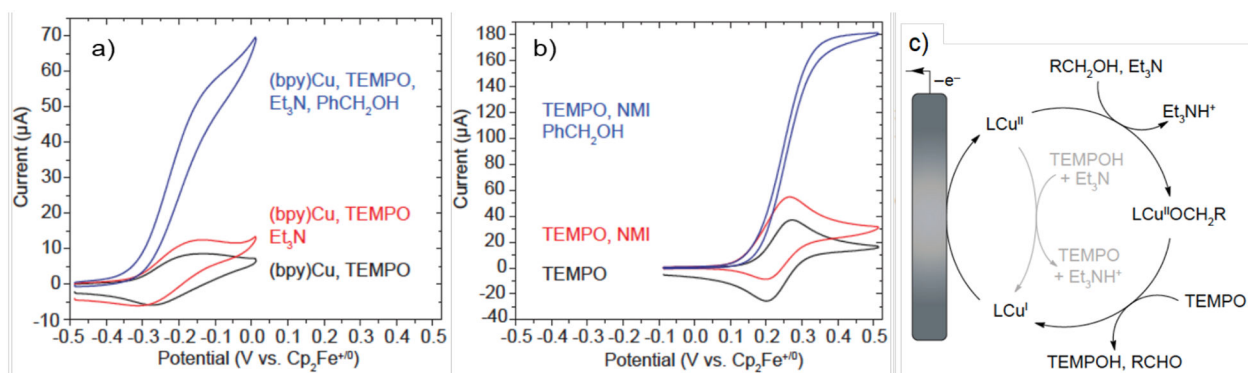
Linear-free-energy correlations for aminoxyl-catalyzed oxidation of 1-butanol with NaOCl as a chemical oxidant (blue triangles) and under electrochemical conditions (red squares). Reprinted with permission from ref. 73. Copyright 2015 American Chemical Society.

**Scheme 37.**

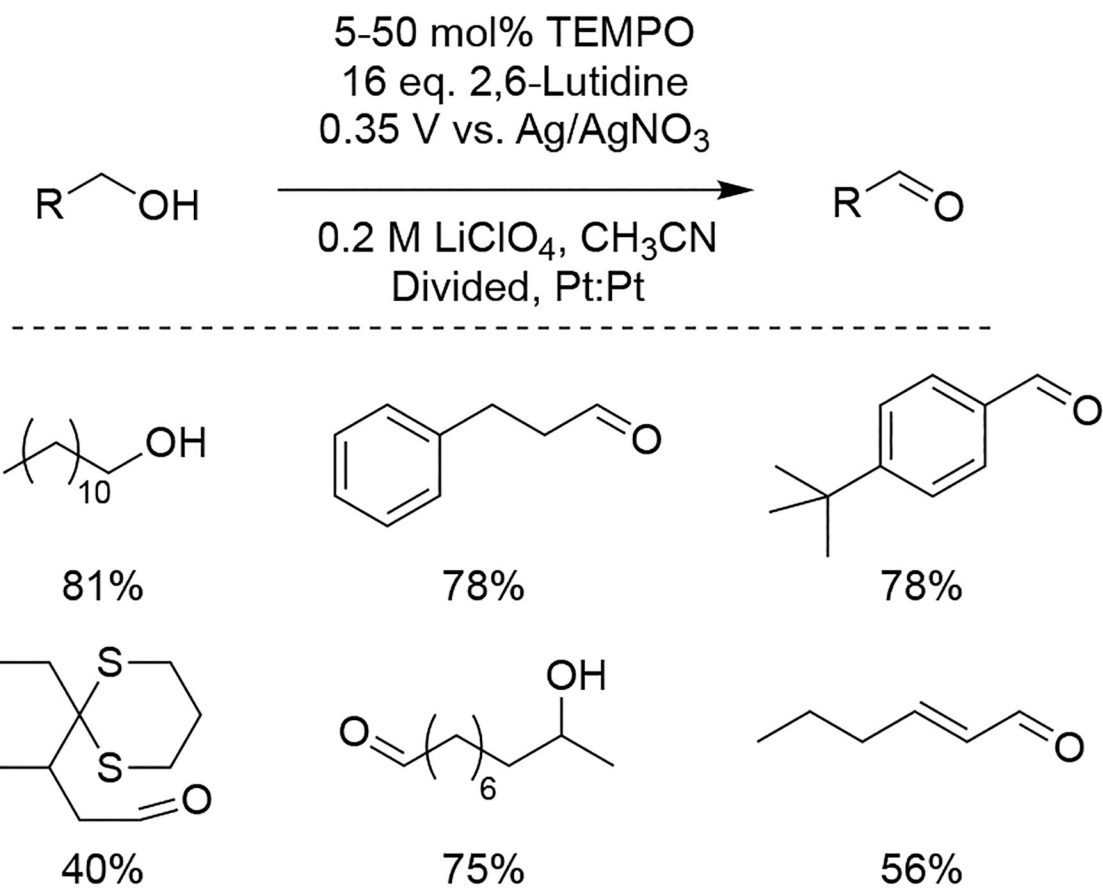
a) Plot demonstrating the asymptotic inverse relationship between E_a and $(i_{pa}/i_{pc})_{cat}$ values for (○) 4-substituted and (▲) 4*N*-substituted TEMPO derivatives and (■) polycyclic species. b) Plot of the computationally predicted values of $(i_{pa}/i_{pc})_{cat}$ versus the corresponding experimental values of the (○) training set, (●) the validation set, and (■) an outlier. Predicted values for $(i_{pa}/i_{pc})_{cat}$ were determined from computed values of E_{a1} and E_{a2} performed using B3LYP/6-31+G(d,p) level of theory with a CPCM solvation model. All experimental values were measured at pH 7. Adapted with permission from ref. 60. Copyright 2015 American Chemical Society.

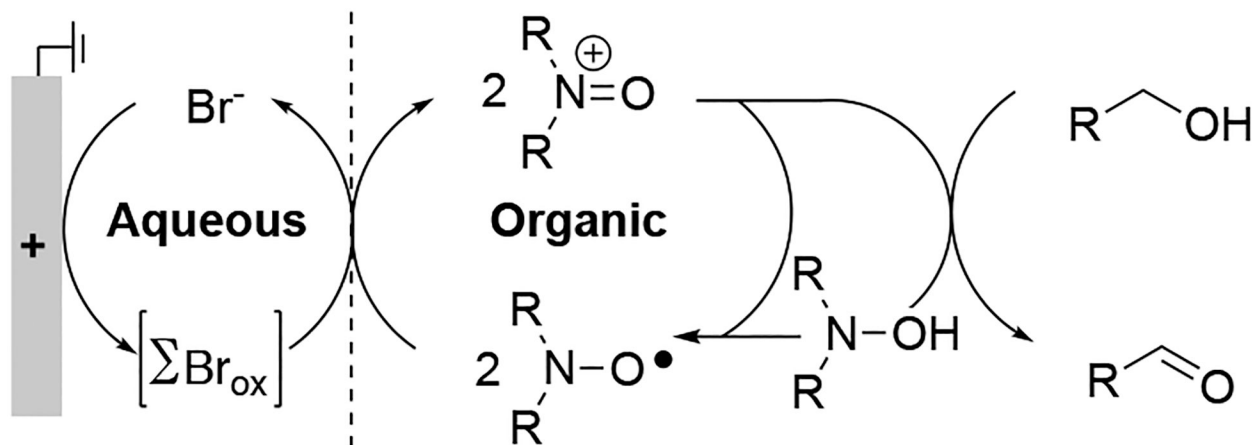
**Scheme 38.**

Plot of the aminoxyl/oxoammonium oxidation potential versus catalytic activity towards glycerol oxidation. (○) 4-Substituted TEMPO derivatives, (▲) 4*N*-substituted TEMPO derivatives, and (■) polycyclic species are represented by different shapes. Representative examples of the aminoxyl radicals in each quadrant are shown below. Adapted with permission from ref. 60. Copyright 2015 American Chemical Society.

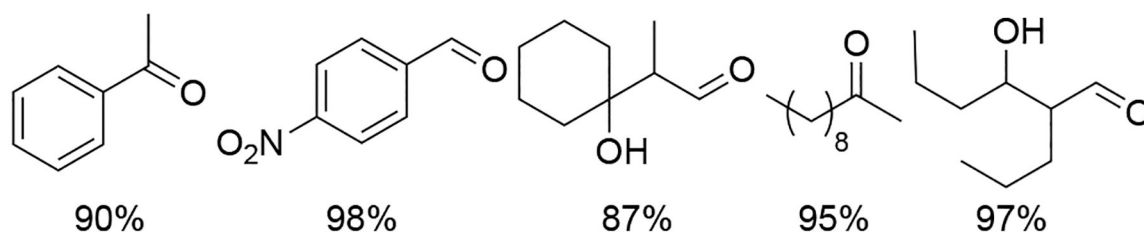
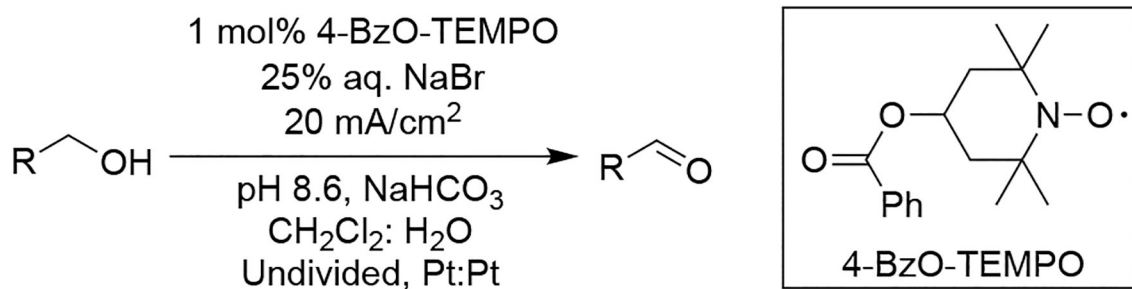
**Scheme 39.**

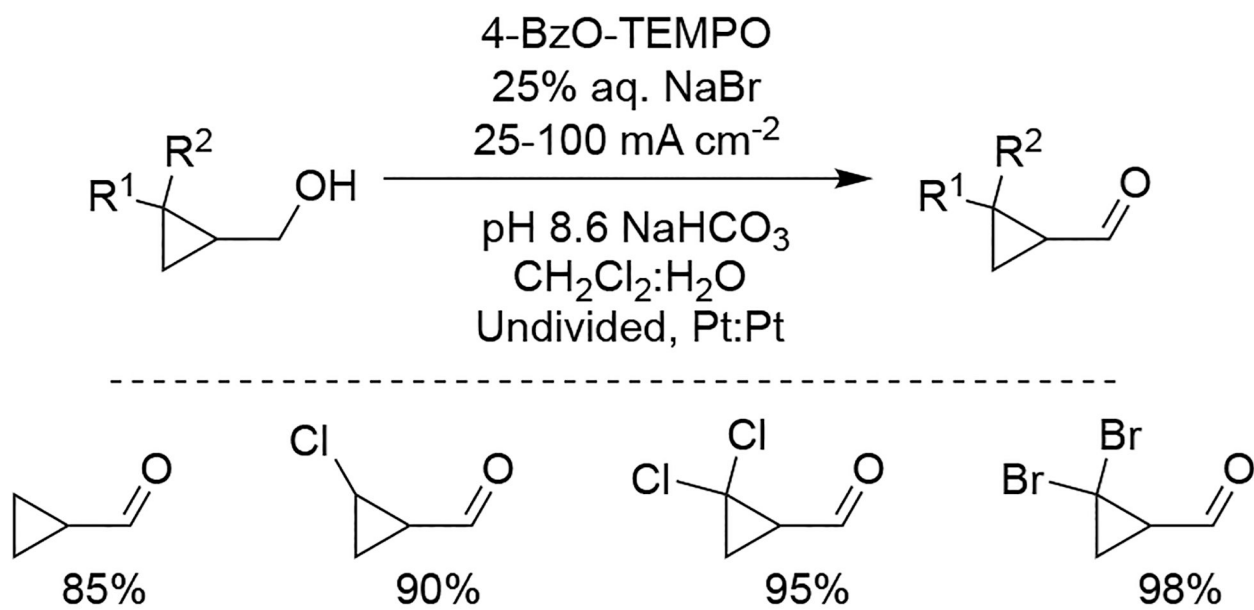
a) CVs of 100 mM benzyl alcohol in the presence of 5 mM TEMPO, 1 mM Cu^IOTf, 1 mM 2,2'-bipyridine (bpy), and 40 mM triethylamine (NEt₃) and b) CVs of 100 mM benzyl alcohol in the presence of 1 mM TEMPO and 450 mM *N*-methyl imidazole. c) Proposed mechanism of cooperative alcohol electrooxidation. Reprinted with permission from ref. 101. Copyright 2016 Nature Publishing Group.

**Scheme 40.**Electrochemical oxidation of aliphatic alcohols with catalytic amounts of TEMPO.⁸⁹

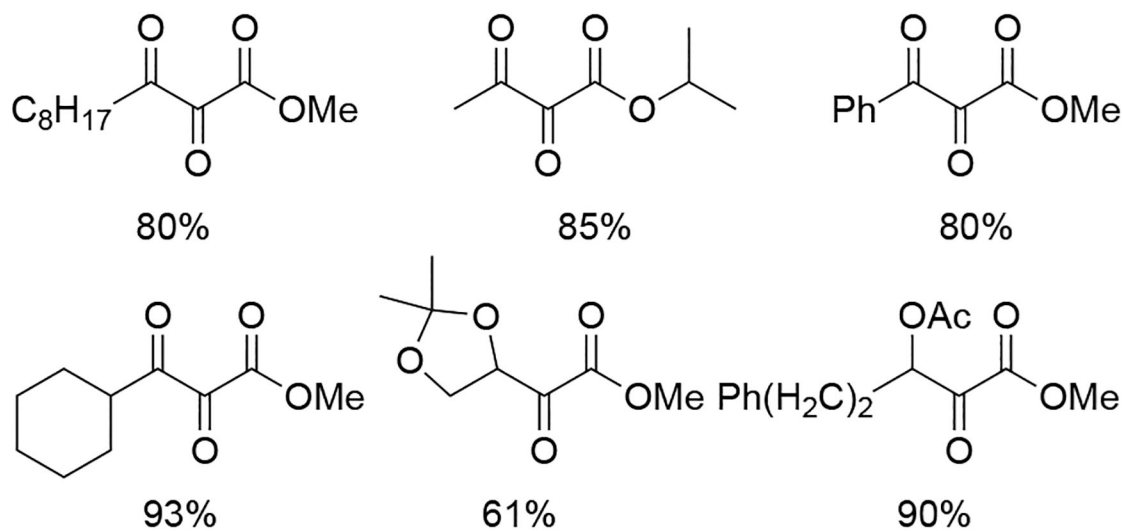
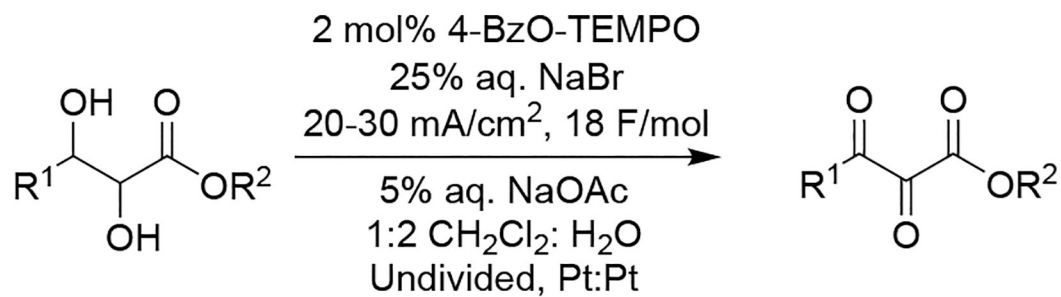
**Scheme 41.**

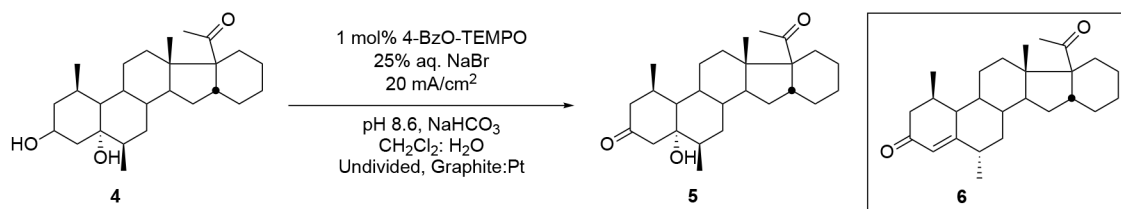
Bromide/aminoxyl double mediatory process for electrochemical alcohol oxidation where ΣBr_{ox} denotes possible bromide electrooxidation products.¹¹⁸

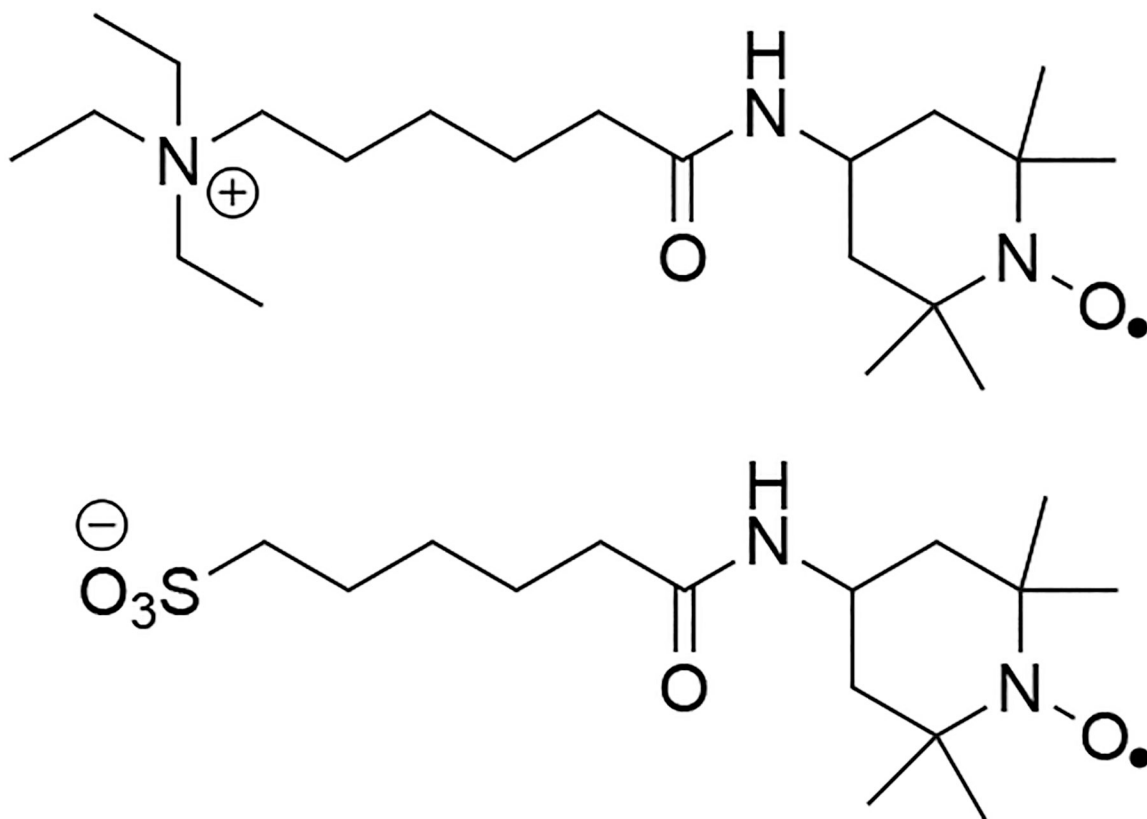
**Scheme 42.**Double mediatory electrochemical oxidation of aliphatic alcohols.¹¹⁸



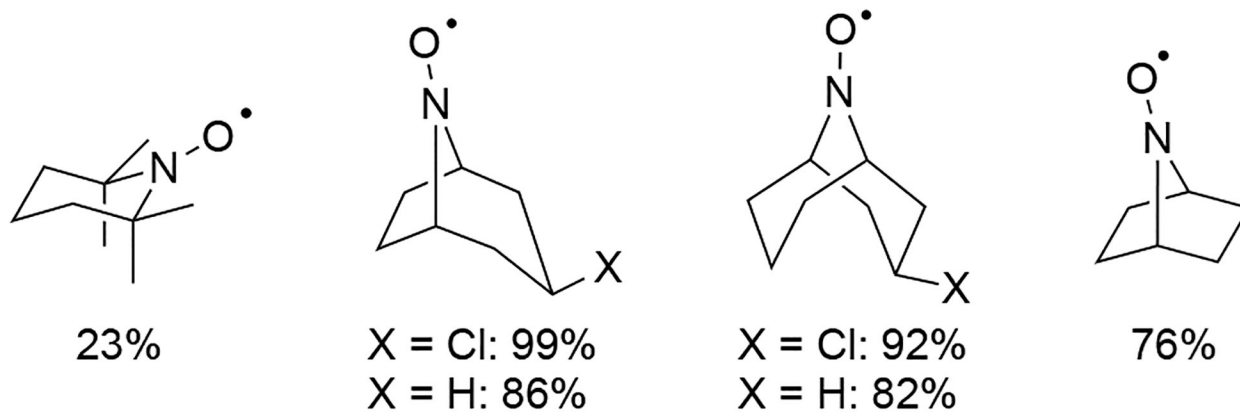
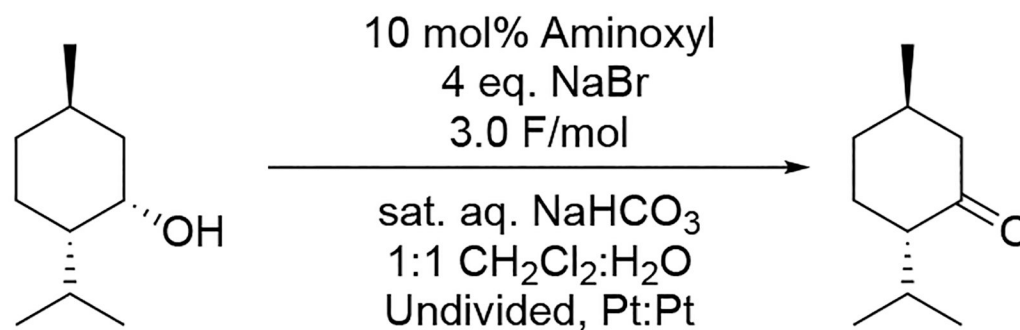
Scheme 43.
Electrochemical oxidation of cyclopropylcarbinols.¹²¹

**Scheme 44.**Double mediatory electrochemical oxidation of dihydroxyalkanoates.¹²²

**Scheme 45.**Oxidation of 6 β -methyl-3 β ,5 α -dihydroxy-16 α ,17 α -cyclohexanopregnan-20-one **4**.¹²³

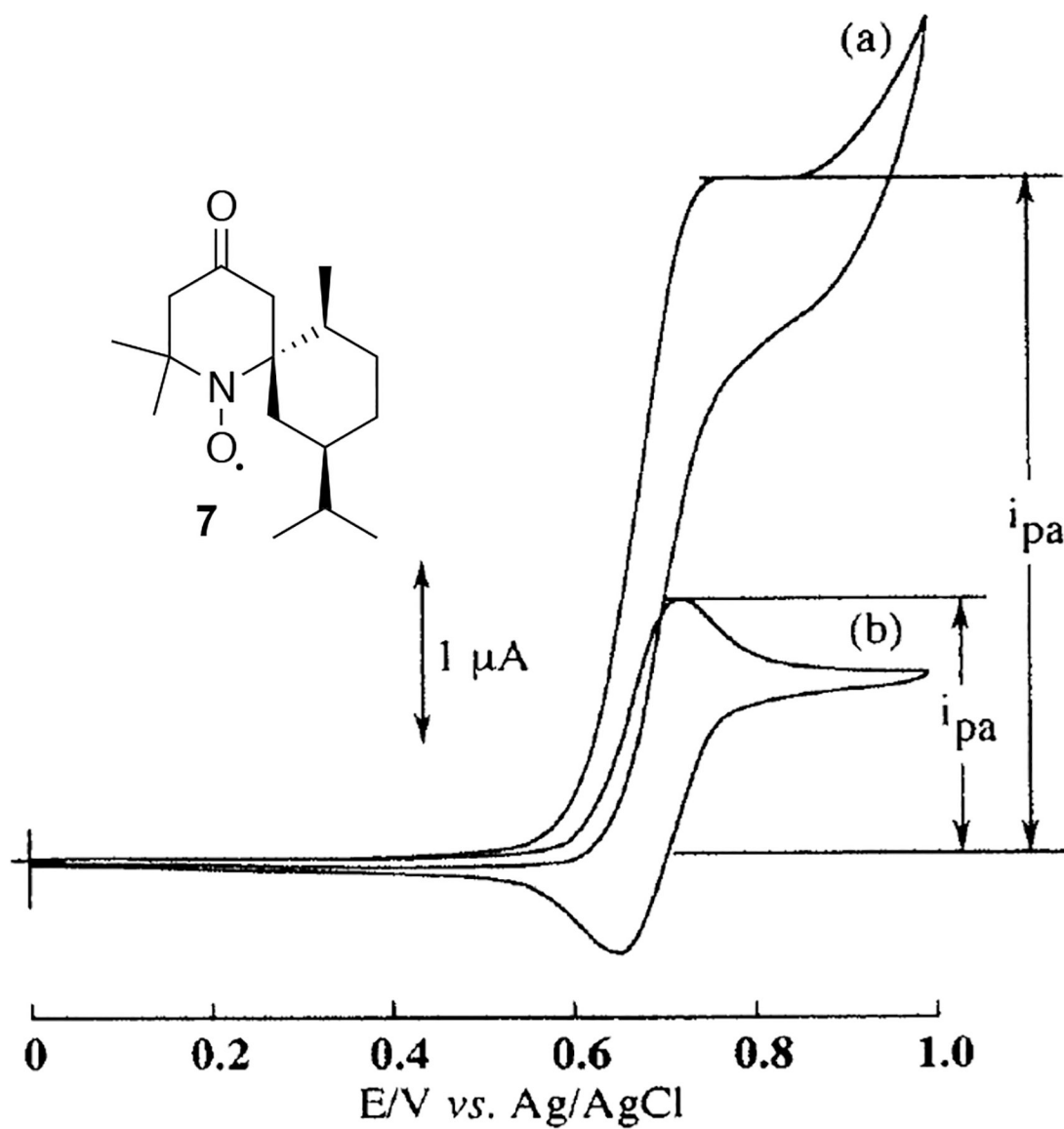
**Scheme 46.**

Cationic and anionic water-soluble TEMPO-derivatives employed by Tanaka.¹²⁴



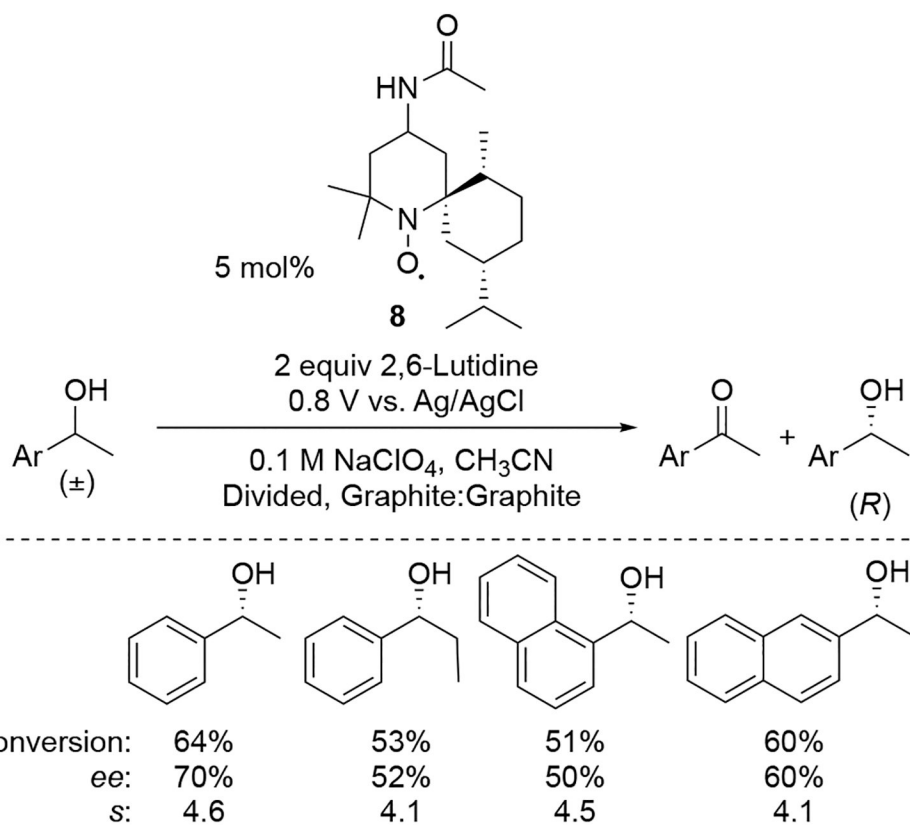
Scheme 47.

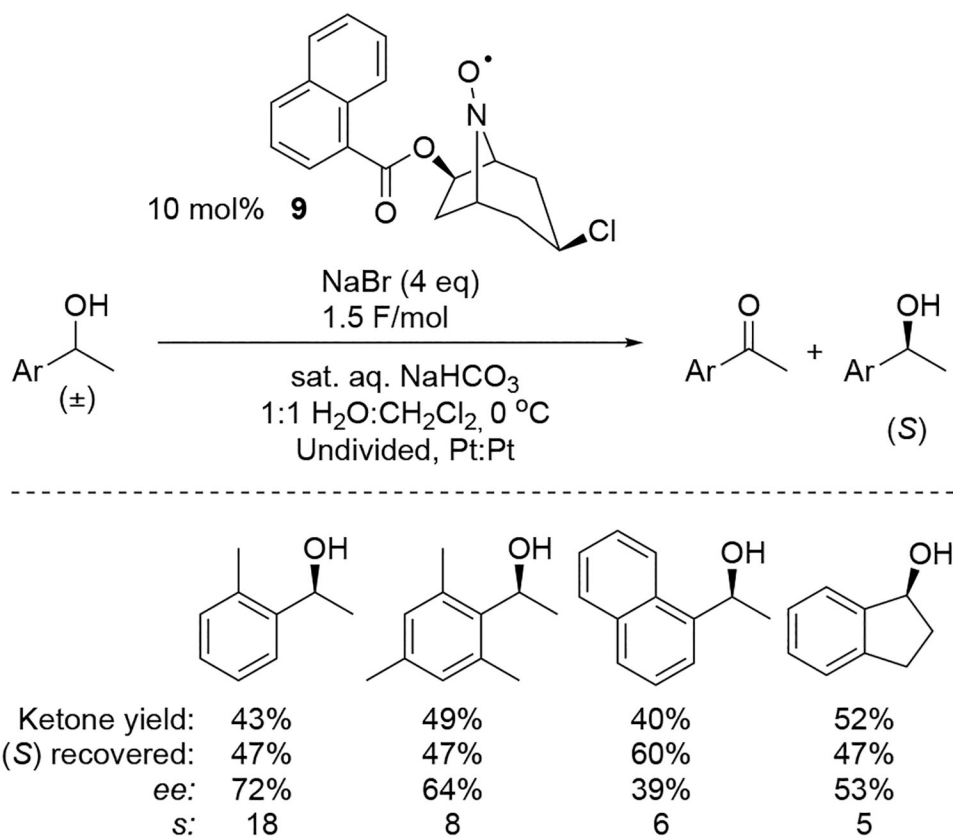
Electrooxidation of menthol catalyzed by aminoxy radicals.¹²⁸



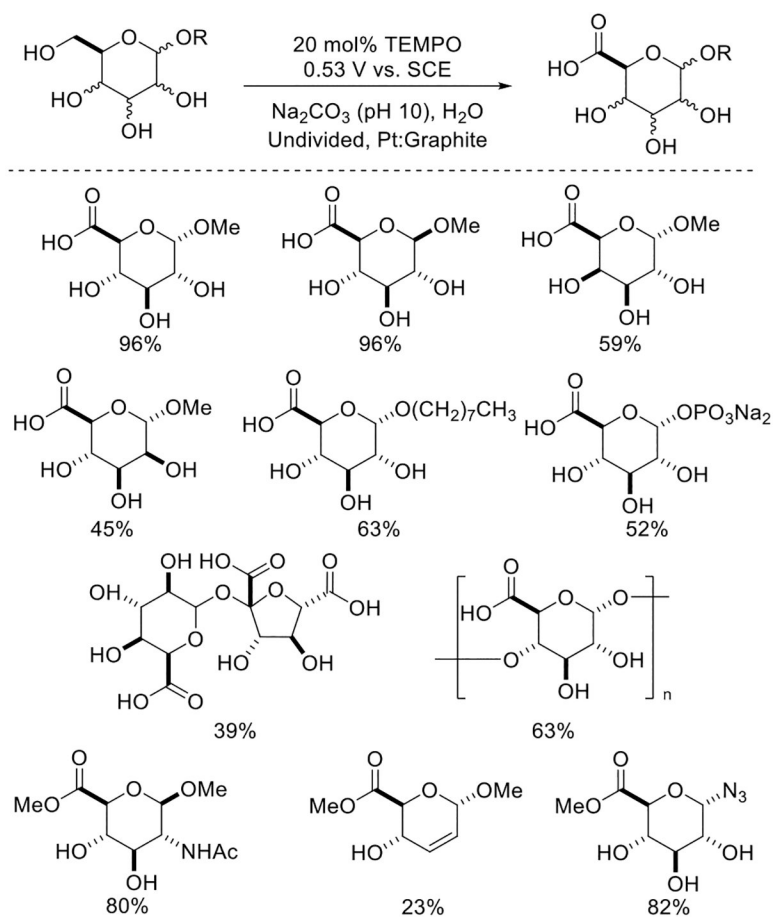
Scheme 48.

CVs of 7 in the presence of (a) (R) -1-phenylethanol and (b) (S) -1-phenylethanol. Adapted with permission from ref.129. Copyright 1999 The Pharmaceutical Society of Japan.

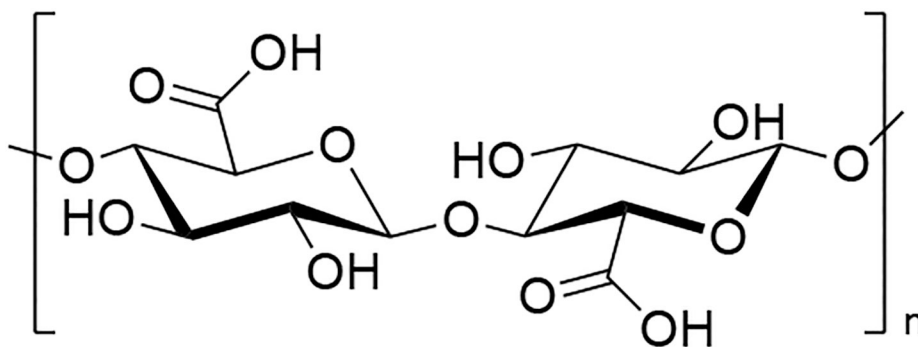
**Scheme 49.**Oxidative kinetic resolution of racemic *sec*-benzylic alcohols by **8**.¹³¹

**Scheme 50.**

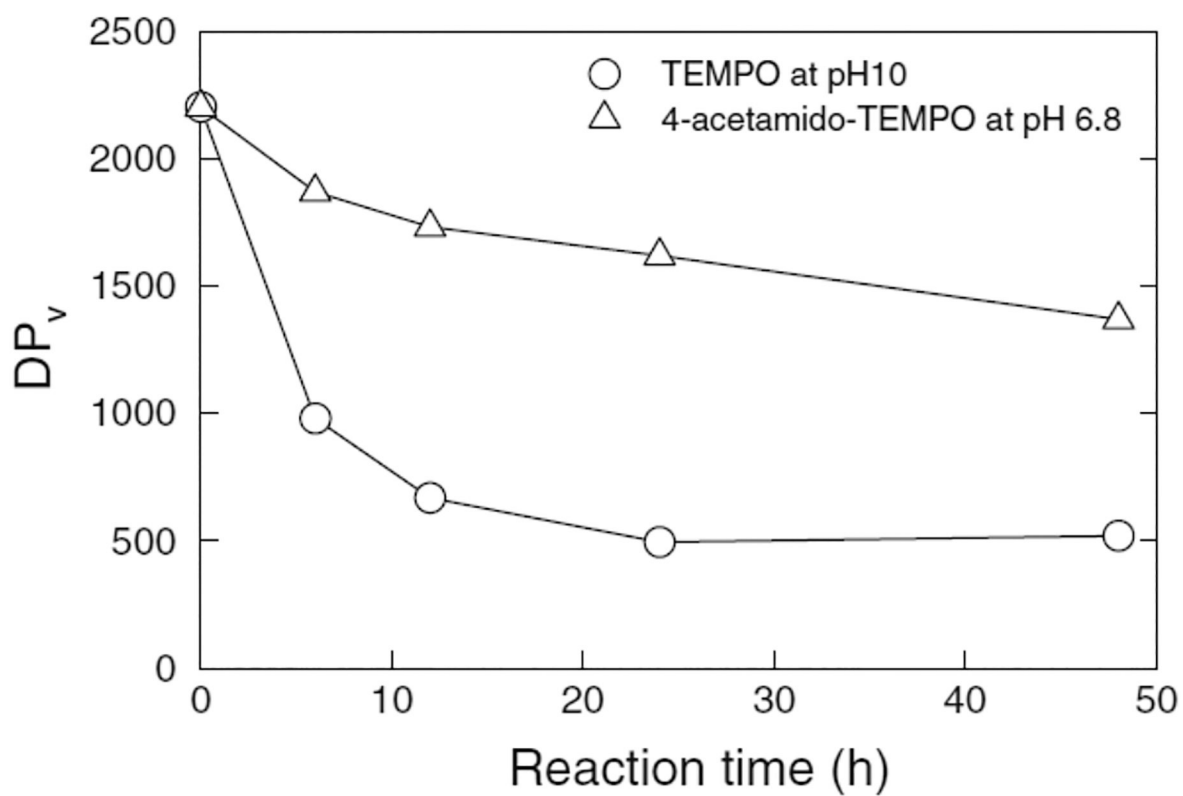
Oxidative kinetic resolution of racemic *sec*-benzylic alcohols by **9**.¹³²

**Scheme 51.**

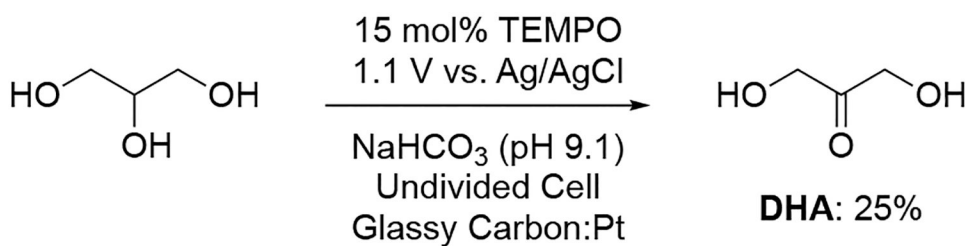
Selective oxidation of carbohydrates reported by Schäfer. Oxidation of glycosyl azides was performed in a divided cell.^{135–137}

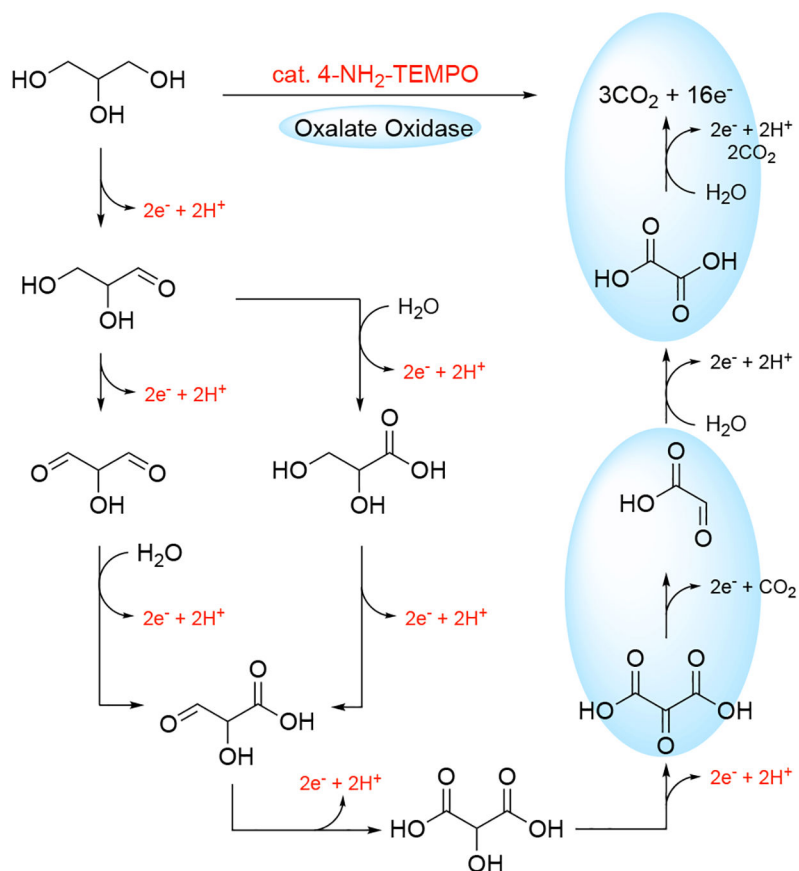


Scheme 52.
Carboxylated cellulose

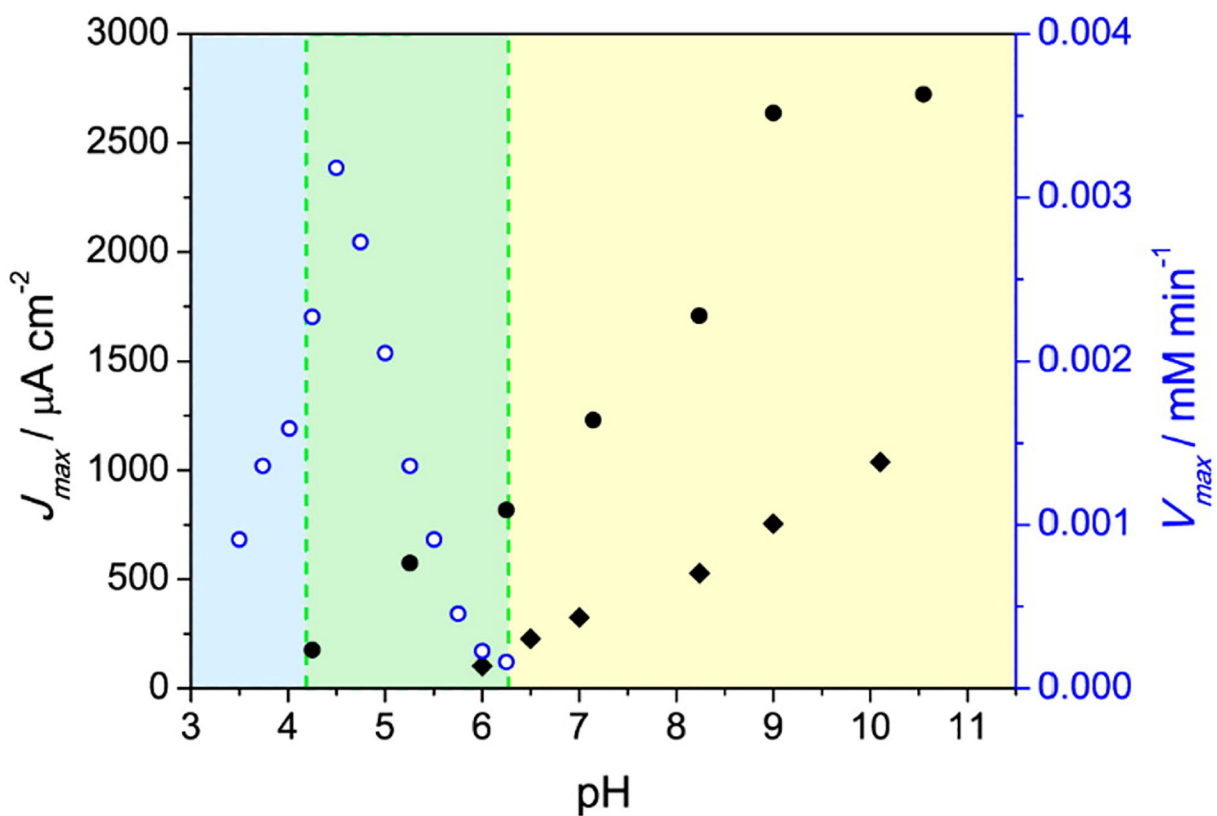
**Scheme 53.**

The viscosity average degrees of depolymerization (DP_v) of softwood bleached kraft pulp native cellulose following aminoxyl-mediated electrooxidation at different pH. Reprinted with permission from ref. 146. Copyright 2010 Springer.

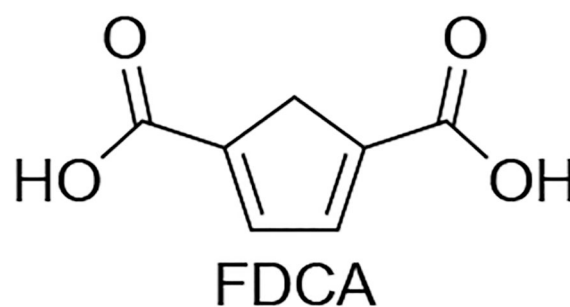
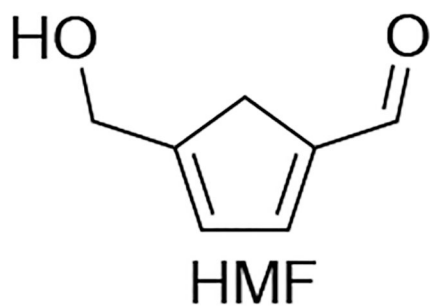
**Scheme 54.**Oxidation of glycerol to 1,3-dihydroxyacetone (DHA).¹⁵²

**Scheme 55.**

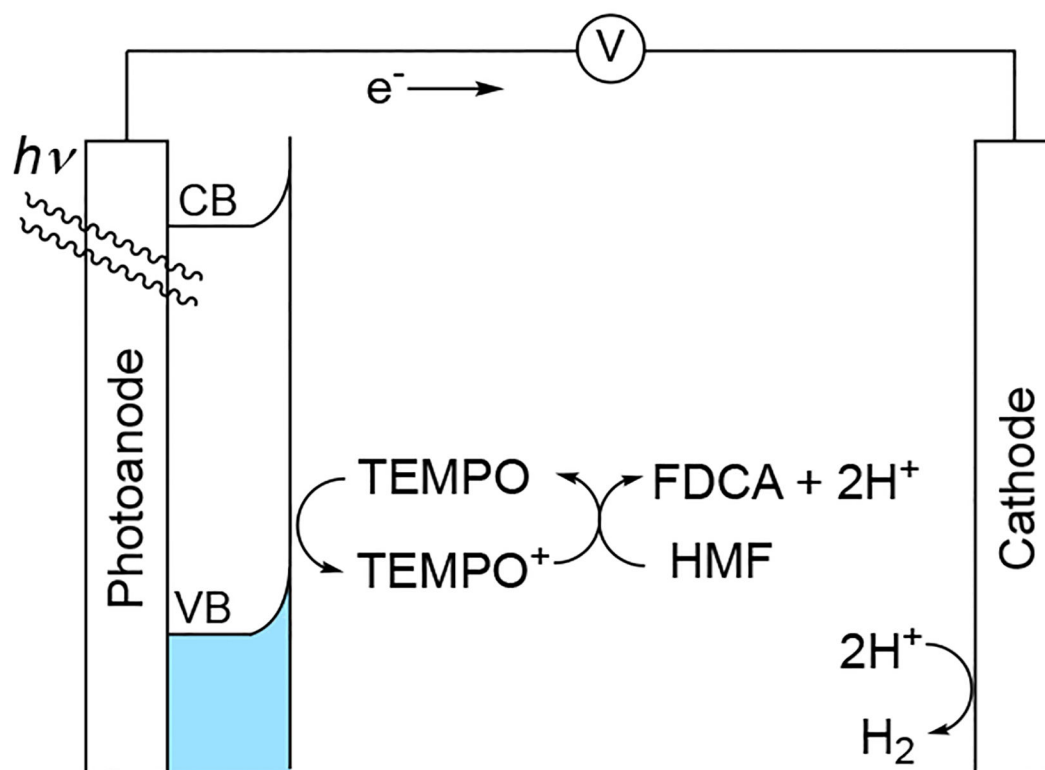
Proposed route for the complete oxidation of glycerol catalyzed by 4-NH₂-TEMPO and oxalate oxidase. Enzyme-mediated steps are highlighted in blue ovals.¹⁵³

**Scheme 56.**

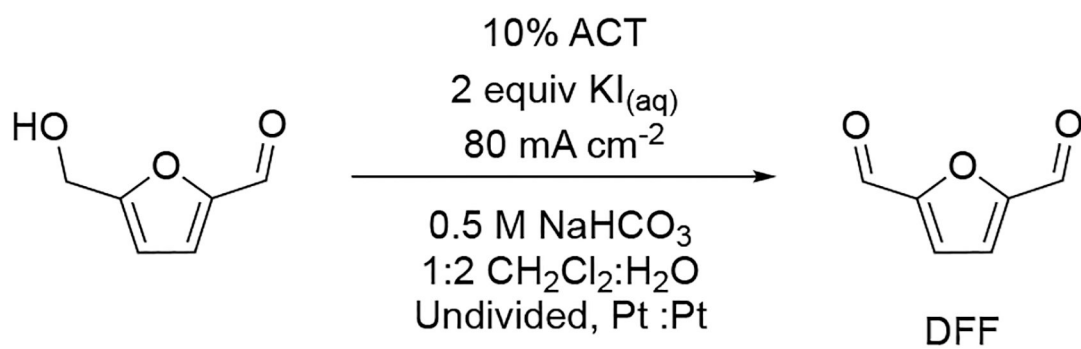
The pH profiles of (O) oxalate oxidase, (◆) TEMPO, and (●) 4-NH₂-TEMPO for catalytic reactivity towards oxalic acid (for oxalate oxidase) and glycerol (for TEMPO and 4-NH₂-TEMPO). Reprinted with permission from ref. 153. Copyright 2014 American Chemical Society.



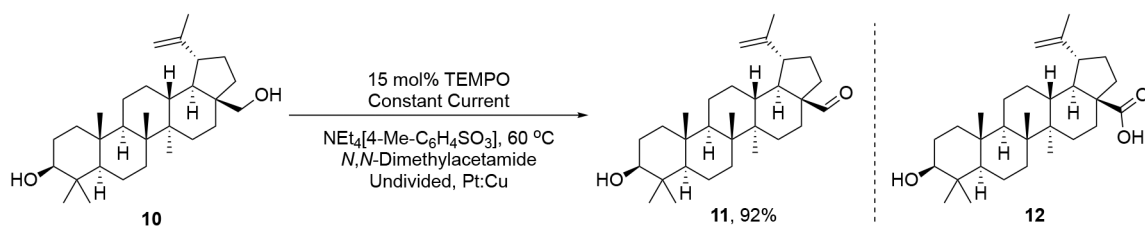
Scheme 57.
5-hydroxymethylfurfural (HMF) and its oxidation product, 2,5-furandicarboxylic acid (FDCA).¹⁵⁴



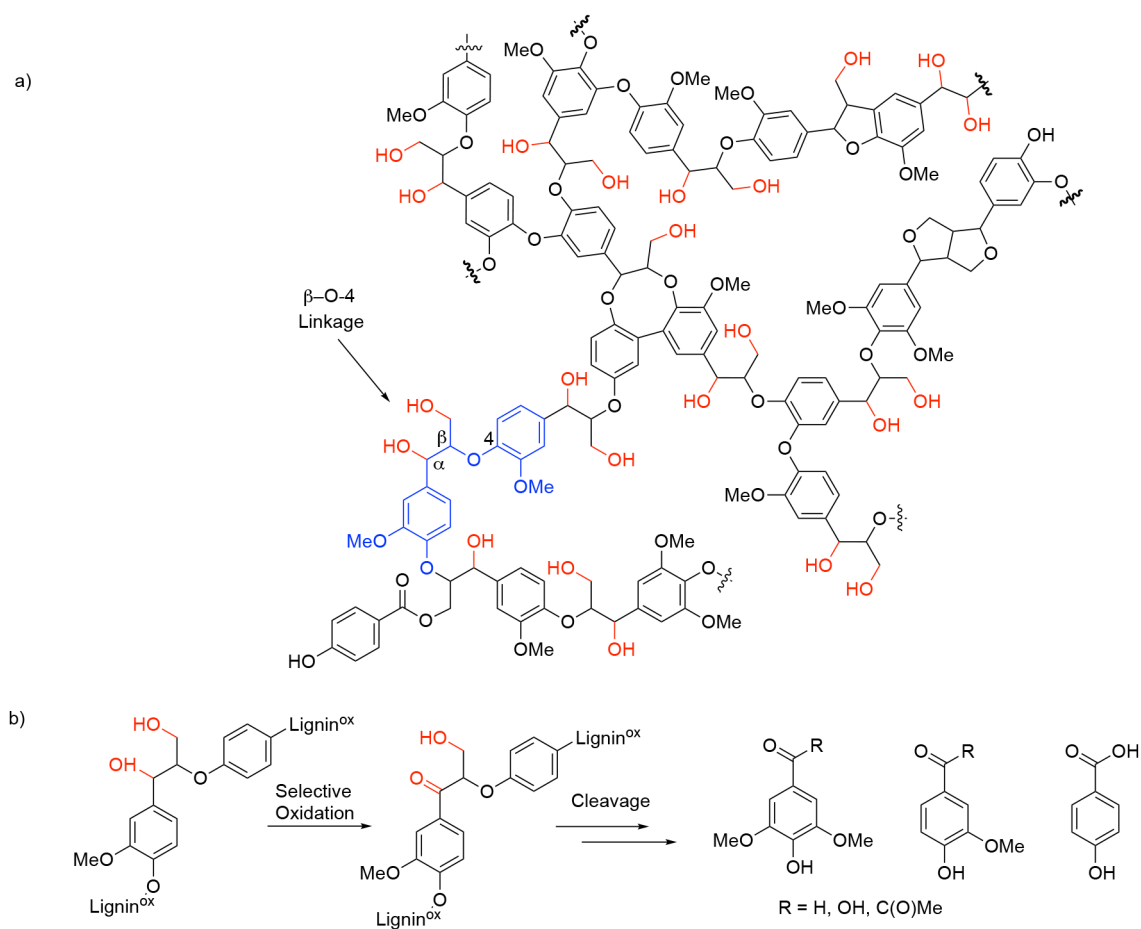
Scheme 58. TEMPO-mediated oxidation of HMF and H₂ generation in a photoelectrochemical cell.¹⁵⁴

**Scheme 59.**

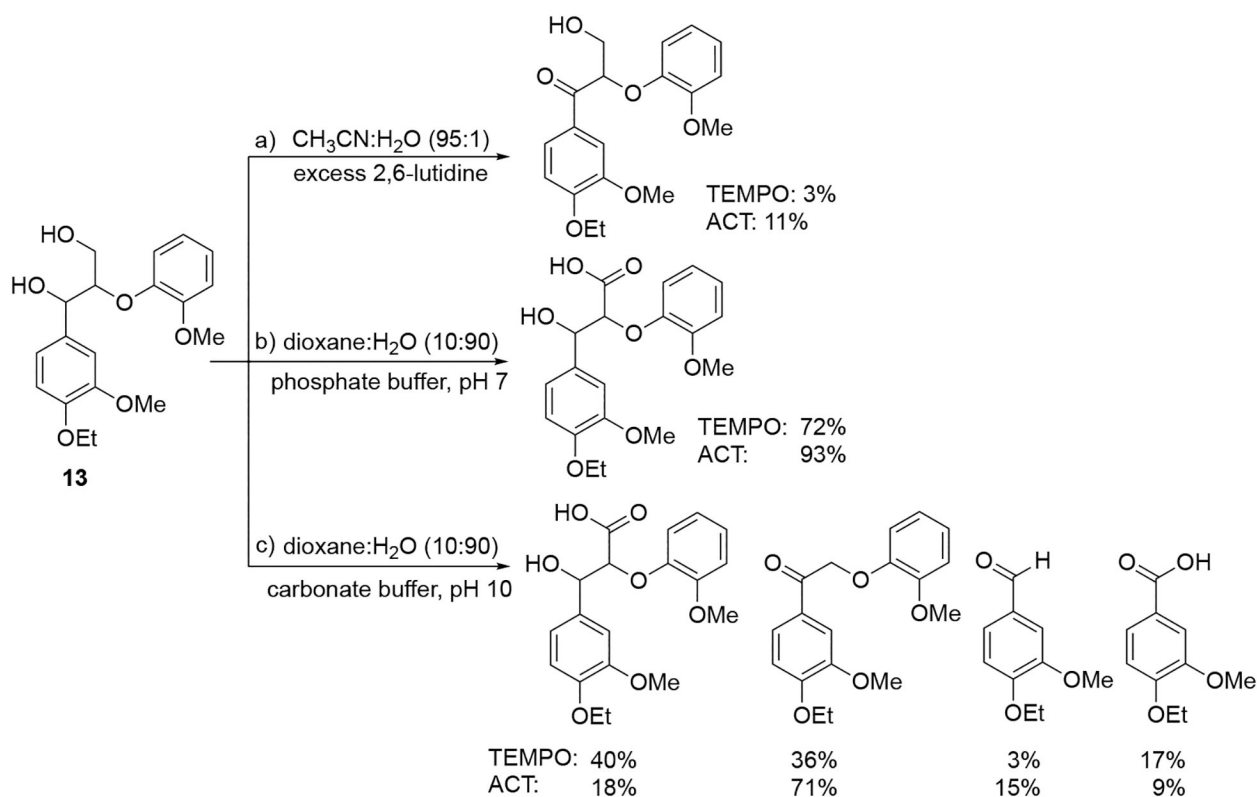
Oxidation of HMF to DFF mediated by ACT/I⁻ under biphasic conditions.¹⁷²



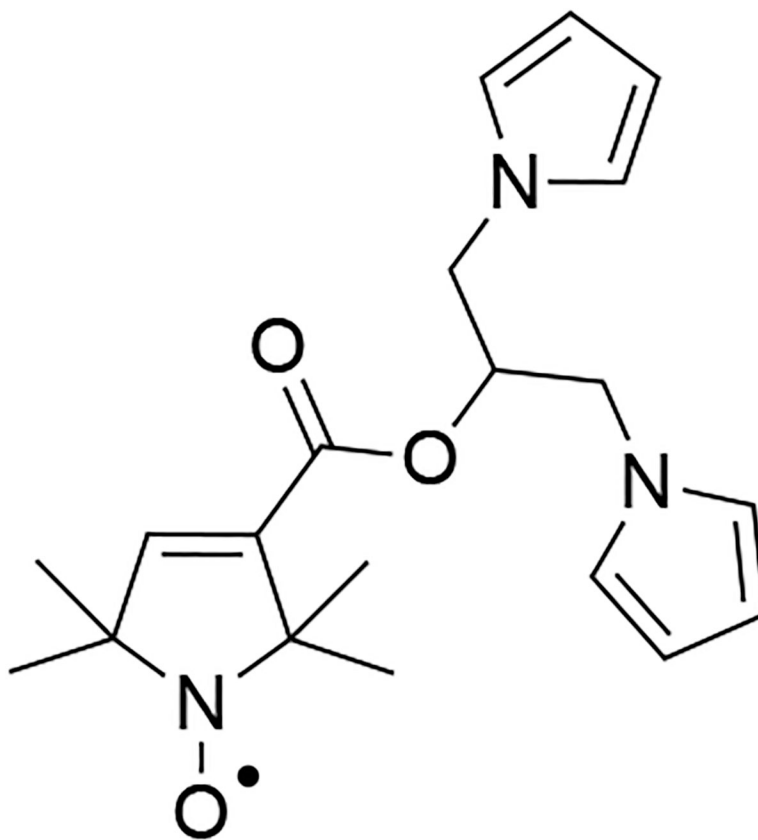
Scheme 60.
Oxidation of betulin to betulin aldehyde.¹⁶⁰

**Scheme 61.**

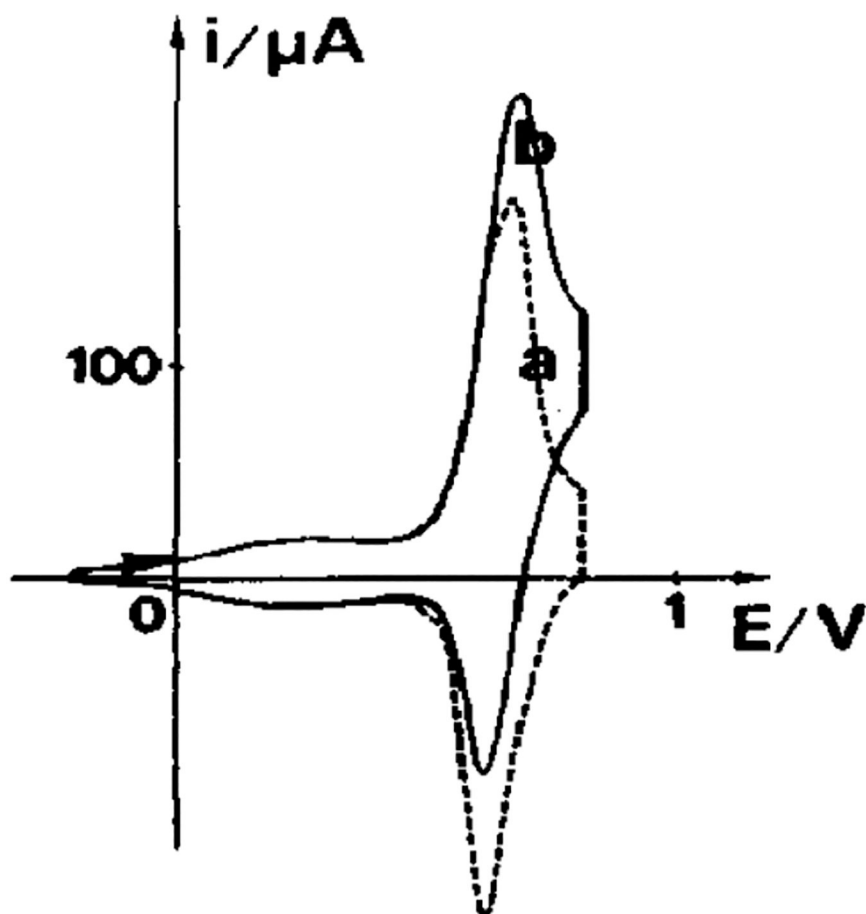
a) Representative structure of lignin highlighting hydroxyl groups (red) and the β -O-4 linkage (blue), and the b) oxidation/hydrolysis sequence that has been shown to afford high yields of low molecular weight aromatics from lignin.¹⁶⁴

**Scheme 62.**

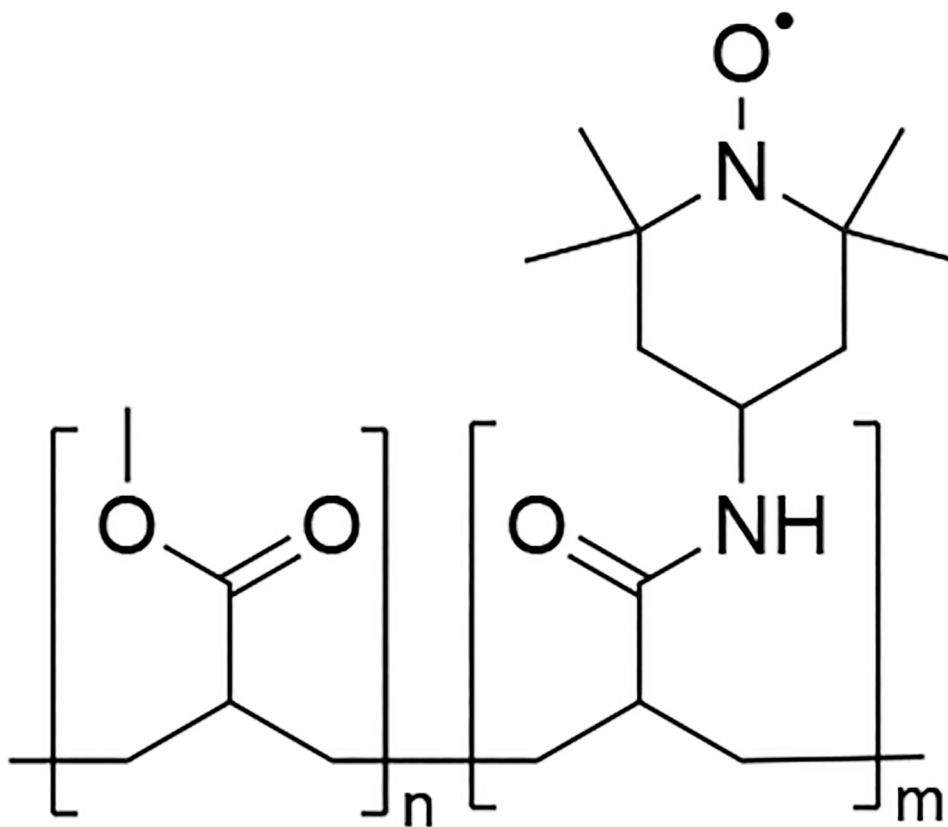
Aminoxy-mediated electrooxidation of lignin β -O-4 model compound **13**. Conditions (a): 0.1 M LiClO_4 in 95% $\text{CH}_3\text{CN}/\text{H}_2\text{O}$, 5 equiv. of 2,6-lutidine; condition (b): 10% dioxane in pH 7 phosphate buffer; condition (c): 10% dioxane in pH 10 carbonate buffer. All electrolysis reactions were performed with 2.5 mM substrate and 0.5 mM aminoxy in a divided cell with a carbon felt anode and platinum wire cathode. Electrolyses were conducted at constant potential.¹⁷²



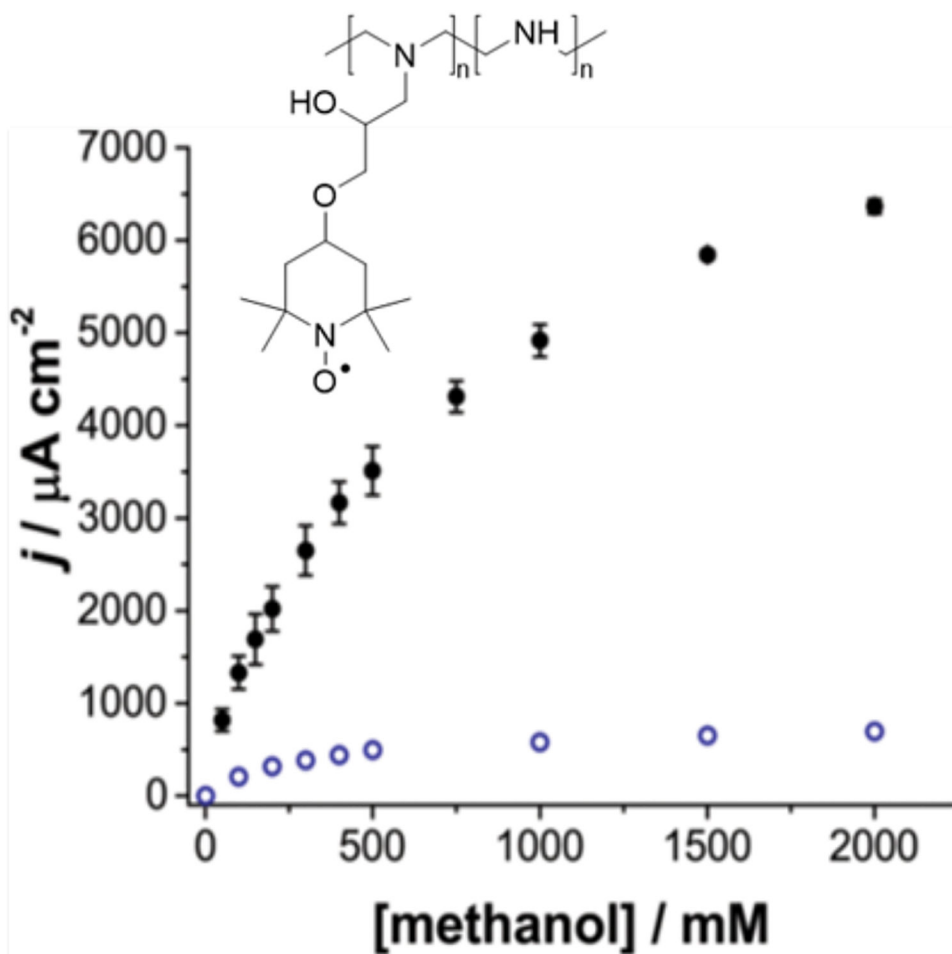
Scheme 63.
Pyrrole-tethered 2,2,5,5-tetramethyl-3-pyrolin-1-oxyl.

**Scheme 64.**

a) CV trace of the pyrrole-tethered 2,2,5,5-tetramethyl-3-pyrrolin-1-oxyl film on a platinum electrode, (b) CV trace of the polypyrrole-aminoxyl film on a platinum electrode upon addition of 4-methoxybenzyl alcohol. CVs recorded in 0.1 M *n*-Bu₄NClO₄ and 0.01 M 2,4,6-collidine in CH₃CN. Scan rate = 50 mV s⁻¹. Potential referenced against Ag^{0/+}. Adapted with permission from ref. 174. Copyright 1987 Elsevier.

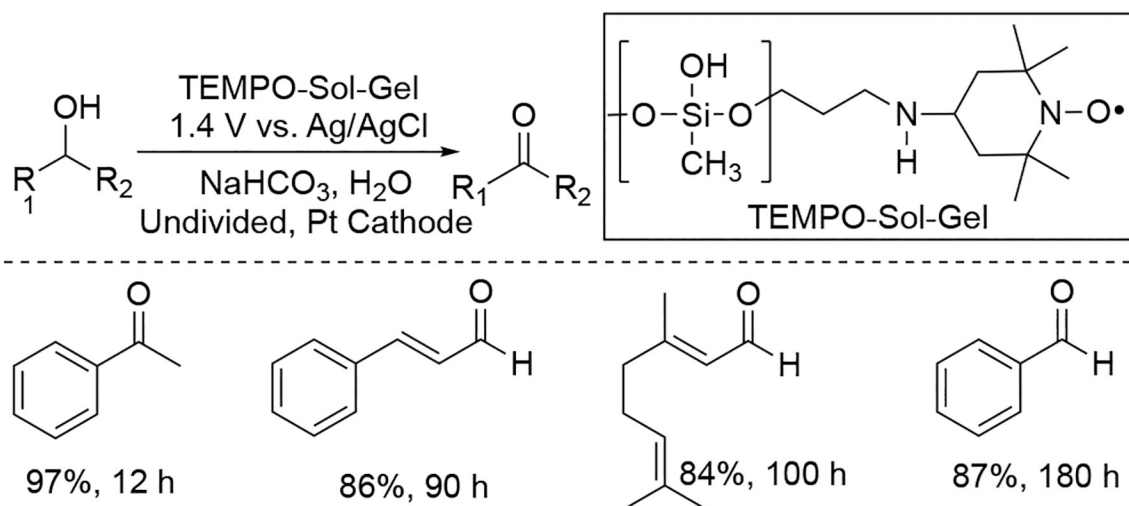


Scheme 65.
TEMPO-PAA film after methylation of free acid residues.

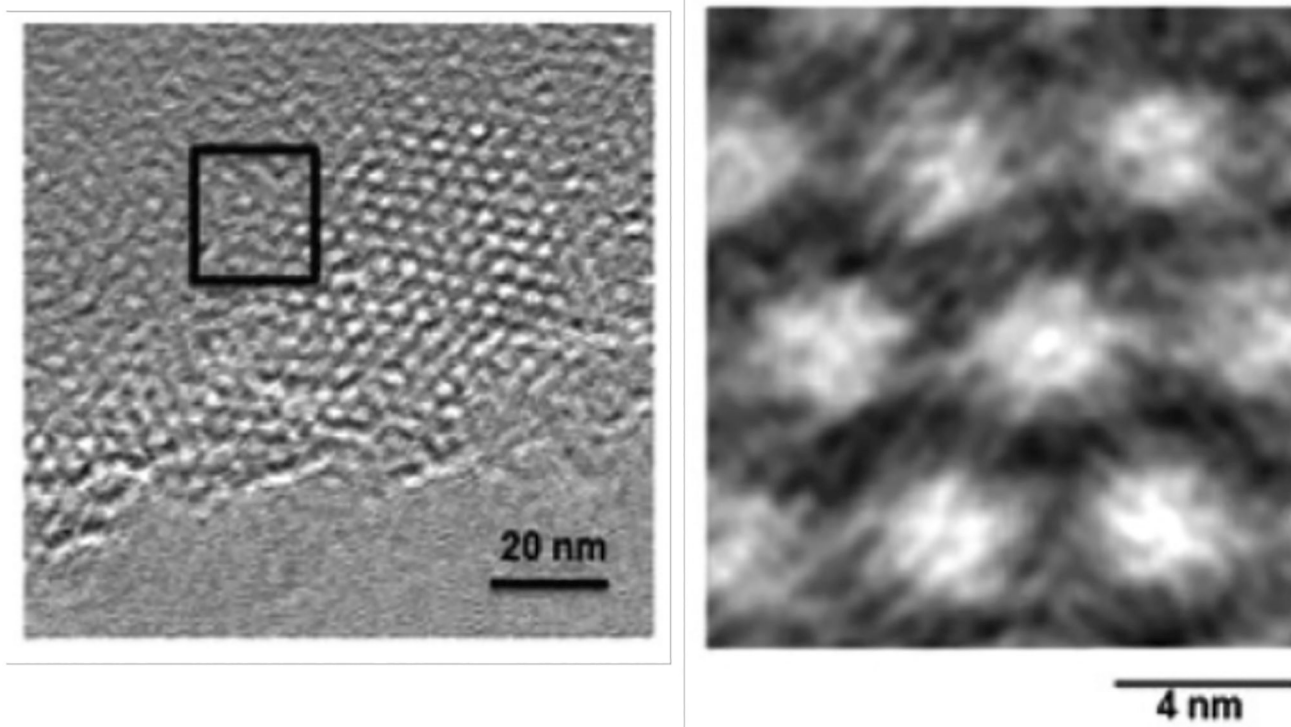


Scheme 66.

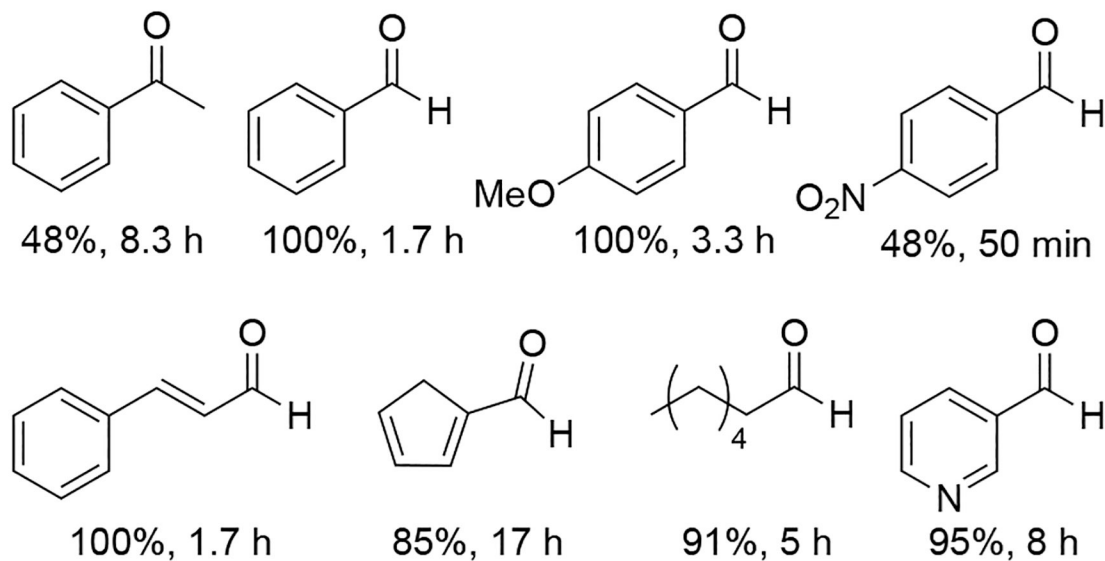
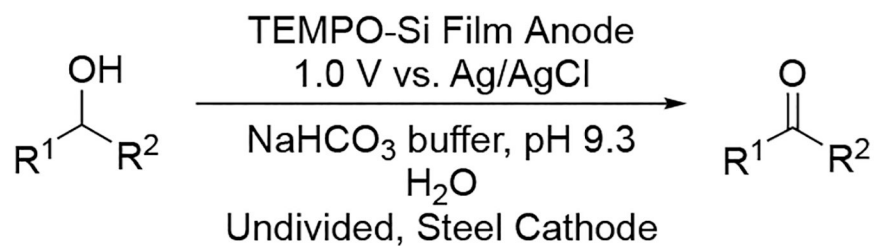
Catalytic activity for the electrooxidation of MeOH by (●) electrode-supported TEMPO-linked poly(ethylamine) and (○) 4-OMe-TEMPO. Inset: TEMPO-linked poly(ethylamine). Reprinted with permission from ref. 188. Copyright 2015 American Chemical Society.

**Scheme 67.**

Electrooxidation of benzylic and allylic alcohols (0.5 mmol) by aminoxy-doped solgel electrode.¹⁸⁹

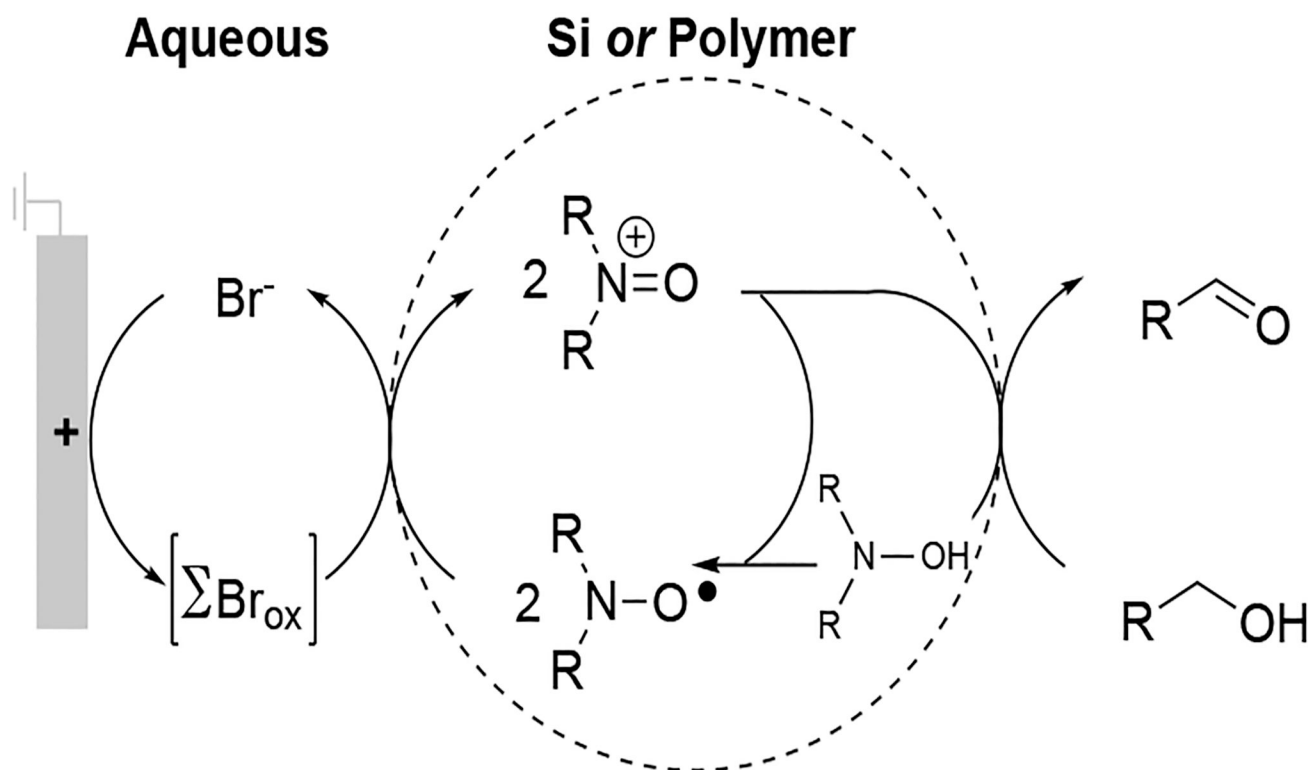
**Scheme 68.**

Transmission electron microscopy images of aminoxy-linked mesoporous silica film.
Reprinted with permission from ref. 191. Copyright 2014 Royal Society of Chemistry.

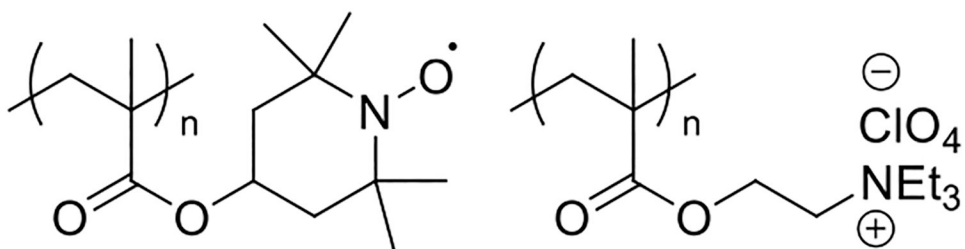
**Scheme 69.**

Electrooxidation of alcohols (1 mmol) mediated by aminoxyl-linked mesoporous silica film.

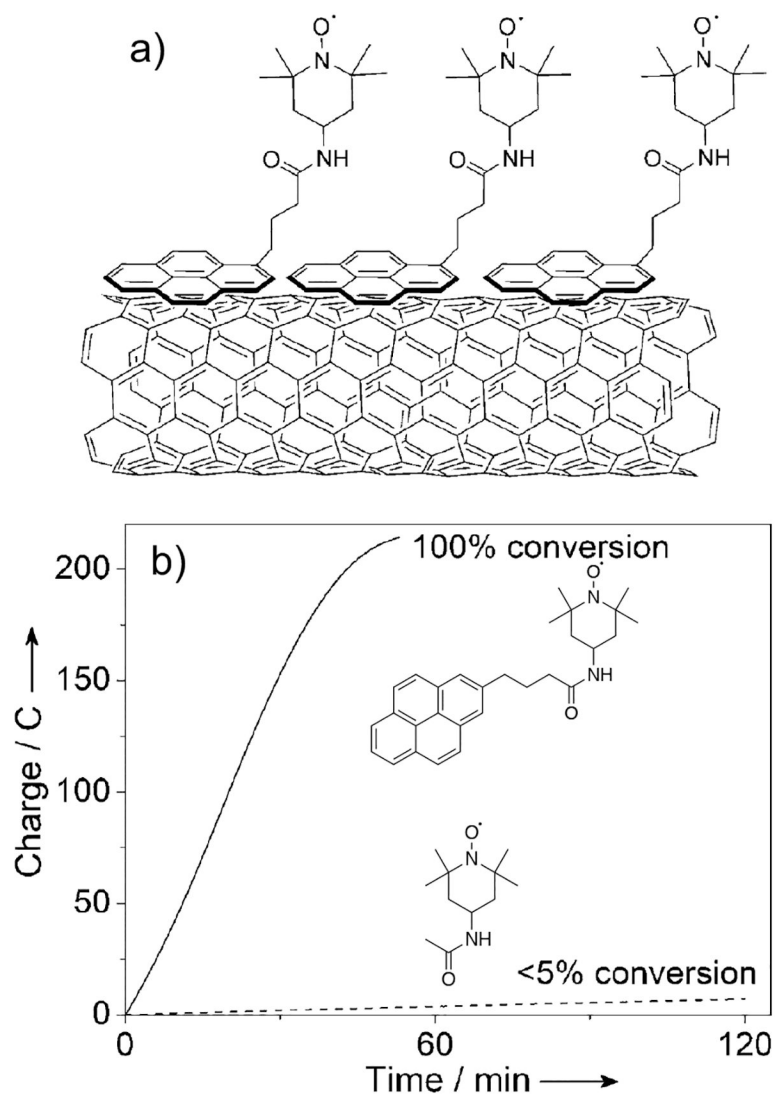
191

**Scheme 70.**

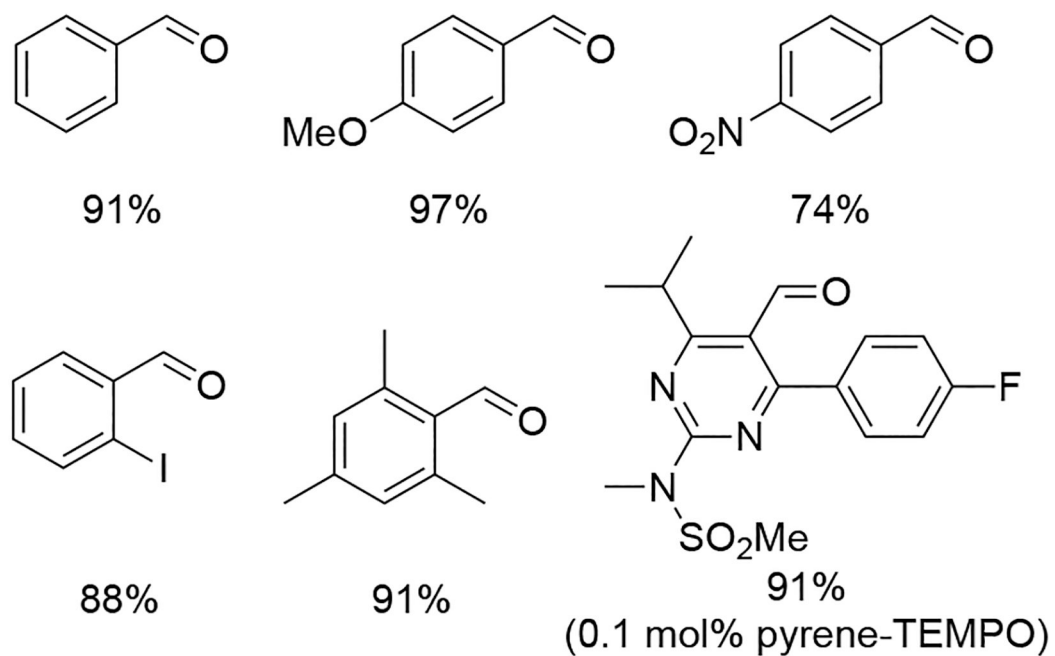
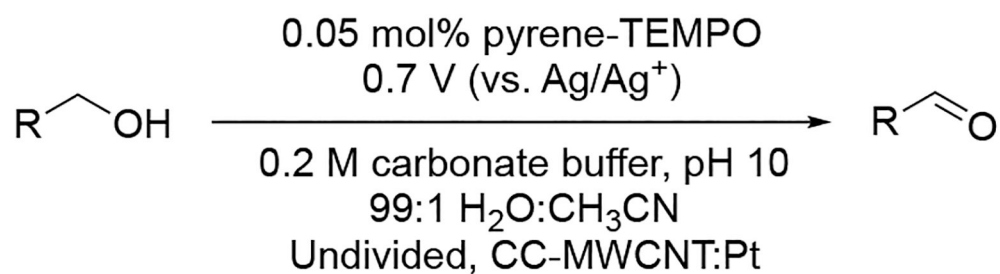
Electrooxidation of alcohols by aminoxyl radical species immobilized in solid particles.¹⁹⁶



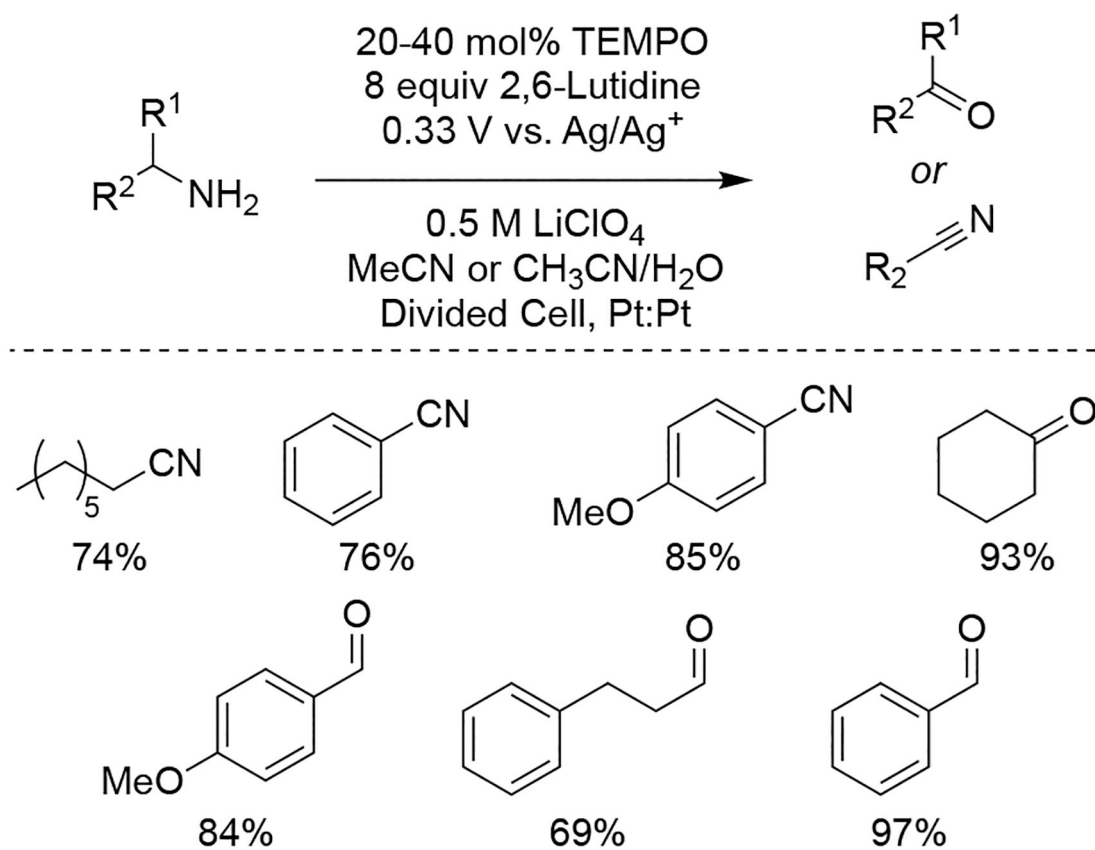
Scheme 71.
Poly(methacrylate)-TEMPO and polyelectrolyte.²⁰⁰

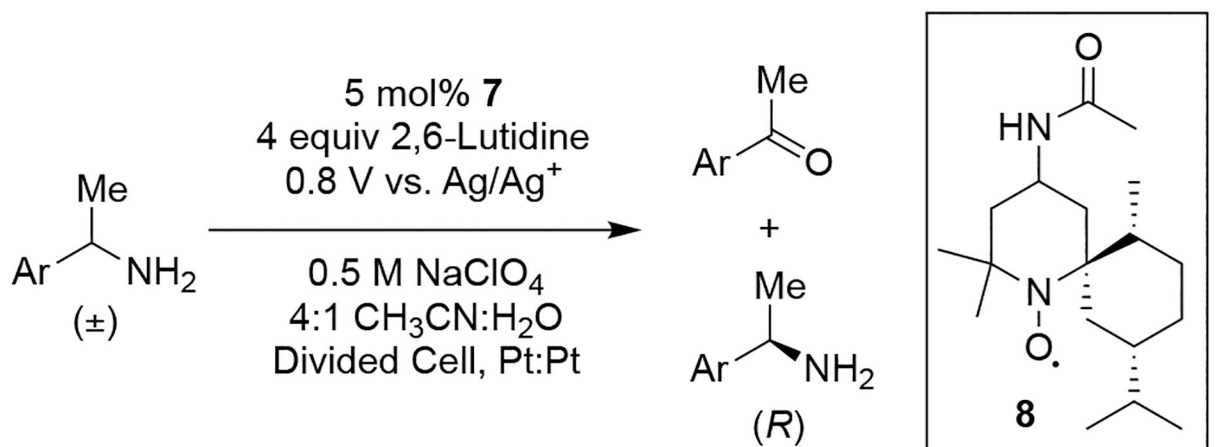
**Scheme 72.**

a) Schematic representation of pyrene-TEMPO immobilization via noncovalent interaction with a MWCNT. b) Comparison of bulk electrolysis of benzyl alcohol to benzaldehyde using dissolved (dashed line) and immobilized (solid line) aminosyls. Reaction conditions: 10 mL carbonate buffer pH 10, 0.1 M benzyl alcohol, 5×10^{-5} M ACT or pyrene-TEMPO, bulk electrolysis at 0.7 V vs. Ag/AgCl. Reprinted with permission from ref. 201. Copyright 2017 John Wiley and Sons.



Scheme 73.
 Pyrene-TEMPO mediated electrooxidation of alcohol substrates.²⁰¹

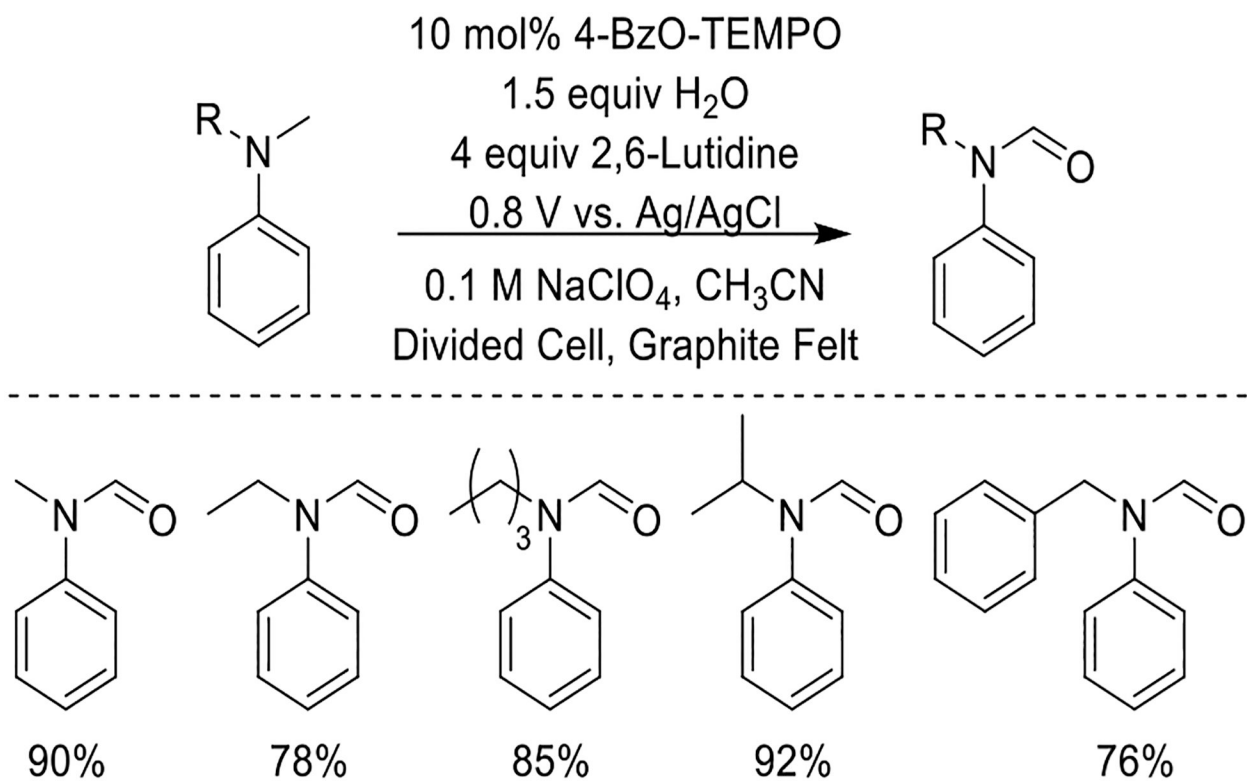
**Scheme 74.**Oxidation of primary and secondary amines to give the corresponding nitrile or carbonyl.²⁰⁵

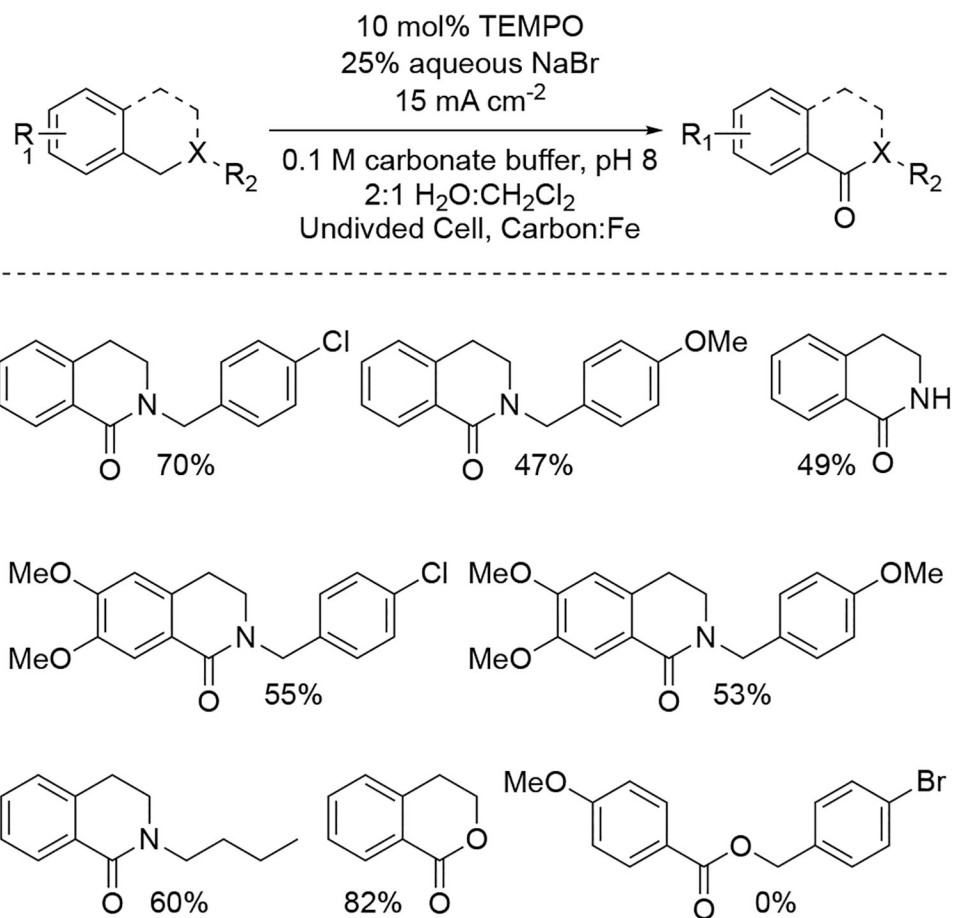


Conversion	65%	66%	54%	60%
ee:	78%	75%	62%	66%
s:	5.3	4.7	5.8	4.9

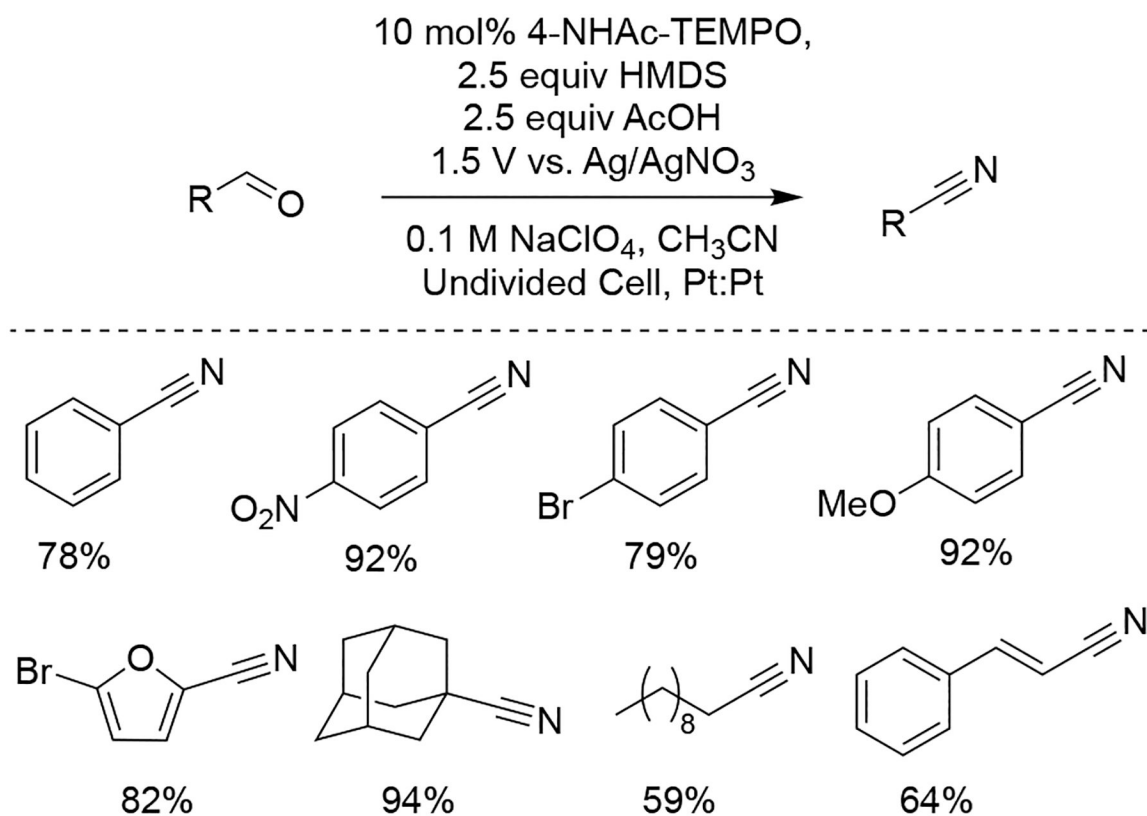
Scheme 75.

Kinetic resolution of benzylic primary amines catalyzed by chiral aminoxy radical **8**.²⁰⁶

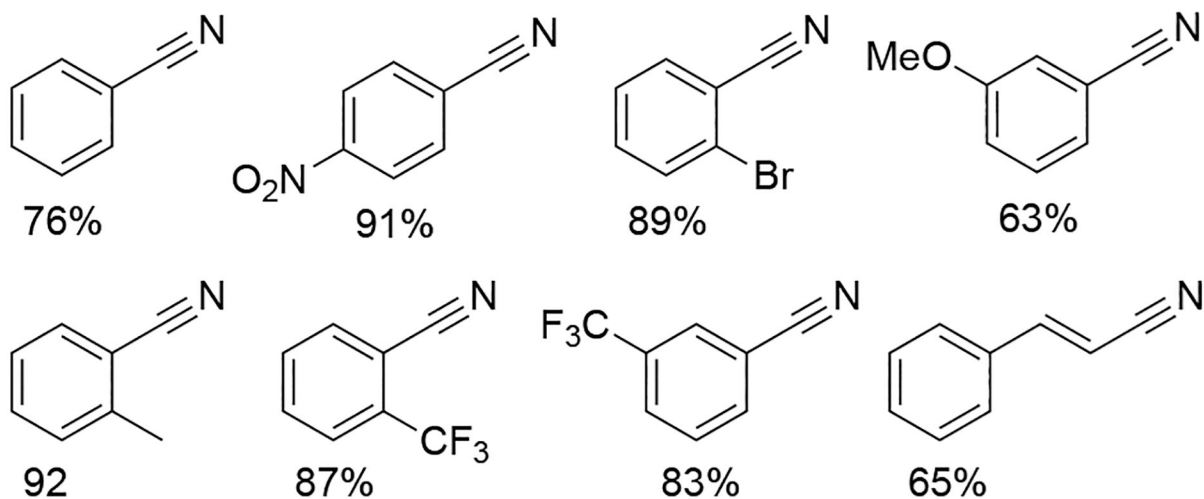
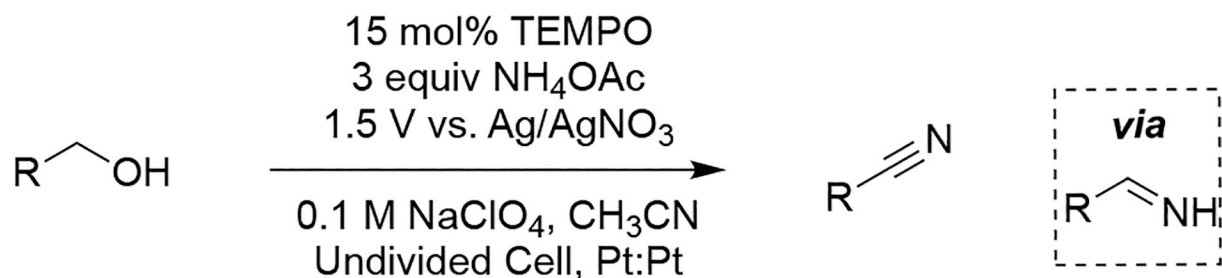
**Scheme 76.**Oxidation of tertiary amines catalyzed by 4-BzO-TEMPO.²⁰⁷



Scheme 77.
 Oxidation of tetrahydroisoquinolines and related compounds.²⁰⁸

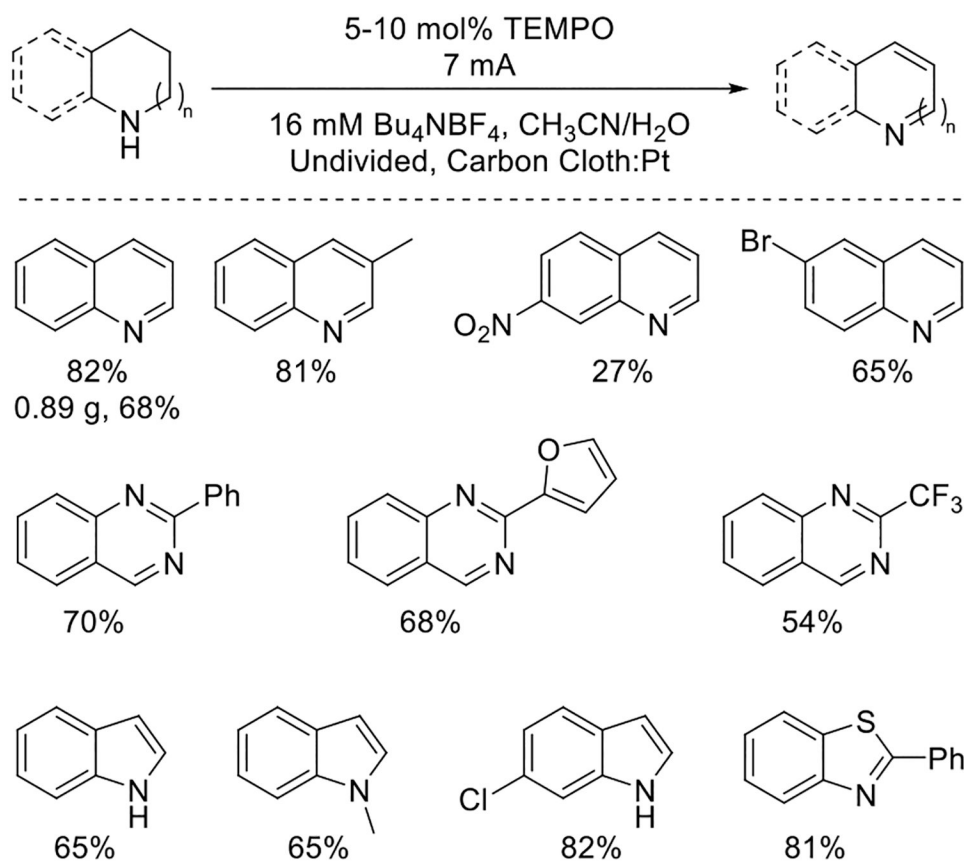
**Scheme 78.**

Aminoxyl-catalyzed electrooxidation of aldehydes to nitriles with HMDS as the nitrogen source.²⁰⁹

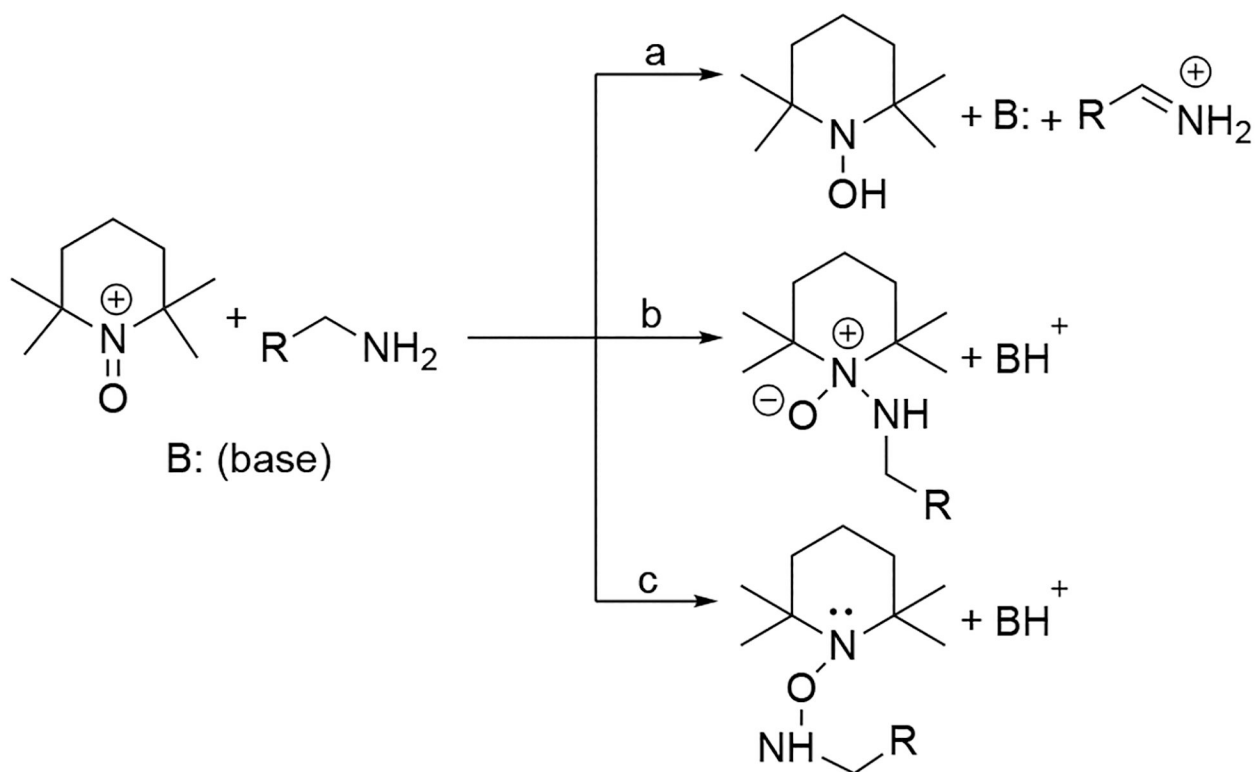


Scheme 79.

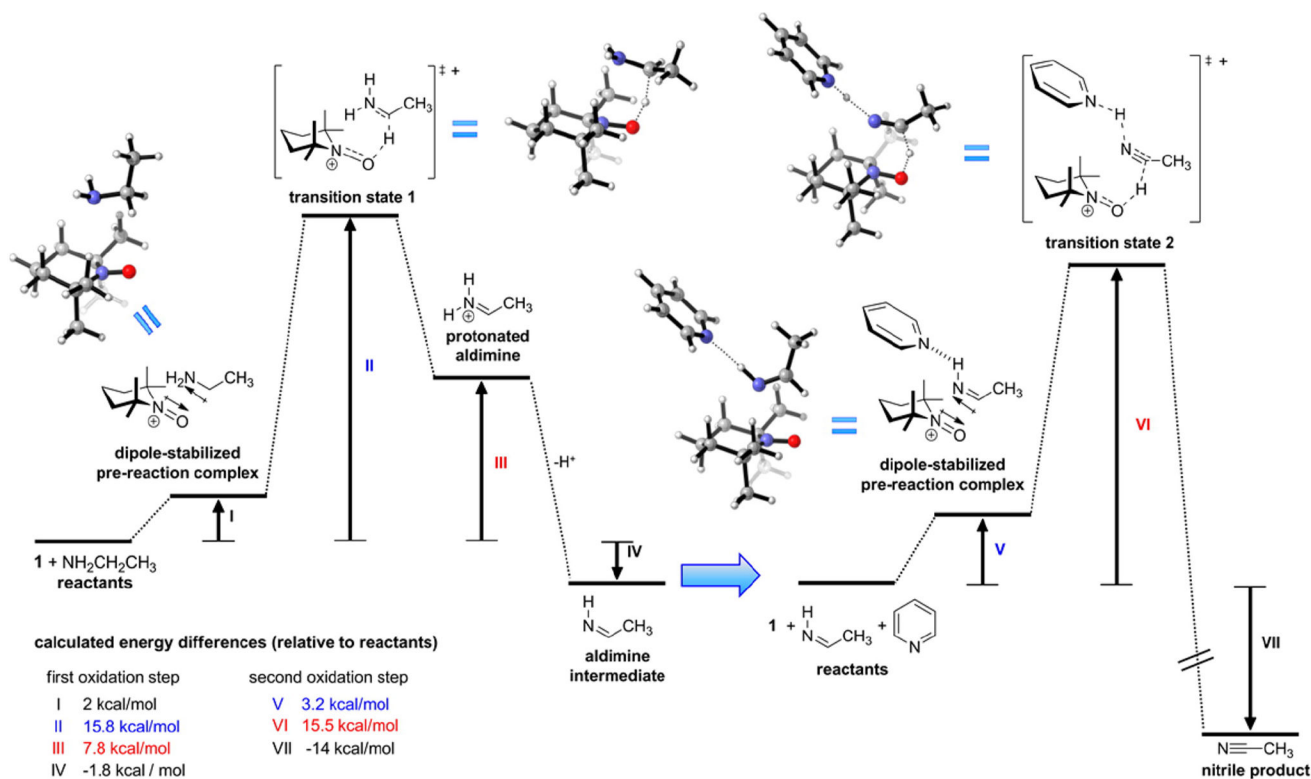
Aminoxy-catalyzed oxidation of alcohols to nitriles with NH₄OAc.²¹¹

**Scheme 80.**

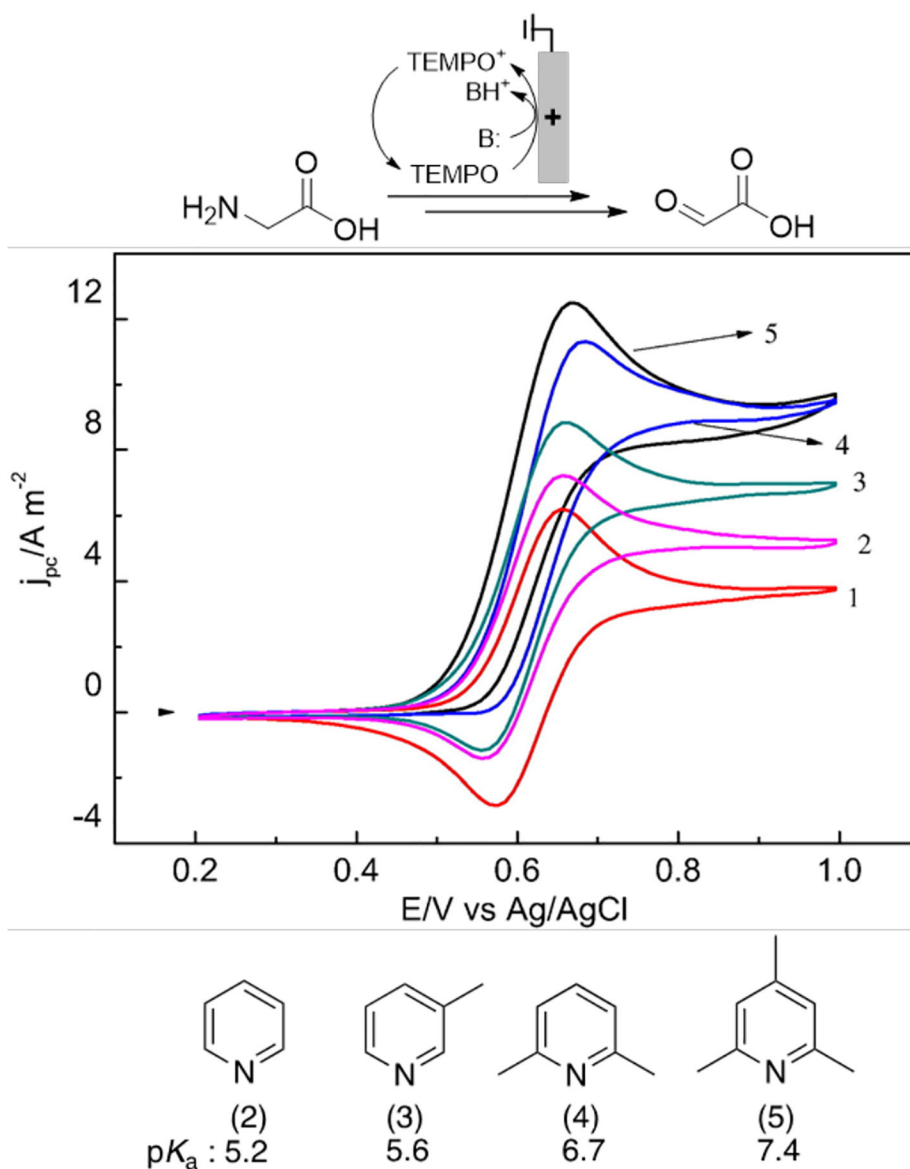
Acceptorless dehydrogenation of saturated *N*-heterocycles.²¹²

**Scheme 81.**

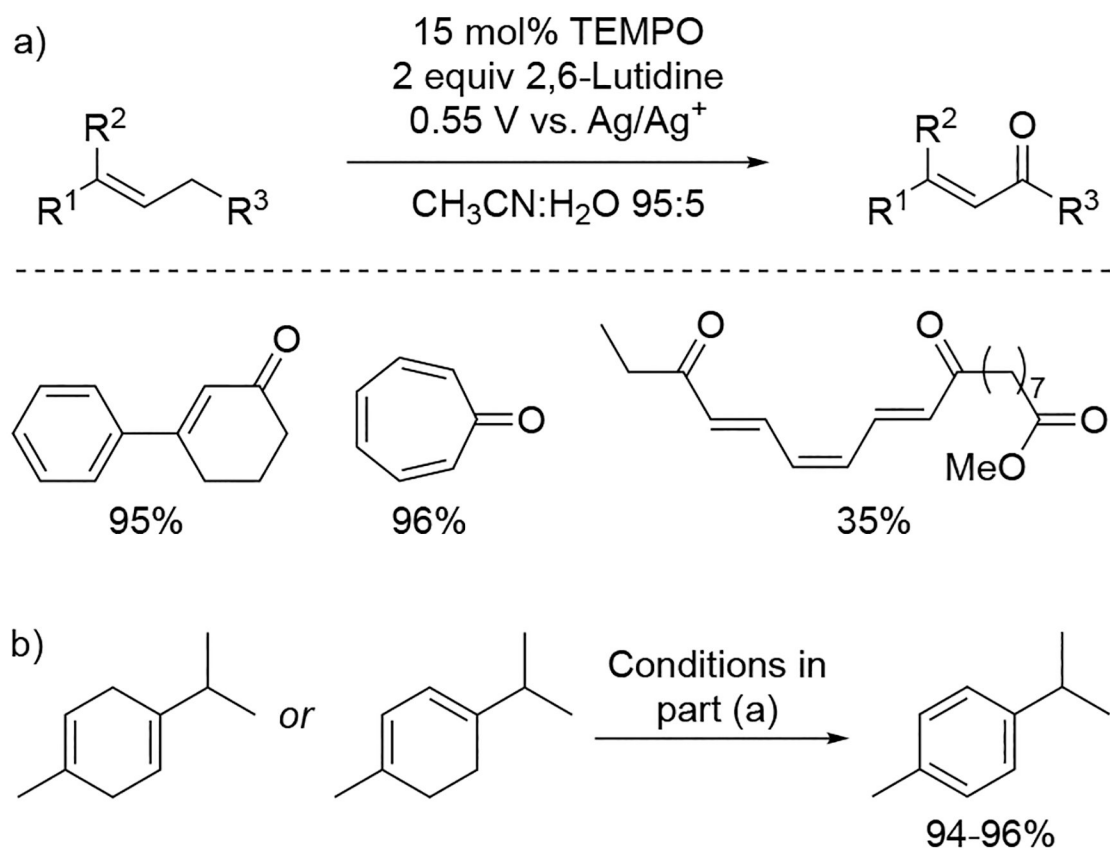
Proposed rate-limiting steps of amine oxidation by oxoammonium.²⁰⁷

**Scheme 82.**

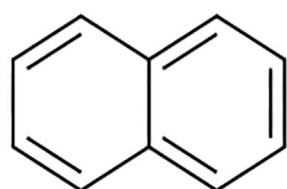
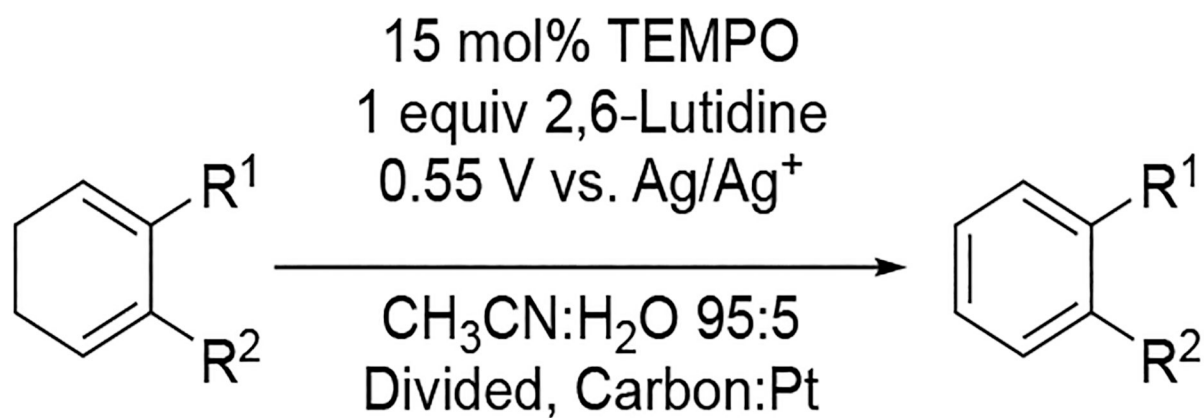
Calculated reaction profile for the oxidation of primary amines to nitriles by oxoammonium (B3LYP/6-311+G*). Reprinted with permission from ref. 215. Copyright 2014 American Chemical Society.

**Scheme 83.**

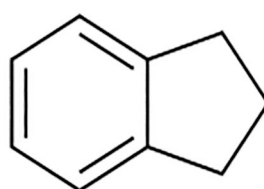
Electrooxidation of glycine by TEMPO in (1) absence of base and presence of 100 mM (2) pyridine, (3) 3-picoline, (4) 2,6-lutidine, and (5) 2,4,6-collidine. CV conditions: 5 mM glycine, 5 mM TEMPO in 0.1 M NaClO₄ in 3:1 CH₃CN:H₂O at platinum electrode. pK_a values are reported for the corresponding pyridinium-type species in water.²¹⁷ Reprinted with permission from ref. 216. Copyright 2017 Elsevier.

**Scheme 84.**

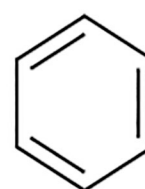
a) Allylic oxidation of activated alkenes, and b) unexpected aromatization of α -terpinene and γ -terpinene to cymene. The electrolyte, electrode materials, and cell design are not addressed in the reference.²¹⁹



93%

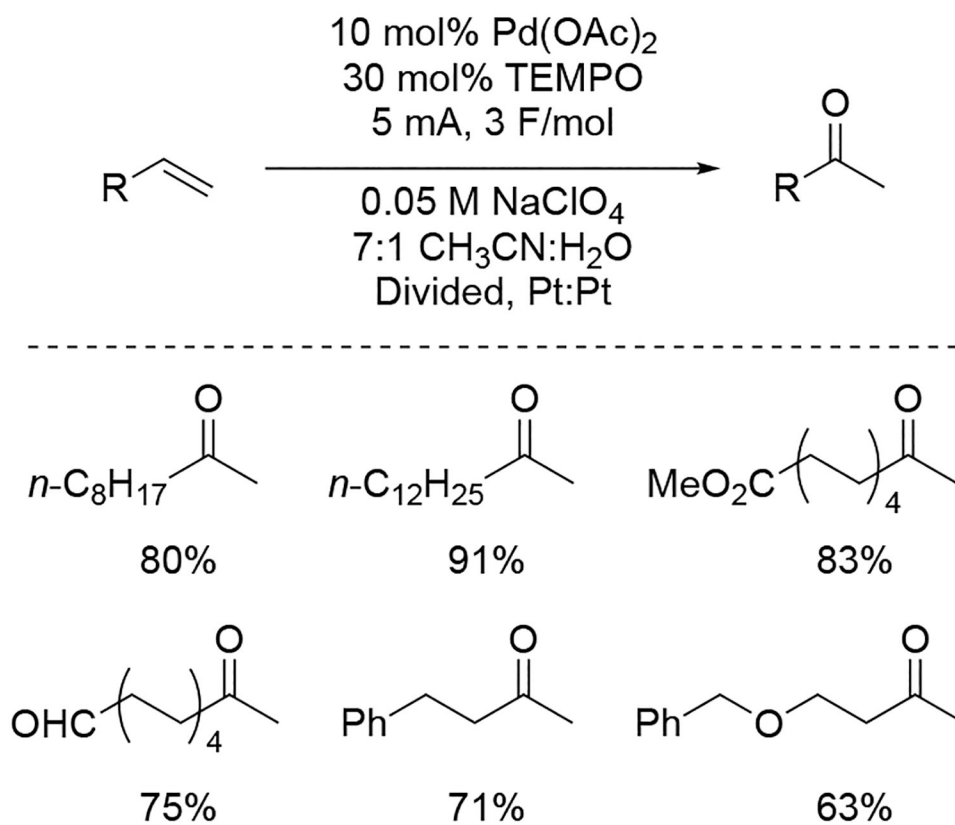


85%

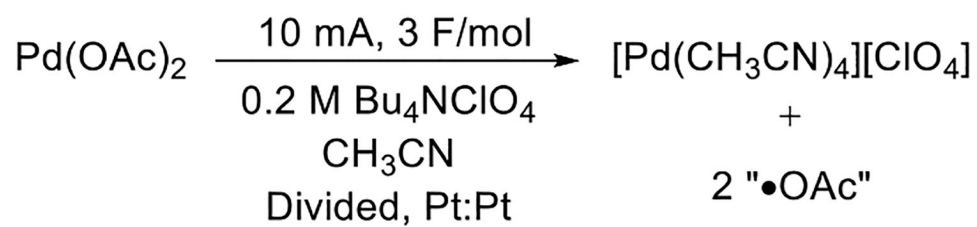


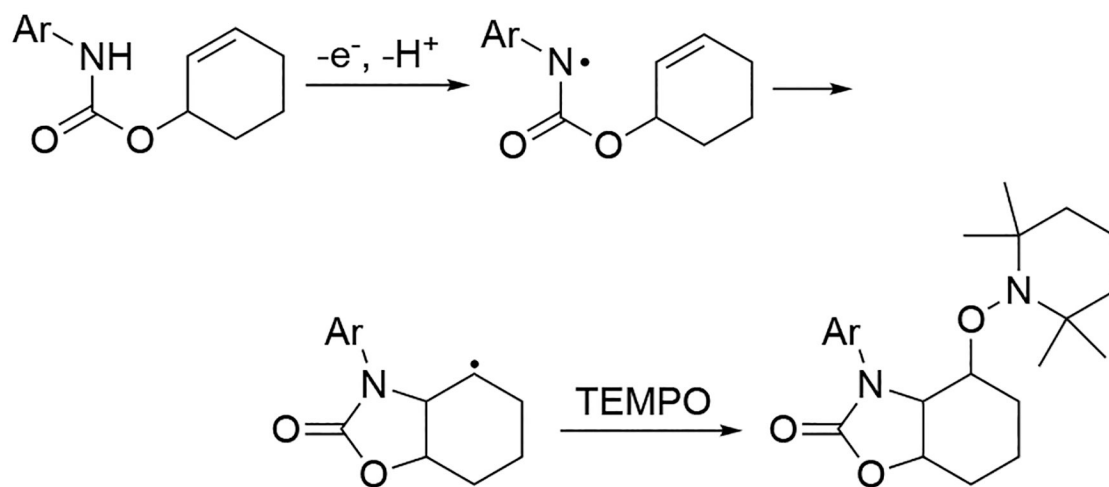
97%

Scheme 85.
Aromatization of cyclohexadienes.²²⁰

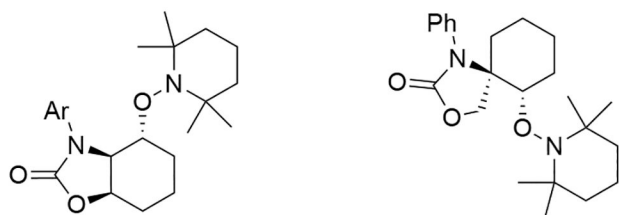
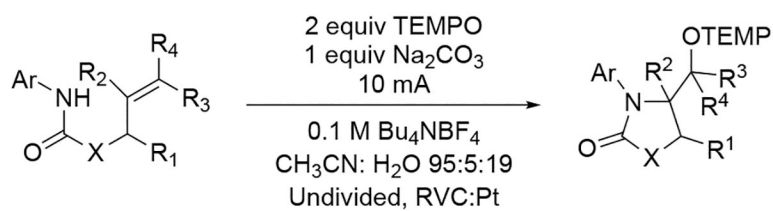
**Scheme 86.**

Wacker-type electrooxidation of terminal alkenes by Pd(OAc)₂ catalysis with co-catalytic TEMPO.²³⁰

**Scheme 87.**Electrochemical generation of cationic Pd²⁺ species.

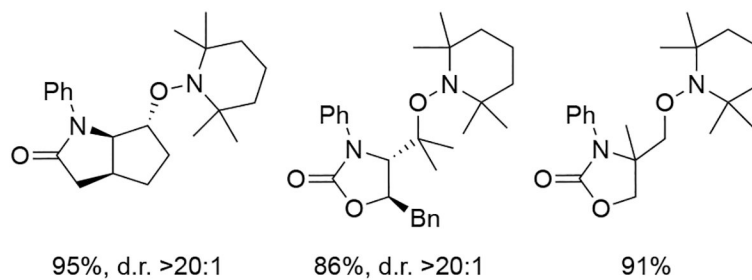


Scheme 88.
Proposed route for aminooxygenation of unactivated alkenes.²³⁵



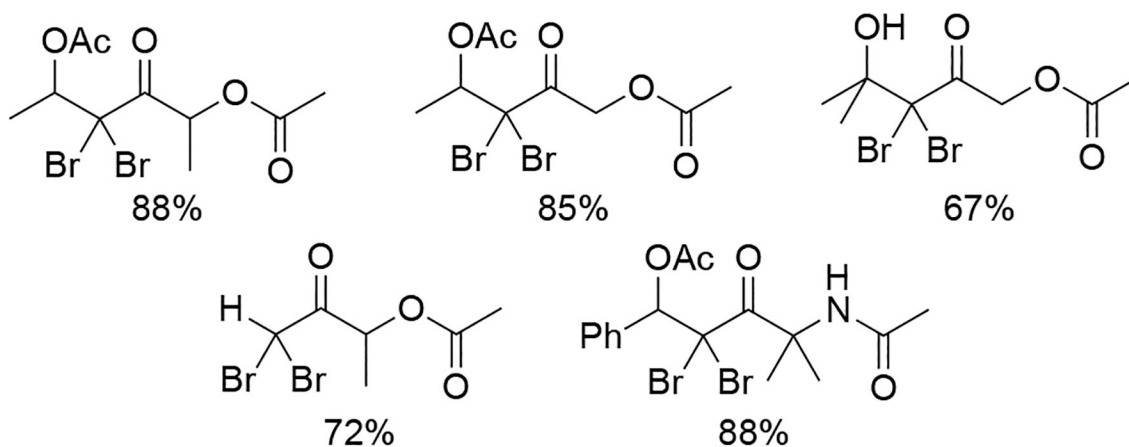
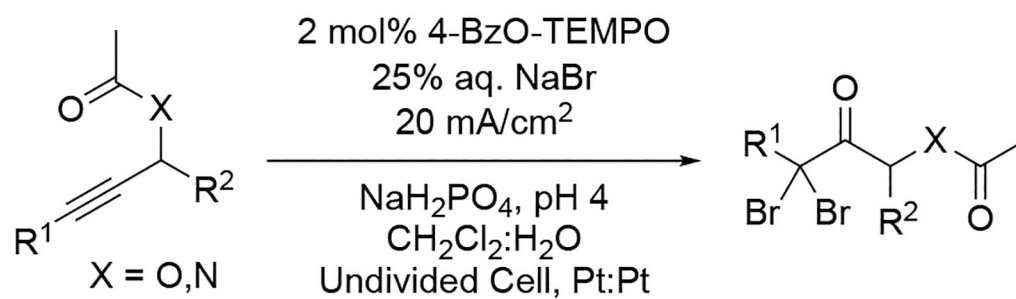
Ar = 4-NO₂Ph, 51%, d.r. >20:1
Ar = CF₃Ph, 83%, d.r. >20:1
Ar = 4-OMePh, 94%, d.r. >20:1
Ar = 2,6-Me₂Ph, 93%, d.r. >20:1

96%, d.r. >20:1

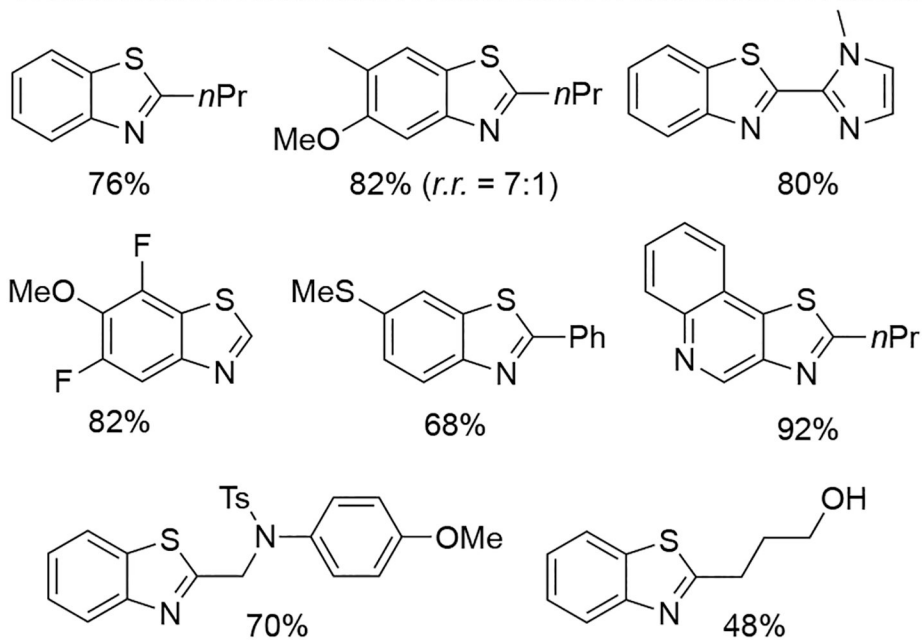
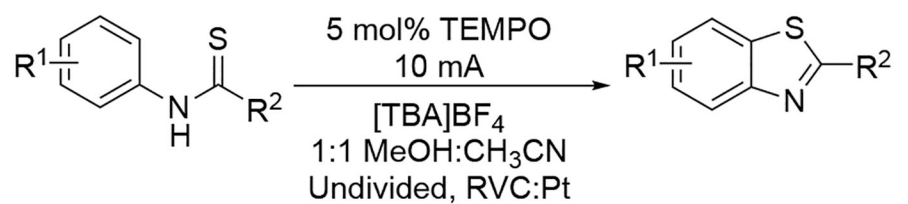


Scheme 89.

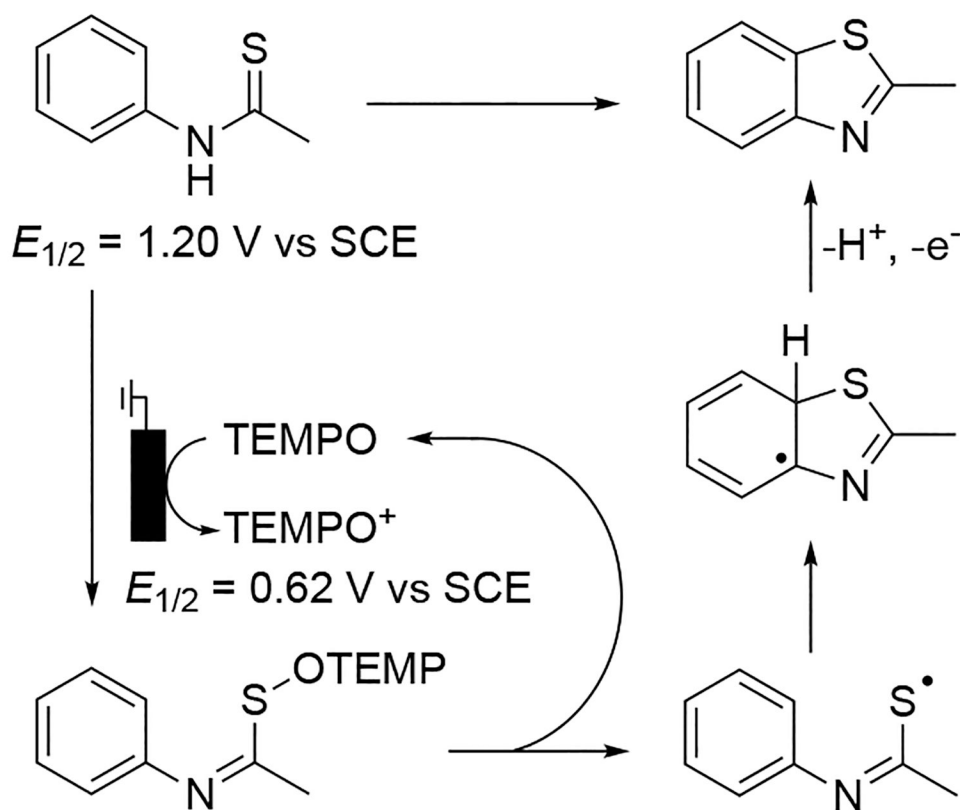
Intramolecular aminooxygenation of unactivated alkenes mediated by TEMPO.²³⁵

**Scheme 90.**

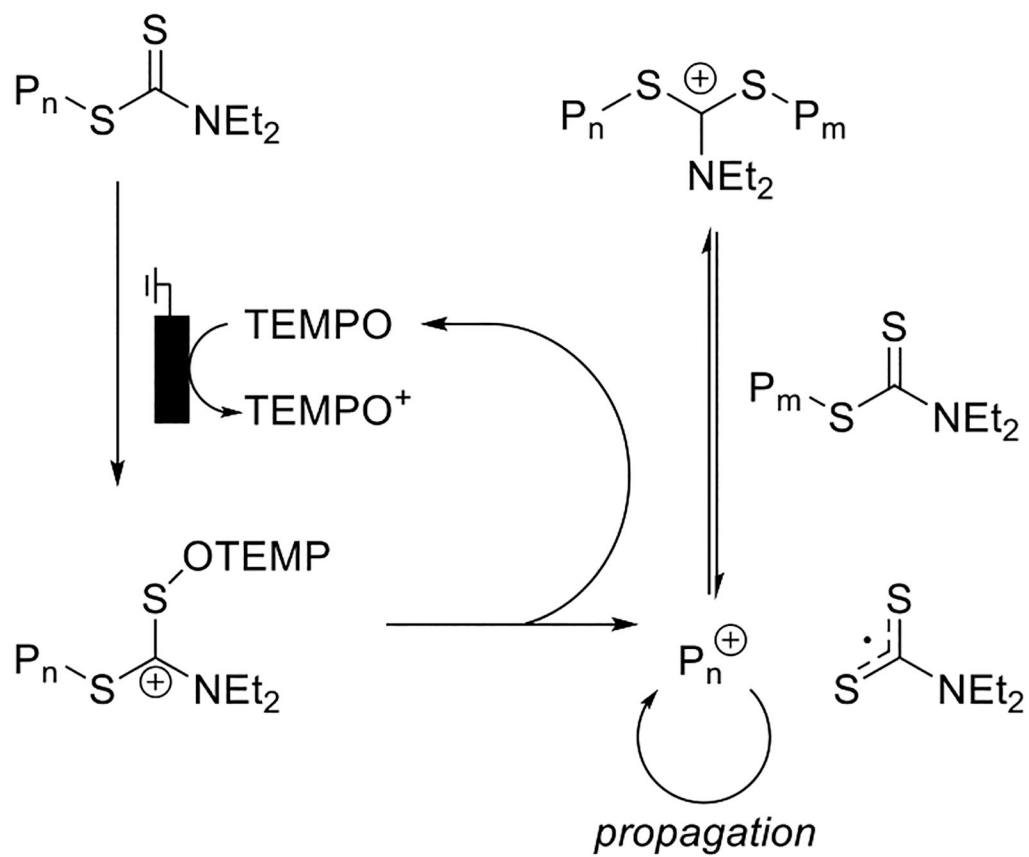
Mediated electrooxidation of propargyl acetates to provide α,α -dihaloketone products.²³⁶

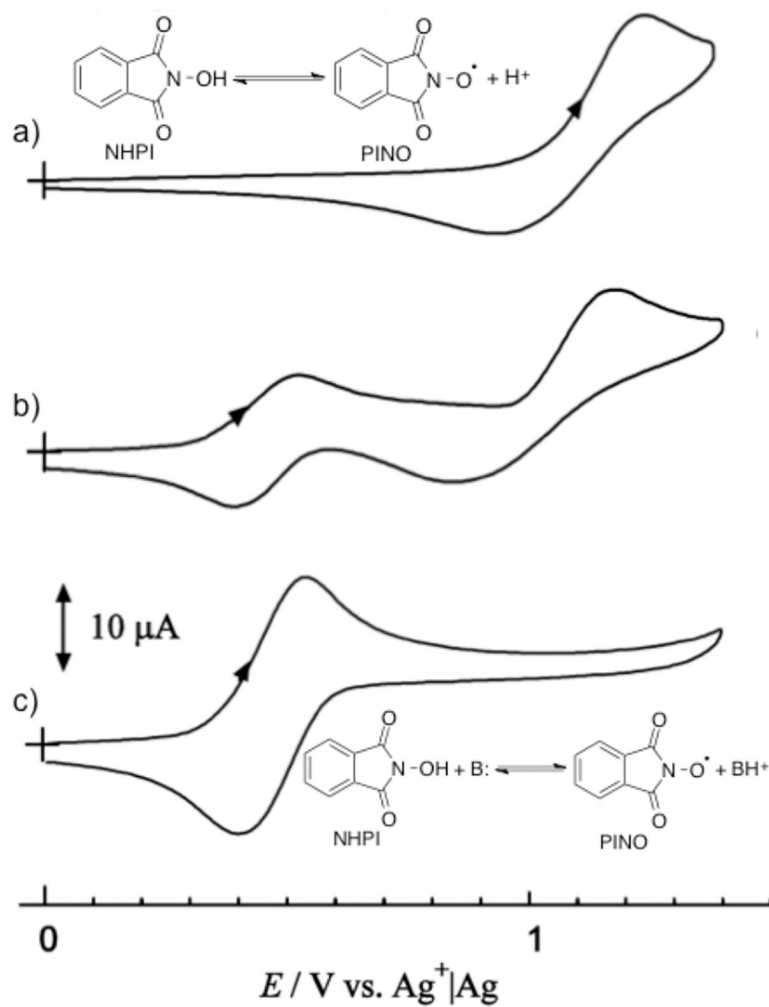


Scheme 91.
Electrooxidation of thioamides by TEMPO.²³⁹

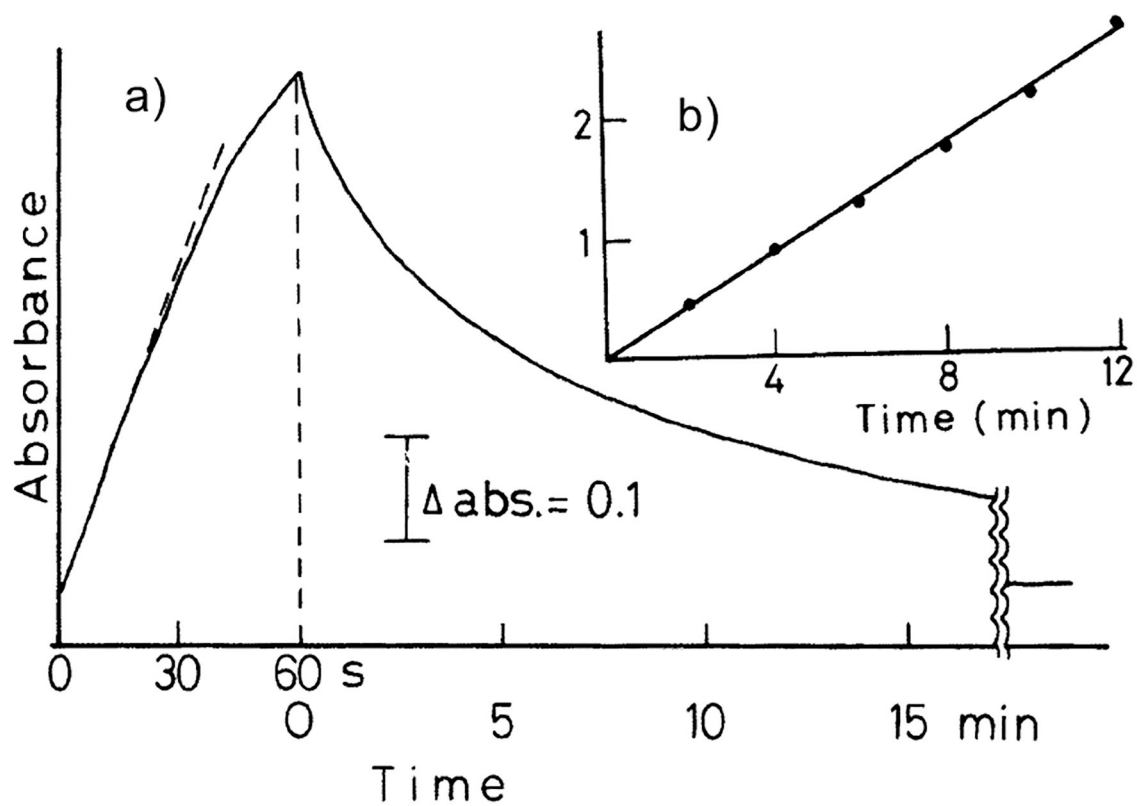
**Scheme 92.**

Proposed mechanism of TEMPO-mediated oxidation of thioamides. The $E_{1/2}$ of TEMPO under these conditions was measured to be 0.62 V vs. SCE.²³⁹

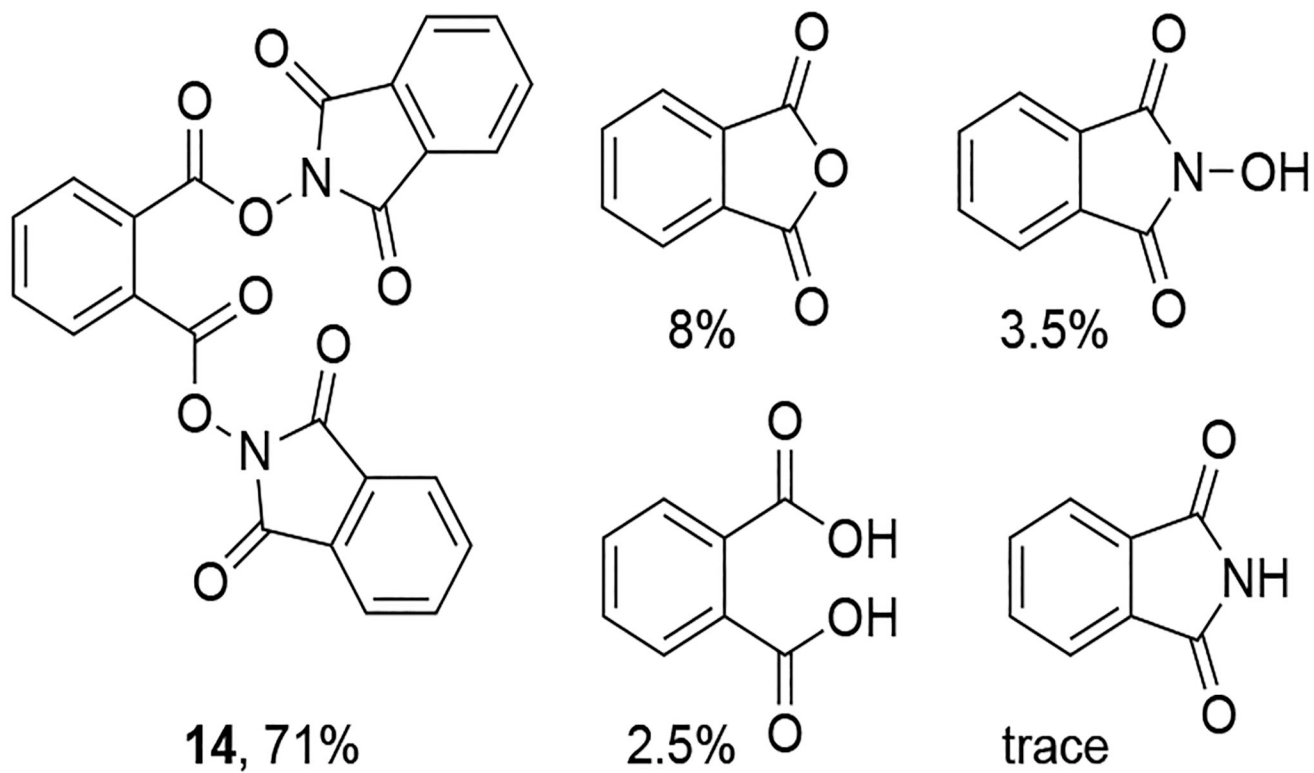
**Scheme 93.**Proposed pathway for TEMPO-mediated electrochemical cationic polymerization.²⁴⁰

**Scheme 94.**

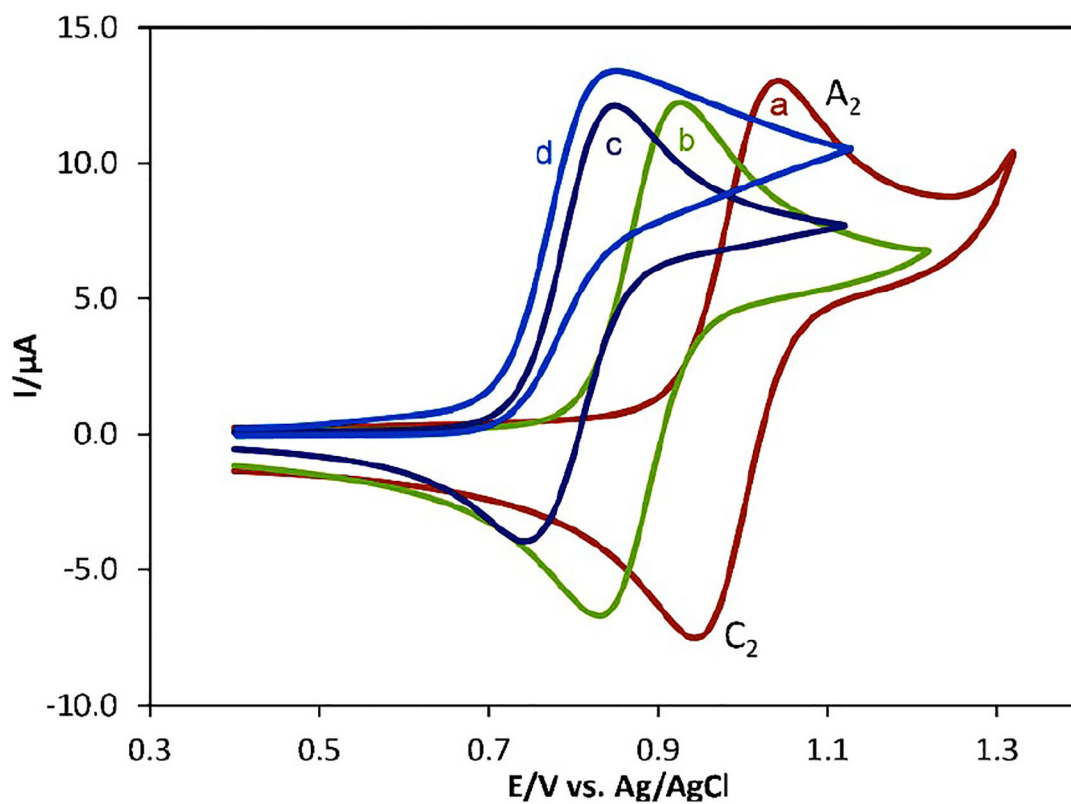
CVs for 5 mM NHPI in 0.1 M Et₄NClO₄ in CH₃CN at a glassy carbon electrode in the (a) absence and (b) presence of 1 mM and (c) 5 mM 2,6-lutidine. Scan rate = 200 mV s⁻¹. Redox reactions added for clarity. Adapted with permission from ref. 242. Copyright 2005 Elsevier.

**Scheme 95.**

a) Absorption-time curve for the generation and decay of PINO and (b) the second-order plot for the decomposition of PINO; the ordinate for the inset plot corresponds to $(A_0 - A)/A_0A$, where A_0 and A are the absorbance at $t=0$ and t , respectively. Reprinted with permission from ref. 44. Copyright 1987 The Pharmaceutical Society of Japan.

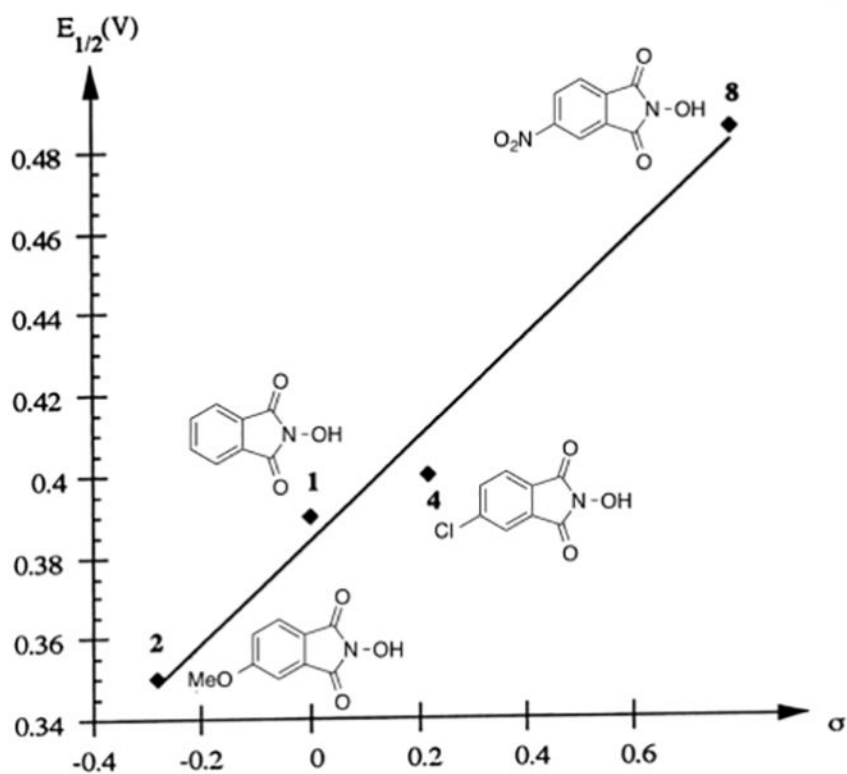
**Scheme 96.**Decomposition products of PINO observed following bulk electrolysis of NHPI in CH₃CN.

44

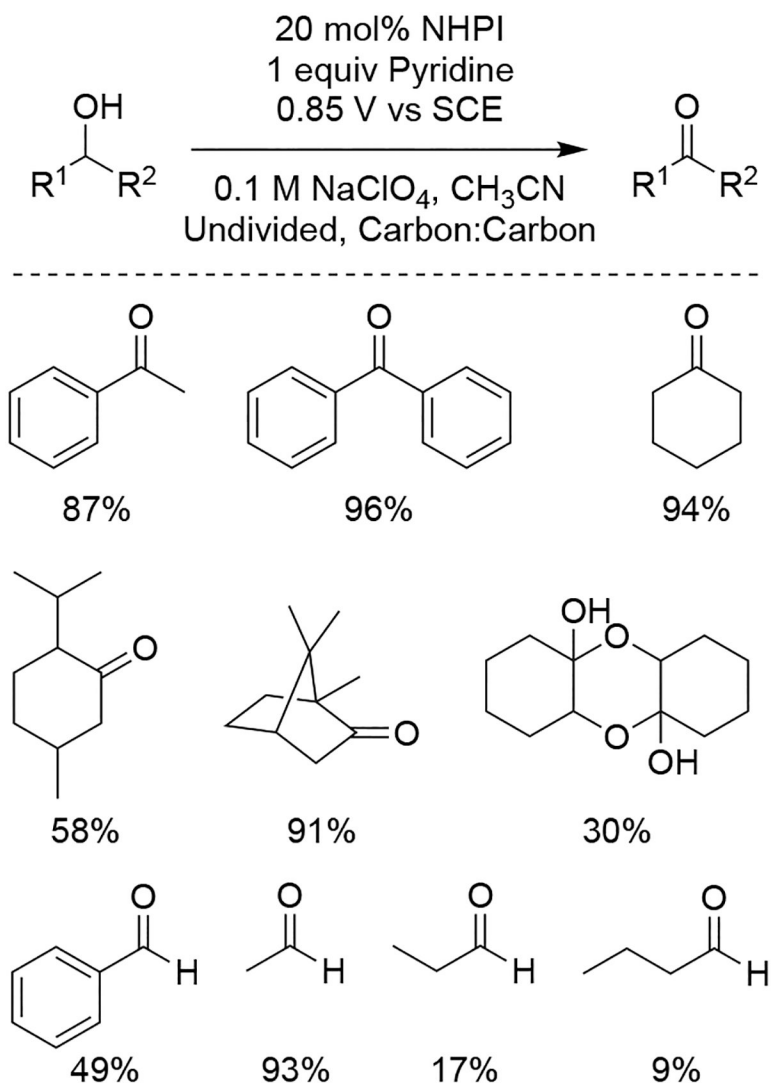
**Scheme 97.**

CVs of 1.0 mM NHPI in buffered solutions at various pH values and the same ionic strength. The solution pHs [from (a) to (d)] are: 2.5, 4.7, 7.2 and 8.3. Scan rate = 100 mV s^{-1} .

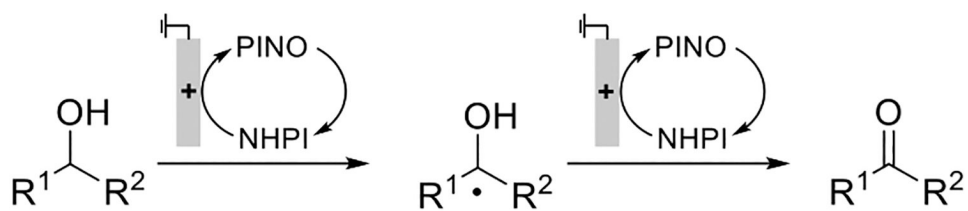
Reprinted with permission from ref. 68. Copyright 2014 John Wiley and Sons.

**Scheme 98.**

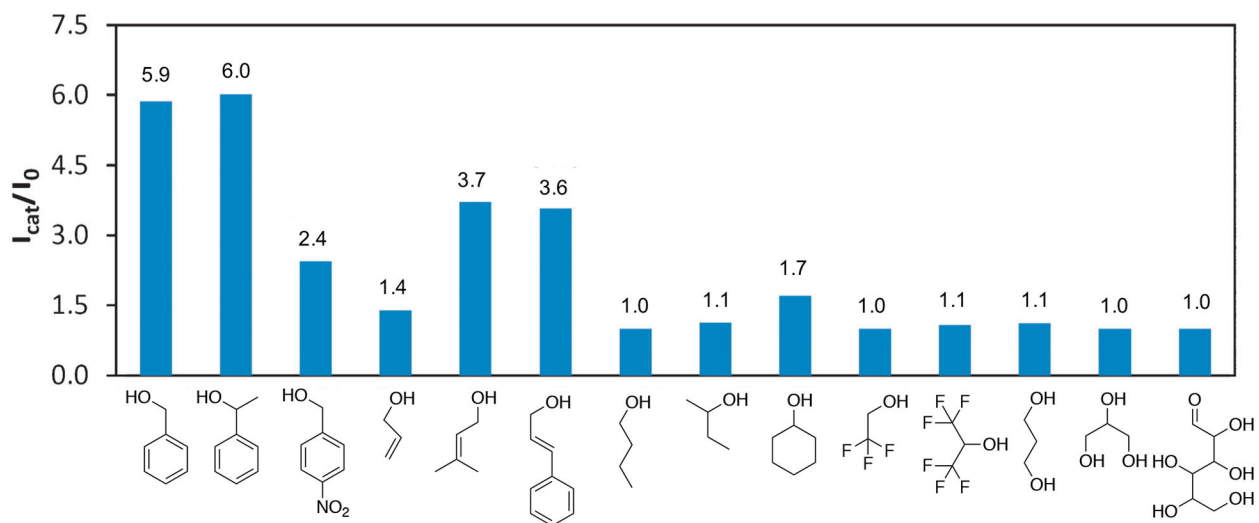
The reported $E_{1/2}$ (vs. Ag/Ag^+) for NHPI derivatives in the presence of collidine versus the σ Hammett parameters for the substituent on 4-position of the NHPI benzene ring. Adapted with permission from ref. 246. Copyright 1998 Elsevier.



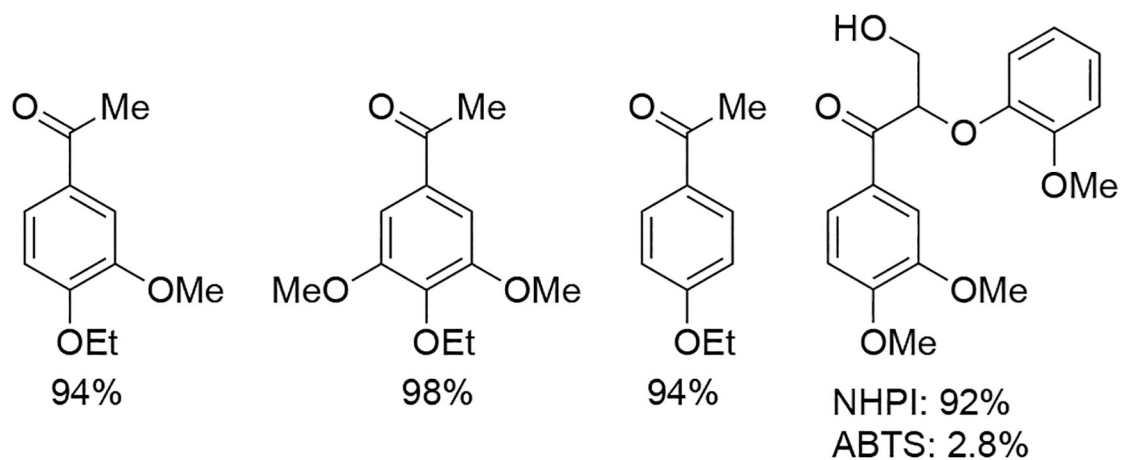
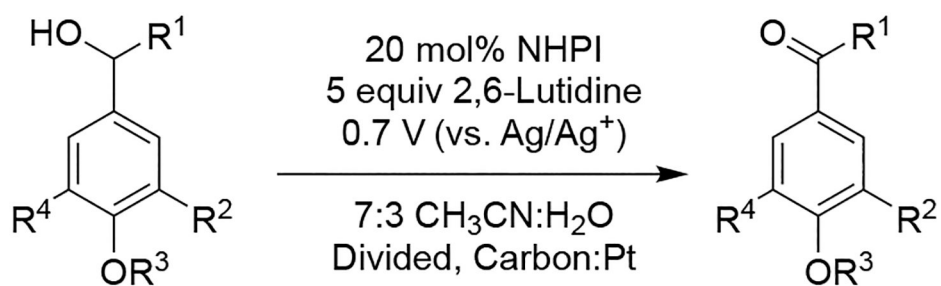
Scheme 99.
NHPI-mediated electrochemical oxidation of alcohol substrates.³⁸

**Scheme 100.**

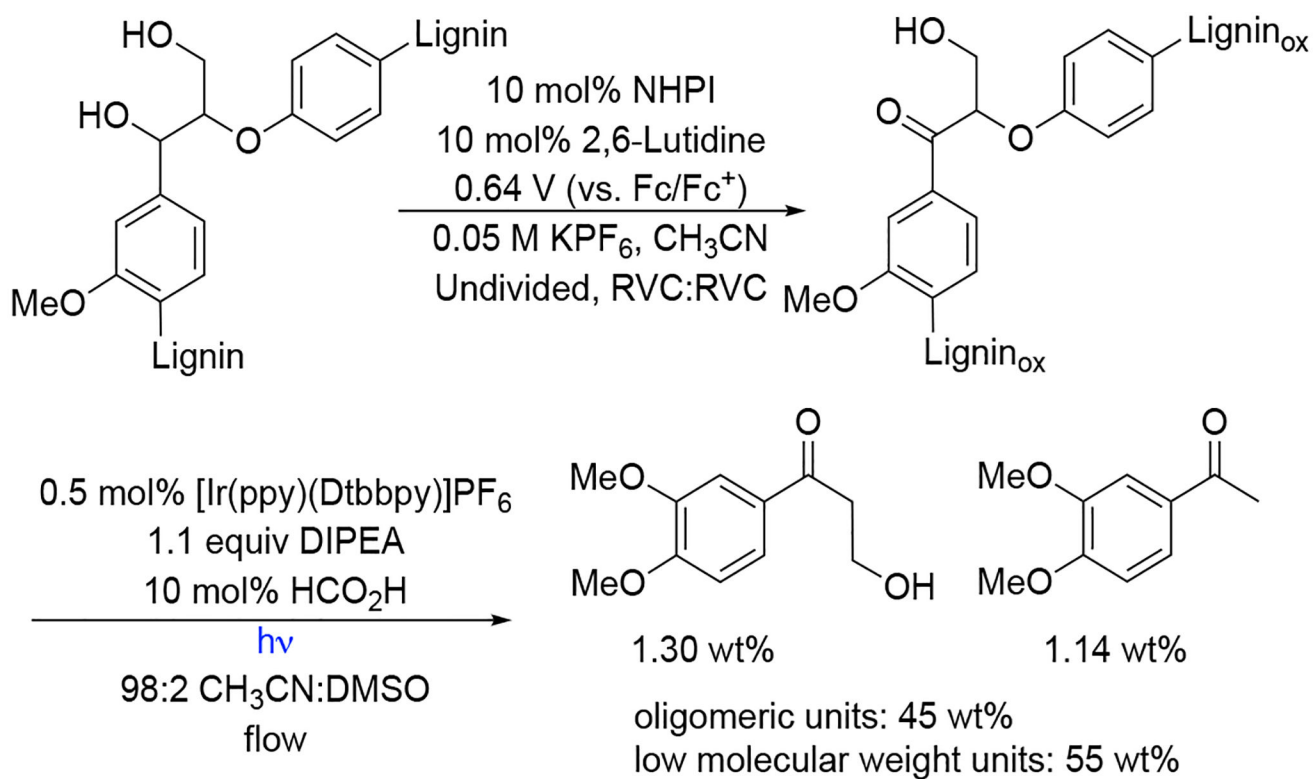
Suggested mechanism of NHPI-mediated electrooxidation of alcohols.

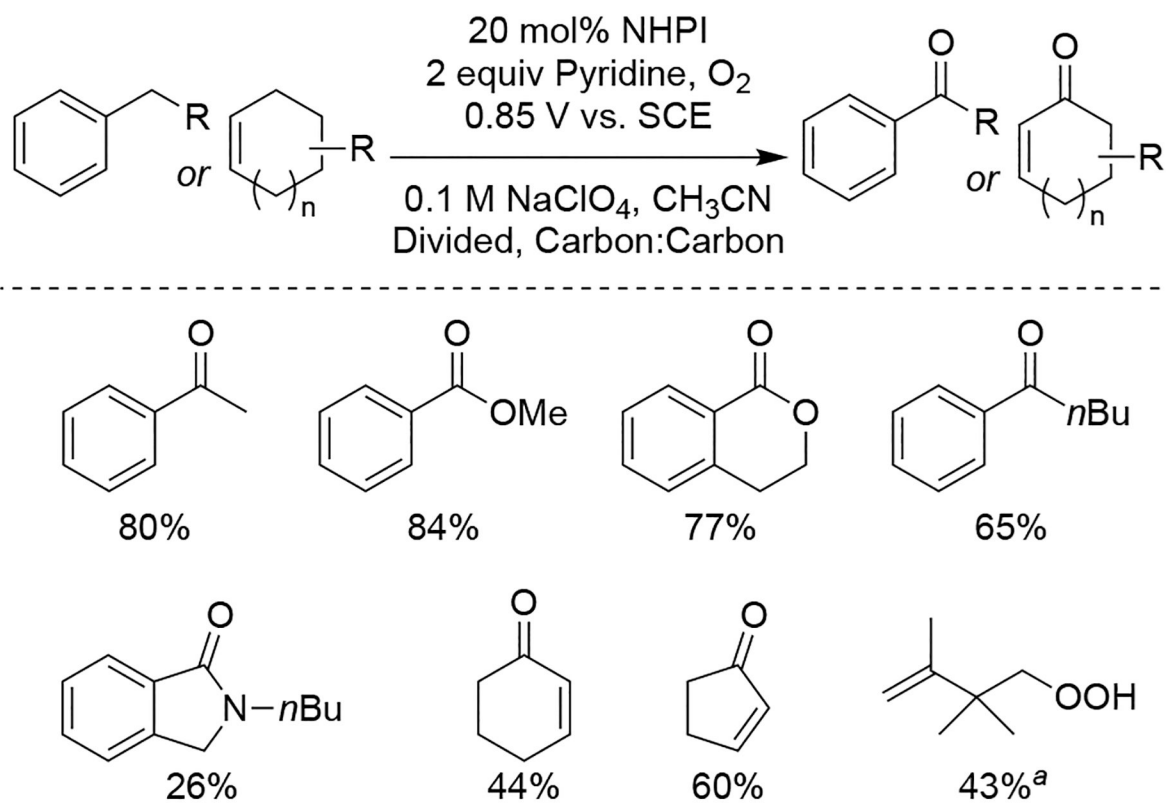
**Scheme 101.**

Ratio of the anodic-peak current (i_{cat}) of NHPI in the presence of alcohols compared to the anodic peak current (i_0) in the absence of alcohols. Reprinted with permission from ref. 68. Copyright 2014 John Wiley and Sons.

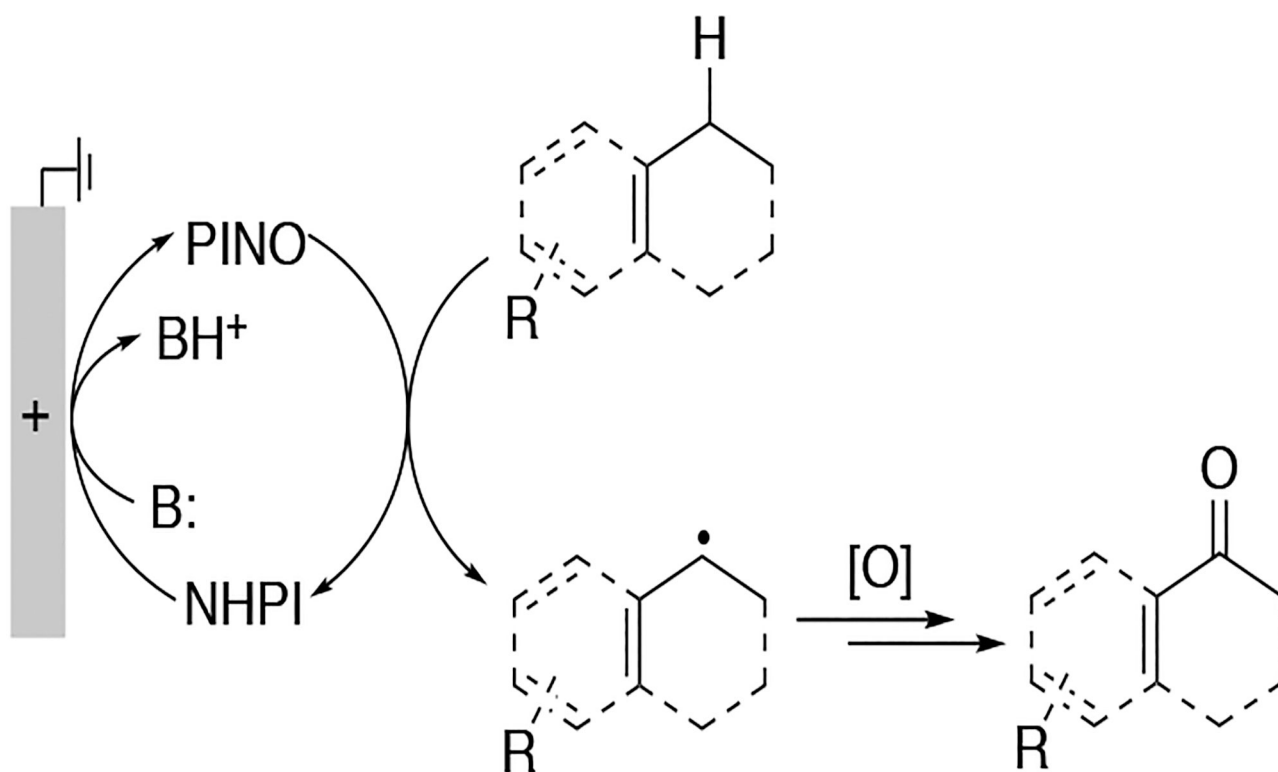


Scheme 102.
NHPI-mediated electrooxidation of lignin models.²⁵¹

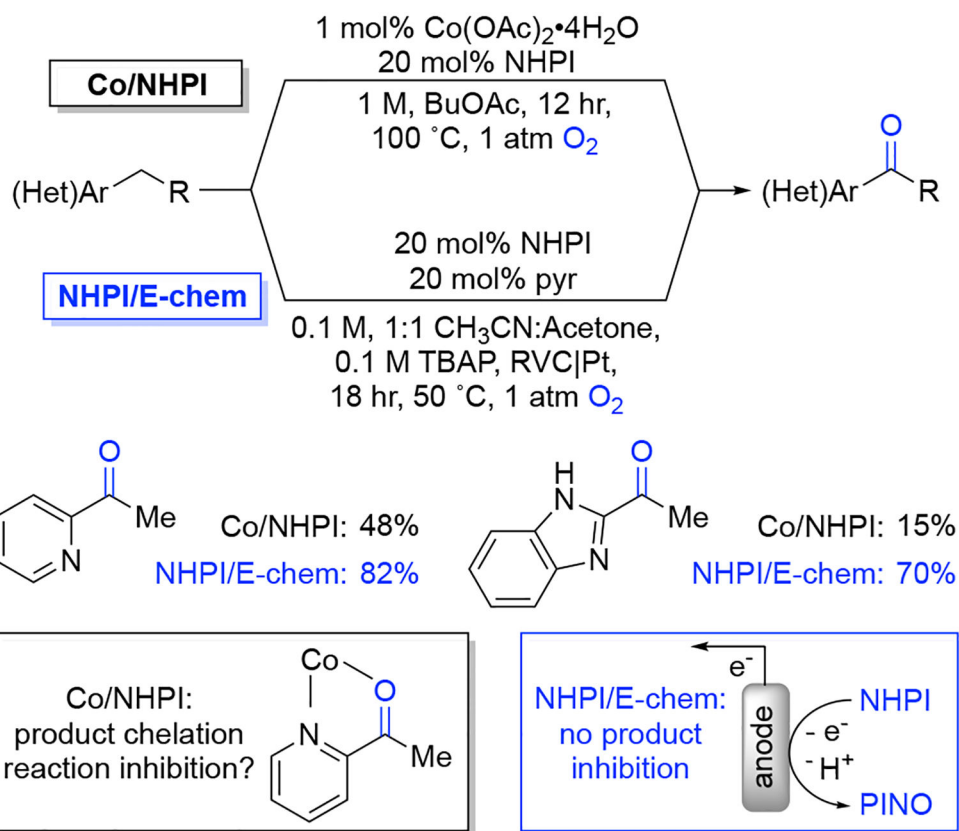
**Scheme 103.**Electrooxidation and photochemical cleavage of native lignin.²⁵²



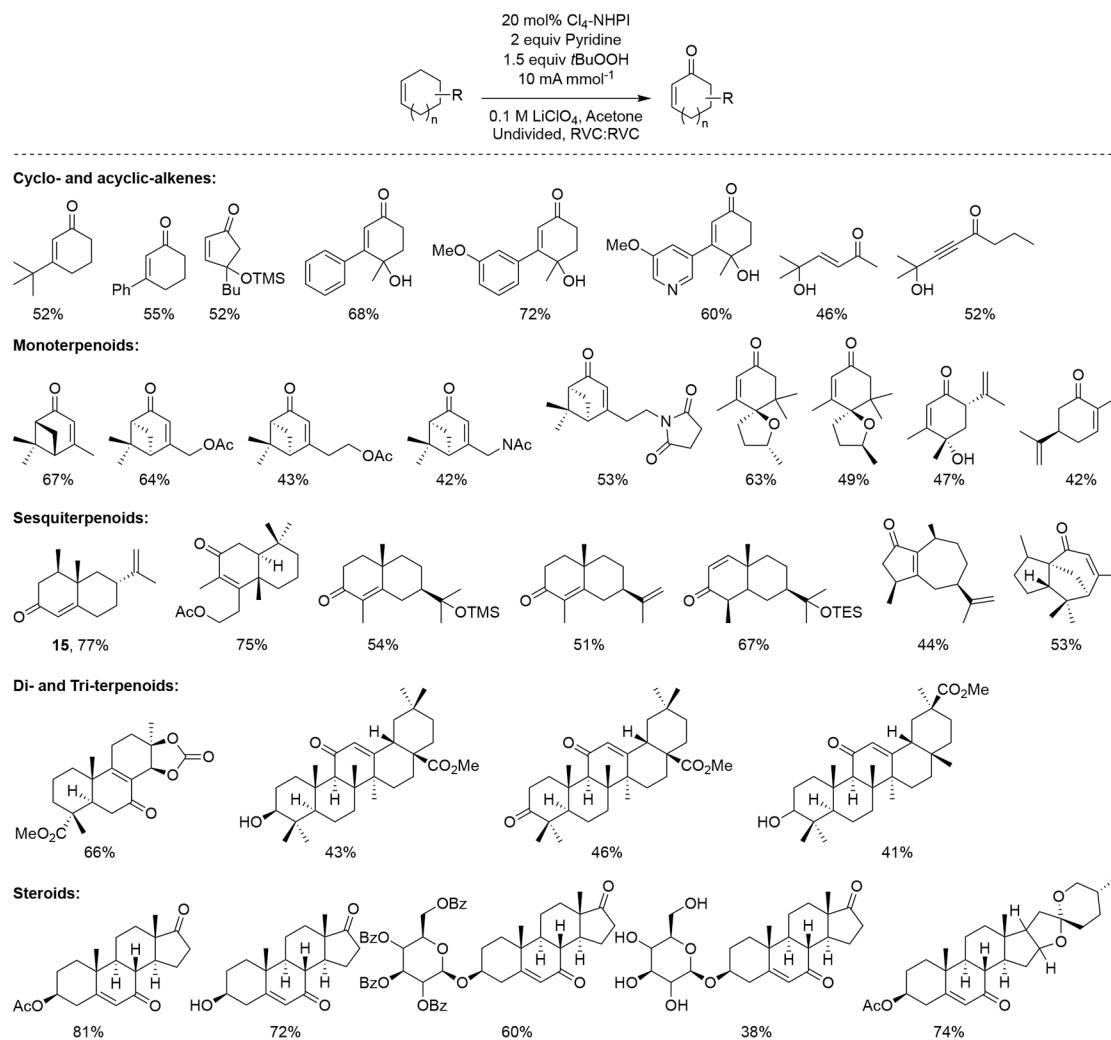
Scheme 104.
 Benzylic and allylic oxygenation mediated by NHPI.³⁹

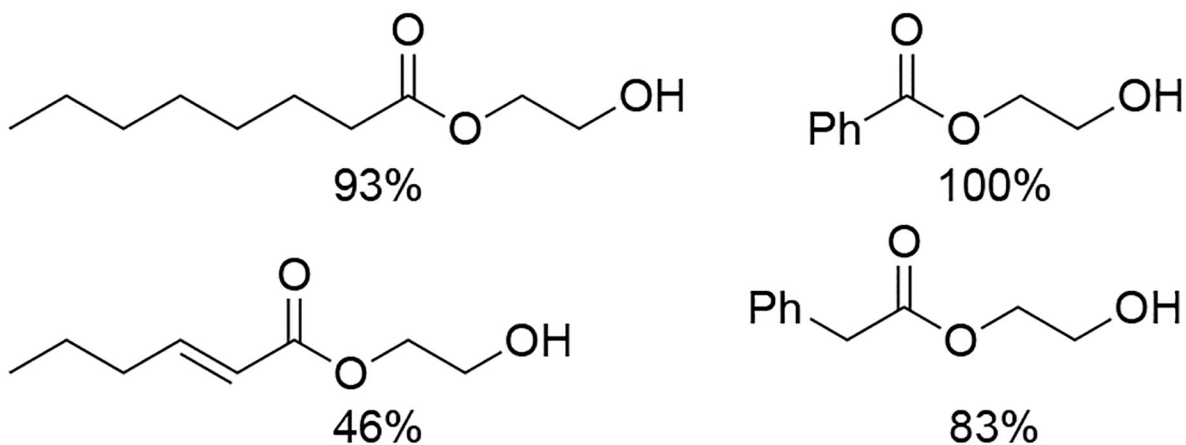
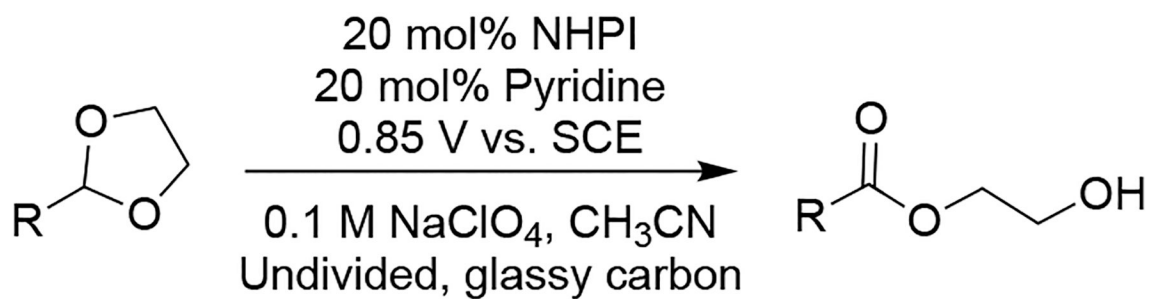
**Scheme 105.**

Electrochemical NHPI/PINO mediated oxygenation of benzylic and allylic bonds.

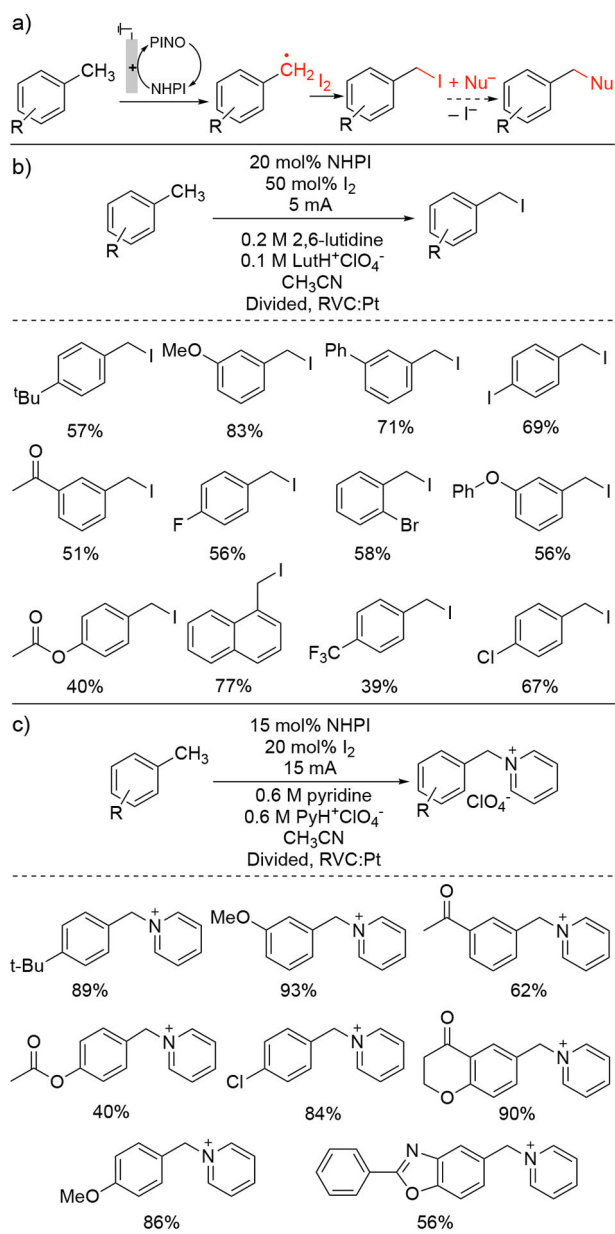
**Scheme 106.**

Comparison of the benzylic oxygenation of heteroaromatic species by NHPI-mediated aerobic and electrochemical methods. Adapted from Ref. 256 with permission from the Royal Society of Chemistry.

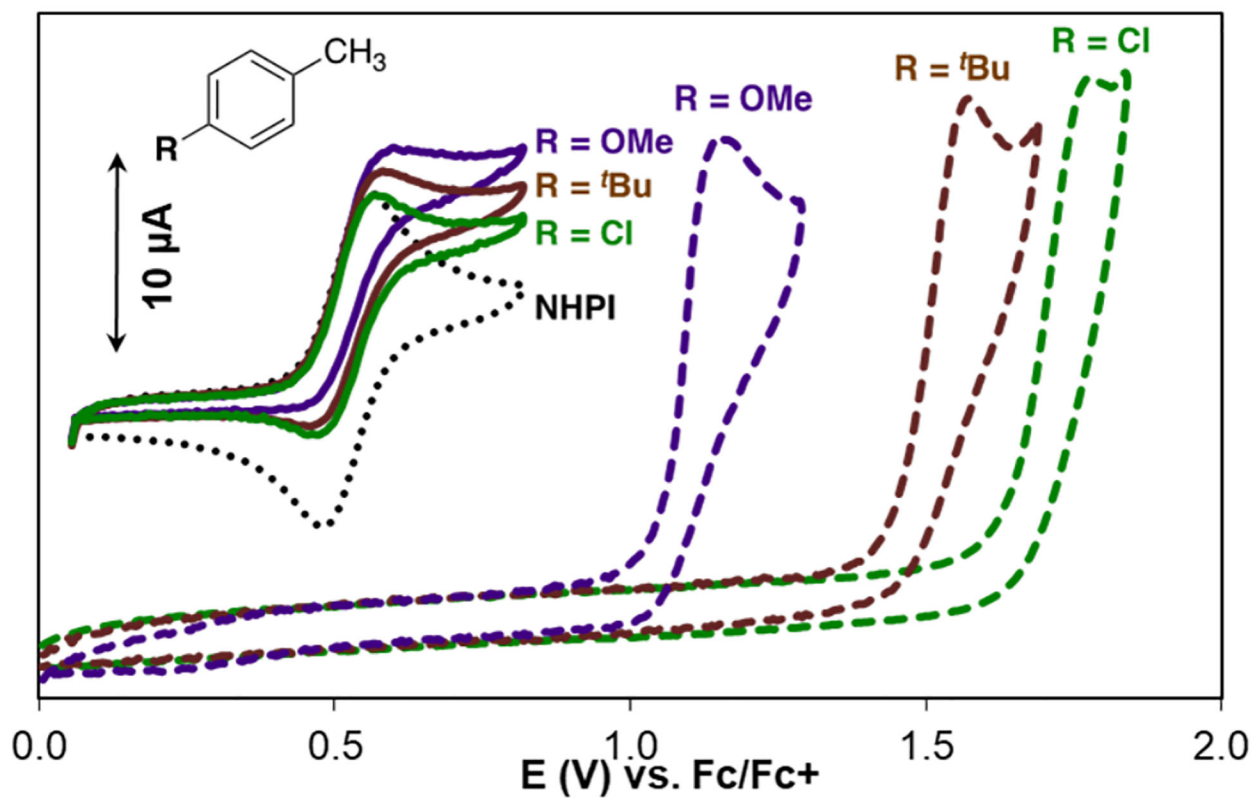
**Scheme 107.**Scope of the oxygenation of allylic C–H bonds mediated by Cl₄-NHPI.²⁵⁷



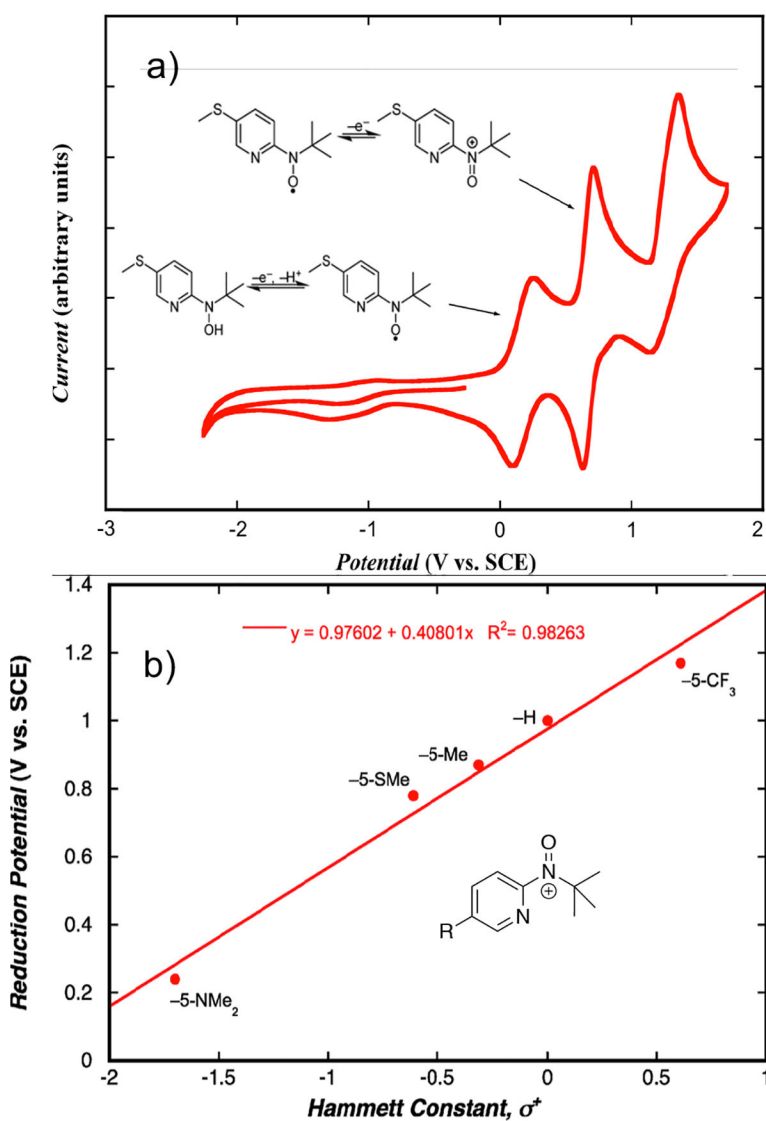
Scheme 108.
NHPI-mediated oxidation of aldehyde acetals.⁴²

**Scheme 109.**

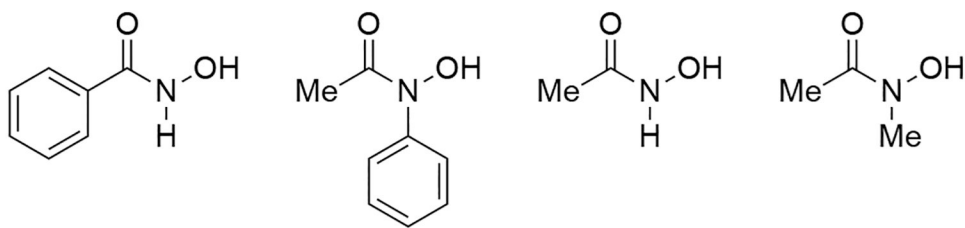
a) Electrochemical NHPI/PINO-mediated iodination/functionalization of methyl arenes b) iodination and c) in situ methylarene iodination/alkylation of pyridine. LutH⁺ = 2,6-lutidinium, PyrH⁺ = pyridinium.

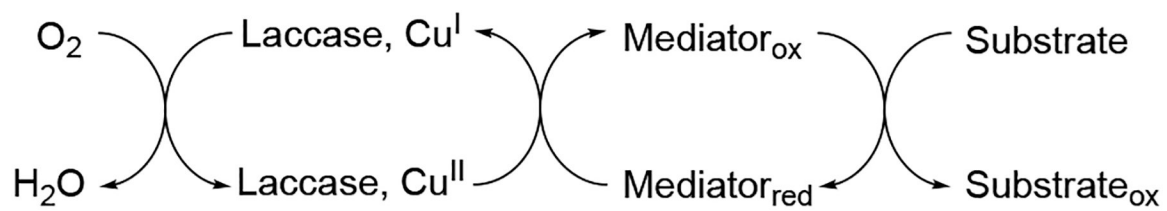
**Scheme 110.**

Comparison of the required potential for NHPI mediated HAT (solid lines), and direct ET (dashed lines) for oxidation of (green) *p*-chlorotoluene, (brown) *p*-*t*-butyltoluene, and (blue) *p*-methoxytoluene. Dotted line shows the CV of NHPI in the absence of substrates. Current units from the original report have been corrected.

**Scheme 111.**

a) CV of acyclic aminoxyl radical derivative. Redox reactions added for clarity. b) Correlation between the reduction potential of acyclic oxoammonium derivatives and substituent Hammett σ^* constants. Adapted with permission from ref. 268. Copyright 2013 American Chemical Society.

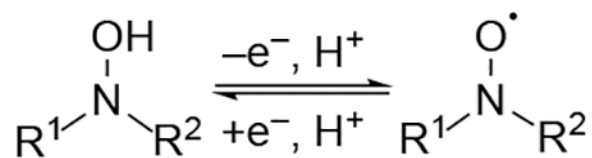
**Scheme 112.**Hydroxamic acids examined by Masui and co-workers.²⁴¹

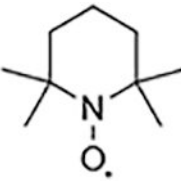
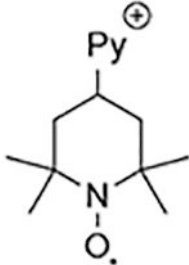
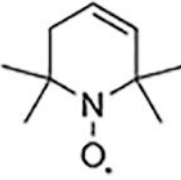
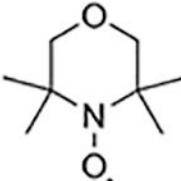
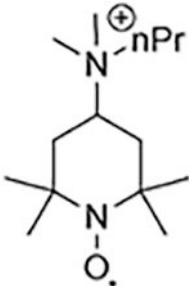
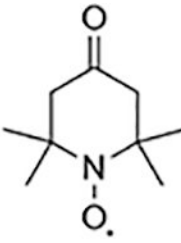
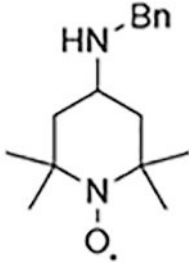


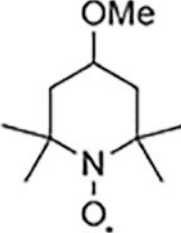
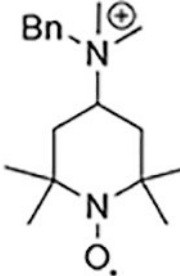
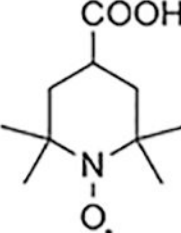
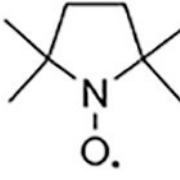
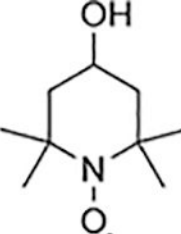
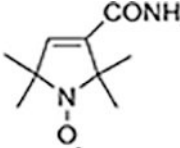
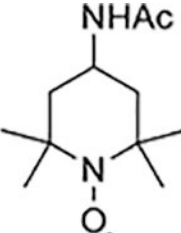
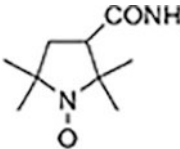
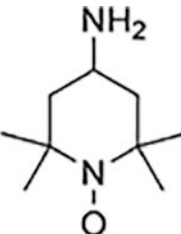
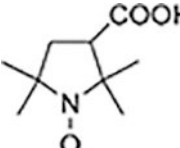
Scheme 113.
Laccase mediated aerobic oxidation

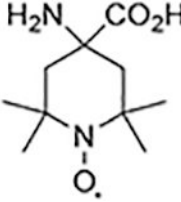
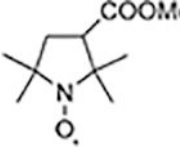
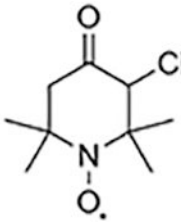
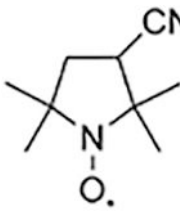
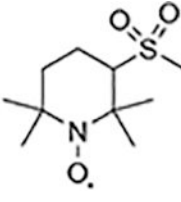
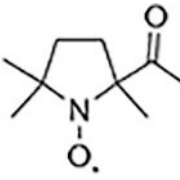
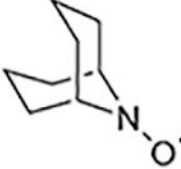
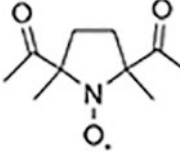
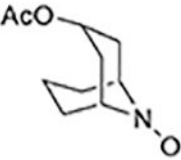
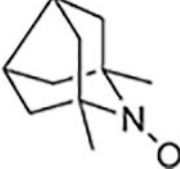
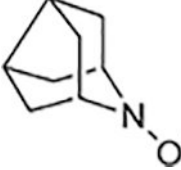
Table 1.

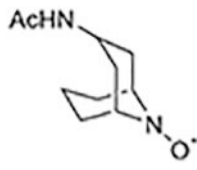
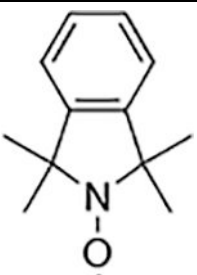
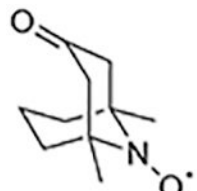
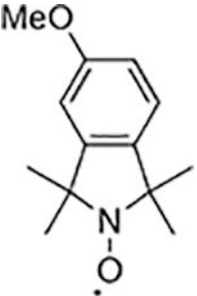
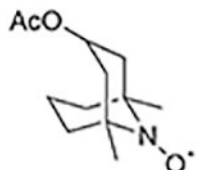
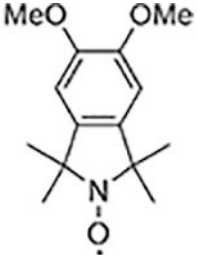
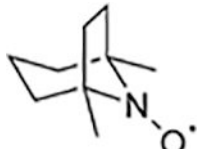
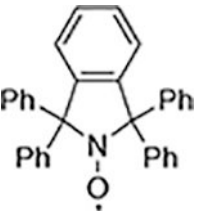

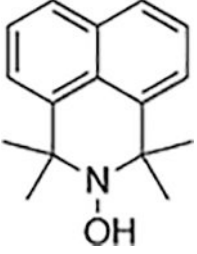
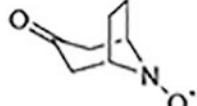
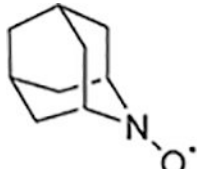
Experimental aminoxyl/oxoammonium redox potentials.

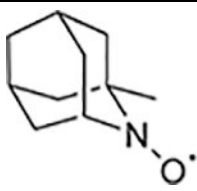
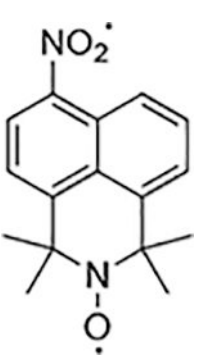
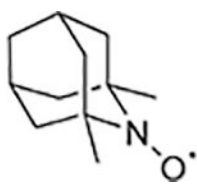
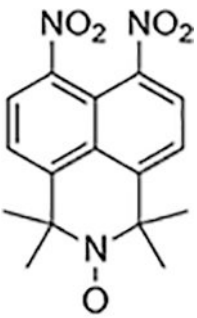
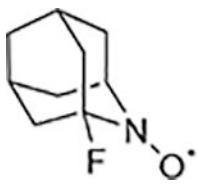
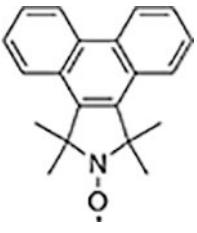
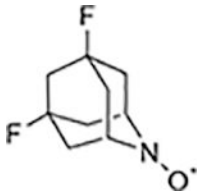
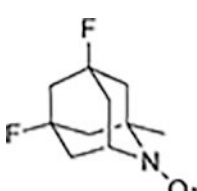


Entry	Aminoxyl Derivative	Potential ^a	Ref.	Entry	Aminoxyl Derivative	Potential ^a	Ref.
1		$E_a = 0.77^b$	60	13		$E_a = 0.95^b$	60
		$E_{1/2} = 0.73^b$	73				
		$E_{1/2} = 0.84^c$	75				
2		$E_{1/2} = 1.00^b$	80				
3		$E_{1/2} = 0.90^b$	63	14		$E_a = 1.00^b$	60
4		$E_a = 0.91^b$	60	15		$E_a = 0.92^b$	60

Entry	Aminoxyl Derivative	Potential ^a	Ref.	Entry	Aminoxyl Derivative	Potential ^a	Ref.
5		$E_a = 0.86^b$	60	16		$E_a = 1.02^b$	60
6		$E_a = 0.82^b$	60	17		$E_{1/2} = 0.89^c$	76
7		$E_a = 0.85^b$	60	18		$E_{1/2} = 0.91^b$	77
8		$E_a = 0.88^b$	60	19		$E_{1/2} = 0.84^b$	74
9		$E_a = 0.91^b$	60	20		$E_{1/2} = 0.88^b$	74

Entry	Aminoxyl Derivative	Potential ^a	Ref.	Entry	Aminoxyl Derivative	Potential ^a	Ref.
10		$E_a = 0.67^b$	60	21		$E_{1/2} = 0.89^b$	74
11		$E_a = 1.01^b$	60	22		$E_{1/2} = 1.00^b$	74
12		$E_{1/2} = 1.05^b$	78	23		$E_{1/2} = 1.10^c$	76
25		$E_a = 0.75^b$ $E_{1/2} = 0.68^b$ $E_{1/2} = 0.80^c$	60 73 75	24		$E_{1/2} = 1.31^c$	76
26		$E_a = 0.86^b$	60	39		$E_a = 0.61^b$	60
				40		$E_a = 0.74^b$	60

Entry	Aminoxyl Derivative	Potential ^a	Ref.	Entry	Aminoxyl Derivative	Potential ^a	Ref.
27		$E_a = 0.85^b$	60	41		$E_{1/2} = 0.97^c$	78
28		$E_a = 1.02^c$	72	42		$E_{1/2} = 0.96^c$	78
29		$E_a = 0.75^b$	60	43		$E_{1/2} = 0.93^c$	78
30		$E_a = 0.68^b$	60	44		$E_{1/2} = 1.23^c$	78
31		$E_{1/2} = 1.00^c$	72	45		$E_{1/2} = 0.94^c$	78
32		$E_{1/2} = 1.06^b$	72				
33		$E_{1/2} = 0.74^b$	60				
		$E_{1/2} = 0.65^b$	73				
		$E_{1/2} = 0.79^c$	75				

Entry	Aminoxyl Derivative	Potential ^a	Ref.	Entry	Aminoxyl Derivative	Potential ^a	Ref.
34		$E_{1/2} = 0.74^c$	75	46		$E_{1/2} = 1.02^c$	78
35		$E_{1/2} = 0.69^c$	75	47		$E_{1/2} = 1.05^c$	78
36		$E_{1/2} = 1.02^c$	75	48		$E_{1/2} = 0.99^c$	78
37		$E_{1/2} = 1.14^c$	75				
38		$E_{1/2} = 1.08^c$	75				

^aPotentials adjusted relative to NHE, as described in ref. 17–19. In ref. 60, only the anodic peak potentials (E_a), not the mid-point potentials ($E_{1/2}$), were reported.

Abbreviations: Ac = acetyl, Bn = benzyl, Py[⊕] = N-pyridinium, nPr=n-propyl.

^bExperimental measurements performed in H₂O.

^cExperimental measurements performed in CH₃CN.

Table 2.Redox leveling in the $1 e^-/1 H^+$ hydroxylamine/aminoxyl redox couple.⁶³

Entry	Aminoxyl Radical	$E_{1/2}$ (vs. NHE) $R_2NOH/R_2NO\bullet$	$E_{1/2}$ (vs. NHE) $R_2NO\bullet/R_2NO^+$	R_2NOH BDE (kcal mol^{-1})
1	TEMPO	0.65	0.75	71 ^a
2	4-AcNH-TEMPO	0.67	0.86	73
3	4-NH ₃ ⁺ -TEMPO	0.61	0.93	72

^a Average of values reported in ref. 35,86

Author Manuscript

Author Manuscript

Author Manuscript

Author Manuscript

Table 3.

Effect of ring structure on the calculated $1 e^-$ potentials for oxidation and reduction of cyclic aminoxy radicals. Gas phase species were optimized at the G3(MP2)-RAD level with B3-LYP/6-31G(d) level of theory. Solvation energies of each species were calculated using the polarized continuum model. Experimental values were measured in CH_3CN with 0.1 M NBu_4BF_4 at a Pt electrode. Values are referenced against NHE.⁷⁸

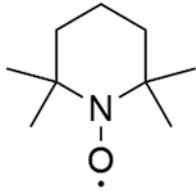
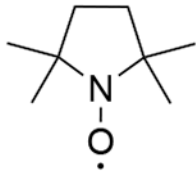
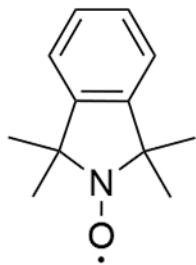
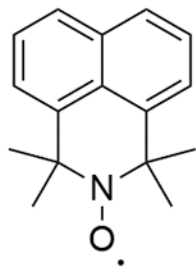
Entry	Aminoxy Radical	Experimental Potential (mV)	Calculated Potential (mV)
1		850	807
2		976	971
3		1045	999
4		1010	474

Table 4.

TOF (h^{-1}) of various aminoxyl radicals for the oxidation of alcohols. Reprinted with permission from ref. 73.
 Copyright 2015 American Chemical Society.

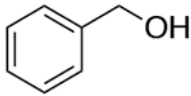
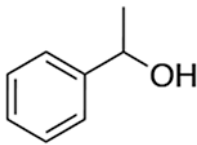
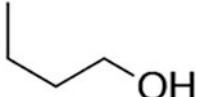
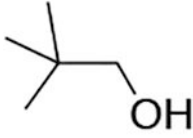
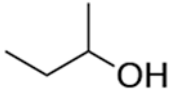
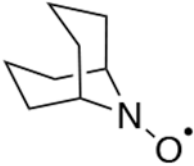
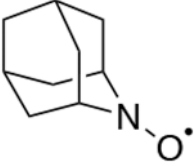
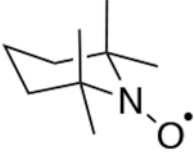
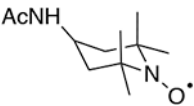
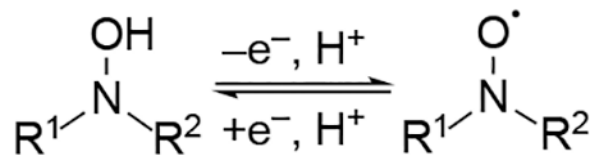
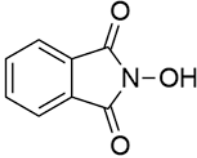
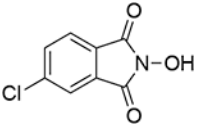
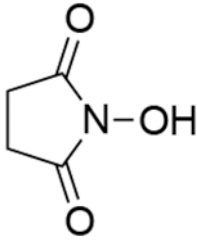
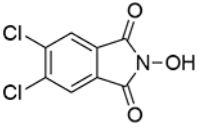
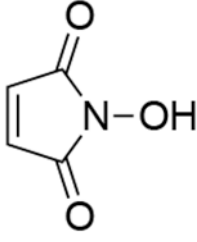
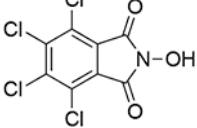
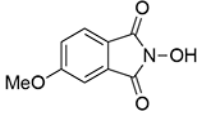
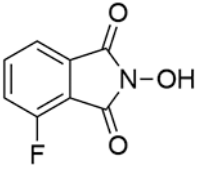
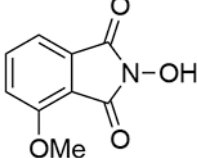
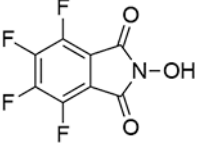
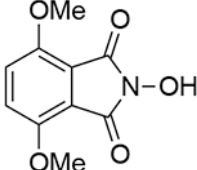
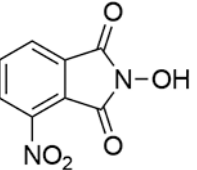
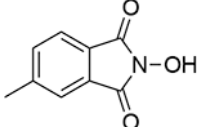
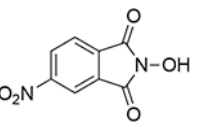
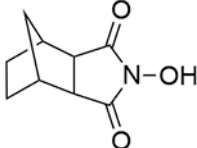
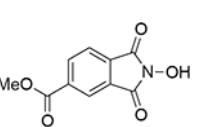
					
	<i>1° benzylic</i>	<i>2° benzylic</i>	<i>1° aliphatic</i>	<i>sterically hindered 1° aliphatic</i>	<i>2° aliphatic</i>
	1088	238	588	337	87
	1128	358	488	298	78
	853	118	568	198	18
	1228	378	708	388	73

Table 5.

Experimental *N*-hydroxyimide/imidoxyl redox potentials vs. NHE.^a

Entry	<i>N</i> -Hydroxyimide Derivative	$E_{1/2}^a$	Ref.	Entry	<i>N</i> -Hydroxyimide Derivative	$E_{1/2}^a$	Ref.
1		0.94 ^b	246	9		0.95 ^b	246
		0.93 ^c	247				
		1.08 ^d	249				
2		1.16 ^c	247	10		0.98 ^b	246
3		1.01 ^c	247	11		1.00 ^b	246
4		0.91 ^b	246	12		1.12 ^b	249
		1.04 ^d	249				
5		1.05 ^d	249	13		1.03 ^b	246

Entry	<i>N</i> -Hydroxyimide Derivative	$E_{1/2}^a$	Ref.	Entry	<i>N</i> -Hydroxyimide Derivative	$E_{1/2}^a$	Ref.
6		1.04 ^d	249	14		1.02 ^b	246
7		1.06 ^d	249	15		0.97 ^b	246
8		1.19 ^d	250	16		0.90 ^b	246

^aPotentials adjusted relative to NHE, as described in ref. 17–19.

^bExperimental measurements performed with 1.7 equivalents 2,4,6-collidine in CH₃CN.

^cExperimental measurements performed with 2 equiv 2,4,6-collidine in CH₃CN.

^dExperimental measurements performed in 50 mM citrate buffer (pH 5).

^eExperimental measurements performed 45 mM phosphate buffer (pH 6).²⁵⁰

Table 6.Second order rate constants of the reaction of PINO with alcohol substrates.³⁸

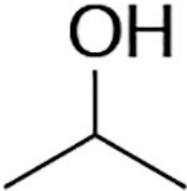
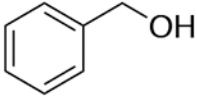
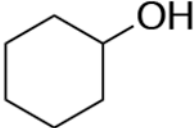
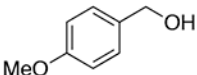
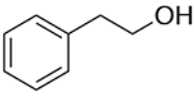
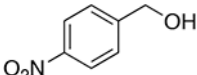
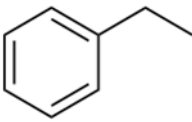
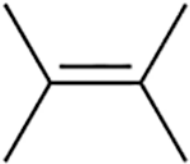
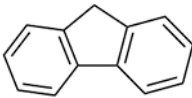
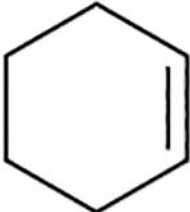
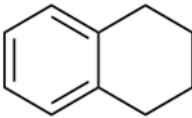
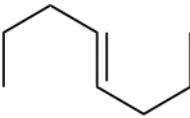
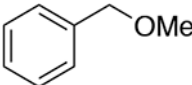

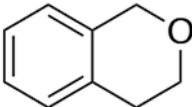
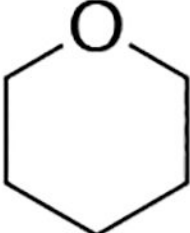
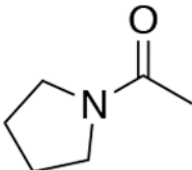
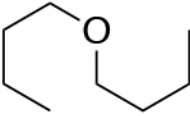
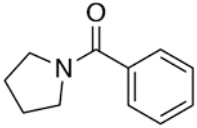

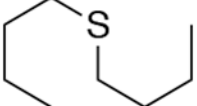
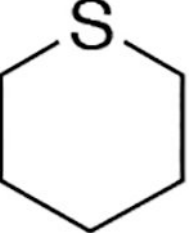
Substrate	k ($M^{-1} s^{-1}$)	Substrate	k ($M^{-1} s^{-1}$)
	1.89		15.6
	4.52		51.8
	0.776		10.3

Table 7.Second order rate constants of the reaction of PINO with substrates containing activated C–H bonds.⁴⁴

Substrate	k ($M^{-1} s^{-1}$)	Substrate	k ($M^{-1} s^{-1}$)
	1.85		77.6
	26.2		20.2
	43.2		12.8
	10.9		2.88
	156		--
	47.6		1.50

Substrate	k ($M^{-1} s^{-1}$)	Substrate	k ($M^{-1} s^{-1}$)
	26.2		96.2
	36.3		15.3

Author Manuscript

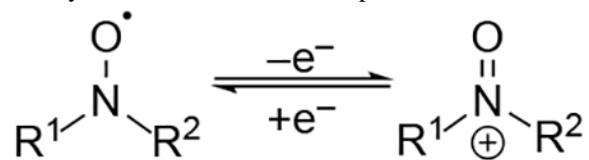
Author Manuscript

Author Manuscript

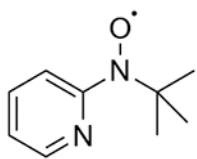
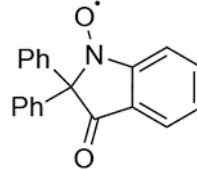
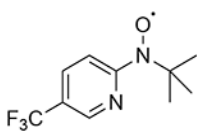
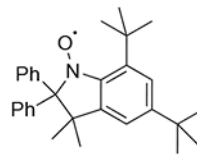
Author Manuscript

Table 8.

The redox potential of the aminoxy to oxoammonium redox process for various *N*-oxyl radicals.



Entry	Aminoxy Derivative	$E_{1/2}^a$	Ref.	Entry	Aminoxy Derivative	$E_{1/2}^a$	Ref.
1		1.36 ^b	264	10		0.69 ^c	266
2		0.78 ^c	72	11		0.63 ^c	266
3		1.01 ^d	265	12		0.95 ^c	267
4		0.48 ^c	268	13		0.57 ^c	267
5		1.00 ^c	268	14		1.14 ^c	267
6		1.02 ^c	268	15		1.05 ^c	267
7		1.11 ^c	268	16		0.98 ^c	267

Entry	Aminoxyl Derivative	$E_{1/2}^a$	Ref.	Entry	Aminoxyl Derivative	$E_{1/2}^a$	Ref.
8		1.24 ^c	268	17		1.20 ^c	273
9		1.41 ^c	268	18		1.20 ^c	273

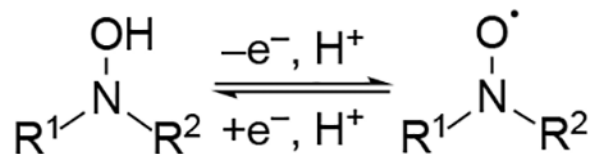
^aPotentials adjusted relative to NHE, as described in ref. 17–19.

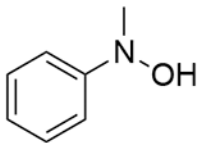
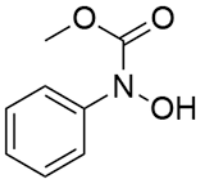
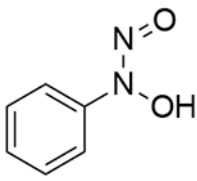
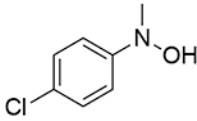
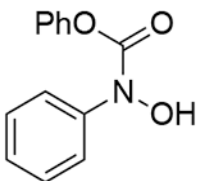
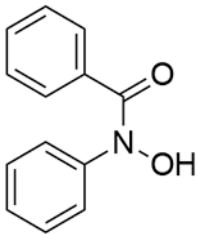
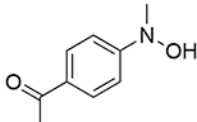
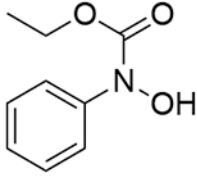
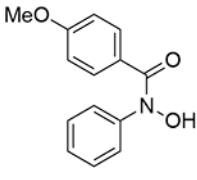
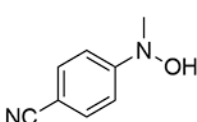
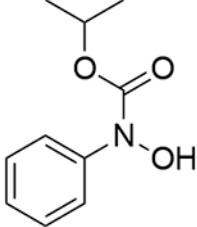
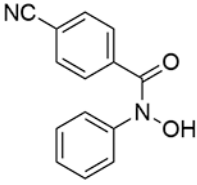
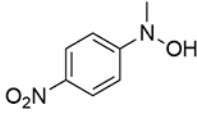
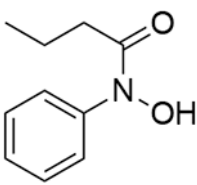
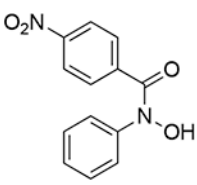
^bStandard potential.

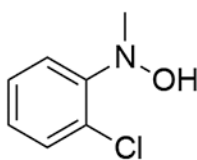
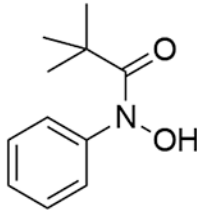
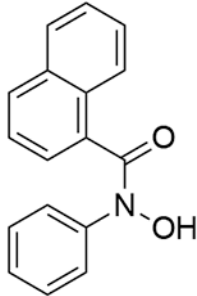
^cExperimental measurements performed in CH₃CN. ^b and ^c experimental measurements performed in H₂O.

Table 9.

Redox potentials (V vs. NHE) of *N*-aryl hydroxylamines, hydroxyamic acids, and other acyclic *N*-hydroxy derivatives as determined by CV or differential pulse voltammetry. Measurements were conducted in phosphate buffer (pH 6).250



Entry	<i>N</i> -Hydroxy Derivatives	$E_{1/2}$	Entry	<i>N</i> -Hydroxy Derivatives	$E_{1/2}$	Entry	<i>N</i> -Hydroxy Derivatives	$E_{1/2}$
1		0.721	7		0.687	13		0.680
2		0.723	8		0.740	14		0.730
3		0.745	9		0.679	15		0.700
4		0.753	10		0.676	16		0.750
5		0.759	11		0.709	17		0.730

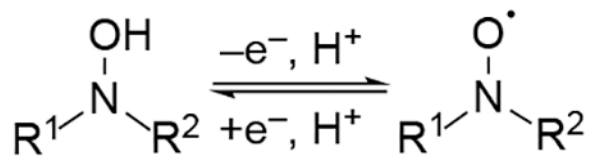
Entry	<i>N</i> -Hydroxy Derivatives	$E_{1/2}$	Entry	<i>N</i> -Hydroxy Derivatives	$E_{1/2}$	Entry	<i>N</i> -Hydroxy Derivatives	$E_{1/2}$
6		0.803	12		0.720	18		0.740

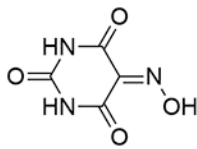
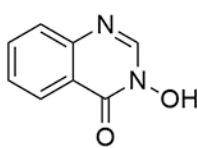
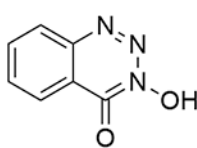
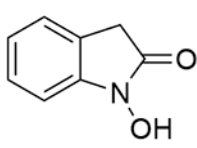
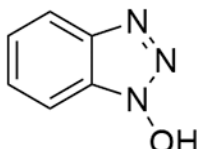
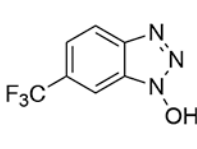
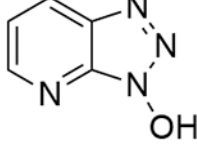
Author Manuscript

Author Manuscript

Author Manuscript

Author Manuscript

Table 10.The redox potential of heterocyclic *N*-hydroxy derivatives.

Entry	<i>N</i> -Hydroxy Derivatives	$E_{1/2}^a$	Ref.
1		0.87 ^b	250
2		1.10 ^c	247
3		1.01 ^c	247
4		0.80 ^d	273
5		1.06 ^b	250
6		1.17 ^b	250
7		1.22 ^b	250

^aPotentials adjusted relative to NHE, as described in ref. 17–19.

^b Experimental measurements performed 45 mM phosphate buffer (pH 6).

^c Experimental measurements performed with 2 equiv 2,4,6-collidine in CH₃CN.

^d Experimental measurements performed in CH₃CN in the absence of base.

Author Manuscript

Author Manuscript

Author Manuscript

Author Manuscript